



# Evoluzione spettrale delle Galassie

Materiale didattico per gli studenti

**A.A. 2019/20 - Laurea Magistrale in  
Astrofisica e Cosmologia**

**Prof. Alberto Buzzoni**

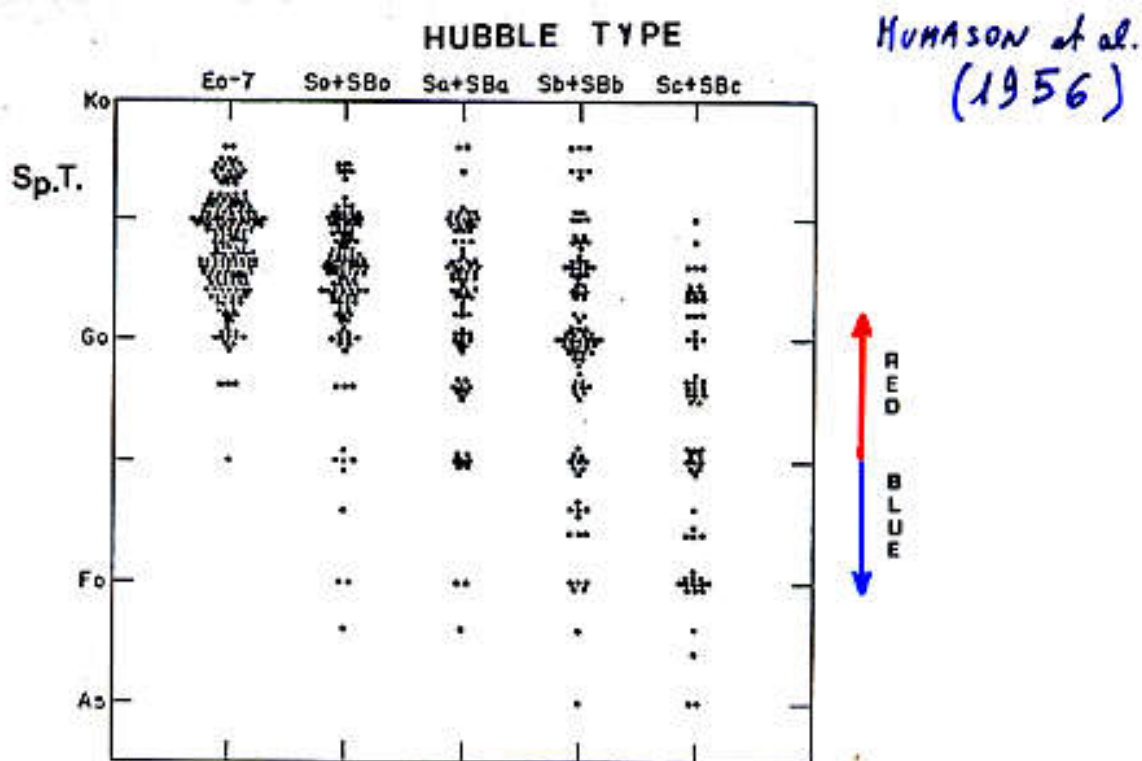
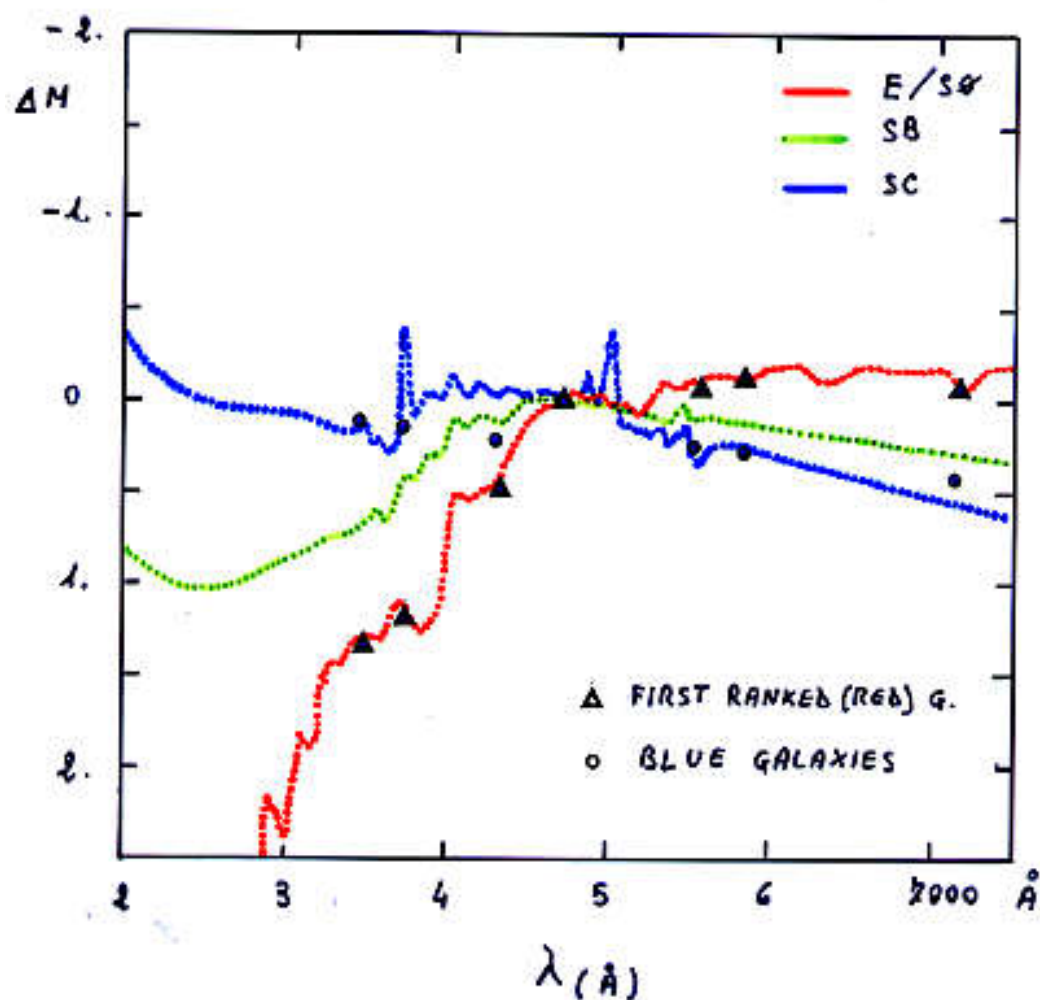
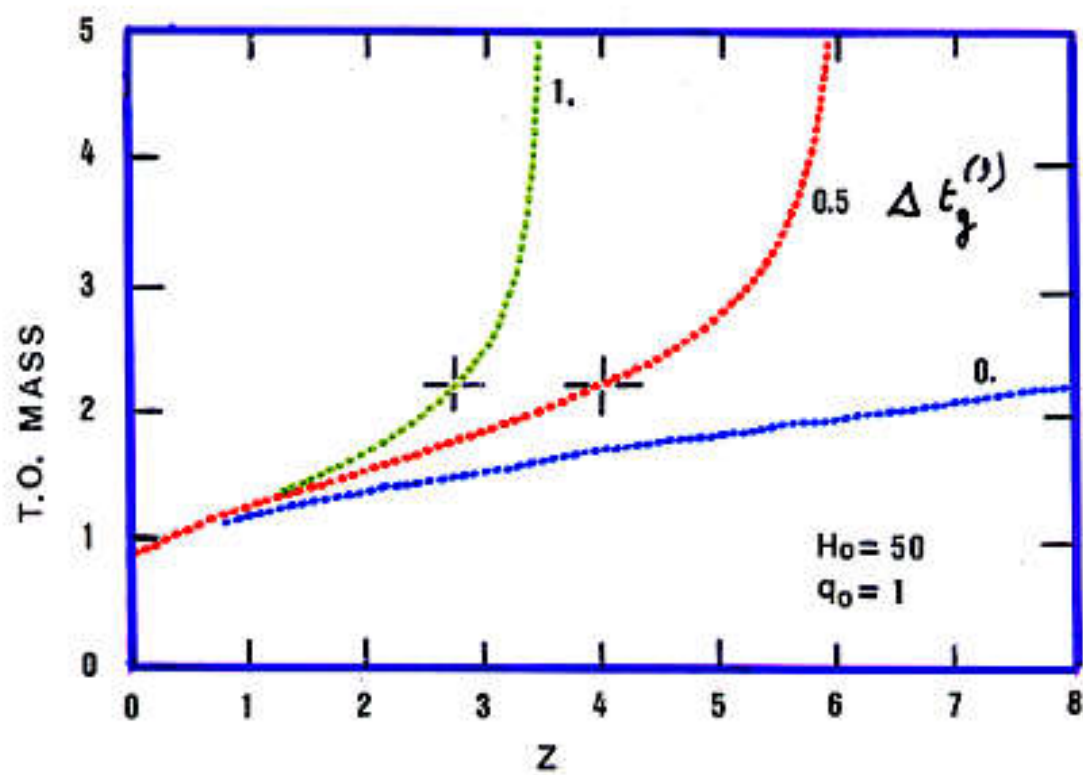
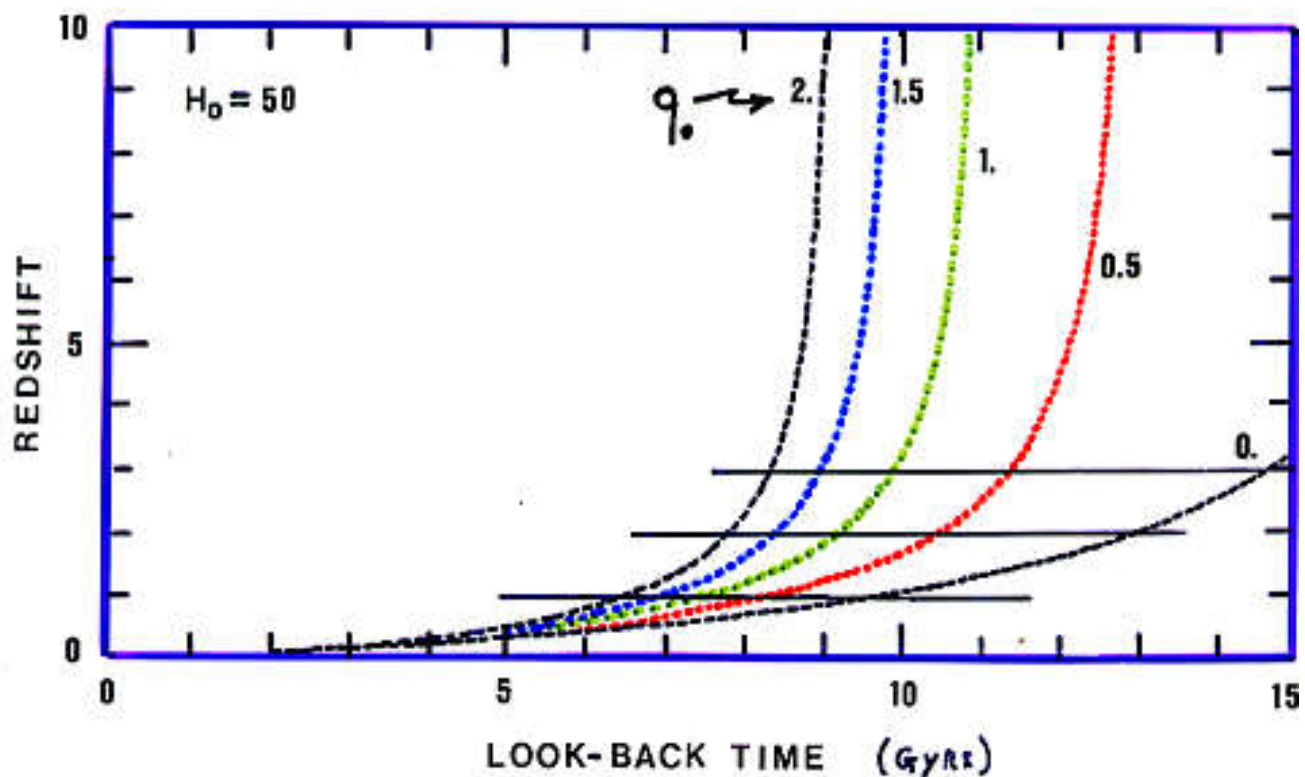


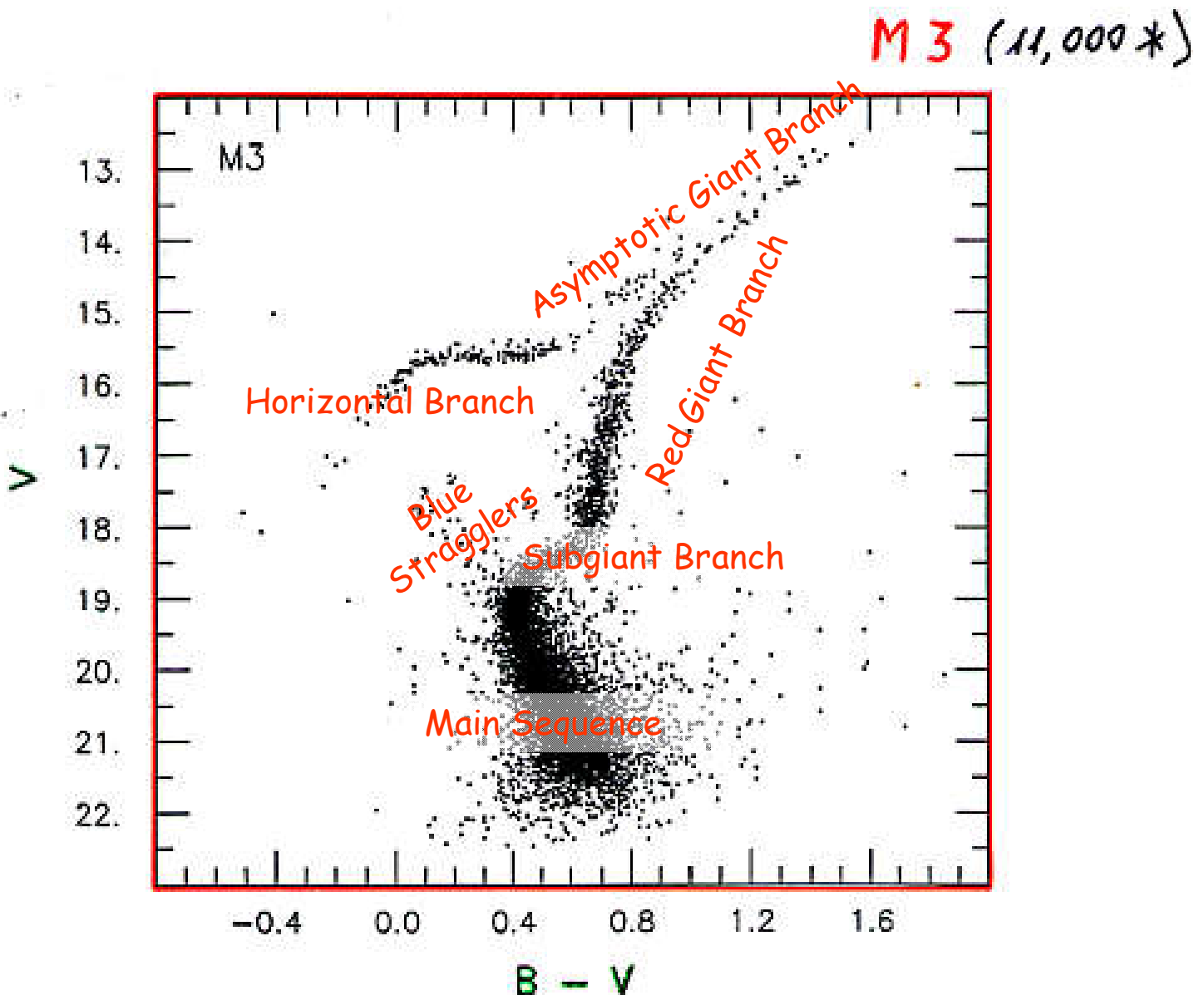
Figure 2. The distribution of spectral type as a function of nebular type for 546 nebulae from Tables I and II.



# Cosmologia & Look-back time



# Un diagramma colore-magnitudine tipo (l'ammasso globulare M3)



Buonanno et al.  
(1994)

# B<sup>2</sup>FH (1956)

5 October 1956, Volume 124, Number 3223



Scanned at the American Institute of Physics

# SCIENCE

## Origin of the Elements in Stars

F. Hoyle, William A. Fowler,  
G. R. Burbidge, E. M. Burbidge

Experimental (*1, 1a*) and observational (*2–6*) evidence has continued to accumulate in recent years in support of the theory (*7–10*) that the elements have been and are still being synthesized in stars. Since the appearance of a new and remarkable analysis by Suess and Urey (*11*) of the abundances of the elements, we have found it possible to explain, in a general way, the abundances of practically all the isotopes of the elements from hydrogen through uranium by synthesis in stars and supernovae. In this article we wish to outline in a qualitative fashion the essentially separate mechanisms which are required in stellar synthesis (*12*).

### Thermal Conversion of Pure Hydrogen through Helium to Iron

As long as extremely high temperatures in excess of  $5 \times 10^9$  degrees Kelvin are not under consideration, the general tendency of nuclear reactions inside stars is to increase the average binding energy per nucleon. For a given temperature and density and for a given time scale of op-

in some cases by resonance penetration. Since barrier effects become less severe as the temperature increases, it follows that the binding energies increase with temperature. This will become clear from the following examples.

At temperatures from about  $10^7$  to  $5 \times 10^7$  degrees in main-sequence stars, hydrogen is transformed to helium,  $4\text{H}^1 \rightarrow \text{He}^4$ , with an average binding energy of 7.07 million electron volts (Mev) per nucleon. We emphasize that the proton-proton sequence of reactions makes possible the production of helium starting only with hydrogen. The recent discovery of the free neutrino as reported by Cowan *et al.* (*1a*) leads to increased confidence in the existence of the primary proton-proton interaction which proceeds through prompt electron-neutrino emission. At temperatures from  $10^8$  to  $2 \times 10^8$  degrees in red giant stars,  $\text{He}^4$  is transformed principally to  $\text{C}^{12}$ ,  $\text{O}^{16}$ , and  $\text{Ne}^{20}$  with an average binding energy of 7.98 Mev per nucleon. The important roles of the ground state of  $\text{Be}^8$  and of the second excited state of  $\text{C}^{12}$  in expediting the primary process of helium fusion,  $3\text{He}^4 \rightarrow \text{C}^{12}$ , have recently been

appreciably greater atomic weight than  $\text{Fe}^{56}$ .

The situation, then, is that a thermal "cooking" of pure hydrogen yields principally  $\text{He}^4$  and the  $\alpha$ -particle nuclei with  $A = 4n$ ,  $Z = 2n$ ,  $n = 3, 4, 5, 6, 7, 8, 9$ , and  $10$  ( $\text{C}^{12}$  to  $\text{Ca}^{40}$ ), together with nuclei centered around  $\text{Fe}^{56}$ . These are the most abundant nuclei. Moreover, the relative abundances that have been calculated for these nuclei, and particularly for the 20-odd isotopes of titanium, vanadium, chromium, manganese, iron, cobalt, and nickel, show good agreement with observed abundances. The original equilibrium calculations by Hoyle (*7*) have been considerably improved by taking into account the low-lying excited states of the iron-group nuclei and of the radioactive nuclei which ultimately decay to them, and by statistically weighting each state according to its observed spin or that expected on nuclear shell theory. Typical results for the equilibrium abundances of the chromium isotopes at  $3.8 \times 10^8$  degrees are indicated in Table 1.

We regard results similar to those presented in Table 1 as giving strong support to the view that the elements under consideration were synthesized inside stars and that they became subsequently distributed in space, either by slow emission from late-type giants or by catastrophic explosion, as for instance in supernovae.

### Thermal Reactions of Hydrogen and Helium with Light Elements

More complicated effects arise when the thermal cooking is considered, not of completely pure hydrogen, but of hydrogen adulterated with a small proportion of the elements mentioned in the previous paragraphs. When a second-genera-

# Clocks

$$L t = E$$

KELVIN-HELMHOLTZ  $E = \frac{GM^2}{R}$

$$t_0 \sim \frac{E}{L} \sim \frac{GM^2}{RL} \sim \frac{6 \cdot 10^{-8} (2 \cdot 10^{33})^2}{2 \cdot 10^{10} 4 \cdot 10^{33}} \text{ sec.}$$

$$t_0 \sim \frac{6 \cdot 10^{25}}{2 \cdot 10^{10} 3 \cdot 10^2} \text{ yr} \Rightarrow \frac{2 \cdot 10^8 \text{ yr}}{2}$$

NUCLEARE  $E = \alpha Mc^2$   
 $\downarrow$   
 $0.007$

$$t_0 \sim \frac{E}{L} \sim \frac{\alpha Mc^2}{L} \sim \frac{2 \cdot 10^{-3} 2 \cdot 10^{33} 9 \cdot 10^{20}}{4 \cdot 10^{33}} \text{ sec.}$$

$$t_0 \sim \frac{63}{2} \frac{10^{17}}{3 \cdot 10^2} \text{ yr} \sim \frac{63}{6} 10^{10} \sim 10^{11} \text{ yr}$$

DIPENDENZA DALLA CHIMICA

$$\left\{ \begin{array}{l} t \propto \frac{M}{L} \\ L \propto \frac{M^3 \mu^4}{K} \end{array} \right. \Rightarrow t \propto \frac{M \tilde{K}}{M^2 \mu^4} \propto \frac{1}{M^2} \left( \frac{\tilde{K}}{\mu^4} \right)$$

quindi: se  $M = \text{fix}$   $t \uparrow$  se  $Z \uparrow$   
 $t \downarrow$  se  $Y \uparrow$

se  $t = \text{fix}$   $M_{T_0} \uparrow$  se  $Z \uparrow$

$M_{T_0} \downarrow$  se  $Y \uparrow$

$$\begin{aligned}
 * & \left\{ \begin{array}{l} 1) \quad \nabla P = -\rho g \Rightarrow \frac{P}{R} \propto \rho \frac{M}{R^2} \Rightarrow P \propto \rho \frac{M}{R} \\ 2) \quad \nabla M = 4\pi R^4 \rho \\ 3) \quad \nabla L = 4\pi R^2 \epsilon \\ * \quad 4) \quad \nabla T = -\frac{3\rho k L}{16\pi a c T^3 R^2} \Rightarrow \frac{T}{R} \propto \frac{\rho L}{T^3 R^2} \Rightarrow T^4 \propto \frac{\rho L}{R} \\ * \quad 5) \quad \rho = \frac{\rho k T}{\mu H} \Rightarrow \rho \propto \rho T \end{array} \right. \\
 \end{aligned}$$

$$\rho T \propto \rho \frac{M}{R}$$

↓

$$\left\{ \begin{array}{l} T \propto \frac{M}{R} \\ T^4 \propto \frac{\rho L}{R} \Rightarrow \frac{M^4}{R^4} \propto \frac{M}{R^4} L \Rightarrow \boxed{L \propto M^3} \end{array} \right.$$

$$L t \propto M$$

↓

$$\left\{ \begin{array}{l} t \propto \frac{M}{L} \\ L \propto M^3 \end{array} \right. \Rightarrow \boxed{t \propto M^{-2} \\ t \propto L_{T.O.}^{-2/3}}$$

# Relazioni di scala per le stelle in Sequenza Principale

$$\left\{ \begin{array}{l} \nabla P = -P g \\ P = \frac{\rho k T}{m H} \end{array} \right. \Rightarrow \frac{\lambda k T}{\mu H R} \propto -\lambda \frac{GM}{R^2}$$

↓

$$T \propto \frac{M}{R} \mu$$

$$\nabla T = \frac{-3\rho \tilde{k} L}{16\pi g c R^2 T^3}$$

↓

$$\frac{T^4}{R^4} \propto \frac{M}{R^3} \frac{\tilde{k} L}{R^2}$$

$$\frac{M}{R^4} \cancel{\mu^4} \propto \frac{M}{R^4} \cancel{\tilde{k} L}$$

↑

$$L \propto M^3 \frac{\mu^4}{\tilde{k}}$$

$$\left\{ \begin{array}{l} T \propto \frac{M}{R} \mu \\ L \propto R^2 T^4 \end{array} \right.$$

$$L \propto R^2 T^4 \Rightarrow R \propto \frac{L^{1/2}}{T^2}$$

$$T \propto \frac{M}{L^{1/2}} \mu$$

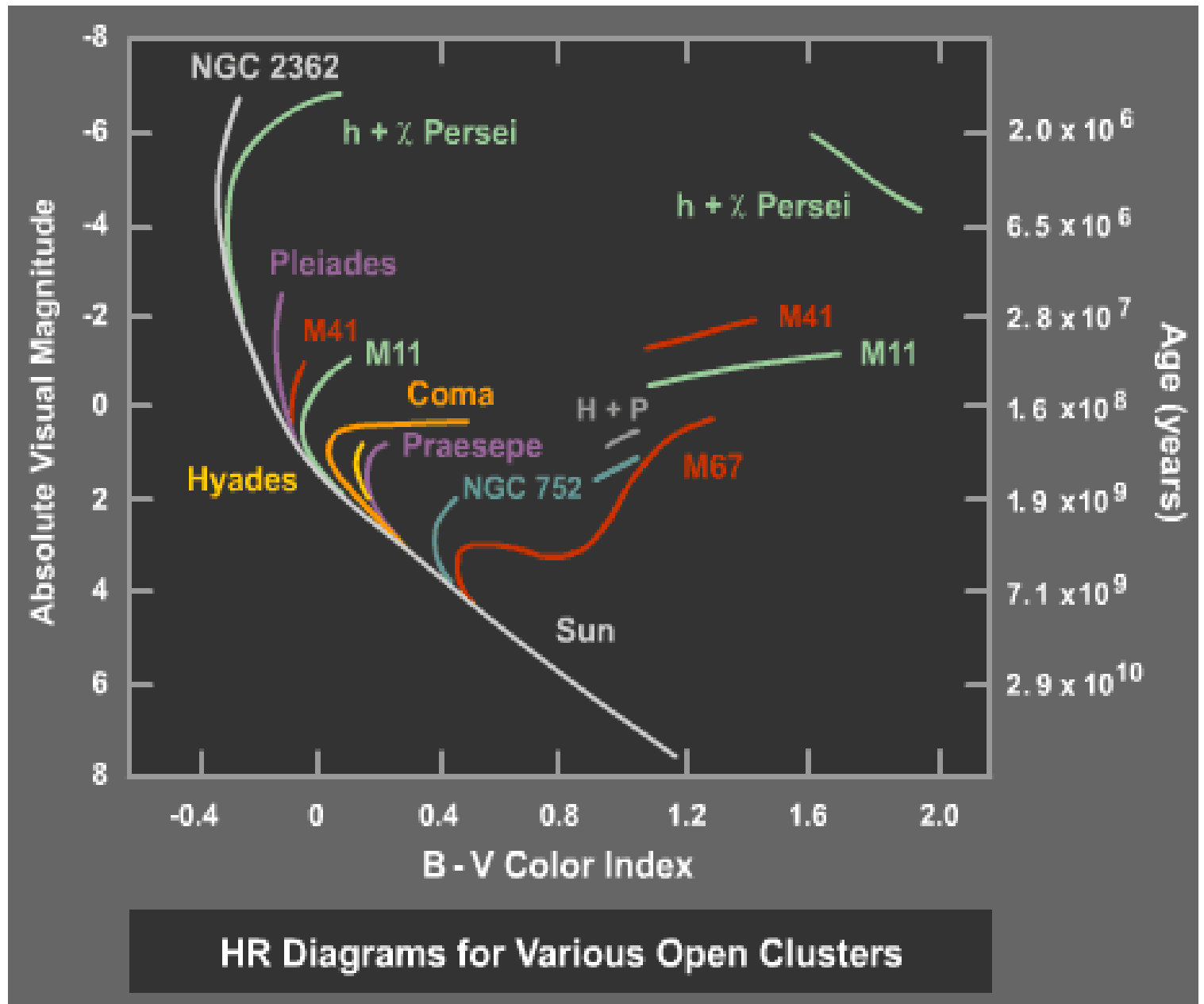
$$\left( \frac{M^2 \mu^4}{L^2 R^2} \right)^{1/2}$$

$$\frac{L^{1/2}}{M \mu} \propto \pi$$

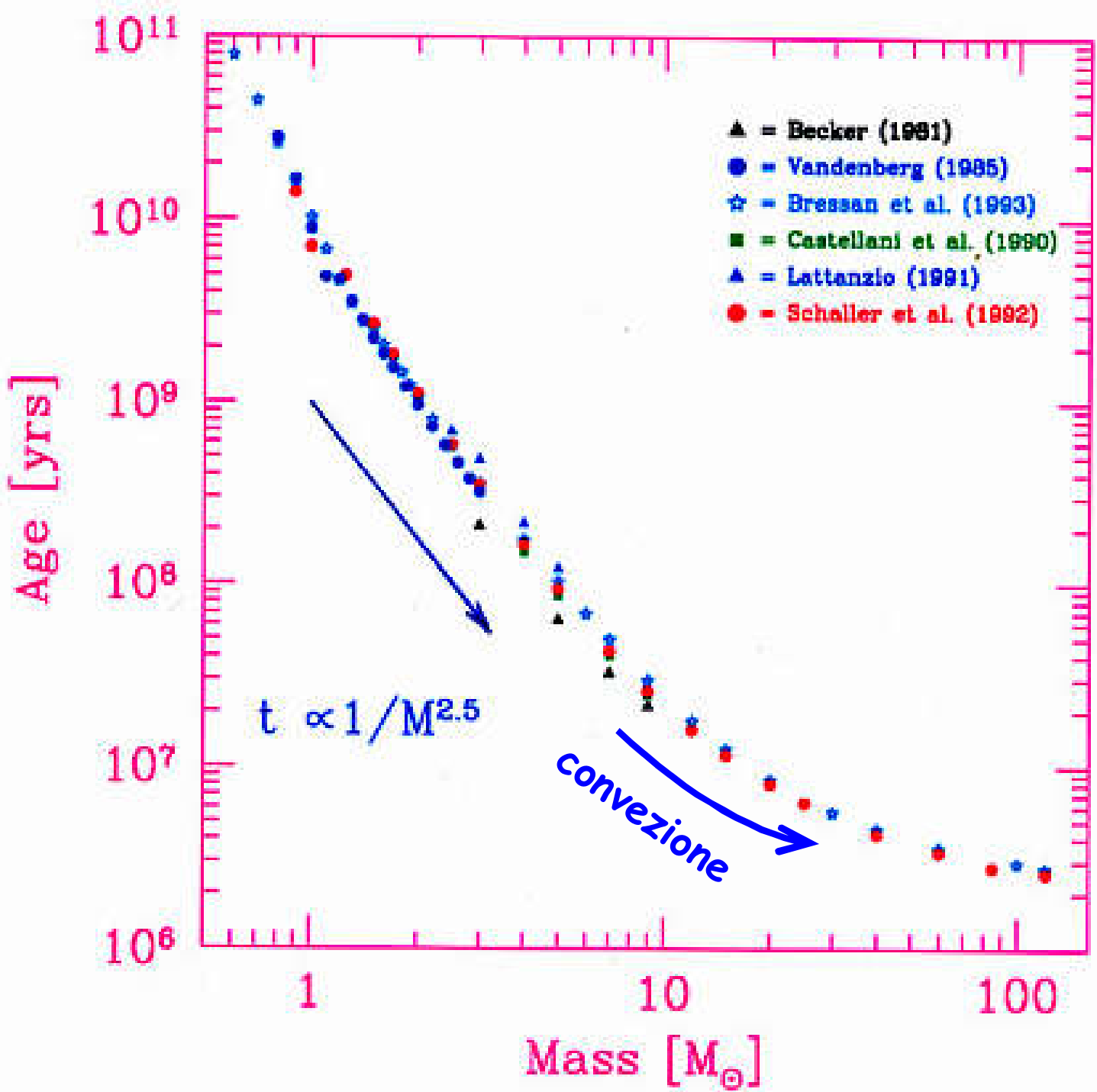
$$T \propto \sqrt{\frac{M}{\tilde{k}}} \mu$$

$$\left\{ \begin{array}{l} L \propto \frac{M^3 \mu^4}{\tilde{k}} \\ T \propto \frac{M^{1/2} \mu}{\tilde{k}^{1/2}} \end{array} \right. \Rightarrow L \propto T^6 \left( \frac{M}{\tilde{k}} \right)^2$$

# Il punto di Turn Off come indicatore di età



# The Clock



# Peso Molecolare Medio

$$\bar{\mu} = \frac{\sum n_j m_j}{\sum n_j}$$

$\forall j =$  tutte le specie chimiche

## GAS NEUTRO

$$\bar{\mu}_N = \frac{\rho_X + \rho_Y + \rho_Z}{\frac{\rho_X}{H} + \frac{\rho_Y}{4H} + \frac{\rho_Z}{2Z}} \sim \frac{H}{X + \frac{Y}{4} + \frac{Z}{2Z}}$$

$\downarrow$   
 $\sim 0$

## PLASMA TOT IONIZZATO

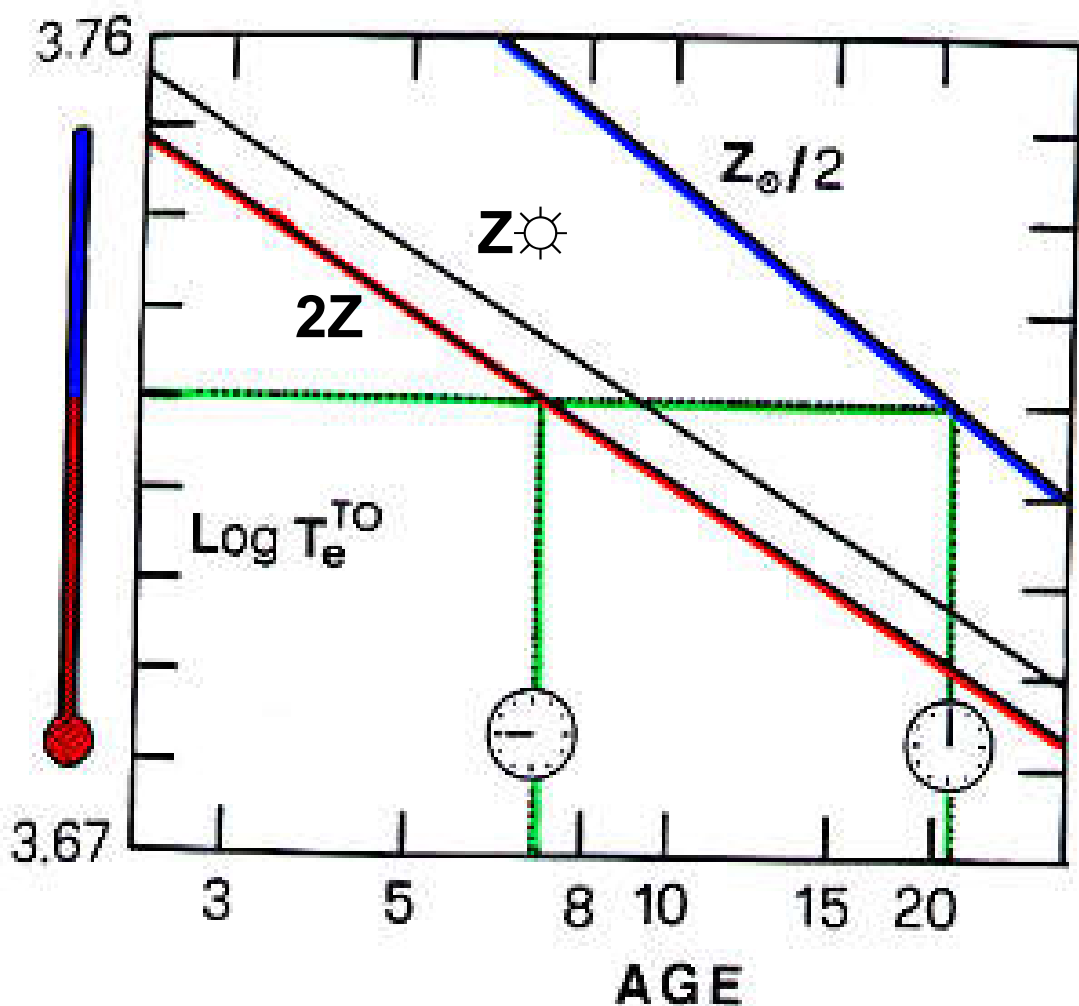
$$\bar{\mu}_i = \bar{\mu}_N + \frac{\rho}{\frac{\rho_X}{H} + \frac{2\rho_Y}{4H} + \frac{2\rho_Z}{2Z}} = \bar{\mu}_N + \frac{H}{X + \frac{Y}{2} + \frac{Z}{2}}$$

$$\bar{\mu}_i = \frac{H}{(X + \frac{Y}{4} + \frac{Z}{2Z}) + (X + \frac{Y}{2} + \frac{Z}{2})} = \frac{H}{2X + \frac{3}{4}Y + \underbrace{(1+\frac{1}{Z})\frac{Z}{2}}_{\sim 1}}$$

$$\bar{\mu}_i \sim \frac{H}{2X + \frac{3}{4}Y + \frac{Z}{2}}$$

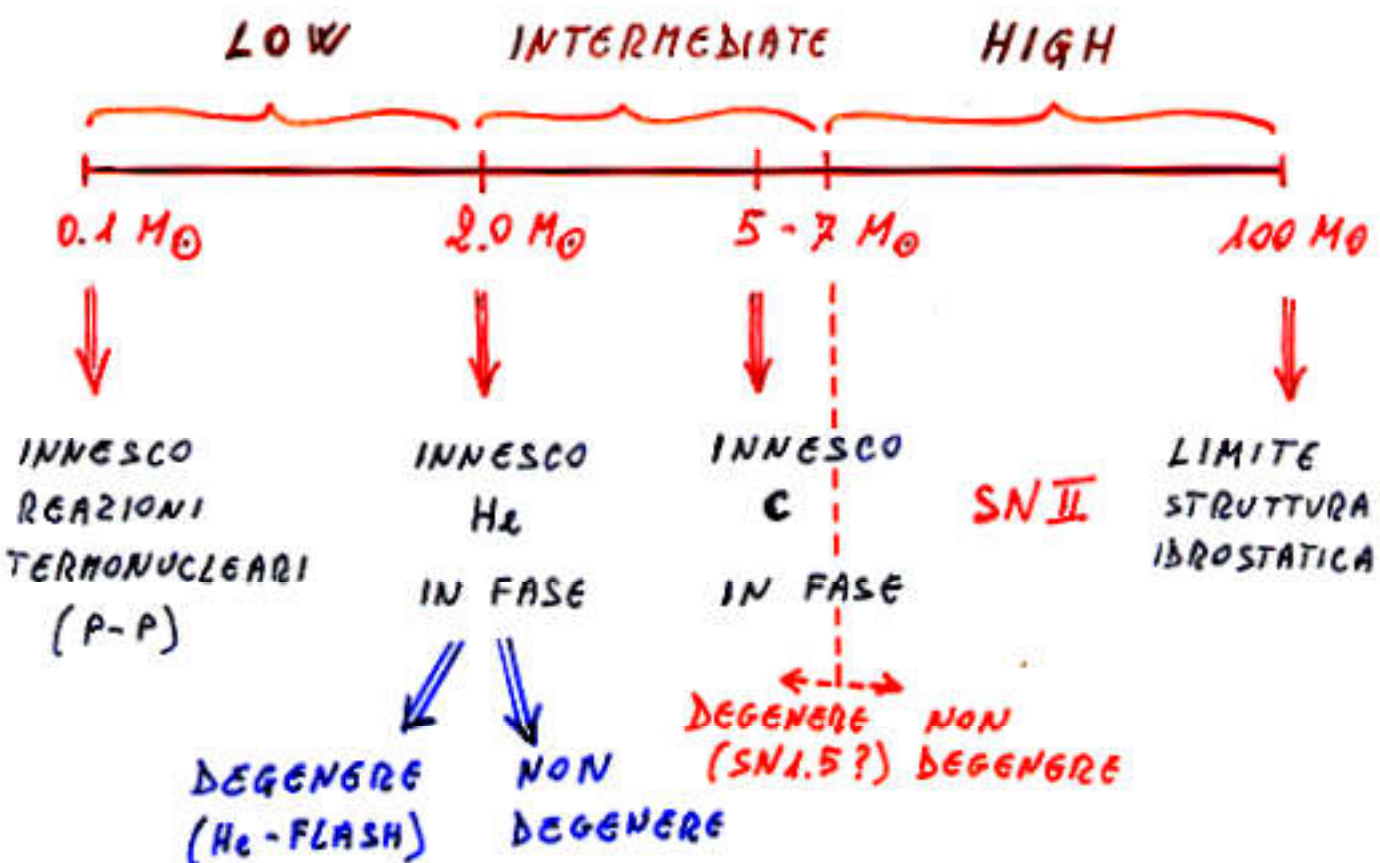
# Thermometers & Clocks (effetto della metallicità)

GLOBAL PROPERTIES OF STELLAR POPULATIONS



Renzini & Buzzoni (1986)

## STELLAR MASSES



FASE	LOW-MASS	HIGH-MASS
CORE H-BURNING	MS	MS
SHELL H-BURNING	{ SGB RGB	1-ST GB
CORE He-BURNING	HB	1-ST BLUE LOOP
DOUBLE (MULTIPLE) SHELL BURNING	AGB	2-NB, 3-NB etc. GBs

---

## DISTINCTIVE PARAMETERS IN A STELLAR POPULATION

---

- 1) AGE  $\Rightarrow t$
- 2) CHEMICAL COMPOSITION  $\Rightarrow z, [Fe/H]$
- 3) STAR MASS DISTRIBUTION  $\Rightarrow IMF$
- 4) STAR FORMATION HISTORY  $\Rightarrow SFR$

---

## CANONICAL ASSUMPTIONS

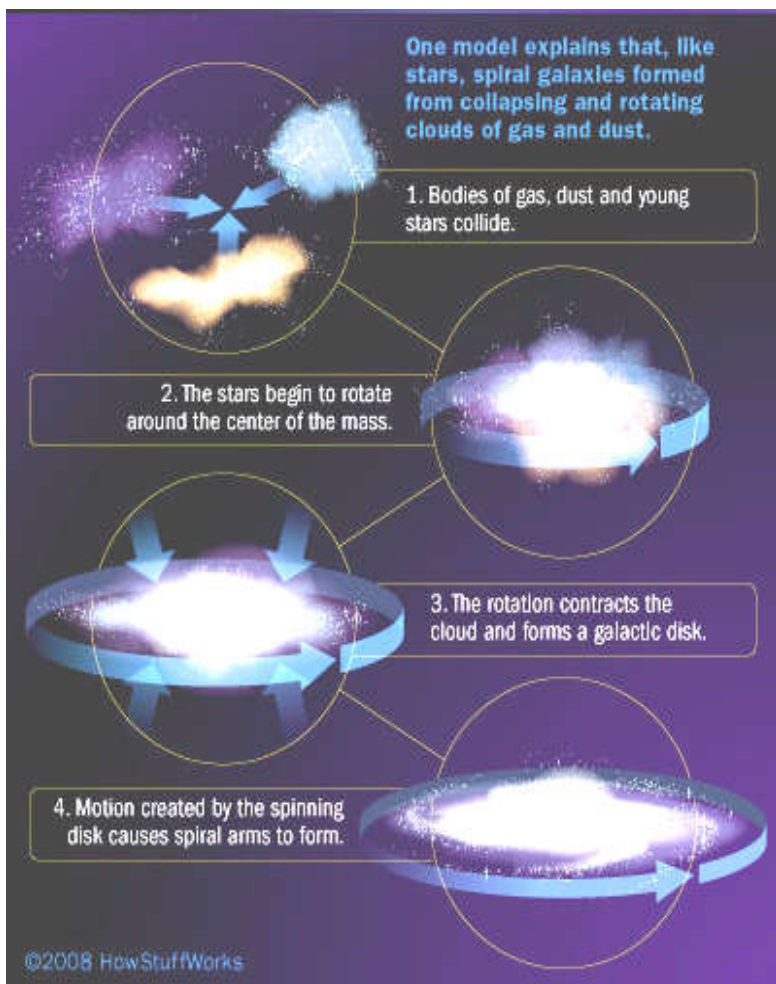
---

- 1) IMF  $N(M) \propto M_*^{-s}$  ( $s = 2.35$ )
- 2) SFR  $\delta(0) \rightarrow SSP$   
 $f(t) \rightarrow CSP$

**Articoli consigliati (vedi Webpage):**  
<http://www.bo.astro.it/~eps/lezioni/lezioni.html>

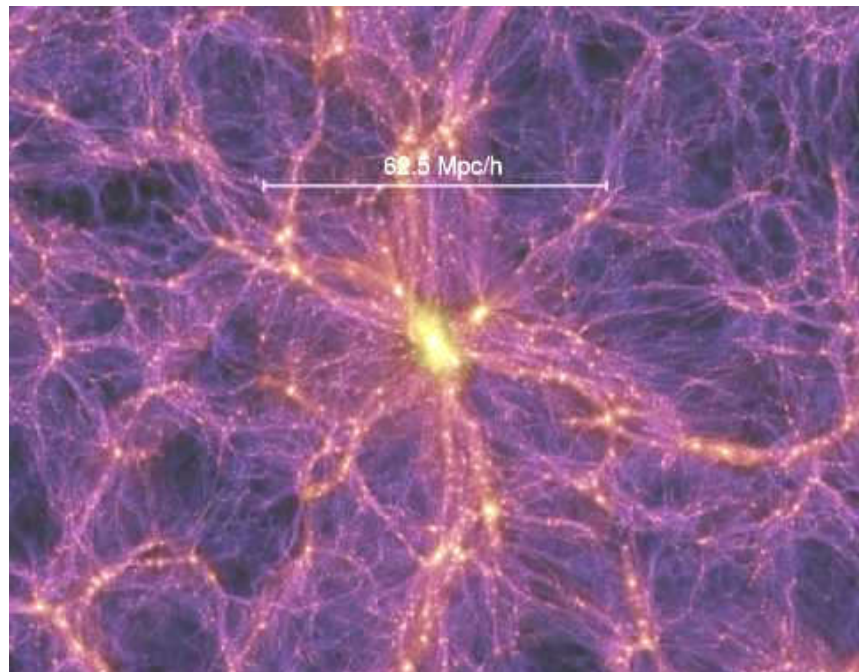
- **SSP Theory (Renzini & Buzzoni 1986)**
- **Galaxy Colors (Buzzoni 2005)**
- **Spectral Properties of Galaxies (Kennicutt 1992)**
- **Energetic & Chemical evolution of Spirals (Buzzoni 2011)**

# Come nascono le galassie?



**Scenario  
“monolitico”  
(Larson 1974, 1975)**

**Scenario  
“gerarchico”  
(Kauffmann &  
White 1993)**



[http://en.wikipedia.org/wiki/GalaxyFormation\\_and\\_Evolution](http://en.wikipedia.org/wiki/GalaxyFormation_and_Evolution)

<http://en.wikipedia.org/wiki/DwarfGalaxyProblem>

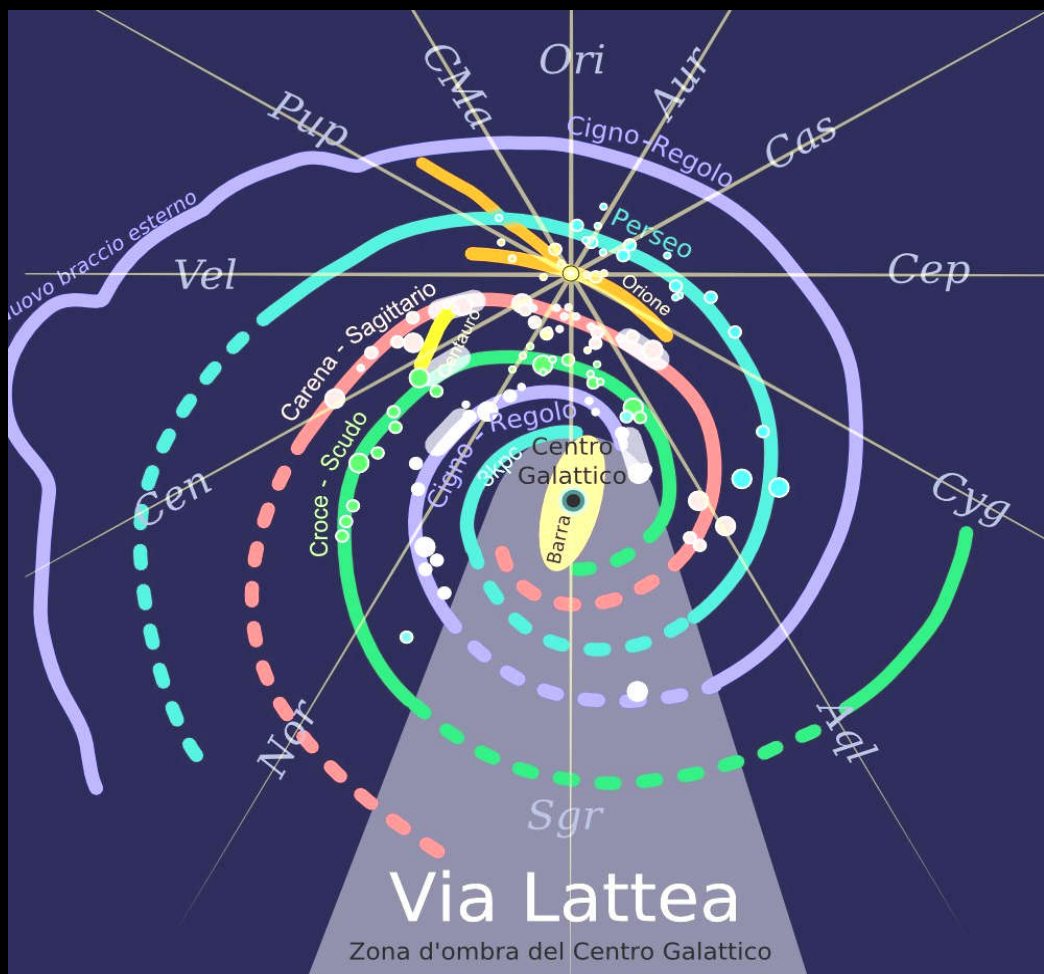
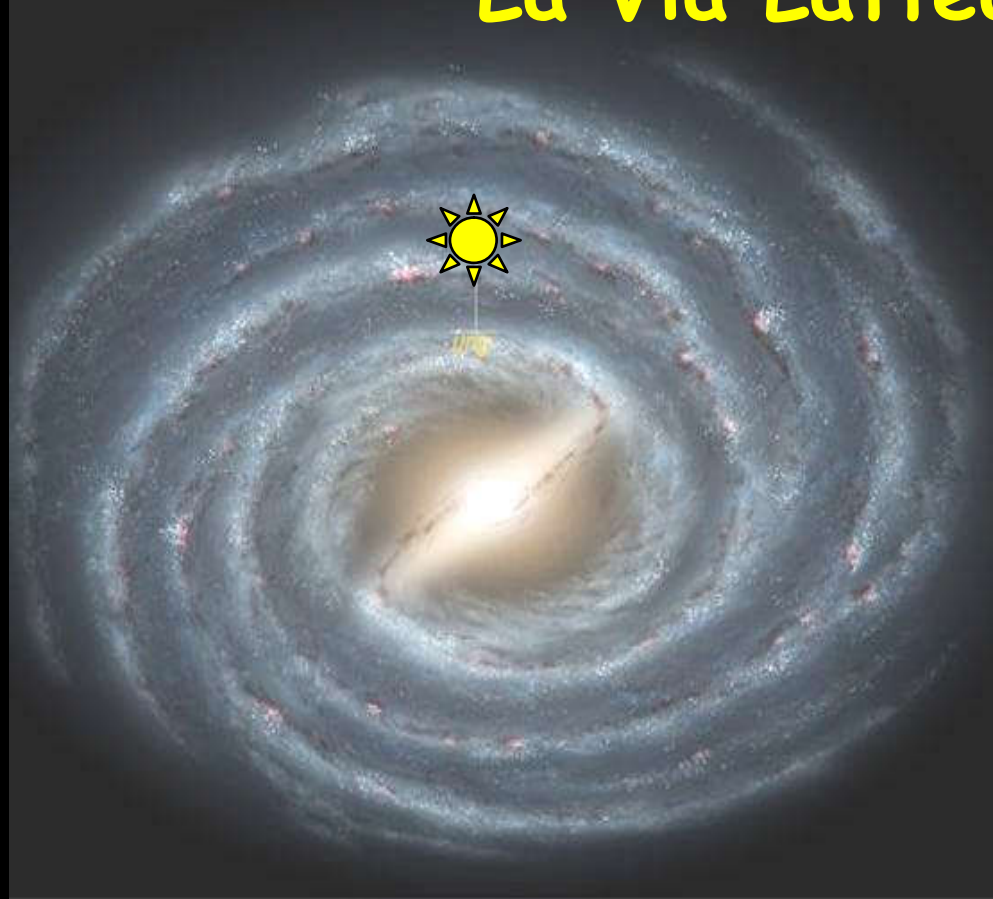
# Scenario Gerarchico & Cosmologia “di consenso”



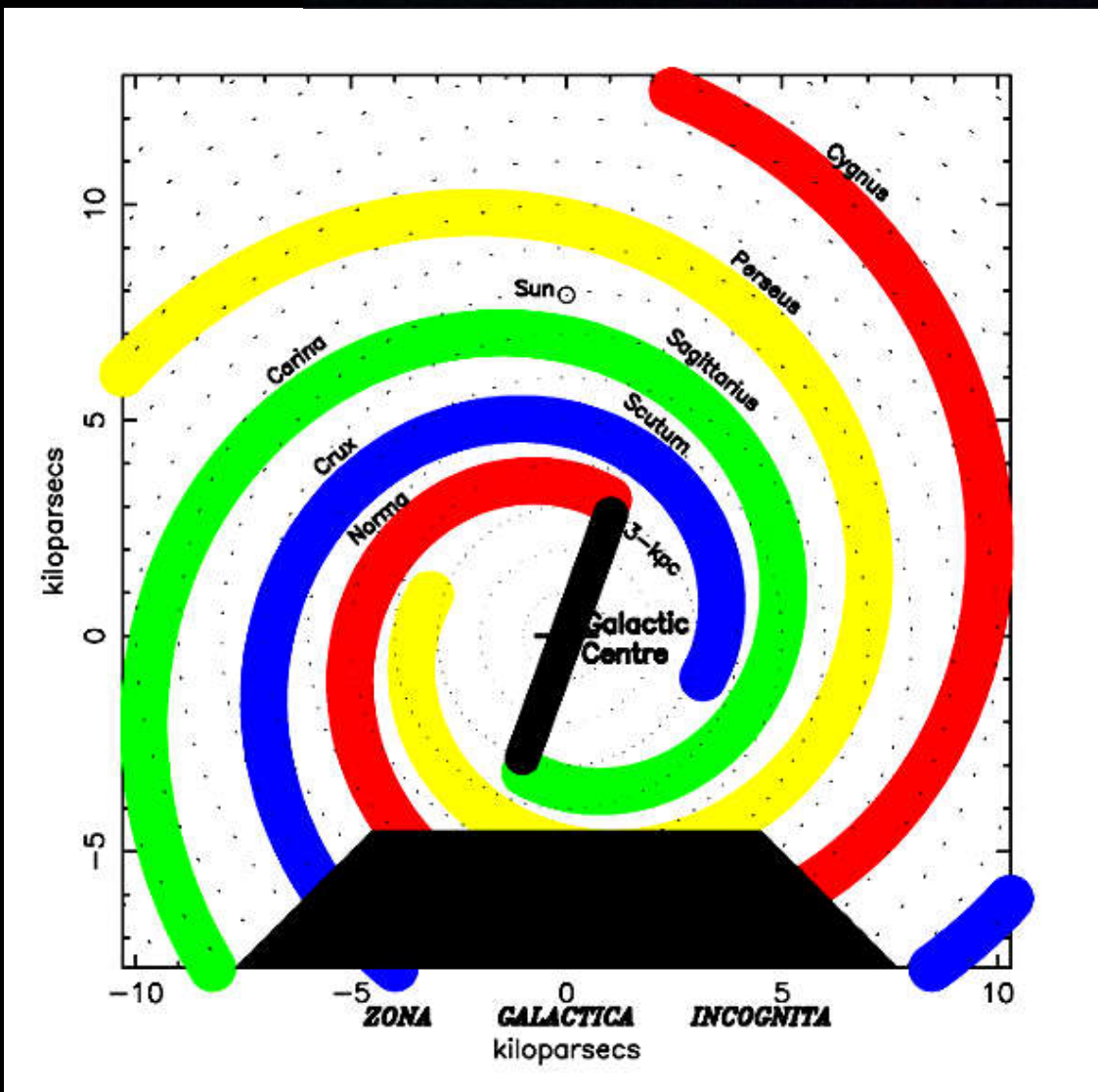
1. Dwarf galaxies must be “older” & metal poor
2. They must “surround” high-mass systems
3. Standard galaxies form “outside in”
4. Ellipticals must be “younger” (i.e. appear at “lower” z) & with a metal-poor bulge
5. Ellipticals could NOT be homologous systems (i.e. Fundamental Plane)

[http://it.wikipedia.org/wiki/Via\\_Lattea](http://it.wikipedia.org/wiki/Via_Lattea)

# La Via Lattea



# I vari bracci della Via Lattea (schematico)



# I diversi sistemi stellari nella Via Lattea

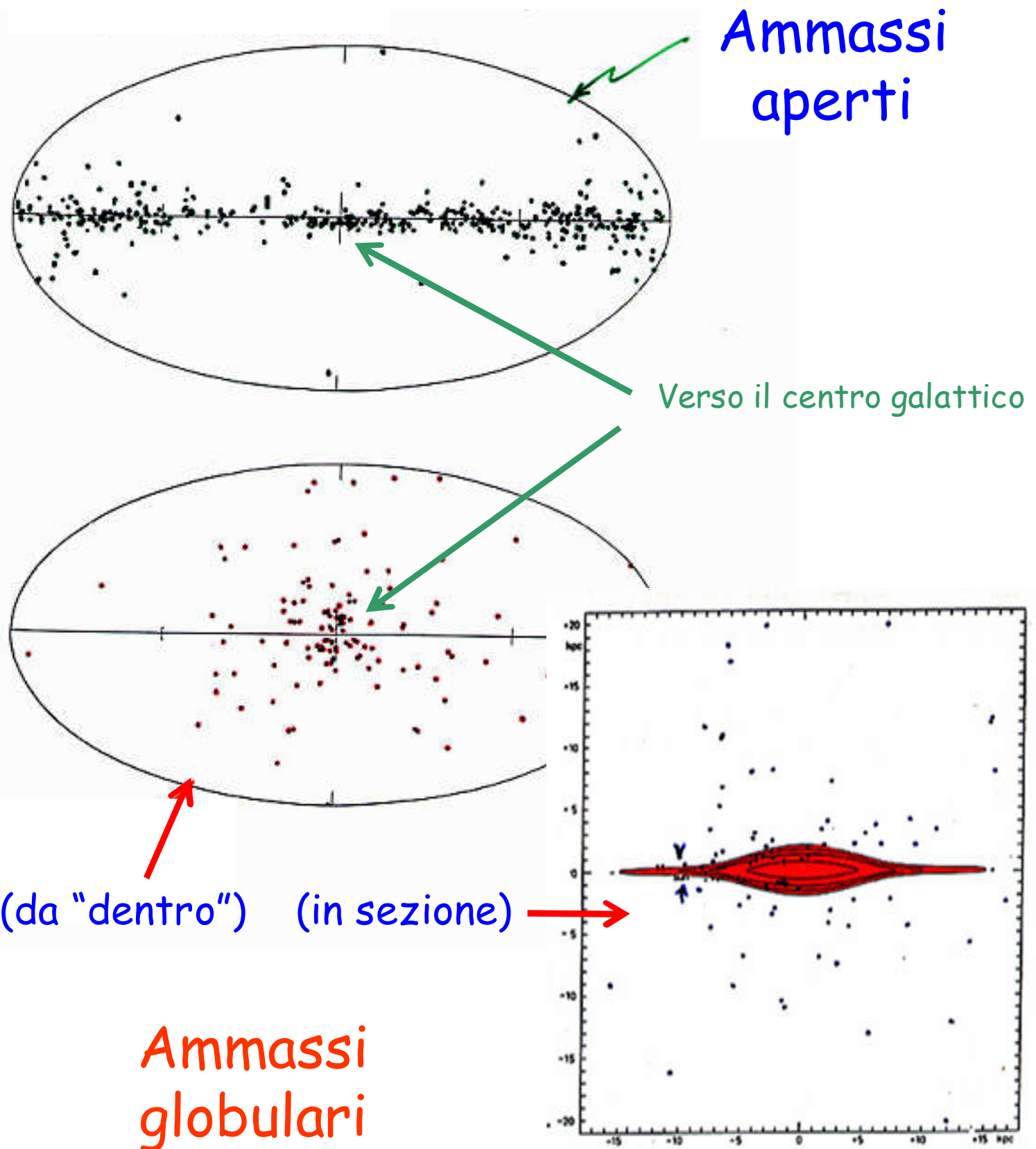
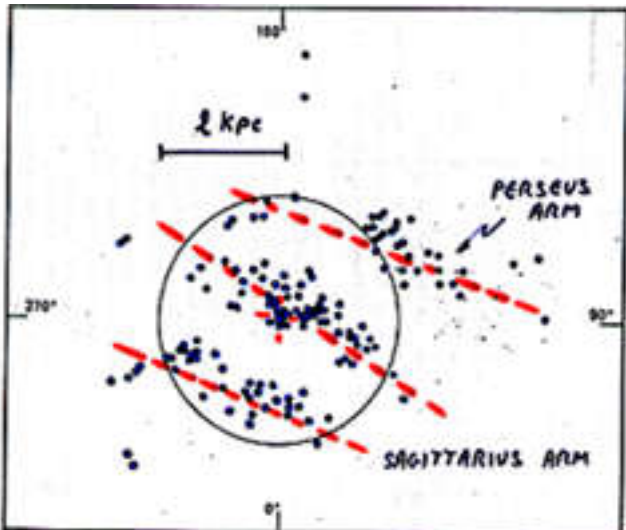
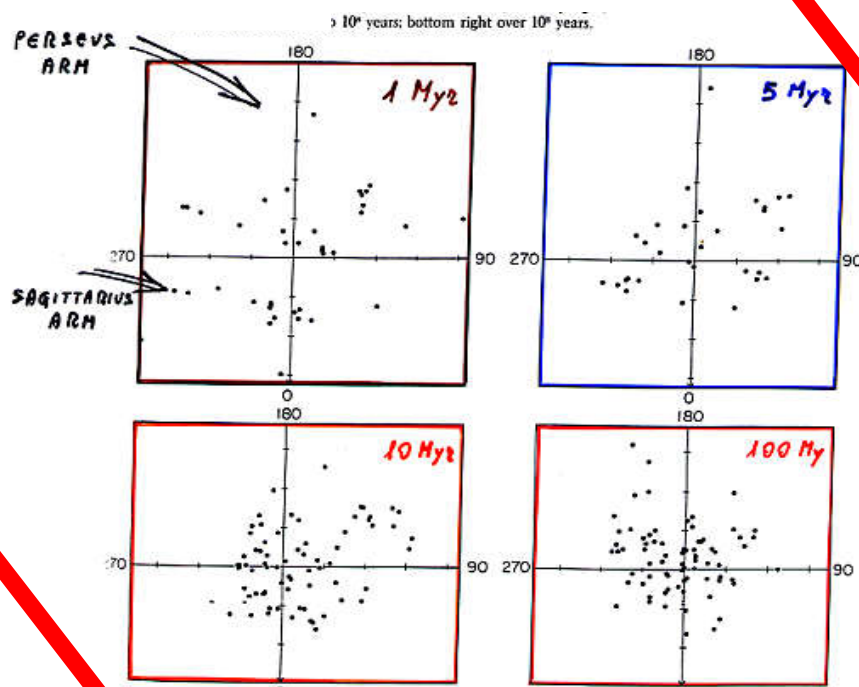


Fig. 23.6: Il sistema galattico: distribuzione spaziale degli ammassi globulari, proiettata su di un piano passante per il sole e perpendicolare al piano galattico, ed aree di uguale densità (riferite alle vicinanze del sole). Nel piano galattico è rappresentato, punteggiato, il sottile strato di materia interstellare con popolazione I estrema (braccio della spirale) (secondo J. H. Oort).

# Gli ammassi aperti come traccianti dei bracci a spirale

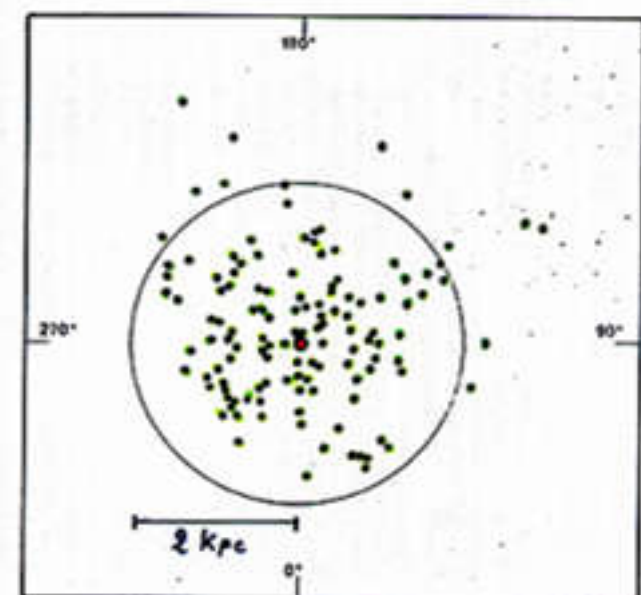


Associazioni O-B (<1 Myr)

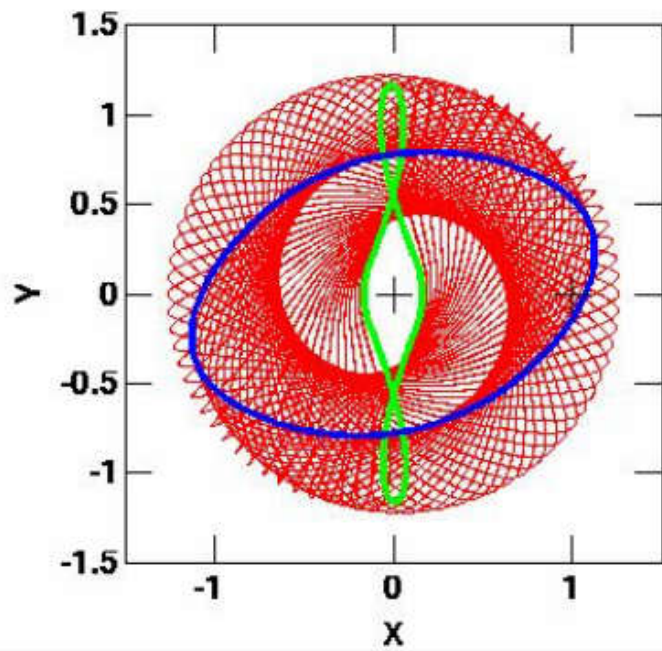
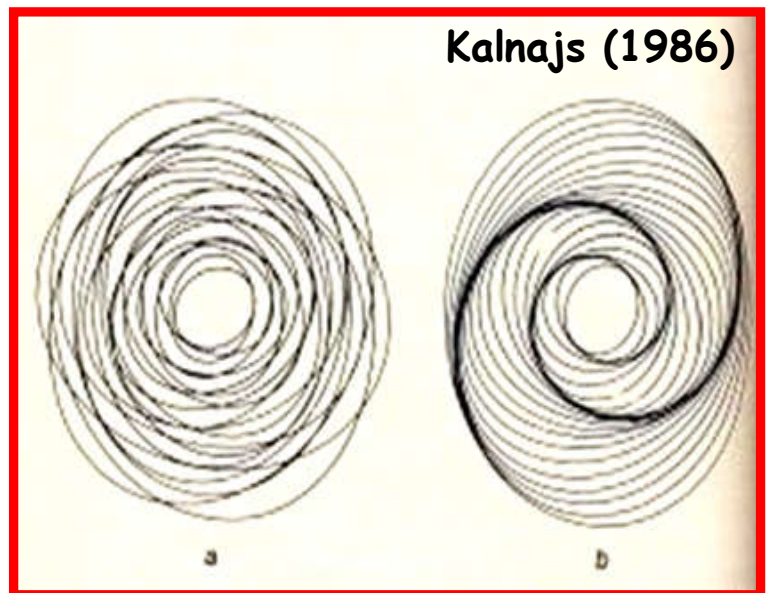
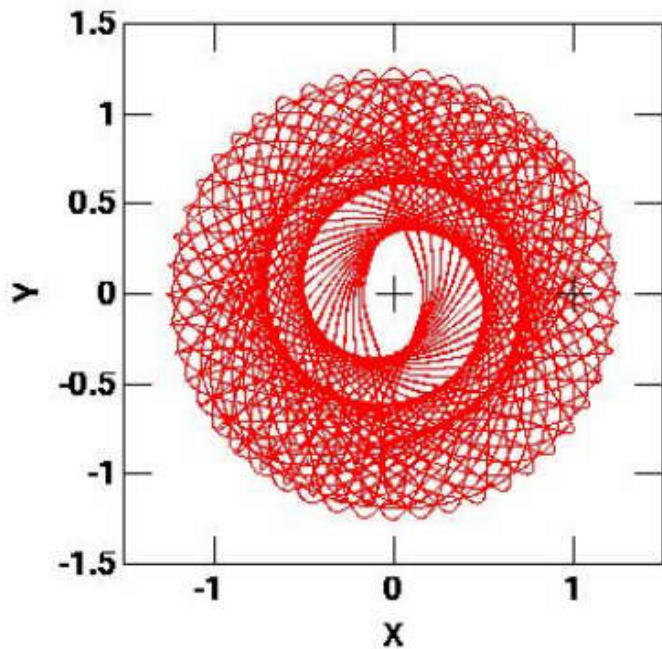


Eta'

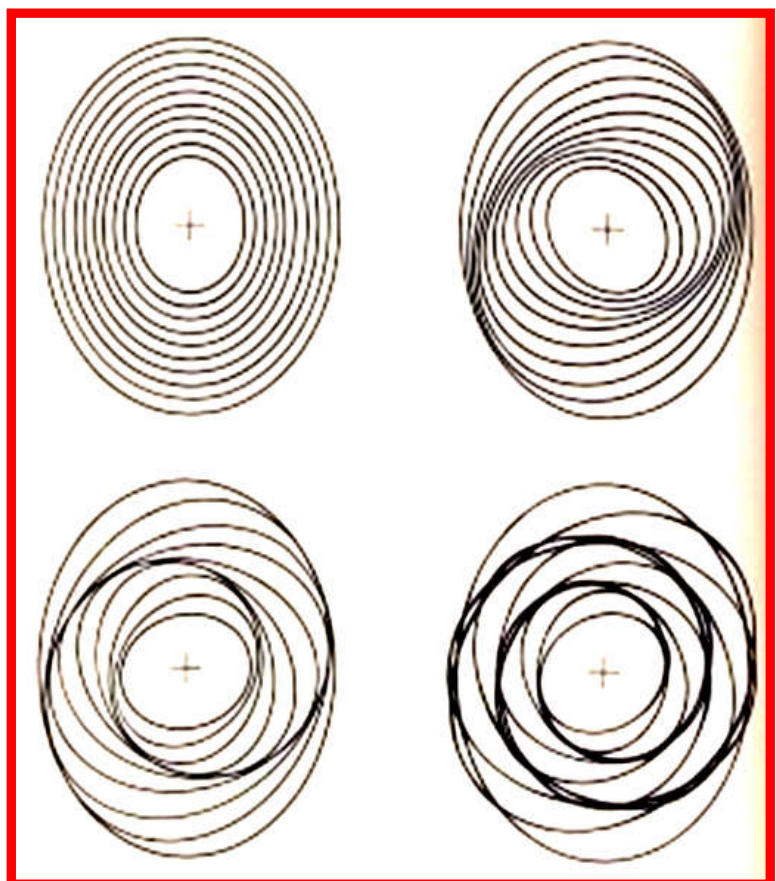
Ammassi aperti (>1Gyr)



# Risonanze orbitali & genesi delle braccia a spirale



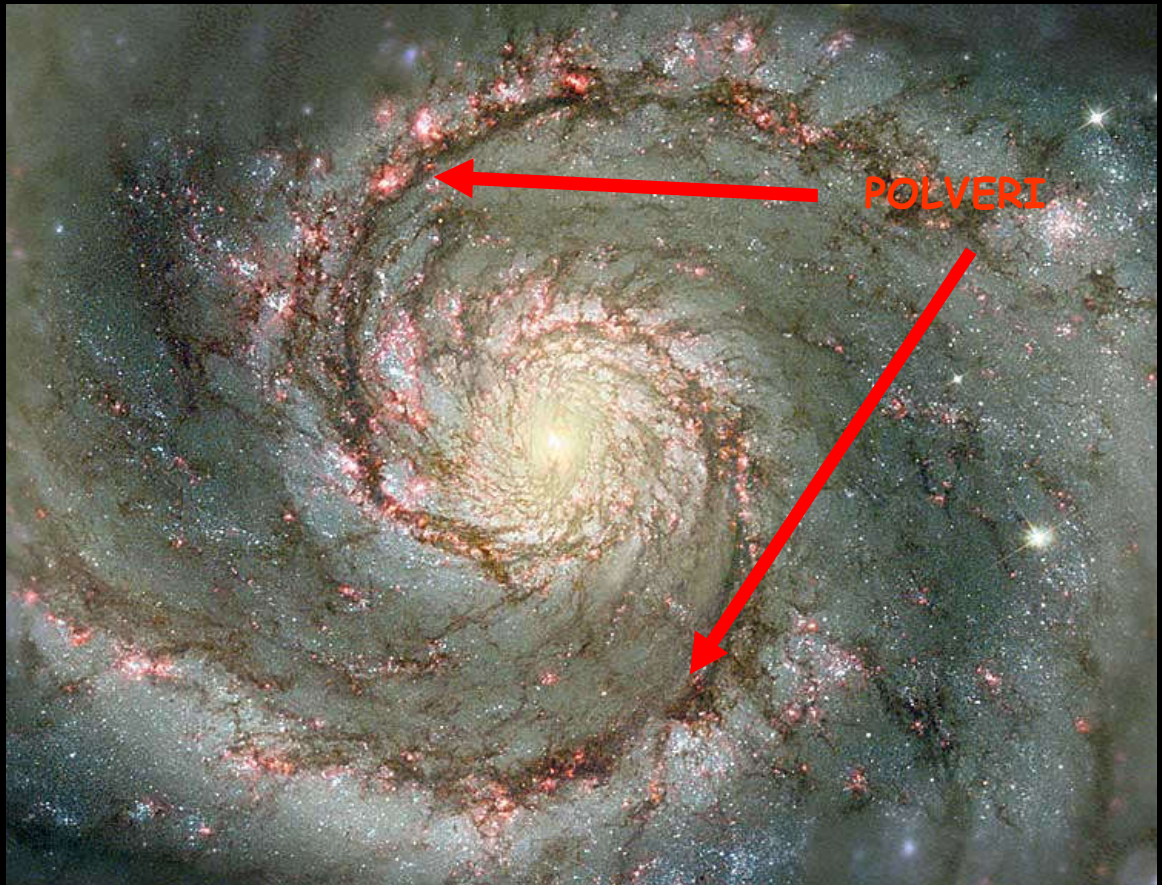
Struck (2015)



# Il meccanismo di formazione stellare

## Il caso di M51

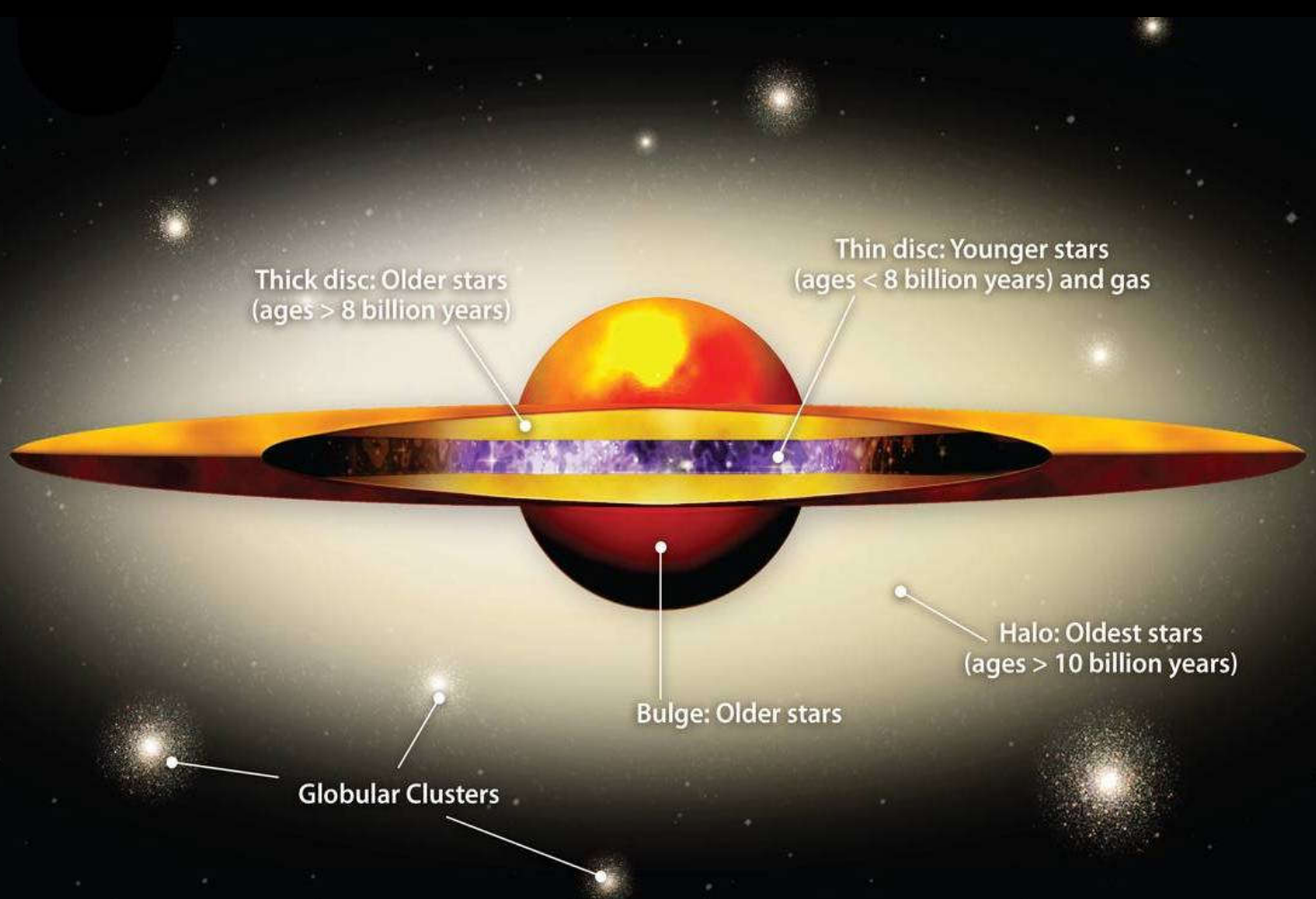
Ottico



Ultravioletto



# Struttura delle galassie a spirale



# Il Diagramma di Bottlinger e la diagnostica delle popolazioni stellari

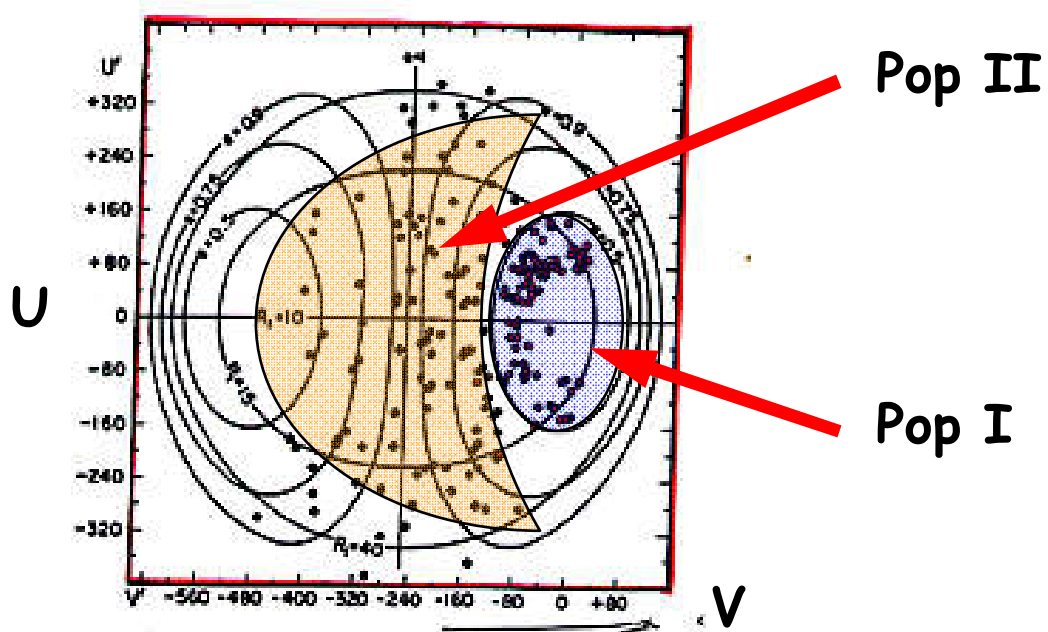
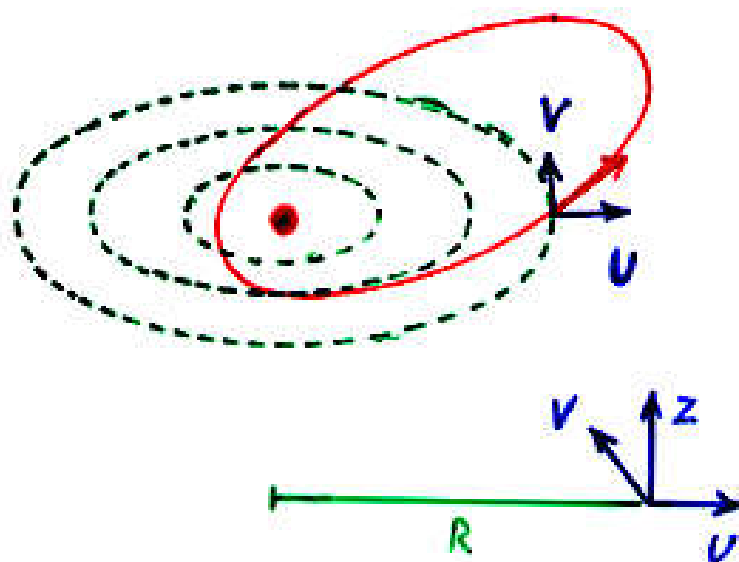
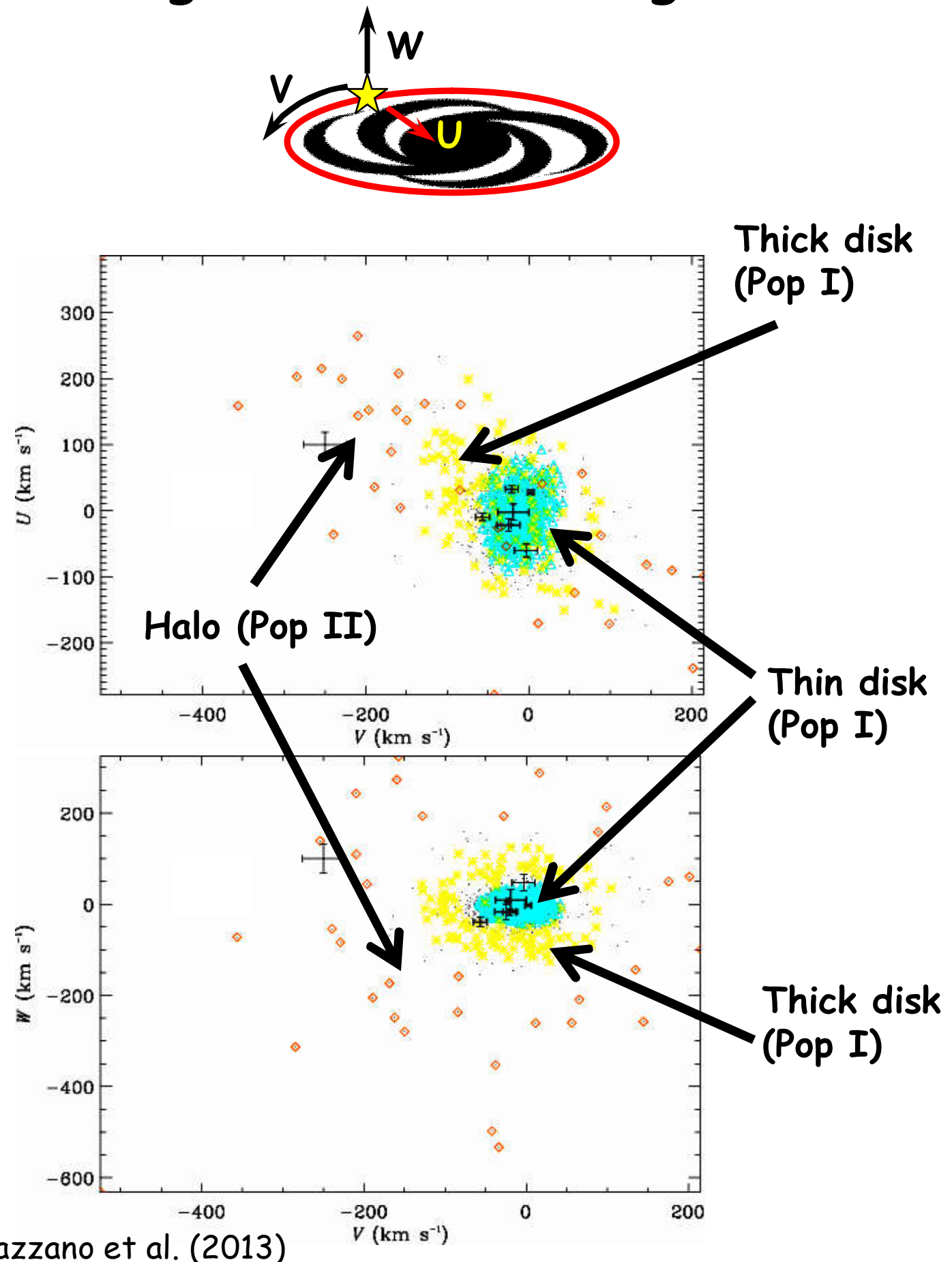


Fig. 23.10: Diagramma di Bottlinger. Sono riportate le componenti delle velocità galattiche  $U'$  (verso l'anticezentro) e  $V'$  (nel senso della rotazione) relative ai dintorni del sole. Gli assi ortogonali rappresentano le  $U$  e  $V$  assolute. Per ogni curva è data l'eccentricità orbitale  $e$  e la distanza apogalattica  $R_i$  in kpc. Nel capitolo 27 diremo sulle stelle (segnate con \*) avendo un eccesso nell'ultravioletto  $\delta(U-B) > +0n.16$ , cioè le stelle povere di metalli della popolazione II di «halo». Queste sono, incidentalmente, stelle veloci con grande velocità spaziale. Con  $\circ$  sono segnate le stelle con  $\delta(U-B) < +0n.16$ , le quali costituiscono una transizione dalla popolazione II di halo alla popolazione del disco galattico, con orbite meno eccentriche (secondo O. J. Eddington).



# Il Diagramma di Bottlinger - 2



# La struttura verticale del disco

SANDAGE (1982)

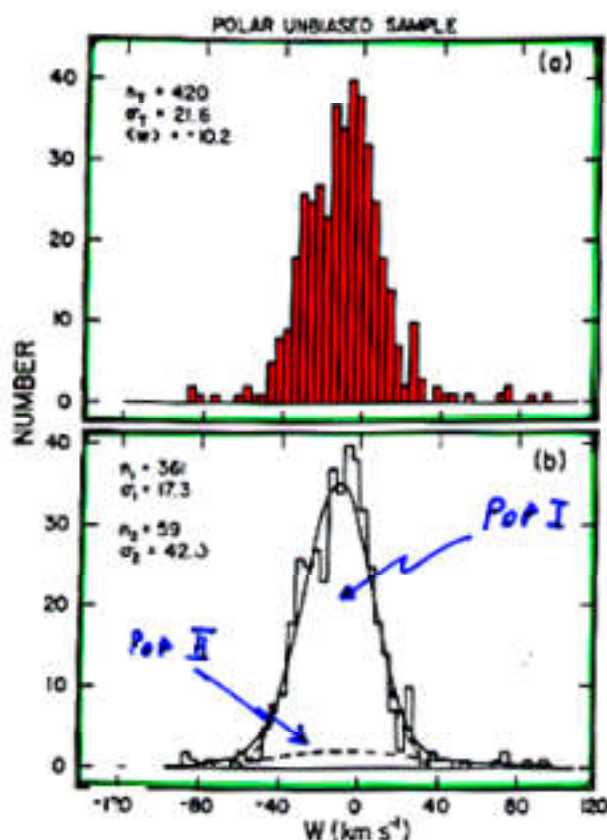


FIG. 2. (Top) Distribution of  $W$  velocities from Table VI for the 420-star sample, binned in  $4 \text{ km s}^{-1}$  intervals. (Bottom) Two-Gaussian fit to the observed distribution. The  $(W)_1$  and  $\sigma_1$  values for the high-velocity component have been assumed.

SANDAGE & FOUTS  
(1987)

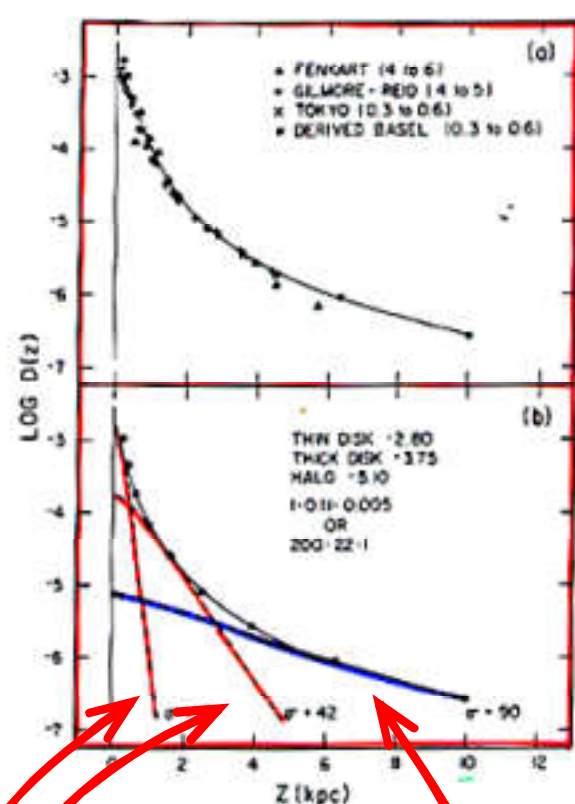


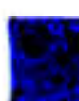
FIG. 2. (Top) The density  $D(z)$  perpendicular to the galactic plane for the four data sets listed in Table II, III, and V. (Bottom) Decomposition of the observed  $\log D(z)$  function into three components using the calculated densities shown in Fig. 1.

HALO

1

THICK DISK 22

THIN DISK 200



$\rho/\rho_{\text{HALO}}$

# Le orbite delle Pop I e Pop II

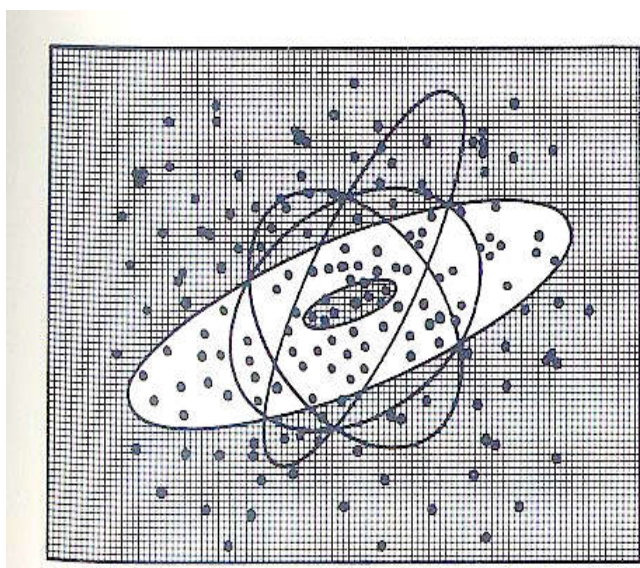


Fig. 11 Schema della costituzione della Galassia. Sono indicate alcune tipiche orbite delle stelle e degli ammassi dell'alone.

Castellani (1986)

# Thick & Thin disk: The G-dwarf problem

TWAROG (1980)

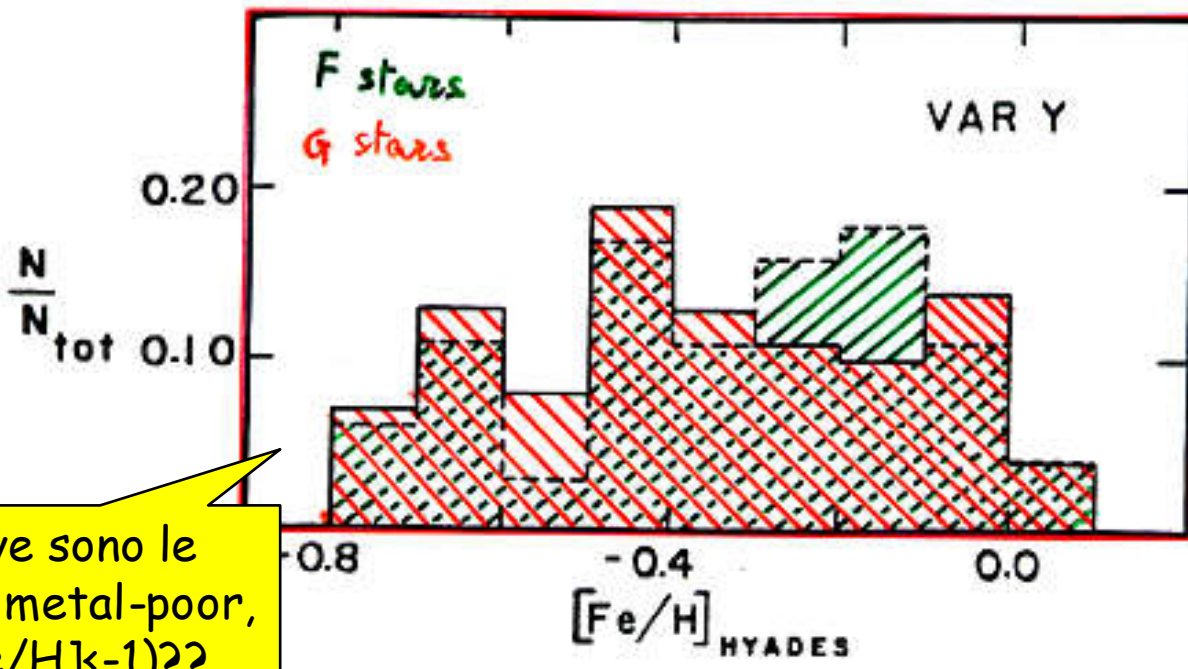
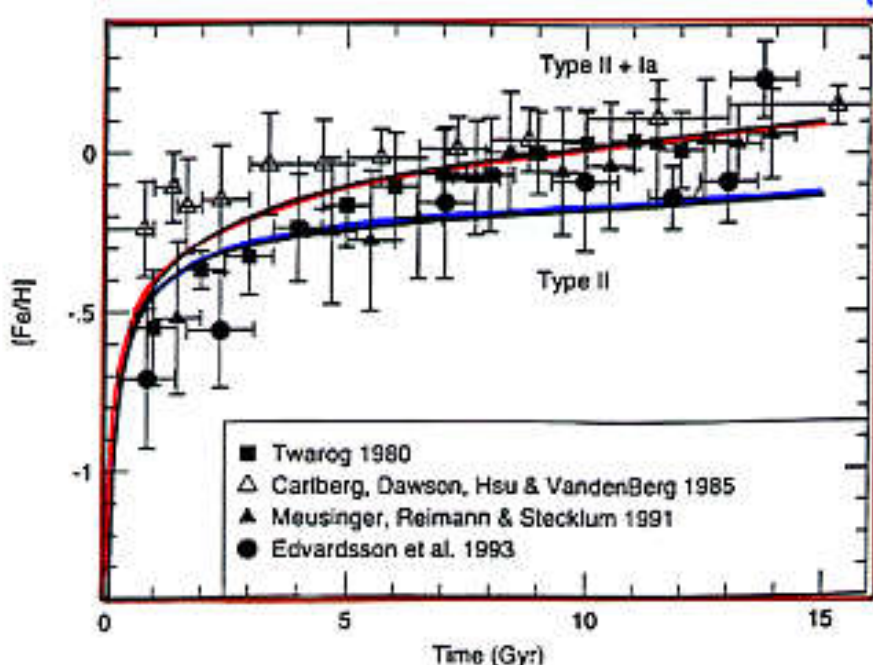


FIG. 8.—F dwarf metallicity distribution (*dashed line*) including corrections for stellar evolution and scale height effects which produce a constant SFR compared to the G dwarfs (*solid line*).

TIMMES et al. (1995)



# Thick & Thin disk e SFR

PARI & FERRINI (1994)

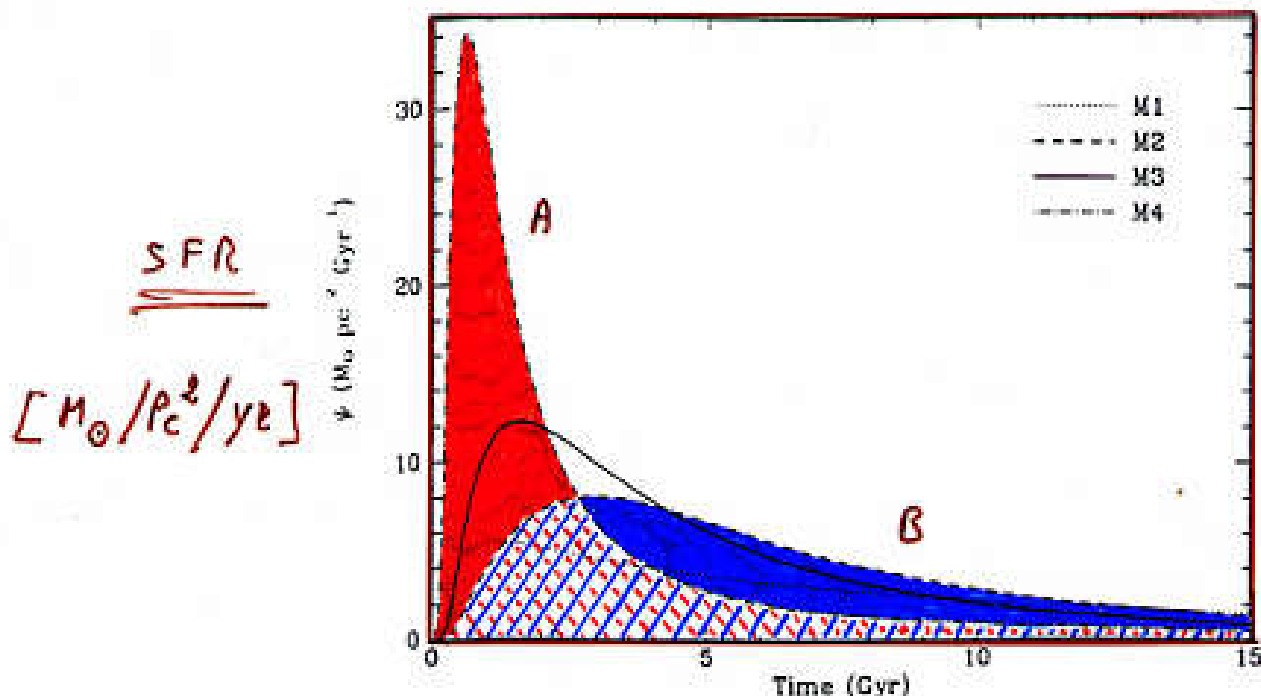


FIG. 3.—SF rate vs. time (M1–M4)

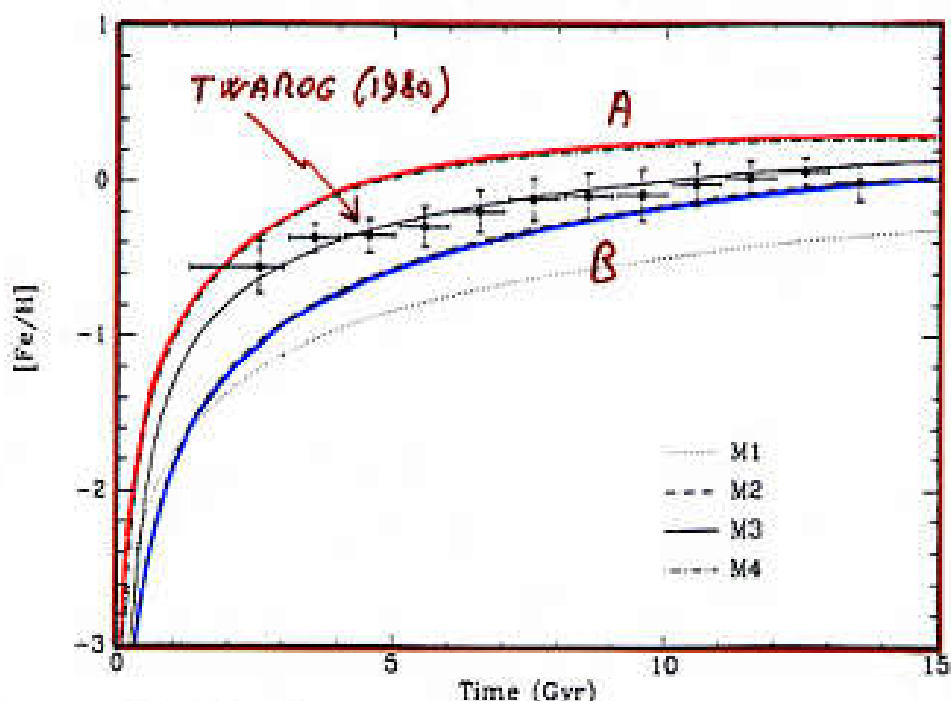
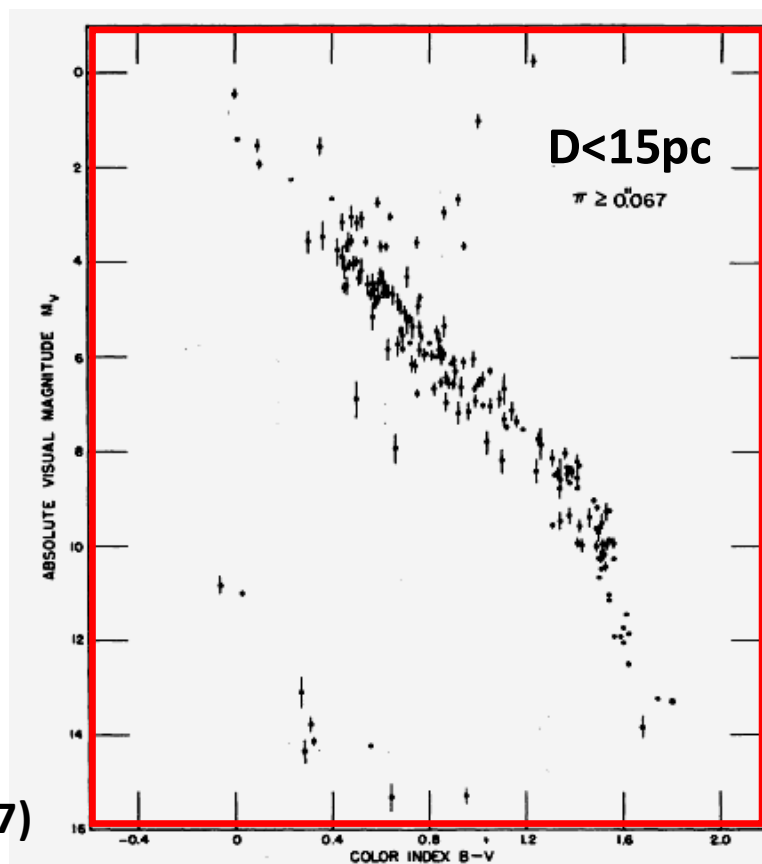
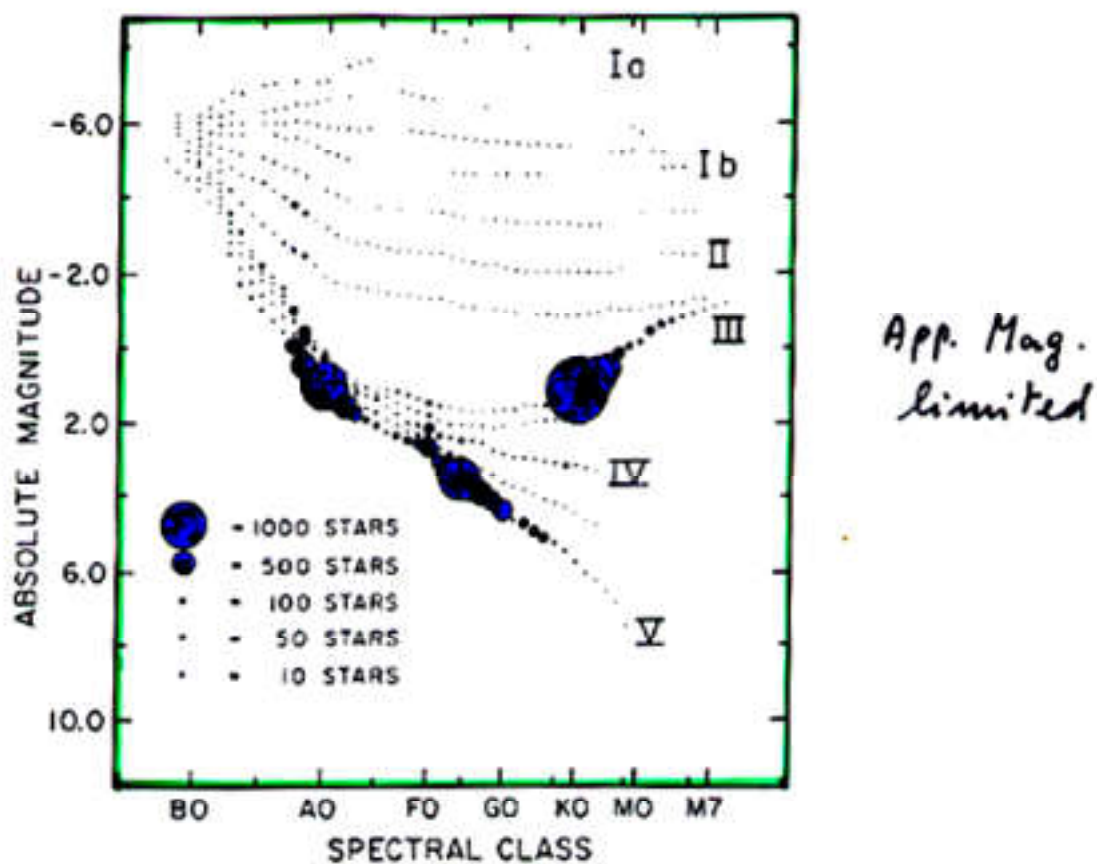


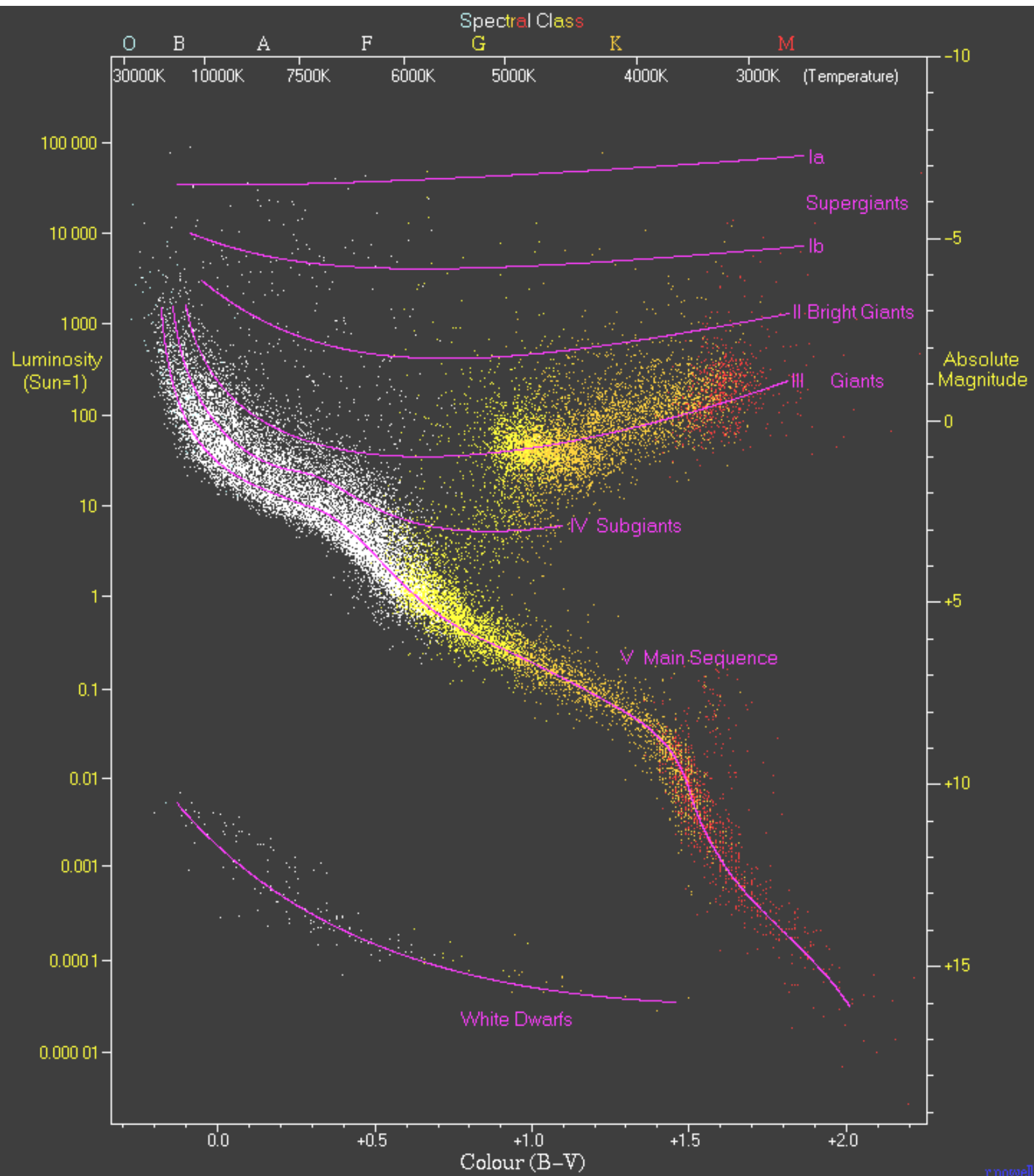
FIG. 4.—[Fe/H] vs. time for the same models of Fig. 3, superposed on data of Twarog (1980).

# I conteggi stellari e la determinazione della IMF

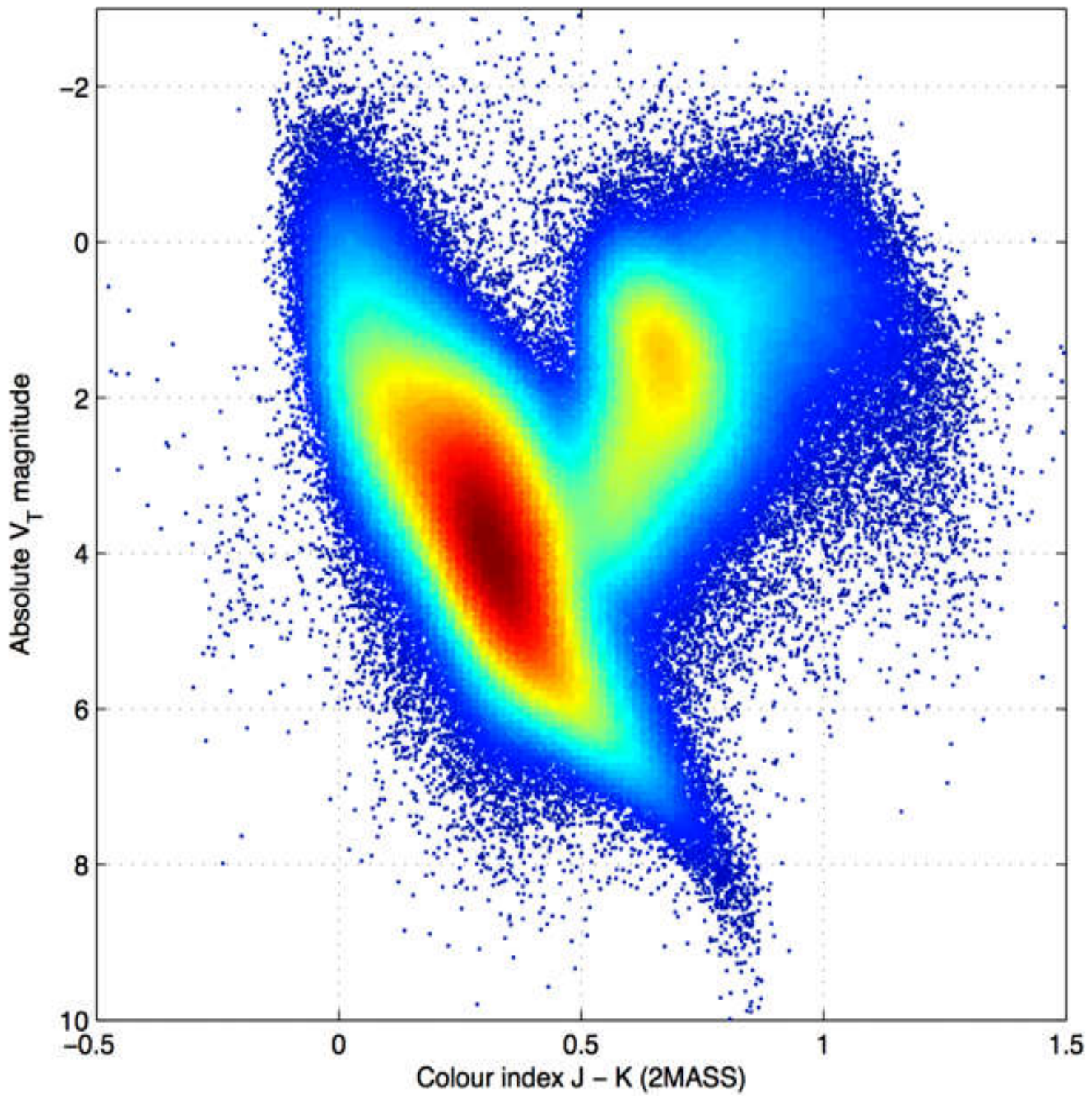


Sandage (1957)

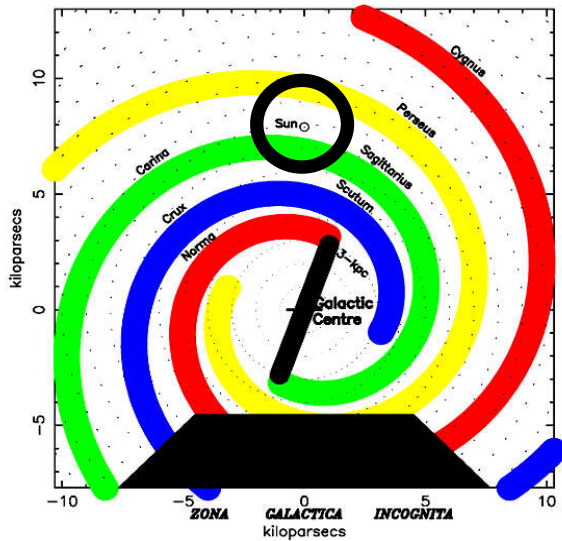
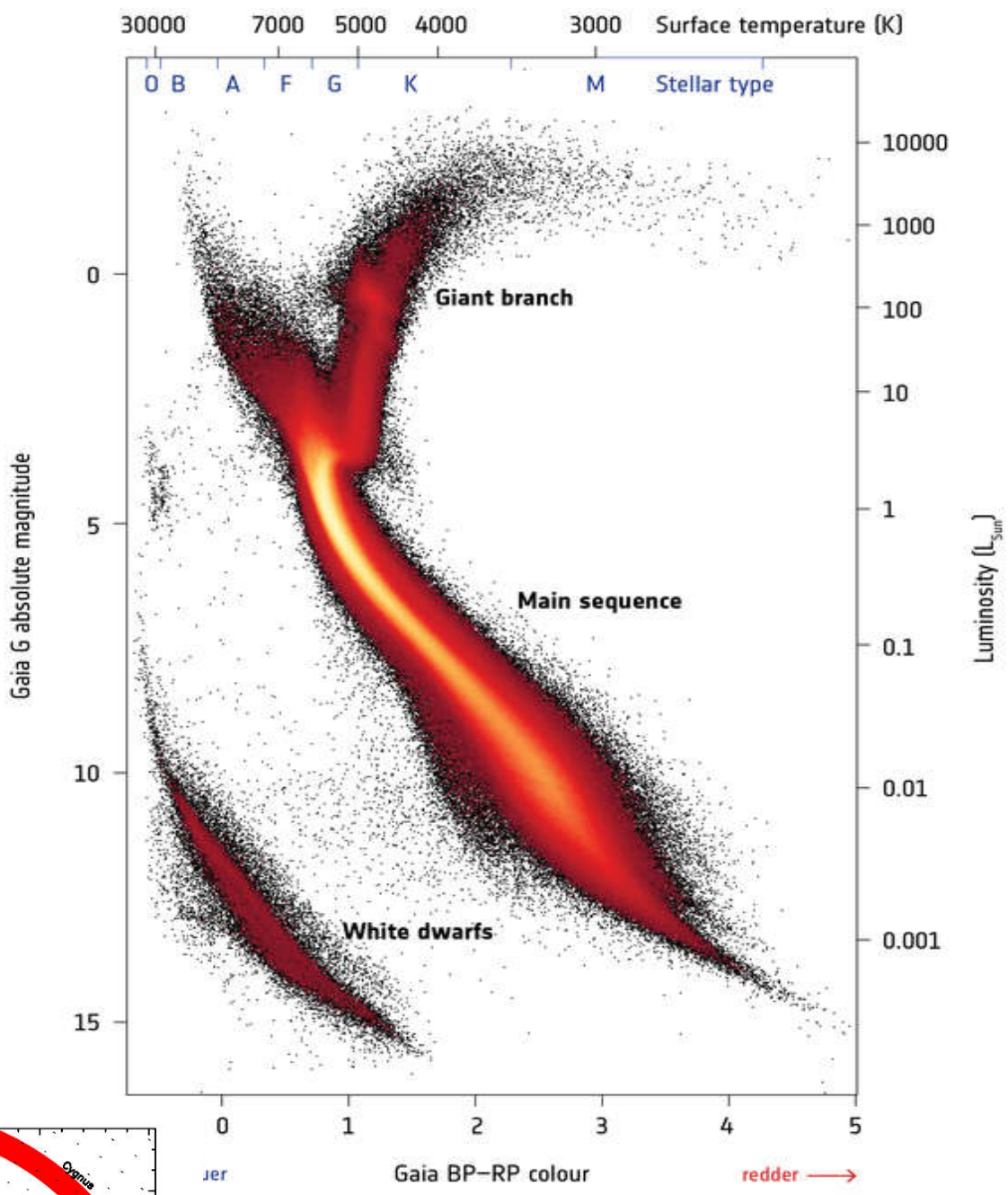
# Hipparcos (1993) (22,000 stars)



# GAIA'S FIRST H-R DIAGRAM ( $\sim 10^6$ stars) (1<sup>st</sup> data release: 2015)



→ GAIA'S HERTZSPRUNG-RUSSELL DIAGRAM  
 2<sup>nd</sup> data release (2018)  
 (~4 10<sup>6</sup> stars < 1.5 kpc)



<http://sci.esa.int/gaia/60198-gaia-hertzsprung-russell-diagram/>

# Il diagramma di Hess

Figure 5.2. Schematic Hess diagram for stars in our neighborhood. Numbers of stars per cubic parsec are shown by contours which refer to 20, 200, 2000, and 20,000 stars. The main sequence runs along the ridge. Probably the peak is reached at about the bottom right corner of the diagram, with about 40,000 stars per cubic parsec. Statistics for fainter stars do not permit us to say how fast the slope falls off from there. The contours for white dwarfs are not shown; these stars populate a moderately high ridge, roughly parallel to the main ridge and separated from it by a deep valley.

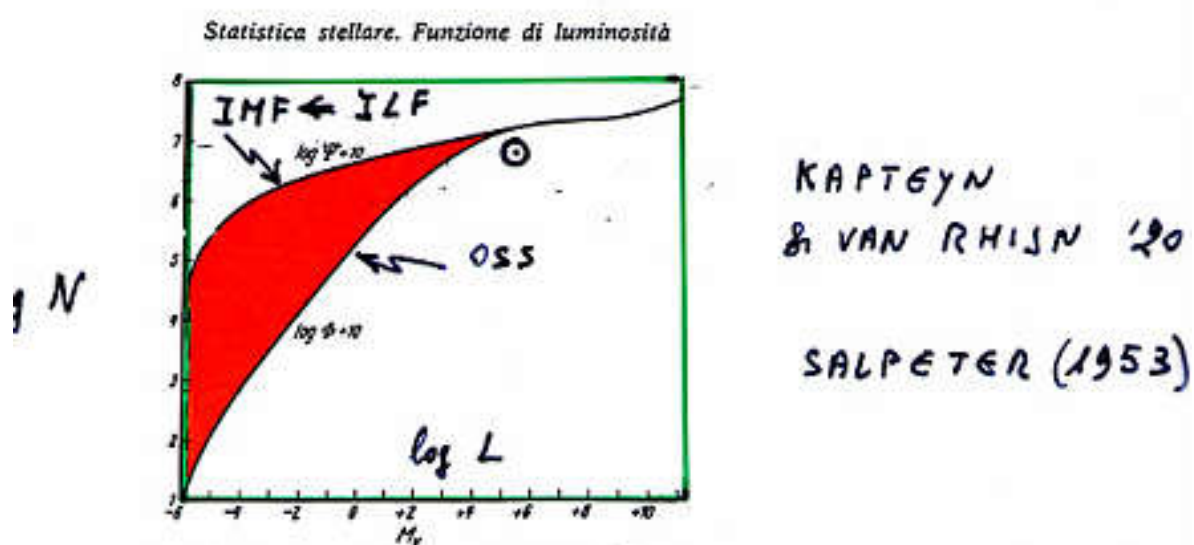
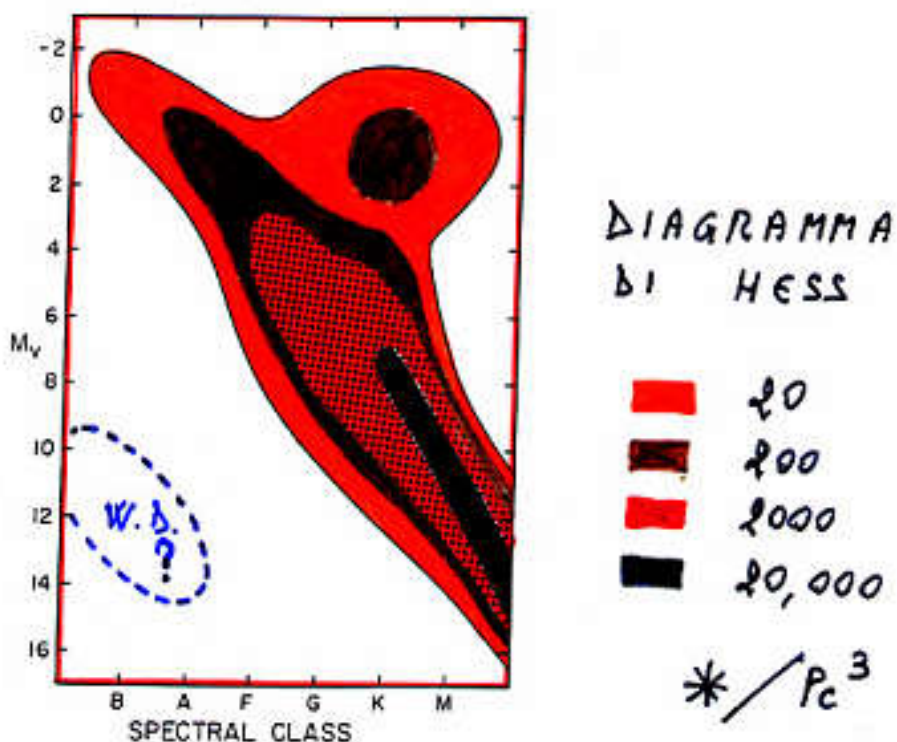


Fig. 26.8: Funzione di luminosità  $\Phi(M_V)$  e funzione iniziale di luminosità  $\Psi(M_V)$ , per stelle della sequenza principale nei dintorni del sole. La  $\Phi$  e la  $\Psi$  danno rispettivamente il numero osservato di stelle per  $\text{pc}^3$  comprese fra  $M_V - 1/4$  ed  $M_V + 1/4$ , e di quelle formatesi a partire dalla formazione della Galassia.

# La IMF

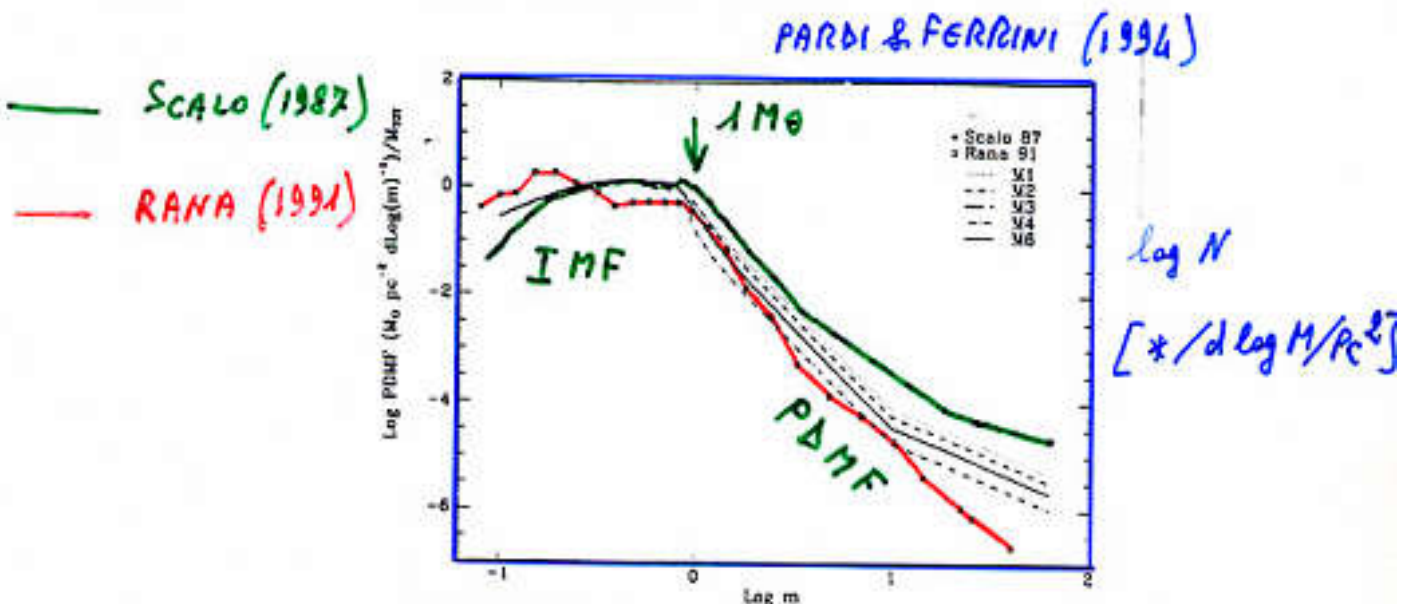
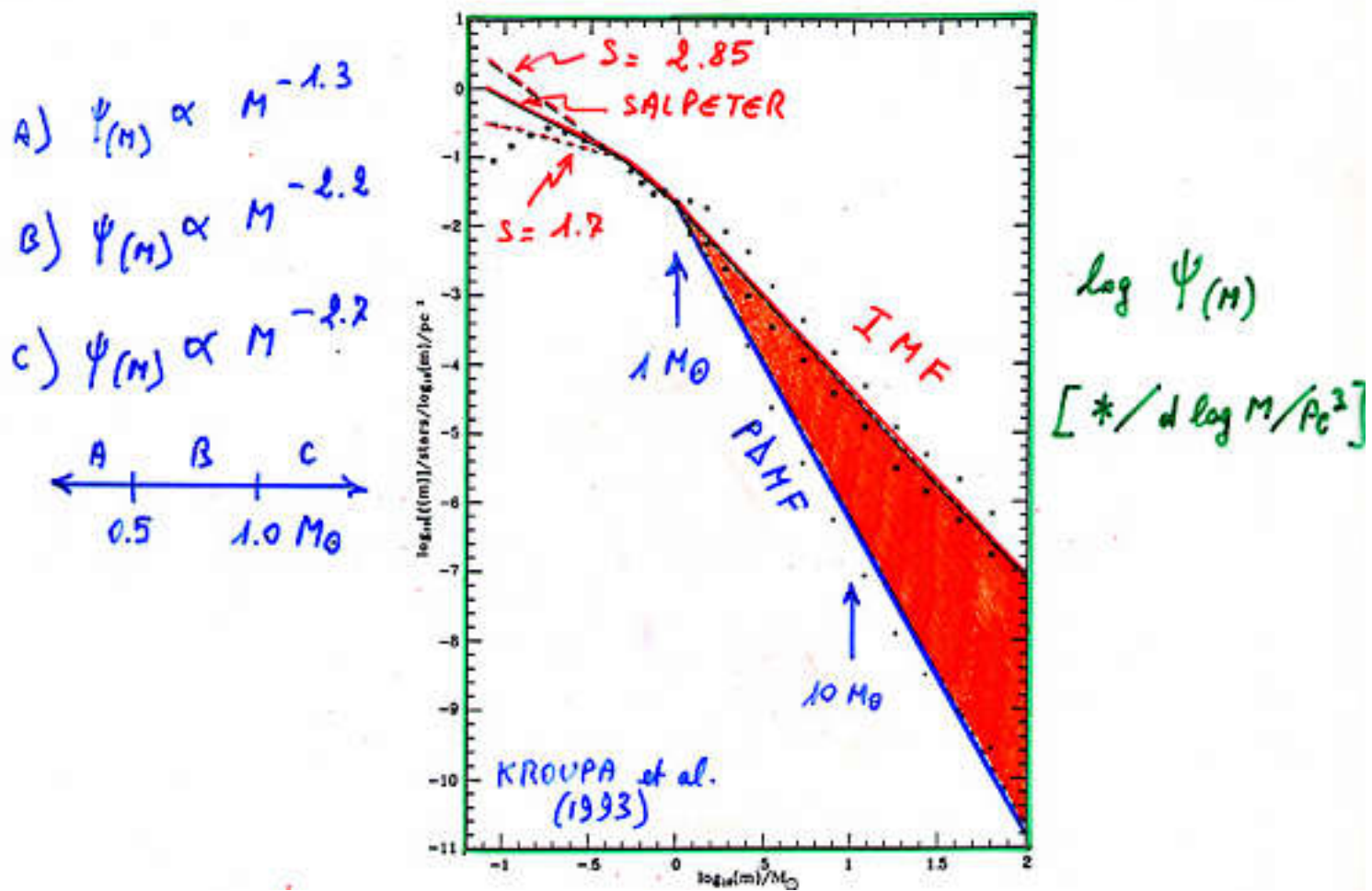


FIG. 12.—PDMFs predicted by the model in cases M1–M4 and M6 superposed on data of Scalo (1987 [triangles]) and Rana (1991 [squares]).



**Articoli consigliati (vedi Webpage):**

<http://www.bo.astro.it/~eps/lezioni/lezioni.html>

- Energetic & Chemical evolution of Spirals (Buzzoni 2011)
- Milky Way mass (Licquia 2015)
- Milky Way mass profile (Taylor 2016)
- MW Disk (Sandage 1987)
- MW thin disk & Bottlinger Diagrams (Gazzano et al. 2013)
- Lindblad orbits (Struck 2015)
- Galaxy Colors (Buzzoni 2005)
- Galaxy mass assembly (Pan 2015)
- IMF (Miller & Scalo 1979)
- IMF (Kroupa et al. 1993)
- IMF (Kalirai et al. 2013)

# Teoria delle Popolazioni Stellari Semplici (SSPs)

Renzini & Buzzoni (1986)

Definition of SSP:

- 1) A generation of COEVAL stars ( $SFR = \delta_0$ )  
(so that we can define an AGE)  
of the population
- 2) Fixed metallicity (unique  $Z$ )

Star partition:

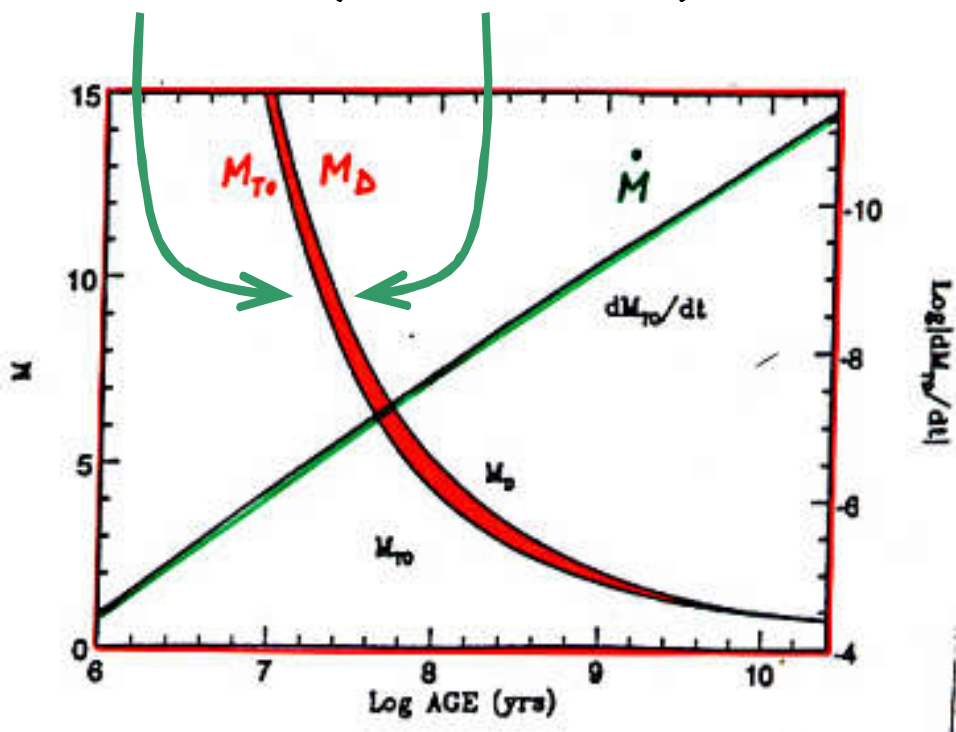
$$MS: \quad N_{(H)} = A M^{-S} \quad (IMF)$$

Post-MS:

$$\Delta M = M_{DYING} - M_{TO} \approx - \frac{dM}{dt} \Big|_{\tau_{PMS}} \approx M_{TO} \frac{\tau_{PMS}}{\tau}$$

$$N_{PMS} = A M_{TO}^{-S} \Delta M = A M_{TO}^{-S} \dot{M}_{TO} \tau_{PMS}$$

Massa al  
Turn Off      Massa finale  
(Nane Bianche)



Renzini & Buzzoni  
(1986)      Flusso evolutivo specifico

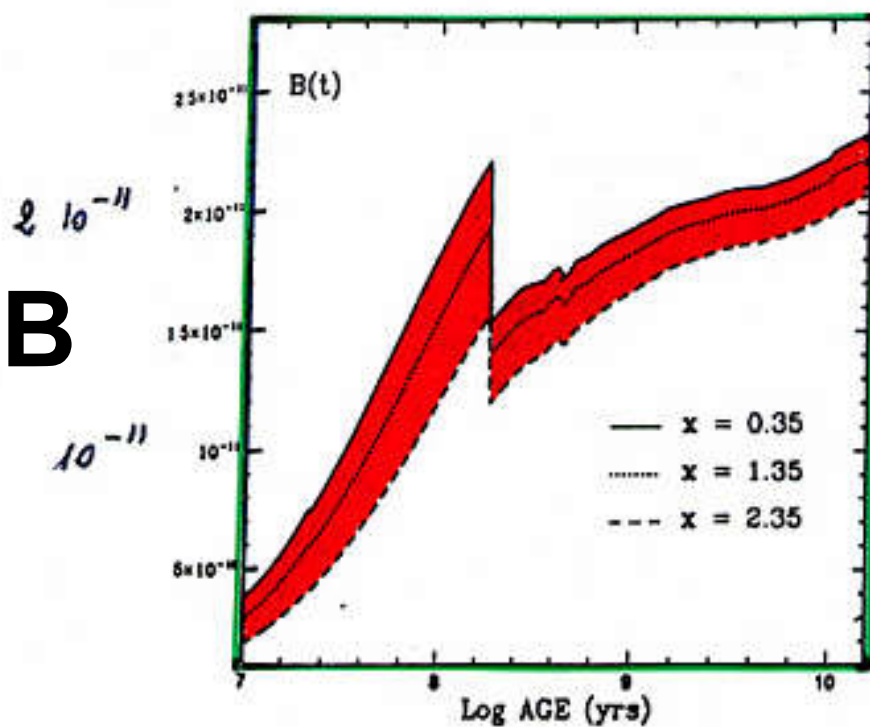


Fig. 1.3: The specific evolutionary flux  $B(t)$  as a function of age for three IMF slopes  $(1+z)$ .

**B** =  $(b/L_{\text{tot}})$

$$N_{\text{PMS}} = \underbrace{A M_{\text{TO}}^{-s} \dot{M}}_{\text{L}} \tau_{\text{PMS}}$$

$$\text{L} = \beta L_{\text{TOT}}$$

$$N_{\text{PMS}} = \beta L_{\text{TOT}} \tau_{\text{PMS}} = 1.7 \cdot 10^{11} \left( \frac{L}{L_0} \right) \left( \frac{\tau}{\text{yr}} \right)$$

↓  
specific Evolutionary  
Flux

## LUMINOSITY

$$L_{\text{MS}} = A \int_0^{\text{TO}} l_* M^{-s} dM \quad \begin{cases} l_* \propto M^3 \\ t_* \propto M^{-2} \end{cases}$$

$$L_{\text{MS}} \approx \frac{A}{4-s} M_{\text{TO}}^{4-s} \quad (s < 4)$$

$$L_{\text{MS}} \propto t^{-\frac{4-s}{2}} \sim t^{-0.85}$$

$$L_{\text{PMS}} = \int_{\text{PMS}} l_* dN = A M_{\text{TO}}^{-s} \dot{M}_{\text{TO}} \underbrace{\int_{\text{PMS}} l_* d\tau}_{\text{Fuel} \sim \text{const.}}$$

$$L_{\text{PMS}} \propto t^{-\frac{3-s}{2}} \sim t^{-0.35}$$

$$\frac{L_{\text{PHS}}}{L_{\text{HS}}} \propto \frac{t^{-\frac{3-s}{2}}}{t^{-\frac{4-s}{2}}} \propto \sqrt{t}$$

Conclusion: MS always dominates with decreasing time

Corollary: Total SSP luminosity is a DECREASING function of time

Model evolutionary rate at different bands

$$L_{\text{BOL}} \propto t^{-0.75}$$

$$z = z_0$$

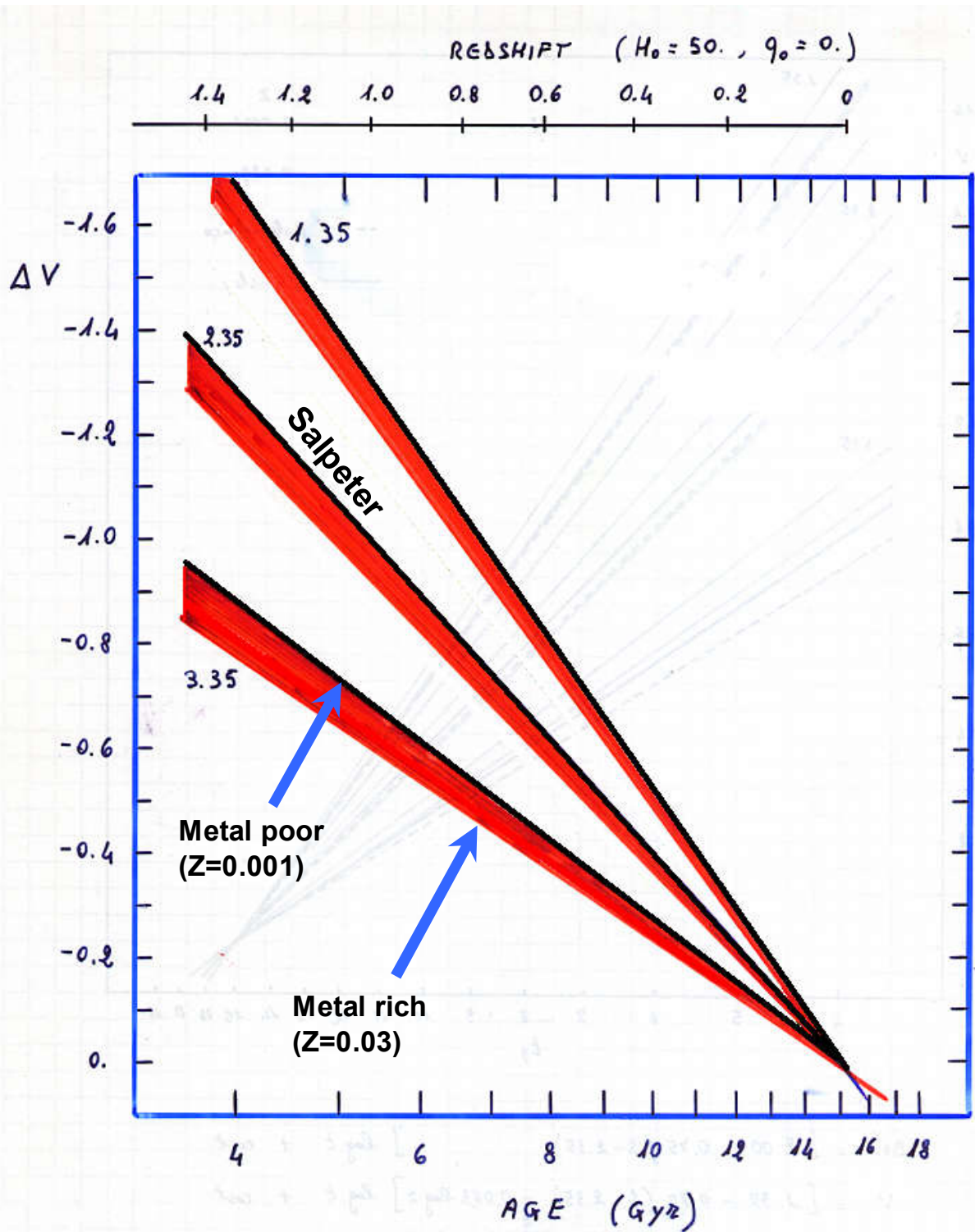
$$s = 2.35$$

$$L_B \propto t^{-0.95}$$

$$L_V \propto t^{-0.86}$$

$$L_I \propto t^{-0.75}$$

$$L_K \propto t^{-0.71}$$



$$t \propto \frac{1}{M^2} \frac{\tilde{k}}{\mu^4}$$

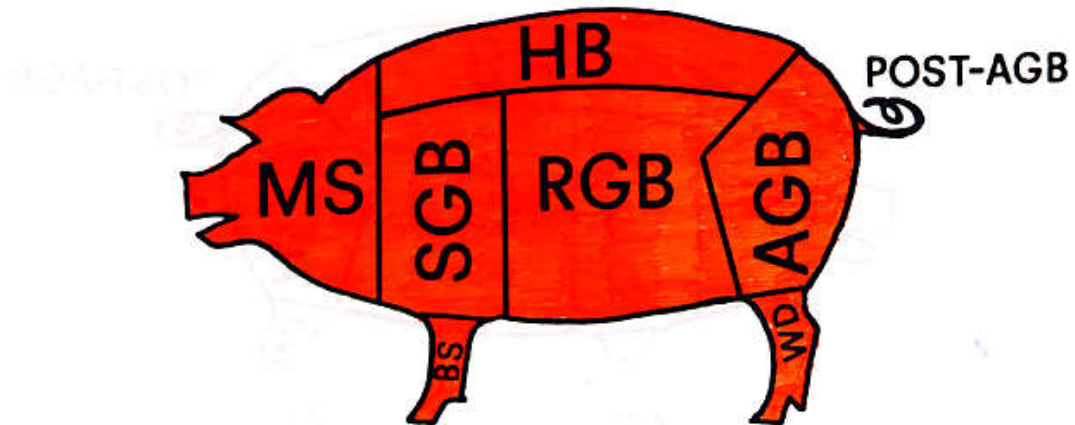
$$\rightarrow \frac{dt}{t} = -\frac{2}{3} \frac{dL_*}{L_*} + \frac{1}{3} \frac{d\tilde{k}}{\tilde{k}} - \frac{4}{3} \frac{d\mu}{\mu}$$

$$L_* \propto M^3 \frac{\mu^4}{\tilde{k}}$$

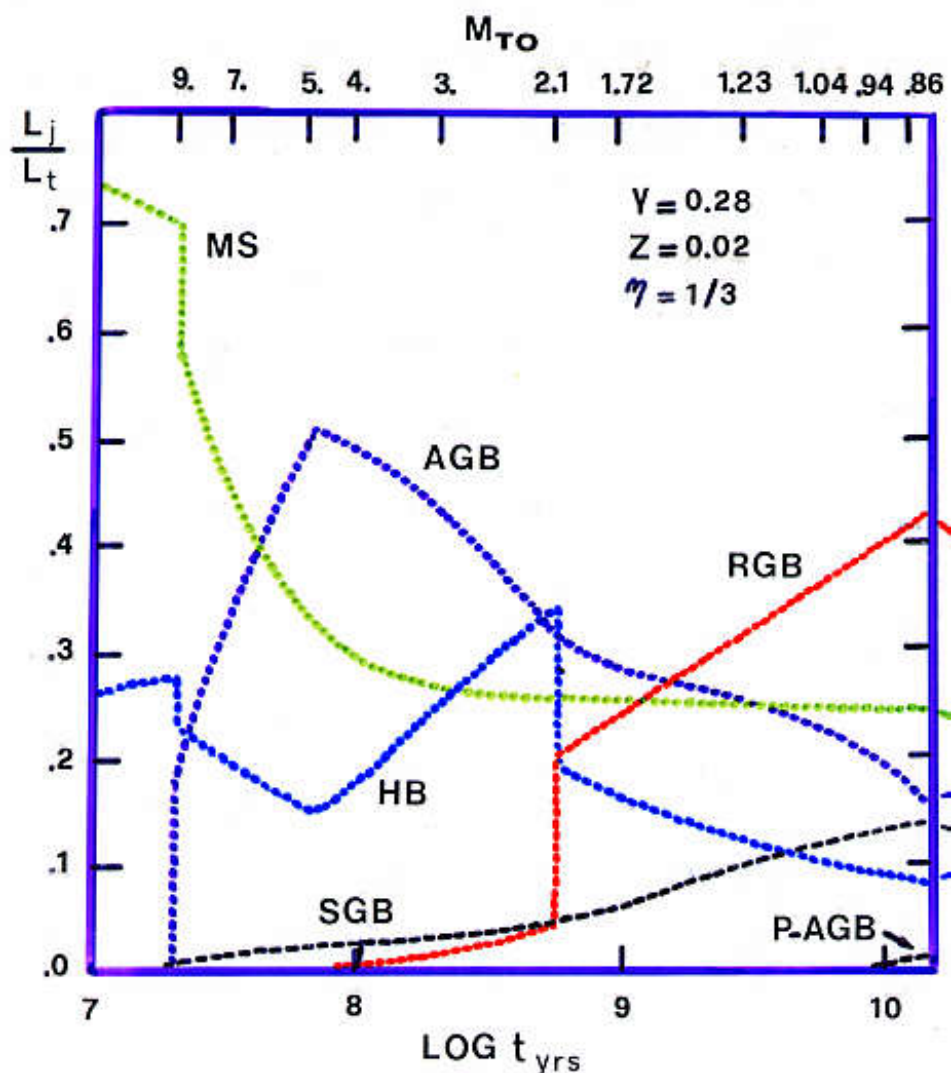
Quindi, la stessa variazione di luminosità  $dL/L$ , avviene su tempi più lunghi ( $dt/t$ ) se  $k$  (ovvero se  $Z$  )

# SSP

## Contributi bolometrici



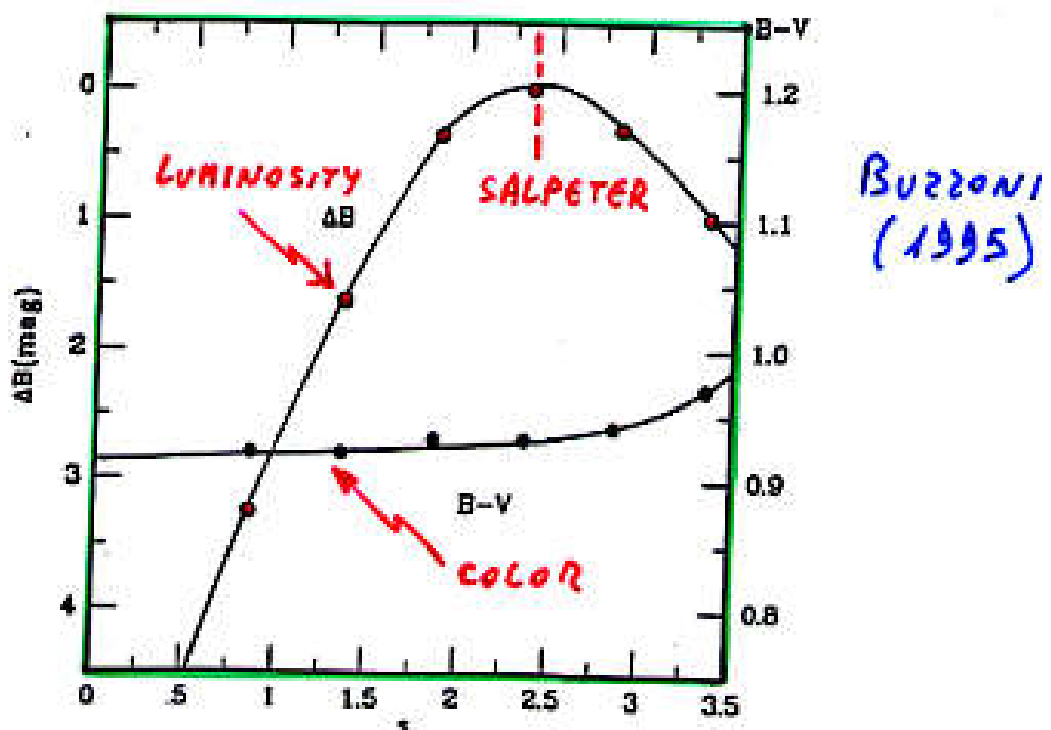
*All the cuts of a stellar population.*



Renzini & Buzzoni (1986)

# IMF e Luminosita' totale

Una IMF alla Salpeter permette alla SSP di rilasciare la max luminosita' per unita' di massa



$$M_{\text{TOT}} = A \int M M^{-s} = \frac{A}{s-1} [M_v^{s-1} - M_l^{s-1}]$$

$s > 1$  DWARF - DOMINATED SSP

$s < 1$  GIANT - DOMINATED SSP

Una IMF alla Salpeter permette alla SSP di rilasciare la max luminosità per unità di massa:  
**DIMOSTRAZIONE**

$$L_{\text{tot}} \propto A M^* M_{\text{TO}}^{-S} \quad \text{solo "A" e } M_{\text{TO}}^{-S} \text{ dipendono da "s"}$$

$$M_{\text{TOT}} = A \int M_*^{-S} M_* dM_* = \frac{A}{2-S} \left[ M_*^{2-S} \right]_{\text{low}}^{\text{up}}$$

Assumiamo  $S > 2$  e vediamo se esiste soluzione all'interno di questo dominio

$$\forall S > 2 \quad A = \frac{M_{\text{TOT}}(2-S)}{M_{\text{low}}^{2-S}}$$

$$L_{\text{tot}} \propto \frac{M_{\text{TOT}}(2-S)}{M_{\text{low}}^2} \left( \frac{M_{\text{TO}}}{M_{\text{low}}} \right)^{-S}$$

(non dipende da "s")

$$\left( \frac{L}{M} \right) \propto \frac{1}{M_{\text{low}}} (2-S) \left( \frac{M_{\text{TO}}}{M_{\text{low}}} \right)^{-S}$$

$$\frac{\partial \left( \frac{L}{M} \right)}{\partial S} = 0 \Rightarrow -1 \left( \frac{M_{\text{TO}}}{M_{\text{low}}} \right)^{-S} = (2-S) \ln \left( \frac{M_{\text{TO}}}{M_{\text{low}}} \right) \left( \frac{M_{\text{TO}}}{M_{\text{low}}} \right)^{-S}$$

$$2-S_{\text{MAX}} = \frac{1}{\ln \left( \frac{M_{\text{low}}}{M_{\text{TO}}} \right)}$$

$$S_{\text{MAX}} = 2 - \frac{1}{\ln \left( \frac{M_{\text{low}}}{M_{\text{TO}}} \right)}$$

$$M_{\text{low}} \sim 0.1 M_{\odot}$$

$$\forall M_{\text{TO}} \rightarrow 0.01 \lesssim \frac{M_{\text{low}}}{M_{\text{TO}}} \lesssim 0.1$$

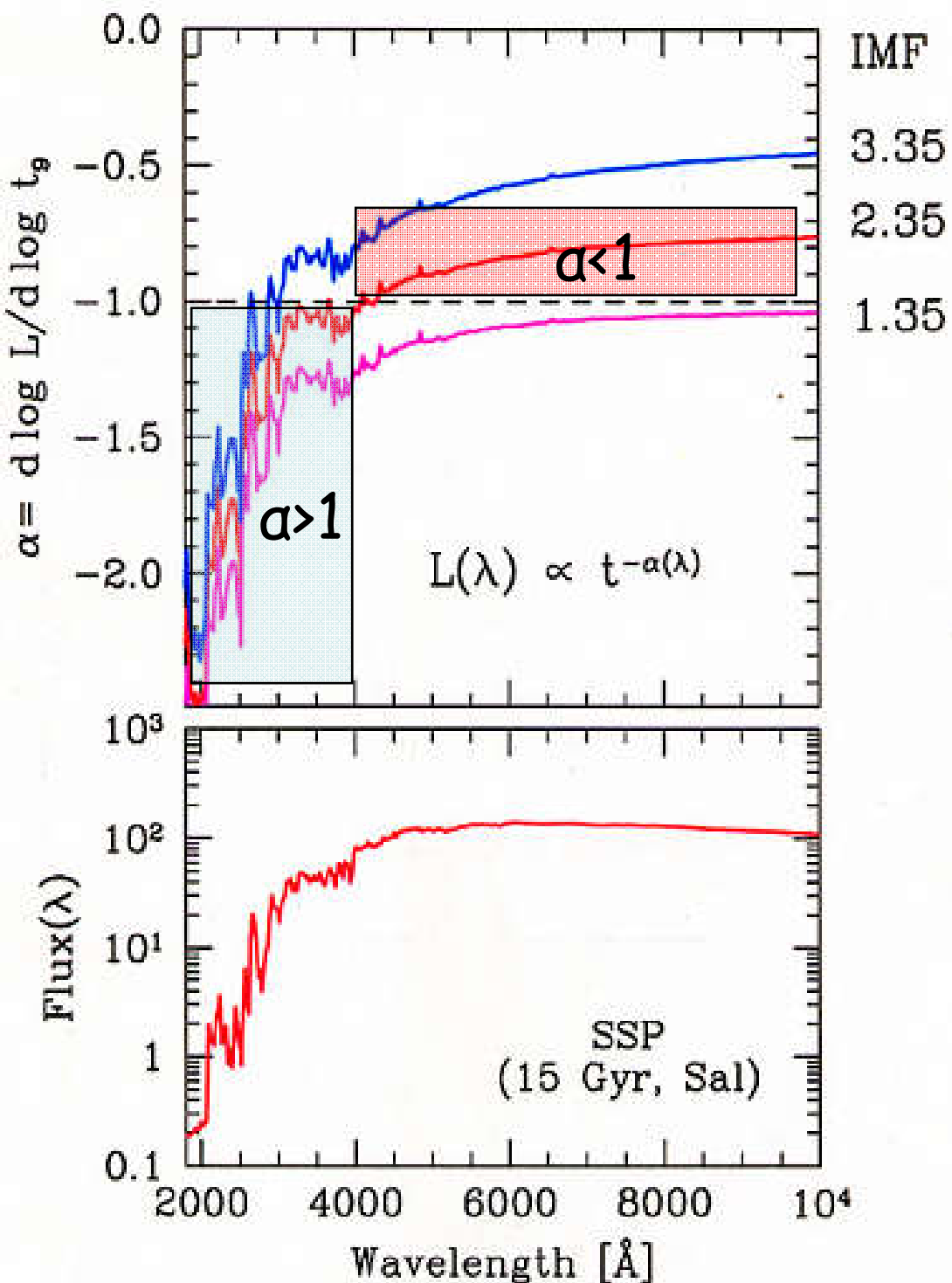
$$2.2 \lesssim S_{\text{MAX}} \lesssim 2.4$$

## **Articoli consigliati (vedi Webpage):**

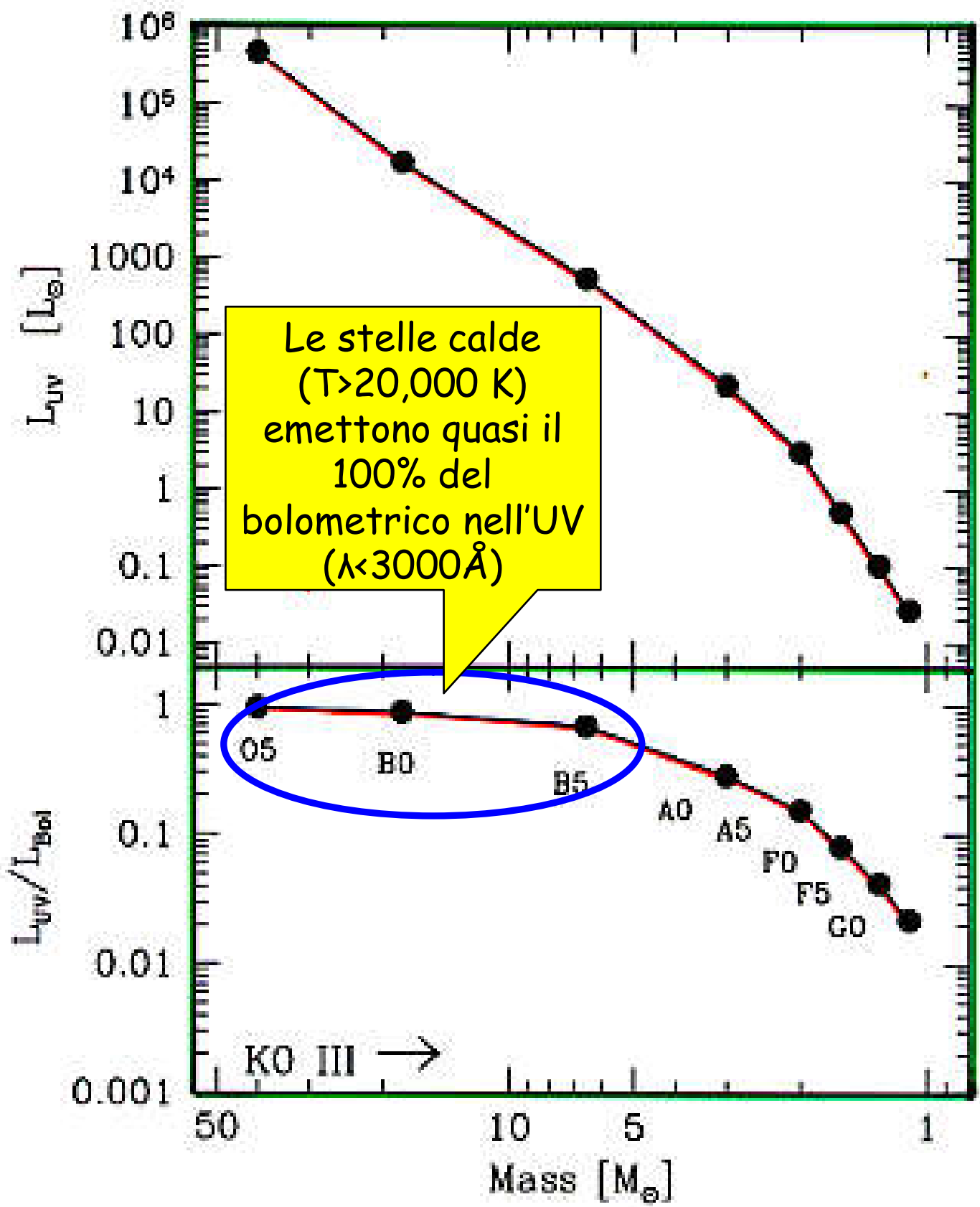
<http://www.bo.astro.it/~eps/lezioni/lezioni.html>

- **SSP Theory (Renzini & Buzzoni 1986)**
- **Energetic & Chemical evolution of Spirals (Buzzoni 2011)**
- **IMF (Miller & Scalo 1979)**
- **IMF (Kroupa et al. 1993)**
- **IMF (Kalirai et al. 2013)**

# Evoluzione fotometrica delle SSP: dal bolometrico al monocromatico



L'evoluzione fotometrica delle SSPs nell'UV avviene più veloce di  $t^{-1}$  !! Dunque, in una CSP, l'UV traccia la SFR recente.

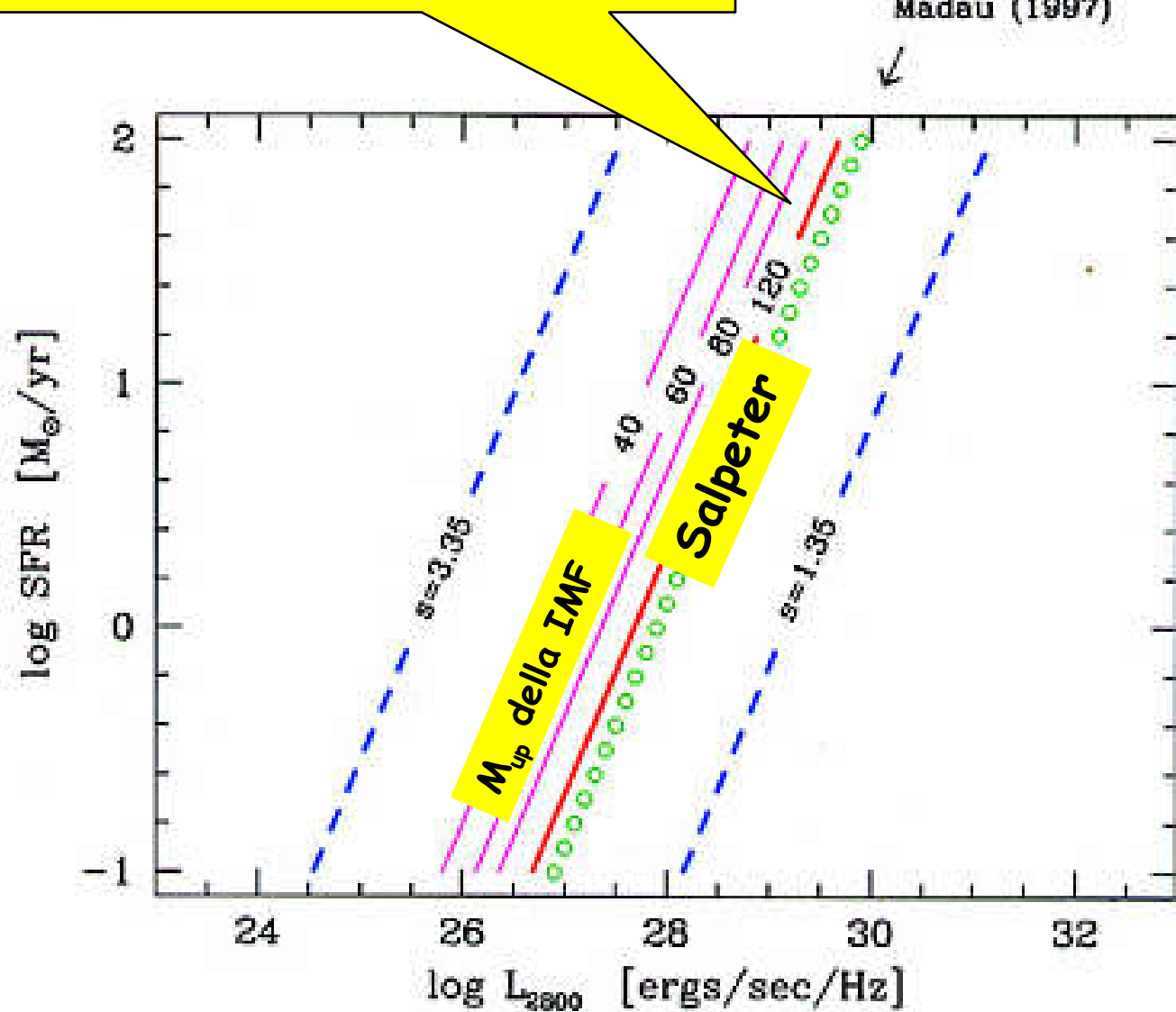


Buzzoni (2002)

$L_{\text{UV}}$   $\rightarrow$  SFR

Deve esserci corrispondenza  
lineare fra  $L_{\text{UV}}$  e SFR

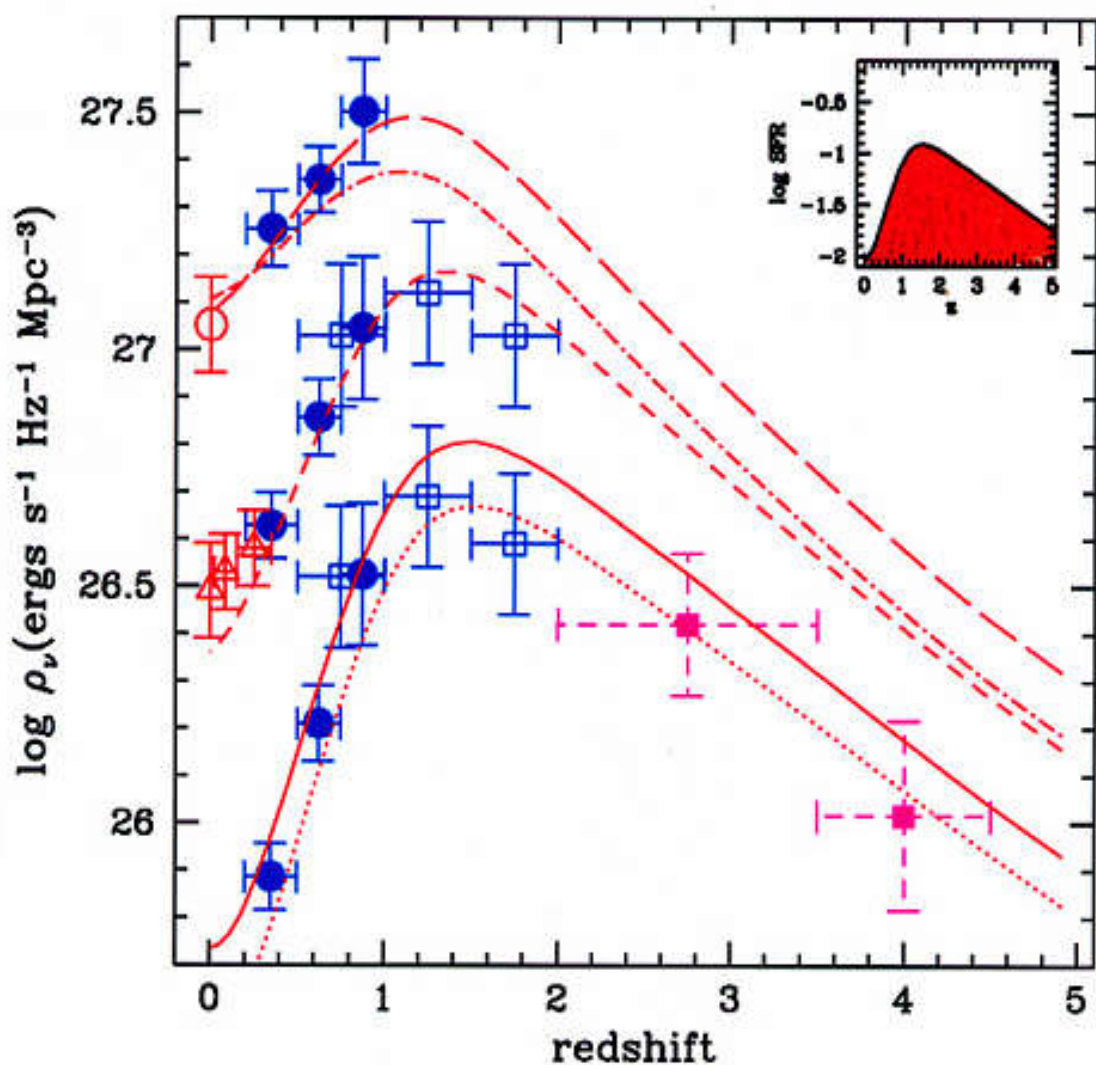
Madau (1997)



(Buzzoni 2002)

# Il "Madau Plot" e la Storia della Formazione Stellare Cosmica

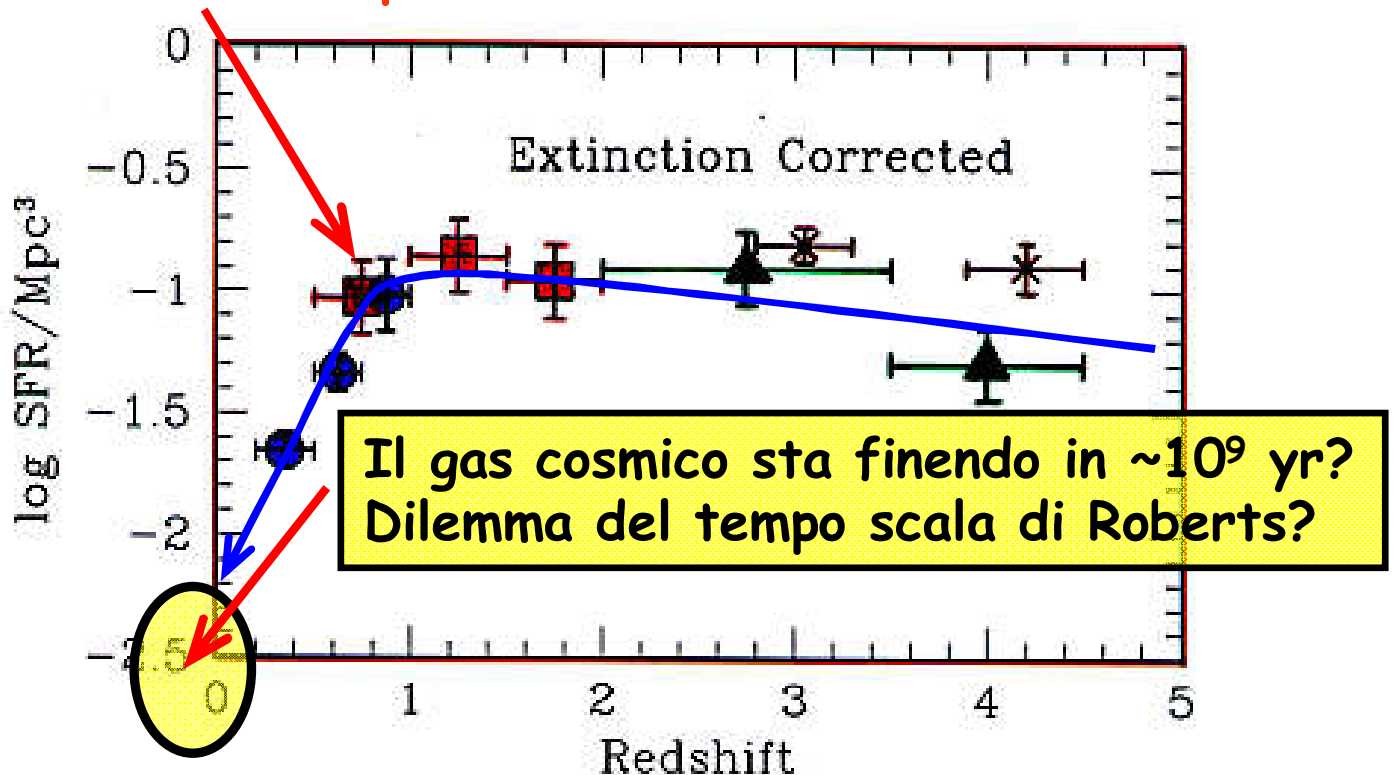
(Madau 1997)



# Evoluzione del Madau plot

(includendo incompletezza, assorbimento polveri etc.)

Cosa e' successo qui?

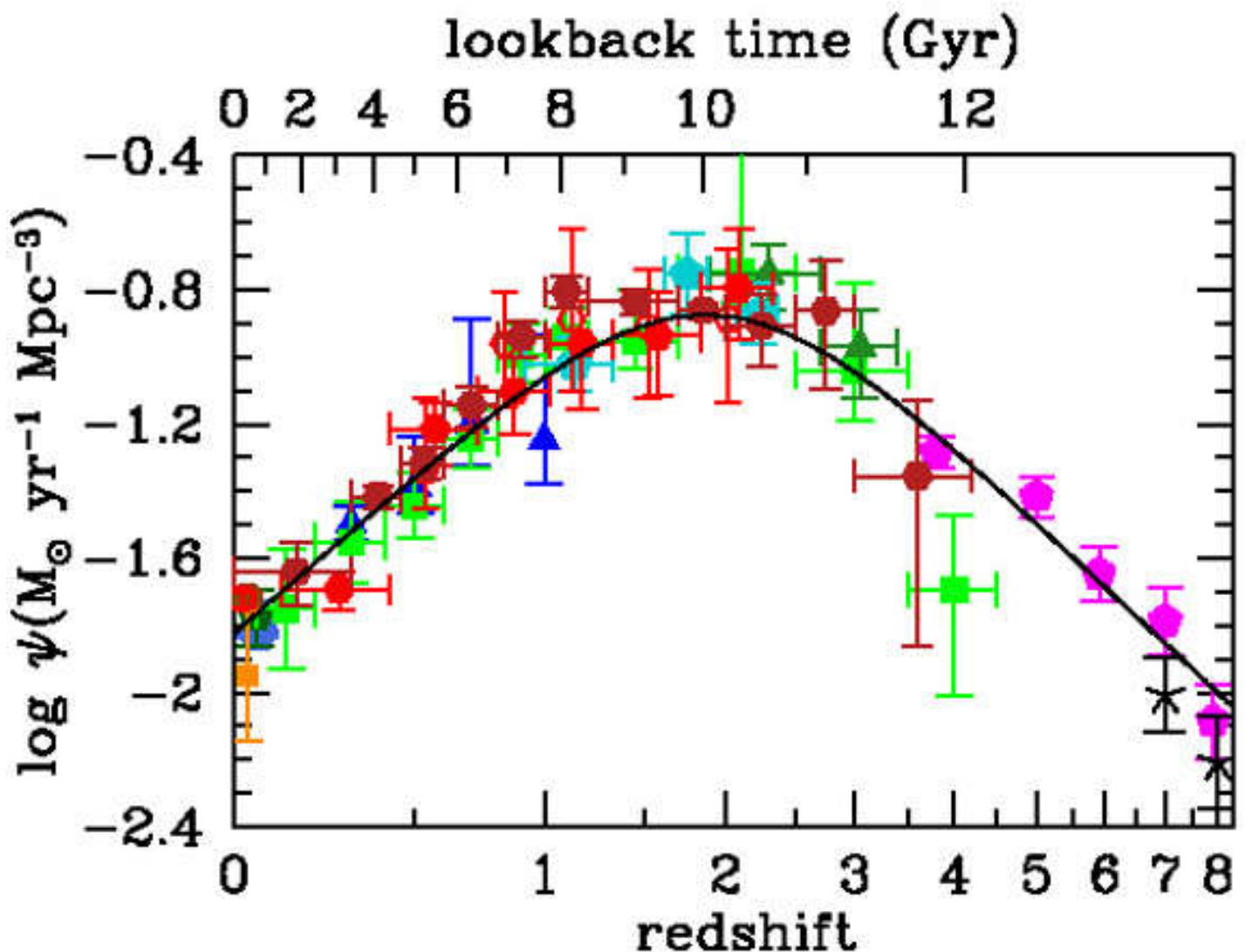


$$(H_0, q_0) = (50, \frac{1}{2})$$

Tempo di Roberts:  $t_R \sim \frac{f_{gas} M_{gal}}{SFR_{now}}$  ma (vedi dopo)  $b = \frac{SFR_{now}}{M_{gal}} t_{gal}$

Combinandole:  $\frac{t_R}{t_{gal}} = \frac{f_{gas}}{b} \sim \frac{\sim 0.1}{\sim 1}$  Quindi  $t_R \sim 1-2$  Gyr max

# Evoluzione del Madau plot



Madau & Dickinson (2014)

Wyder et al. (2005)	blue-gray hexagon	Bouwens et al. (2012ab)	magenta pentagons
Schiminovich et al. (2005)	blue triangles	Schenker et al. (2013)	black crosses
Robotham & Driver (2011)	dark green pentagon	Sanders et al. (2003)	brown circle
Cucciati et al. (2012)	green squares	Takeuchi et al. (2003)	dark orange square
Dahlen et al. (2007)	turquoise pentagons	Magnelli et al. (2011)	red open hexagons
Reddy & Steidel (2009)	dark green triangles	Magnelli et al. (2013)	red filled hexagons
		Gruppioni et al. (2013)	dark red filled hexagons

**Articoli consigliati (vedi Webpage):**

<http://www.bo.astro.it/~eps/lezioni/lezioni.html>

- **SSP Theory (Renzini & Buzzoni 1986)**
- **UV Upturn (O'Connell 1999)**
- **Dropout galaxies (Madau 1996)**
- **Madau Plot (1997)**
- **Cosmic SFR (Madau & Dickinson (2014)**
- **Galaxy mass assembly (Pan 2015)**

# Teoria delle Popolazioni Stellari Composite (CSPs)

Buzzoni (2005)

Definition:

$$[CSP] = \int [SSP] \otimes SFR$$

A relevant case:  $SFR = \text{const}$

$$\mathcal{L}_{CSP} = \int_0^T L_{SSP} dz$$

$\downarrow$   
 $t^{-\alpha}$       ( $\alpha < 1$ )

$$\mathcal{L}_{CSP} \Big|_T = \frac{T^{1-\alpha}}{1-\alpha}$$

$$\mathcal{L}_{CSP} \propto t^{0.15}$$

Conclusion: Total luminosity in a CSP is an **INCREASING** function of time

Color evolution:

SSP

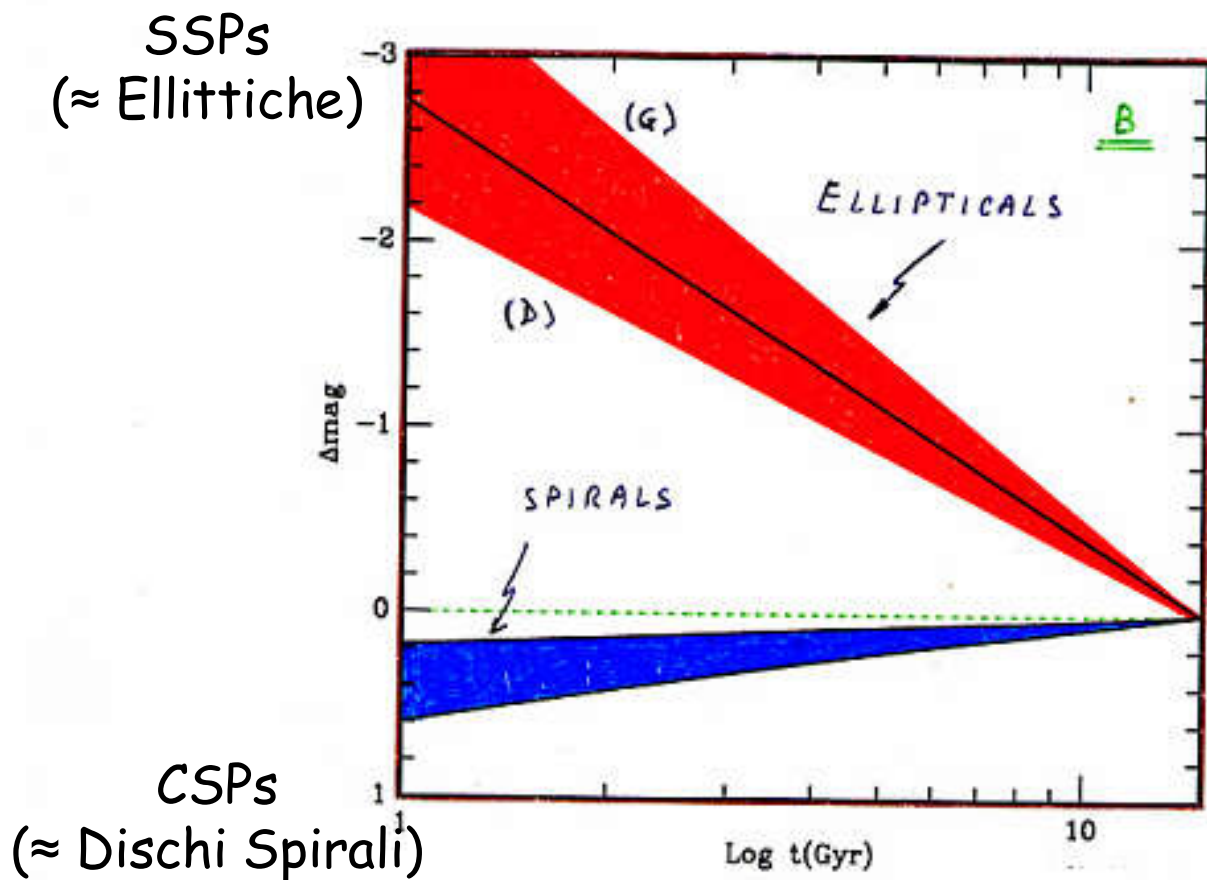
CSP

$$\begin{cases} L_B \propto t^{-\alpha_B} \\ L_V \propto t^{-\alpha_V} \end{cases} \quad \begin{cases} L_B \propto t^{1-\alpha_B} \\ L_V \propto t^{1-\alpha_V} \end{cases}$$

**SAME LAW!**

$$\frac{L_B}{L_V} \propto t^{-(\alpha_B - \alpha_V)}$$

## LUMINOSITY EVOLUTION



Ellipticals

$$L_t \propto t^{-\alpha} \sim t^{-0.8}$$

Spirals  
(disk)

$$L_t \propto t^{1-\alpha} \sim t^{+0.2}$$

# Star Formation Rate (Leggi di Schmidt)

$$SFR = - \frac{d f_{\text{gas}}}{dt}$$

$$\text{PDMF}_{(M,t)} = \int_0^{z \leq T} SFR \times \text{IMF}_{(M)} dt$$

↓

OBSERVED       $0 \leq z \leq T$

ASSUMED

$$SFR \propto f_{\text{gas}}^m \quad m=2 \quad \text{SCHMIDT LAW}$$

$$m=1 \quad SFR = k f = -\dot{f} \quad SFR = k e^{-kt}$$

$$m=2 \quad SFR = k f^2 = -\dot{f} \quad SFR = \frac{k}{(1+kt)^2}$$

$$k = \frac{1}{\tau} \quad (\text{star formation timescale})$$

$$\lim k \rightarrow \infty \quad \tau \rightarrow 0 \quad \Rightarrow \quad \text{SSP}$$

$$SFR \rightarrow \delta(0)$$

# Star Formation Rate (Leggi di Schmidt)

Soluzioni:

$$n=1$$

$$\left\{ \begin{array}{l} SFR = \dot{f}_* = -\dot{f}_{gas} \\ \dot{f}_* = K f_{gas} \end{array} \right\} \rightarrow K f_{gas} = -\frac{df_{gas}}{dt}$$

$$\frac{df_{gas}}{f_{gas}} = -k dt \quad \text{integro: } f_{gas}(t) = f_{gas}(0) e^{-kt}$$

possa assumere  $k = \frac{1}{z}$  tempo  
scala

Quindi, alla fine ha:

$$\left\{ \begin{array}{l} f_{gas} = e^{-kt} \\ SFR = K e^{-kt} \end{array} \right. \quad b = \frac{SFR_0}{\langle SFR \rangle} = \frac{K e^{-kt}}{\frac{K}{t} \int_0^t e^{-kz} dz} = \frac{e^{+kt}}{e^{+kt} - 1} \quad 0 \leq b \leq 1$$

$$n=2 \quad (\text{Legge di Schmidt canonica})$$

$$\left\{ \begin{array}{l} SFR = -\dot{f}_{gas} \\ SFR = K f_{gas}^2 \end{array} \right\} \rightarrow K f_{gas}^2 = -\frac{df_{gas}}{dt}$$

$$\frac{df_{gas}}{f_{gas}^2} = -k dt \quad \text{integro: } \frac{1}{f_{gas}(0)} - \frac{1}{f_{gas}(t)} = -kt$$

$$\left\{ \begin{array}{l} f_{gas} = \frac{1}{1+kt} \\ SFR = \frac{K}{(1+kt)^2} \end{array} \right. \quad b = \frac{K}{(1+kt)^2} \cdot \frac{t}{\int \frac{K}{(1+kt)^2} dt} = \frac{1}{1+kt} \quad 0 \leq b \leq 1$$

# Star Formation Rate (Power Law)

Soluzione:

Assume che l'efficienza del meccanismo di formazione stellare sia un parametro intrinseco della galassia, che solo dipende dalla sua morfologia.

Ne consegue che:

$$\begin{cases} SFR = k t^{-\beta} \\ SFR = -f_{\text{gas}}^* \end{cases} \rightarrow \quad k t^{-\beta} = -\frac{df_{\text{gas}}}{dt}$$

k ha le dimensioni di  $\propto^{+(\beta-1)}$

$$df_{\text{gas}} = -k t^{-\beta} dt \rightarrow 1 - f_{g(t)} = \frac{k}{1-\beta} t^{1-\beta}$$

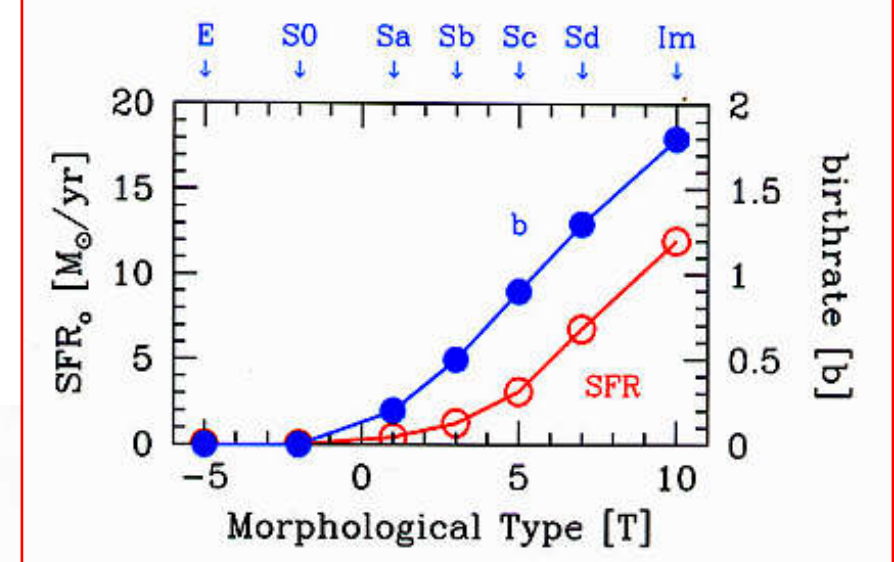
$$\boxed{\begin{cases} f_{g(t)} = 1 - \frac{k t^{1-\beta}}{1-\beta} \\ SFR(t) = k t^{-\beta} \end{cases} \quad b = \frac{k t^{-\beta}}{\frac{k}{1-\beta} t^{1-\beta}} = (1-\beta) \quad \forall t}$$

Quindi il Birthrate è indipendente dal tempo.  
Il gas si esaurisce in un tempo finito:

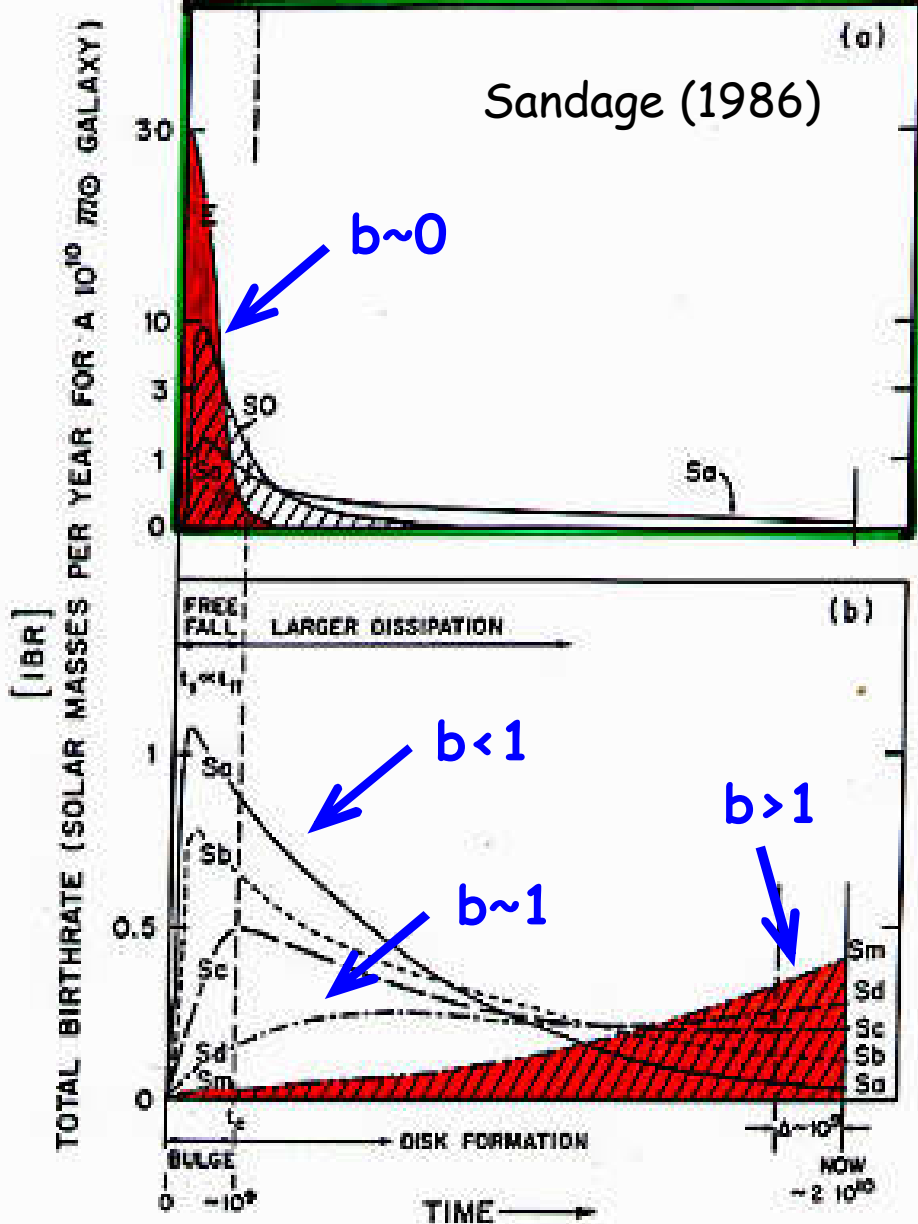
$$t_{\text{MAX}} = \left( \frac{1-\beta}{k} \right)^{\frac{1}{1-\beta}}$$

# SFR & Birthrate

FREE-FALL TIME  
↓



Buzzoni (2002)

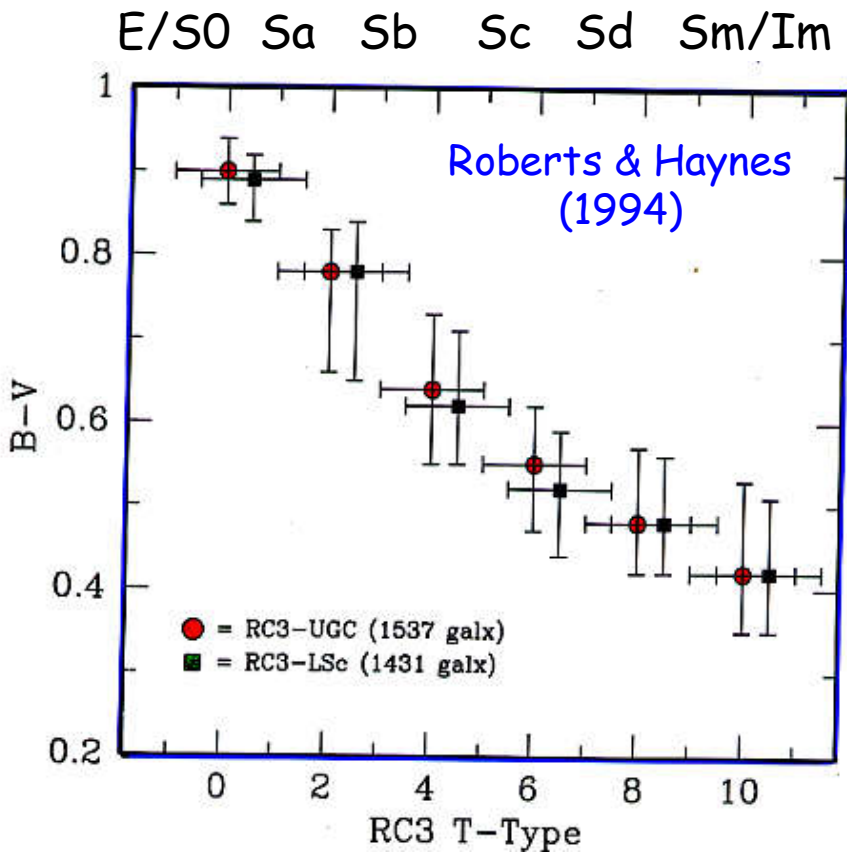


Birthrate

$$b = \frac{SFR_o}{\langle SFR \rangle}$$

Fig. 10. Same as Fig. 9 with later Hubble types shown in the lower panel. The integral under the Sm curve is shaded for illustration. The curves are only schematic showing the trends that have been established by Gallagher et al. (1984).

# Eta' media delle popolazioni e colore integrato delle galassie



Nel caso di una SFR a legge di potenza:

$$SFR = k t^{-\beta}$$

$$\mathcal{L}(t) = k' \int^t \tau^{-\alpha} (t-\tau)^{-\beta} d\tau = k' \frac{\Gamma(1-\alpha) \Gamma(1-\beta)}{\Gamma(2-\alpha-\beta)} t^{1-\alpha-\beta}$$

$$b = \frac{SFR(t)}{\langle SFR \rangle} = \frac{k t^{-\beta} (1-\beta) t}{k t^{(1-\beta)}} = (1-\beta) \quad \forall t$$

Eta' media delle SSP componenti (usata con la luminosita')

$$\langle t \rangle = \frac{k' \int \tau \tau^{-\alpha} (t-\tau)^{-\beta} d\tau}{k' \int \tau^{-\alpha} (t-\tau)^{-\beta} d\tau} = \frac{\int \tau \mathcal{L}(\tau)}{\mathcal{L}(t)}$$

Ricordando che  $\Gamma(1+m) = m! \Gamma(m)$

$$\langle t \rangle = \frac{\Gamma[1+(1-\alpha)] \Gamma(1-\beta)}{\Gamma[2+(1-\alpha)-\beta]} \frac{\Gamma(2-\alpha-\beta)}{\Gamma(1-\alpha) \Gamma(1-\beta)} \frac{t^{2-\alpha-\beta}}{t^{1-\alpha-\beta}}$$

$$\langle t \rangle = \frac{1-\alpha}{2-\alpha-\beta} t$$

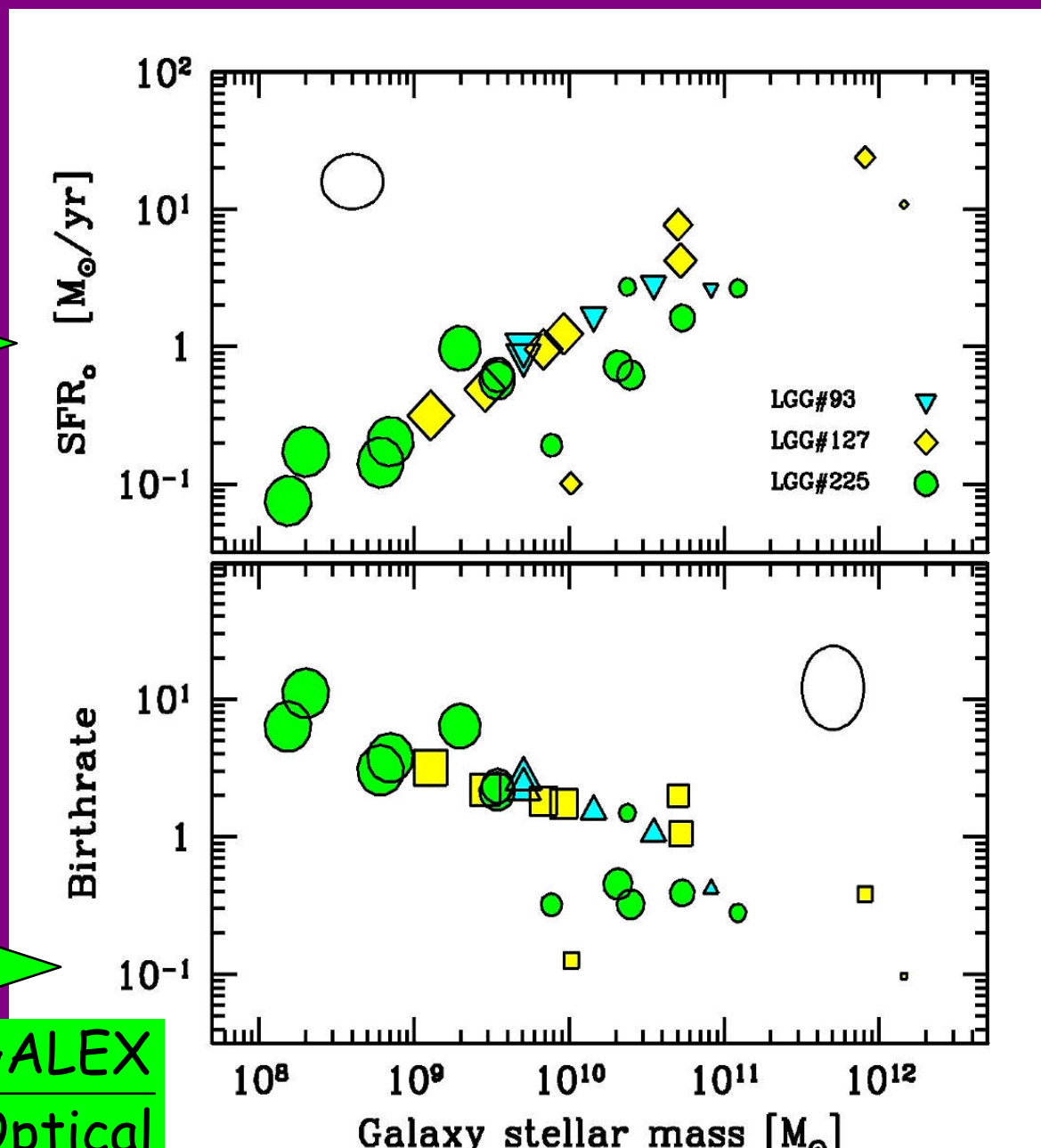
$$\frac{\langle t \rangle}{t} \ll 1 \quad \text{se} \quad b \gg 0$$

# Birthrate & Downsizing

Buzzoni (2011) - Marino et al. (2009)

GALEX

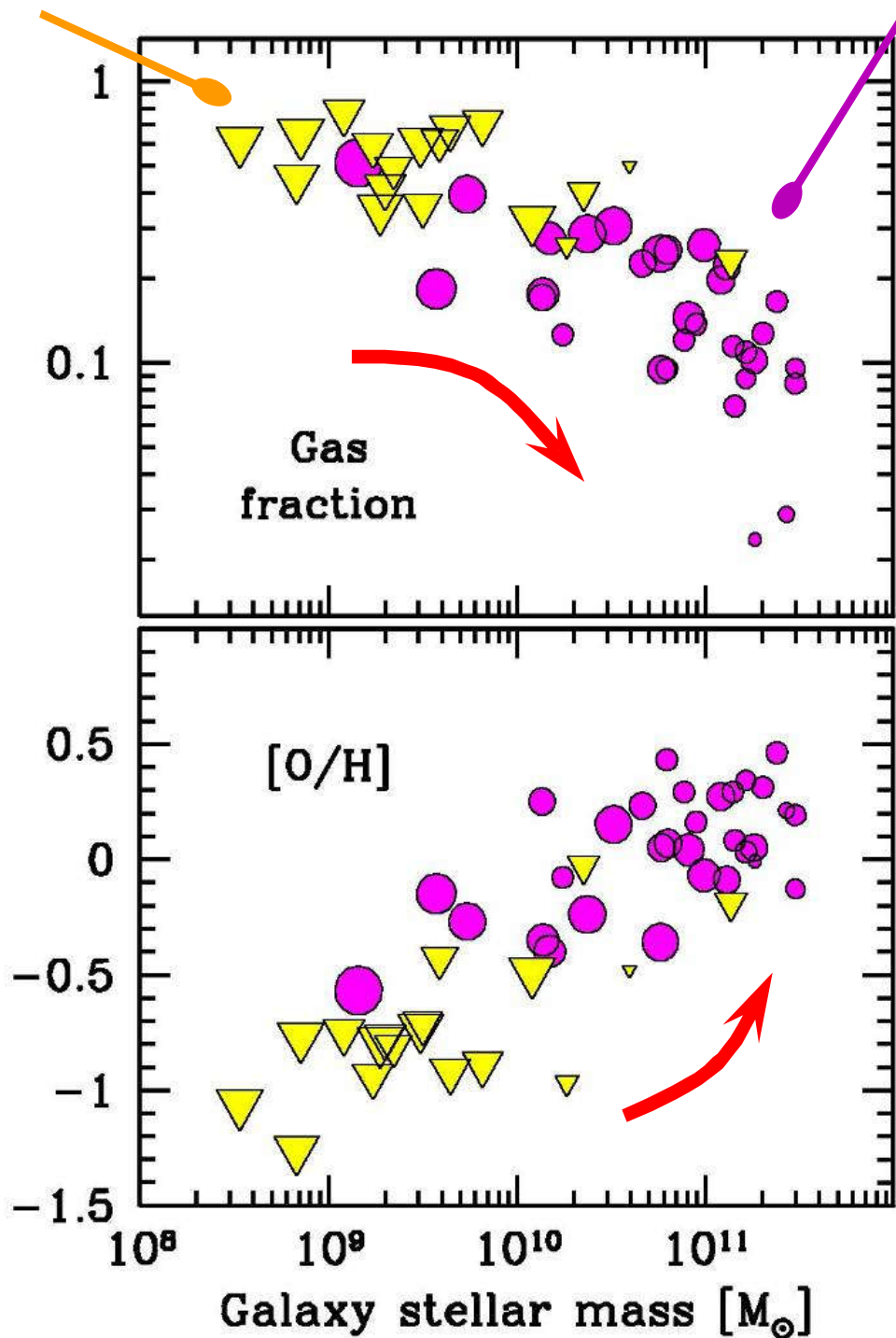
$$b = \frac{SFR}{\langle SFR \rangle} = \frac{GALEX}{Optical}$$



# Gas fraction & ISM Metallicity

Kuzio de Naray et al. (2004)

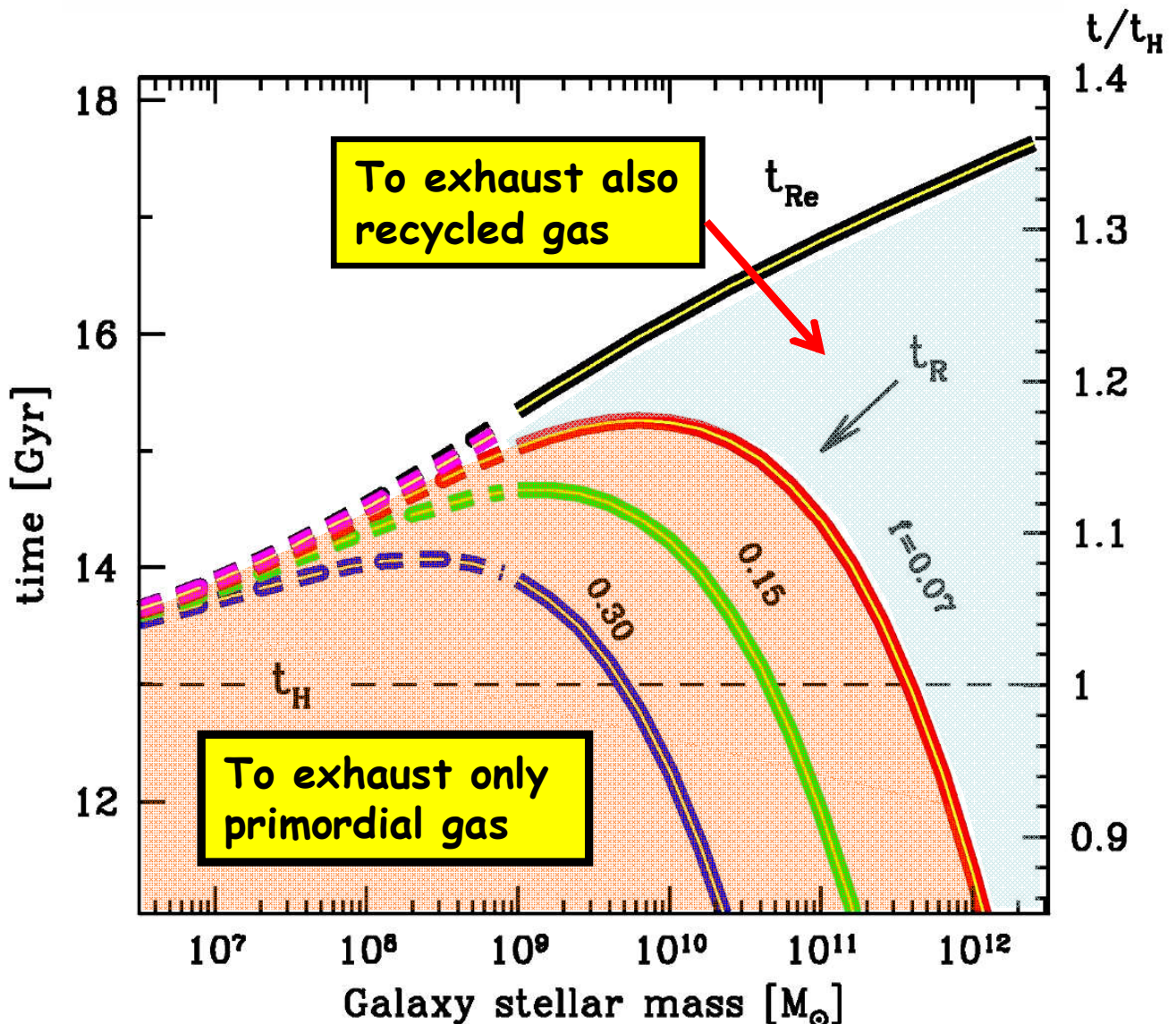
Garnett (2002)



# The Roberts time (hurry up: the party is over!)

**Tempo di Roberts:**  $t_R \sim \frac{f_{\text{gas}} M_{\text{gal}}}{SFR_{\text{now}}} \quad (\text{vedi dopo})$   $b = \frac{SFR_{\text{now}}}{M_{\text{gal}}} t_{\text{gal}}$

Combinandole:  $\frac{t_R}{t_{\text{gal}}} = \frac{f_{\text{gas}}}{b} \sim \frac{\sim 0.1}{\sim 1}$  Quindi  $t_R \sim 1-2 \text{ Gyr max}$



We are (so embarrassingly) close to the final death of galaxies as star-forming systems in the Universe!!

# Energetica nucleare e rapporto M/L delle galassie

## METAL ABUNDANCE

$$X + Y + Z = 1$$

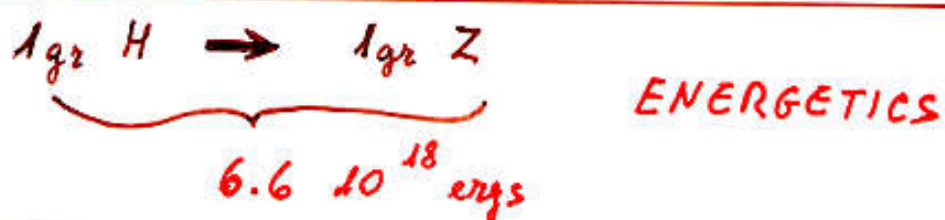
Hydrogen      Helium      "Others"

$$\left[ \frac{F_e}{H} \right] = \log \frac{F_e}{F_{e_0}} - \log \frac{H}{H_0}$$

$$\underline{I F \quad F_e \propto Z}$$

$$\left[ \frac{Fe}{H} \right] = \log \frac{Z}{0.017} - \log \frac{1-Z-y}{0.21} \approx \log Z + 1.8$$

$$(X, y, z)_0 = (0.30, 0.48, 0.017)$$



$$IN\ A\ GALAXY:\ M_2 \sim 2 \cdot 10^9\ M_\odot \sim 4 \cdot 10^{42}\ g_2$$

$$M_2 = \frac{\int L \times t}{6.6 \cdot 10^{18}} \sim \frac{\langle L \rangle \cdot 10^{10} \text{ yr}}{6.6 \cdot 10^{18} \text{ erg/s}}$$

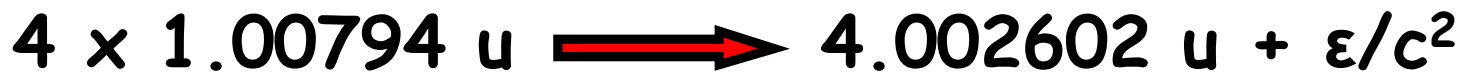
$$\langle L \rangle \sim 2.2 \cdot 10^{10} L_0 \quad \frac{M}{L} \leq 5 \quad \text{in primordial gas}$$

# Energetica nucleare e tempi scala evolutivi

Atomic Number	Element Symbol	Element Name	Atomic Weight
1	H	Hydrogen	1.00794
2	He	Helium	4.002602
3	Li	Lithium	6.941
4	Be	Beryllium	9.012182
5	B	Boron	10.811
6	C	Carbon	12.0107
7	N	Nitrogen	14.0067
8	O	Oxygen	15.9994
9	F	Fluorine	18.9984032
10	Ne	Neon	20.1797
11	Na	Sodium	22.989770
12	Mg	Magnesium	24.3050
13	Al	Aluminium	26.981538
14	Si	Silicon	28.0855
15	P	Phosphorus	30.973761
16	S	Sulfur	32.065
17	Cl	Chlorine	35.453
18	Ar	Argon	39.948
19	K	Potassium	39.0983
20	Ca	Calcium	40.078
21	Sc	Scandium	44.955910
22	Ti	Titanium	47.867
23	V	Vanadium	50.9415
24	Cr	Chromium	51.9961
25	Mn	Manganese	54.938049
26	Fe	Iron	55.845

# Energetica nucleare e tempi scala evolutivi

H burning:  $4 \text{ H} \longrightarrow 1 \text{ He}$



$$E = \frac{4.03176 - 4.002602}{4.002602} c^2 = 6.6 \cdot 10^{18} \text{ erg / gr}$$

He burning:  $4 \text{ He} \longrightarrow 1 \text{ C}^{12}$



$$E = \frac{12.007806 - 12.000000}{12.000000} c^2 = 0.6 \cdot 10^{18} \text{ erg / gr}$$

$4 \text{ He} \longrightarrow 1 \text{ O}^{16}$



$$E = \frac{16.010408 - 16.000000}{16.000000} c^2 = 0.6 \cdot 10^{18} \text{ erg / gr}$$

# Analytic fundamentals

Luminosity of a Composite Stellar Population:

$$\mathcal{L}_{CSP} = \int \ell_{SSP} \otimes SFR \, dt$$

Output energy after "t" years:

$$\mathcal{E}(t) = \int_0^t \mathcal{L}_{CSP}(\tau) d\tau$$

## Analytic fundamentals (2)

Metal enrichment:

$$\frac{M_{YZ}}{M^*} = \frac{K^{-1}\epsilon}{\int SFR} = \frac{\epsilon_0}{KM_0} \left( \frac{t}{t_0} \right)^{0.23}$$

“Yield Metallicity” of processed mass scales with time as a power law:

$$Z \propto \frac{M_{YZ}}{M^*} \propto \left( \frac{t}{t_0} \right)^{0.23}$$

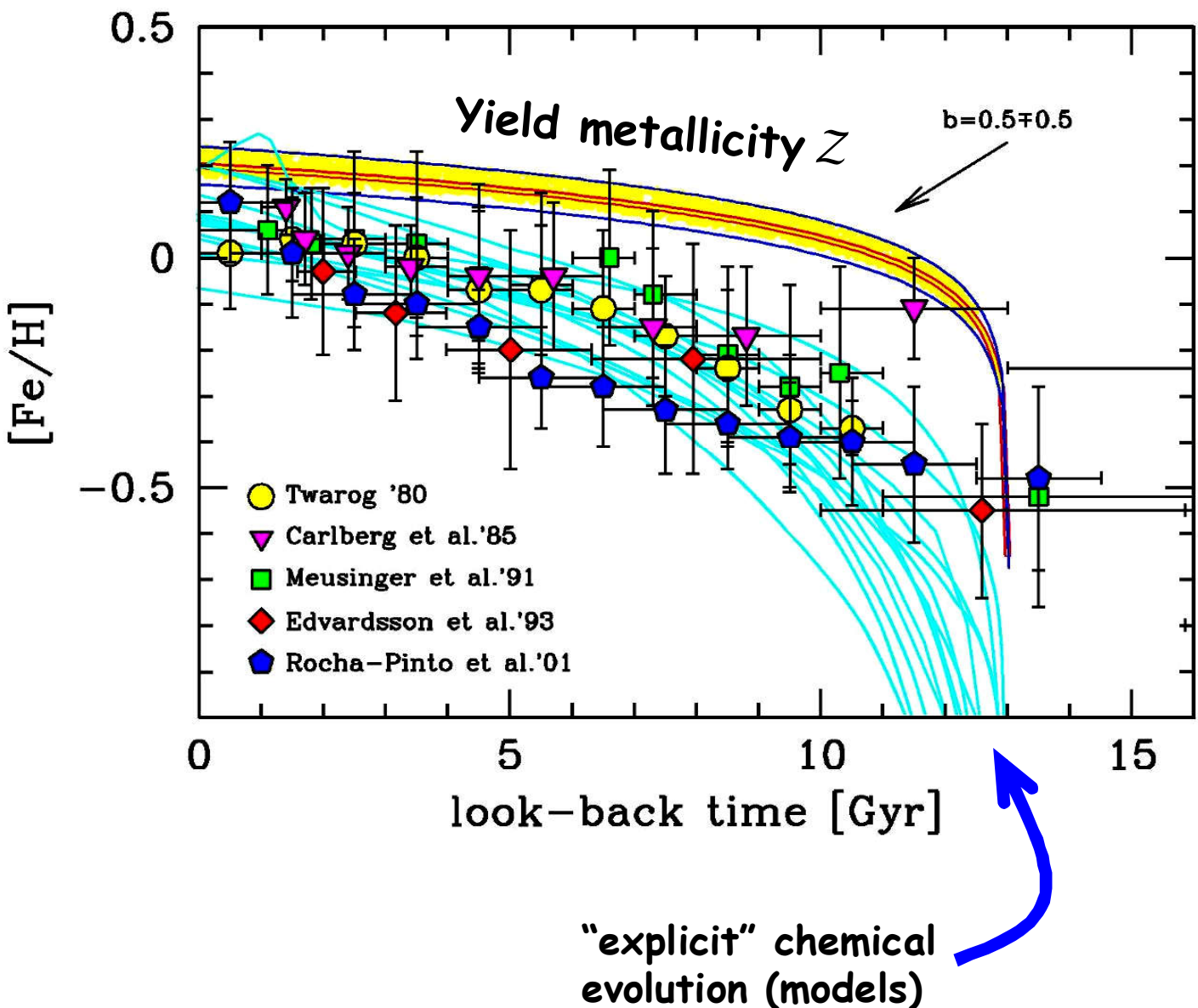
Mass energetic exploitation does (nearly) NOT depend on the galaxy SFR:

$$\mathcal{F} = \frac{\epsilon_0}{KM_0}$$

~ 10 - 13%

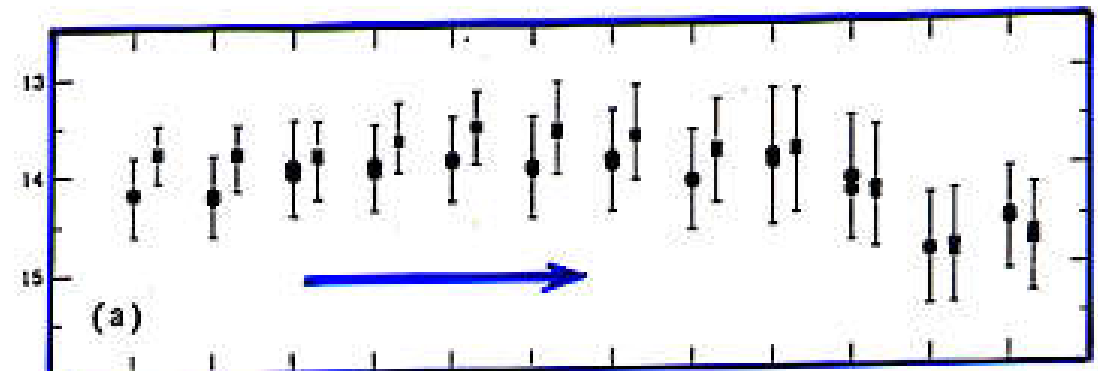
# The Age-metallicity relation (AMR)

Buzzoni (2011)

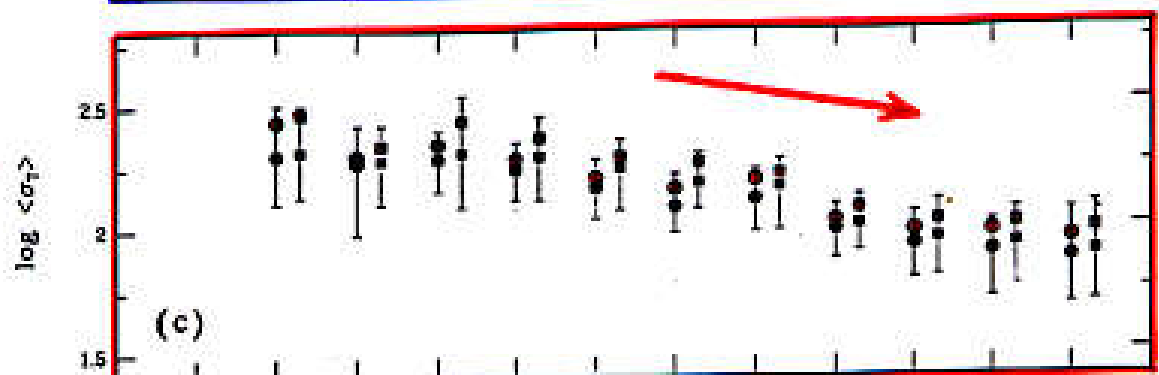


Matteucci & Francois 89 // Wyse & Silk 89 //  
Carigi 94 // Pardi & Ferrini 94 // Prantzos &  
Aubert 95 // Timmes et al. 95 // Giovagnoli & Tosi  
95 // Pilyugin & Edmunds 96 // Mihara & Takahara  
96 // Chiappini, et al. 97 // Portinari et al. 98 //  
Boissier & Prantzos 99 // Alibes et al. 01

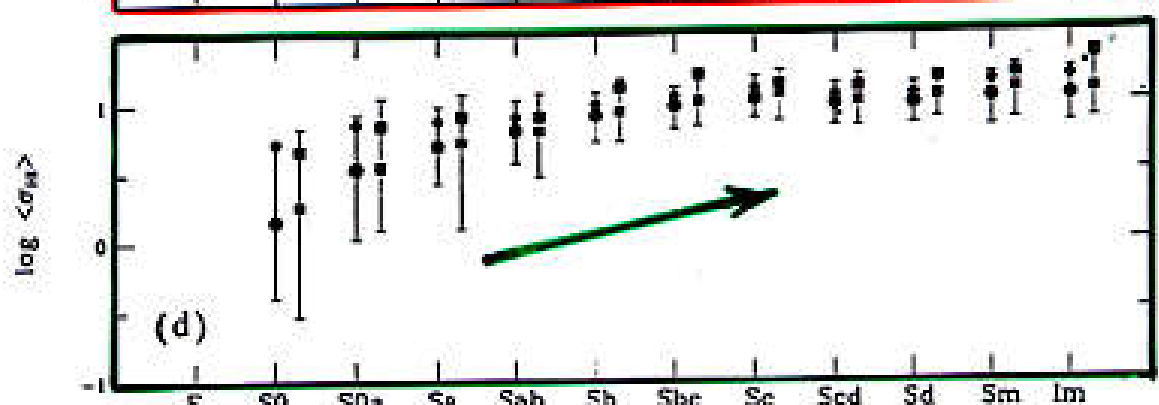
SURFACE  
BRIGHTNESS  
 $\Sigma_B$



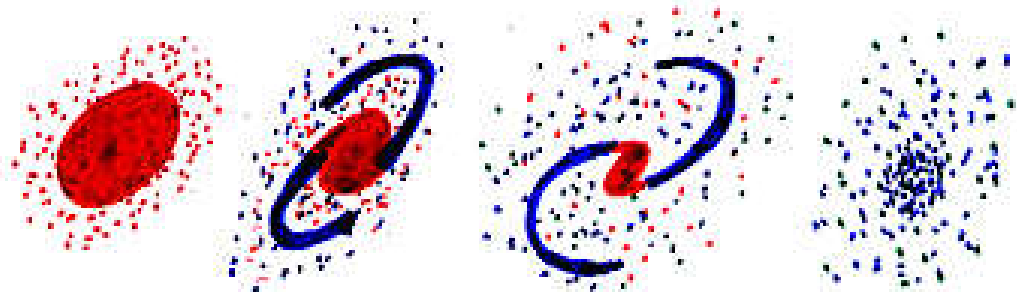
SURFACE  
DENSITY  
 $\sigma_T$



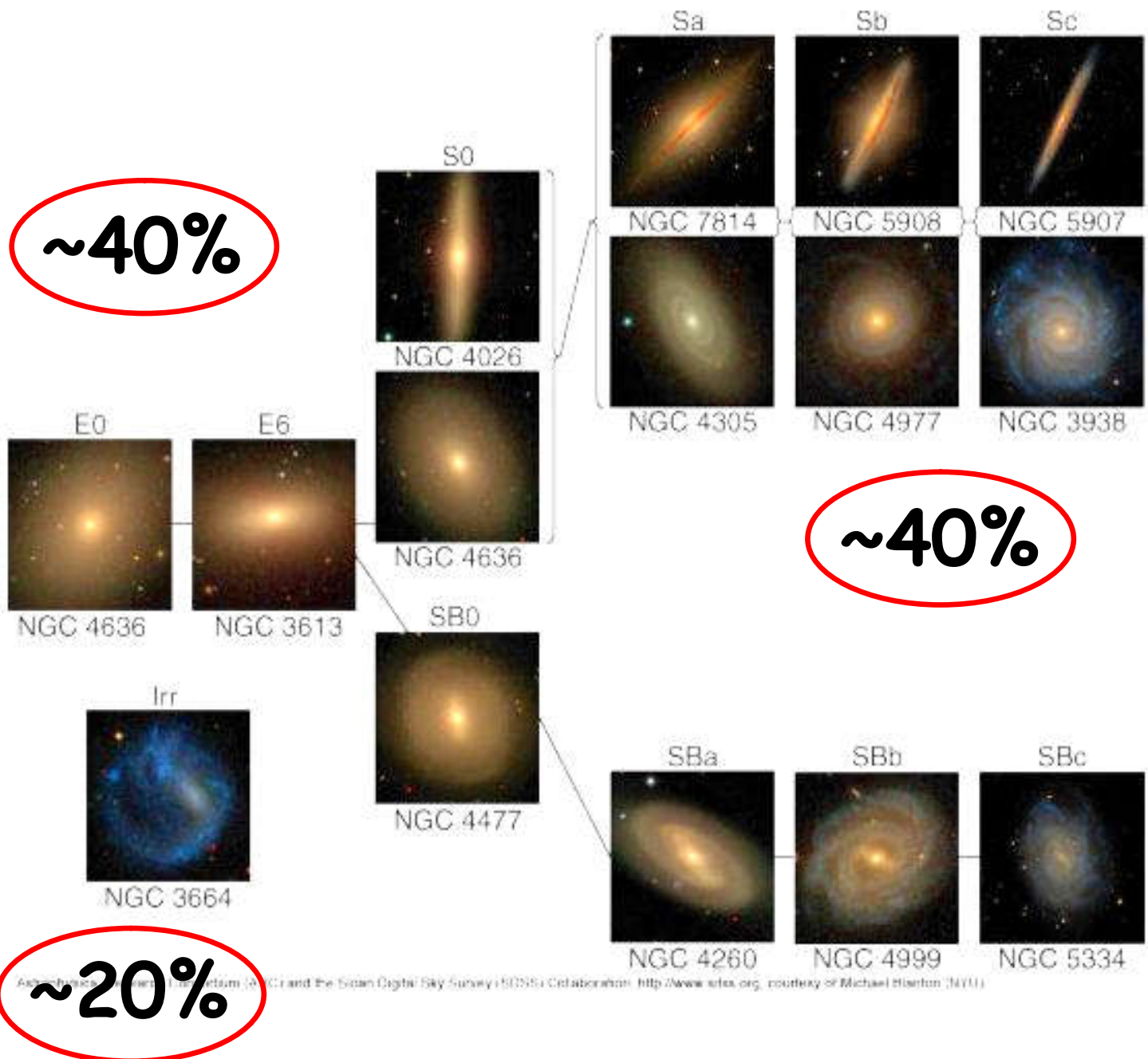
GAS  
(HI)



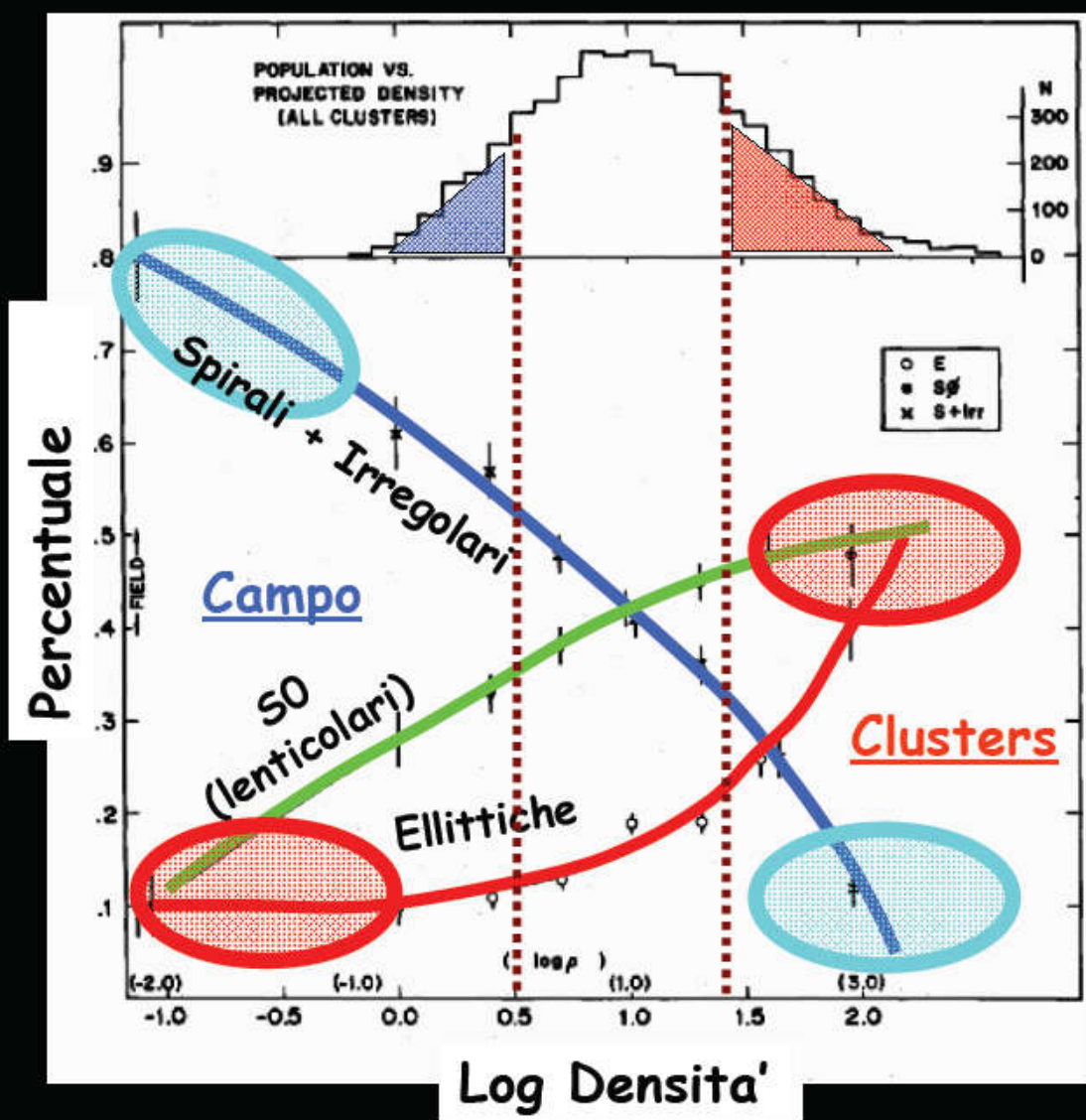
E S0 Sa Sb Sc Sd Sm Im



# Classificazione Morfologica di Hubble

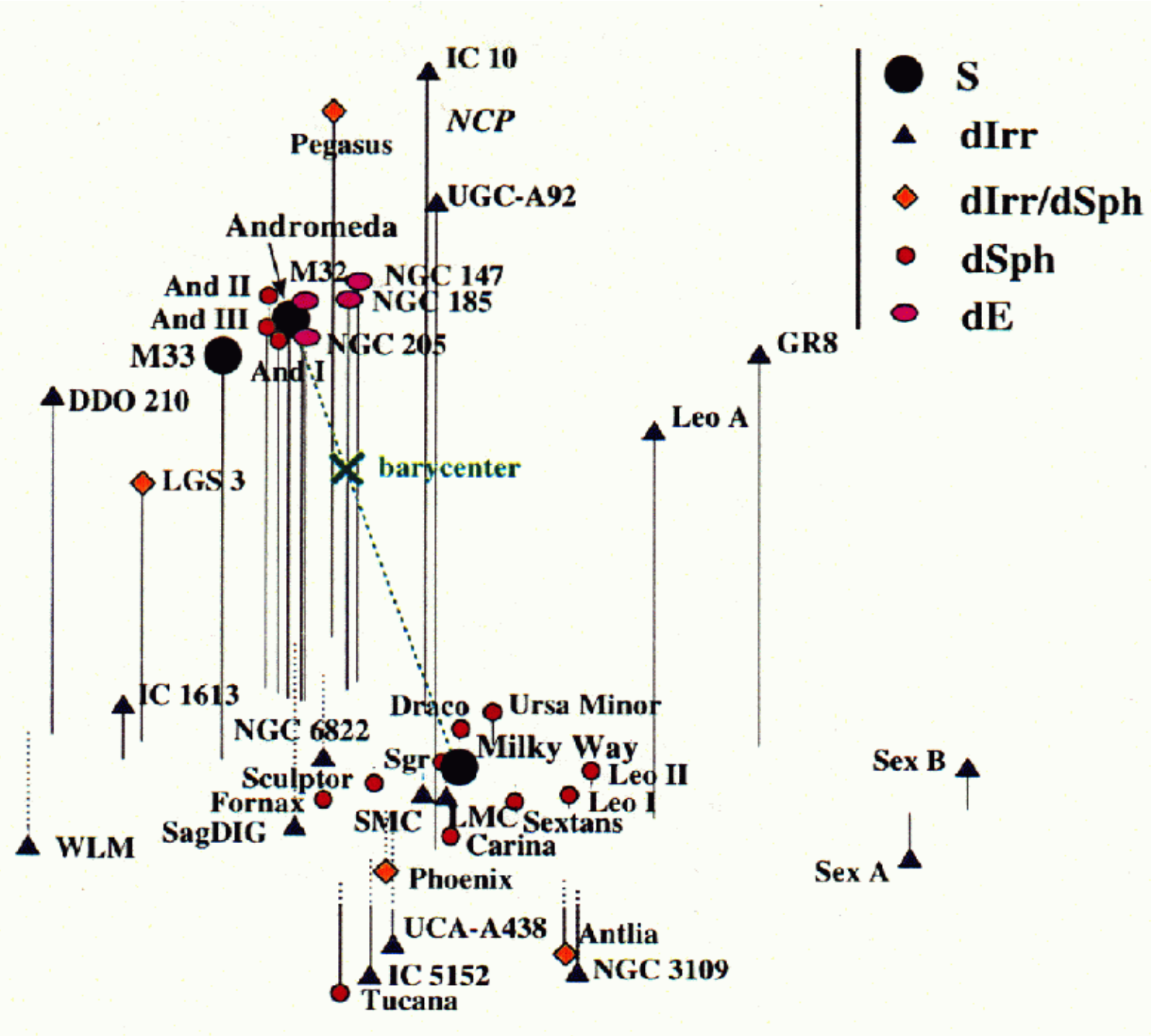


# Distribuzione galattica e tipo morfologico (Segregazione morfologica)

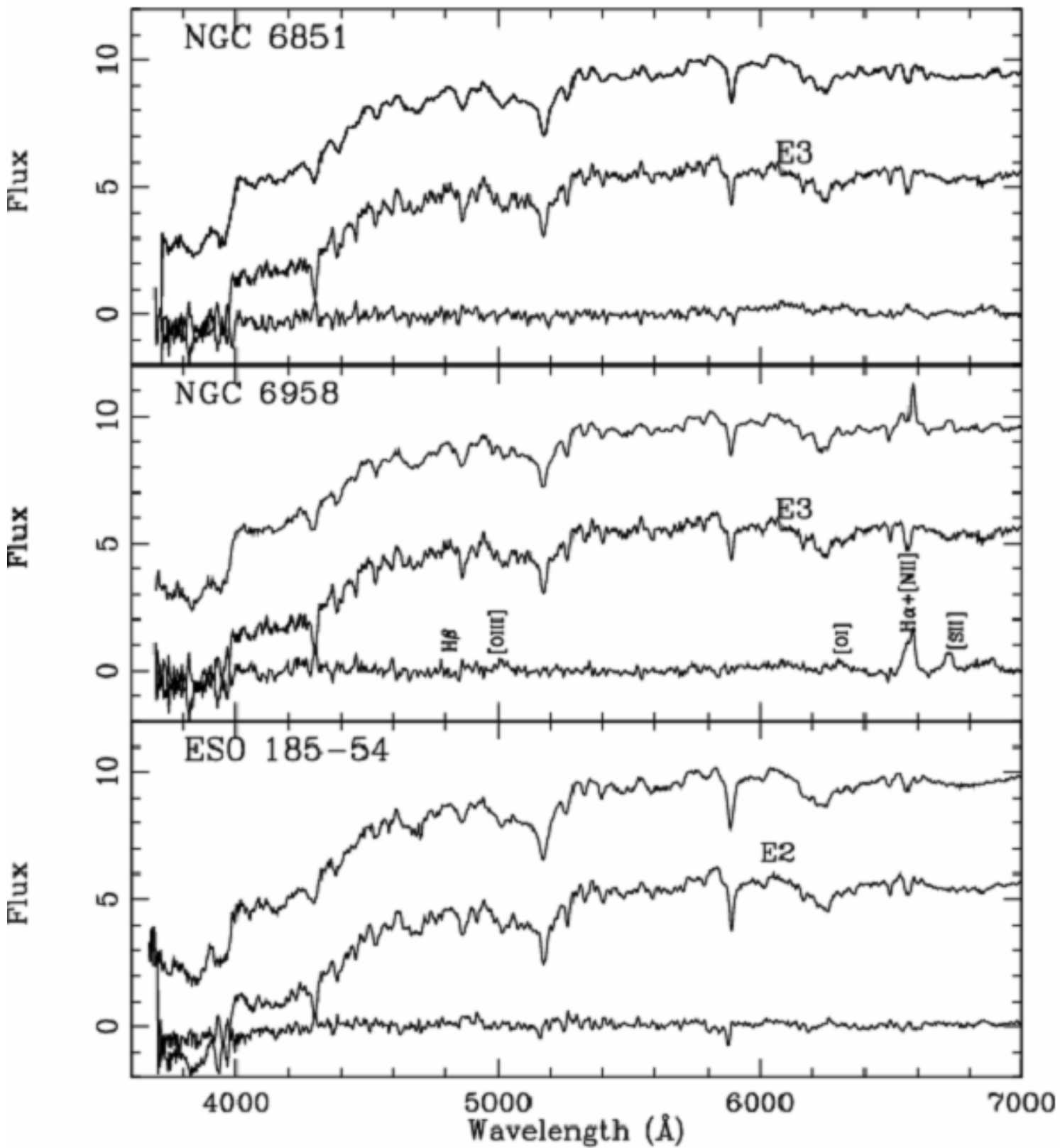


Dressler (1980)

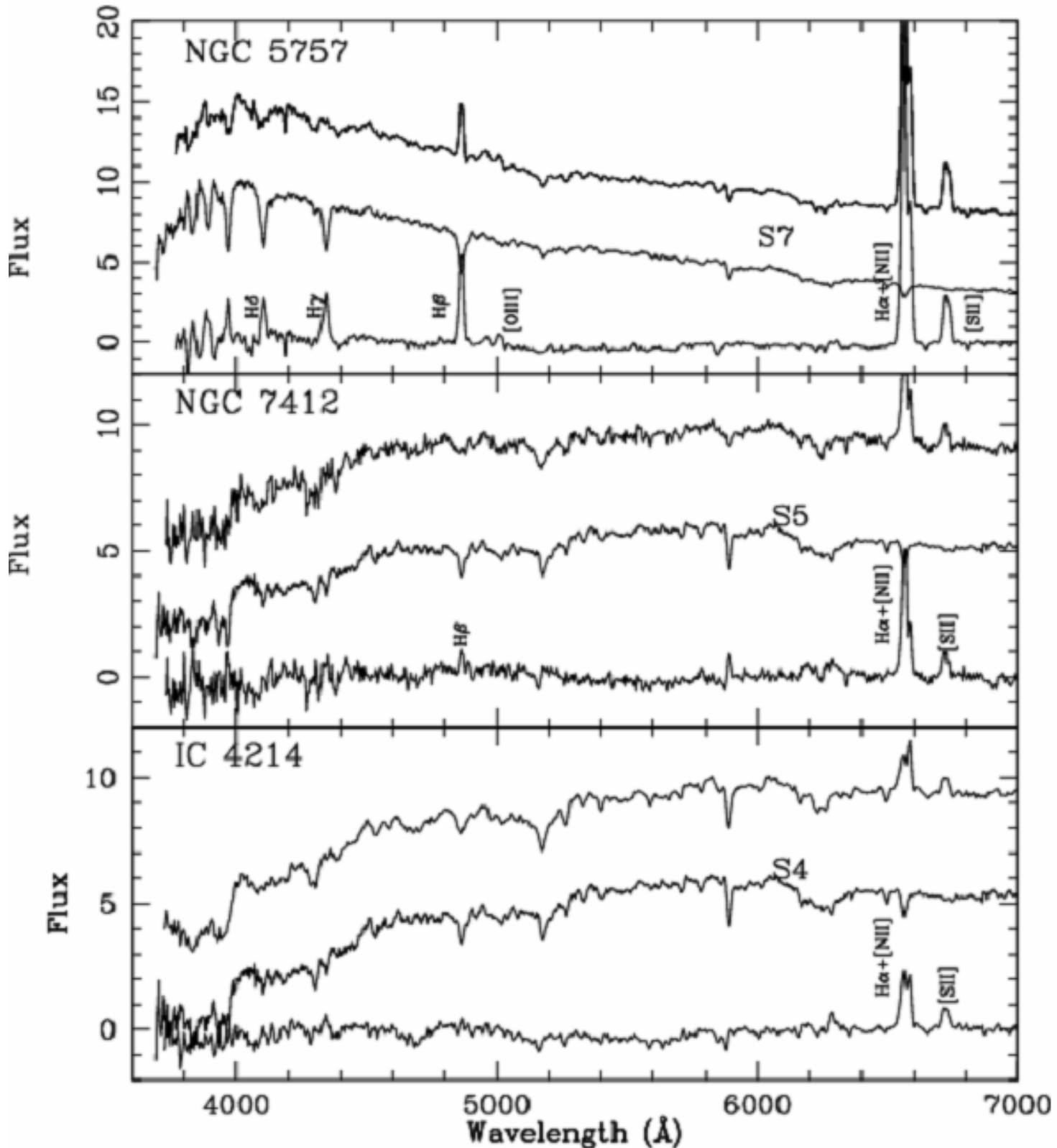
# Il Gruppo Locale



# Lo spettro delle Ellittiche



# Lo spettro delle Spirali



# I principi della spettroscopia (Diffrazione & Interferenza)

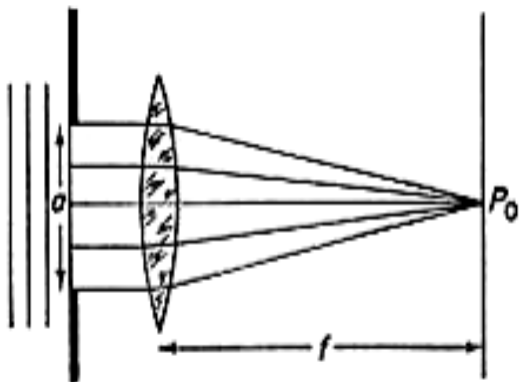


Figura 2. Massimo centrale nella diffrazione di Fraunhofer.

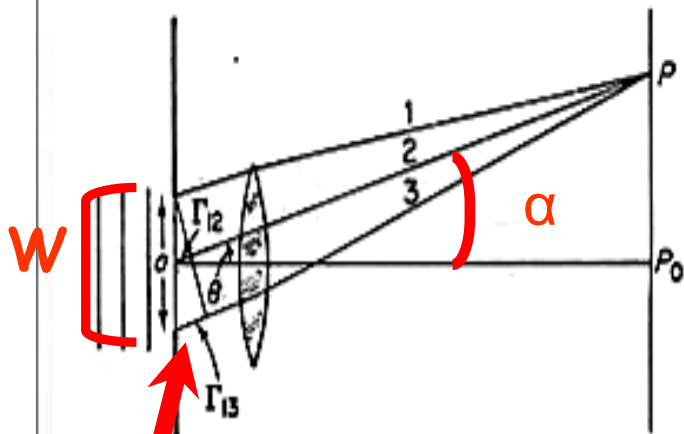


Figura 3. Diffrazione di Fraunhofer.

$$\frac{W}{2} \sin \alpha = \frac{m}{2} \lambda$$



$$\alpha \cong m \frac{\lambda}{W}$$

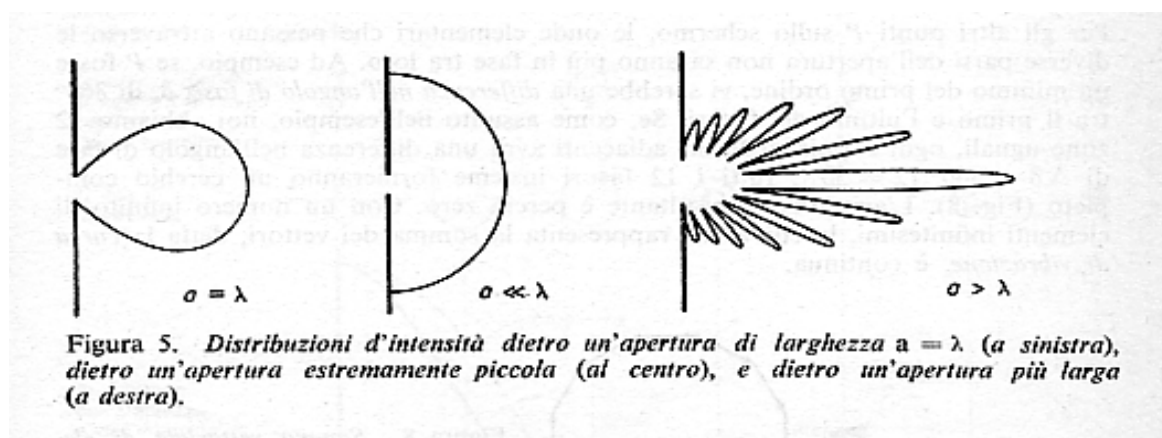
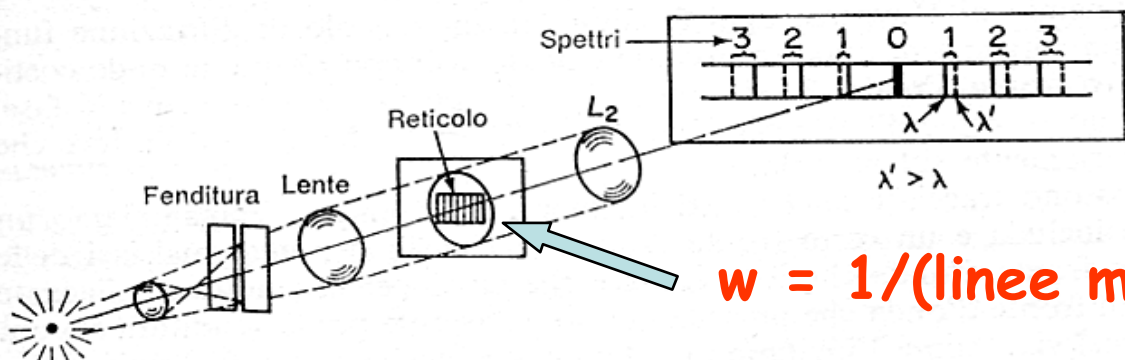


Figura 5. Distribuzioni d'intensità dietro un'apertura di larghezza  $a = \lambda$  (a sinistra), dietro un'apertura estremamente piccola (al centro), e dietro un'apertura più larga (a destra).

# Reticoli di diffrazione



$$w = 1/(\text{linee mm}^{-1})$$

Figura 2. La formazione di una riga spettrale in un reticolo a diffrazione. Viene mostrato lo spettro di una sorgente che emette su due lunghezze d'onda  $\lambda$  e  $\lambda'$ .

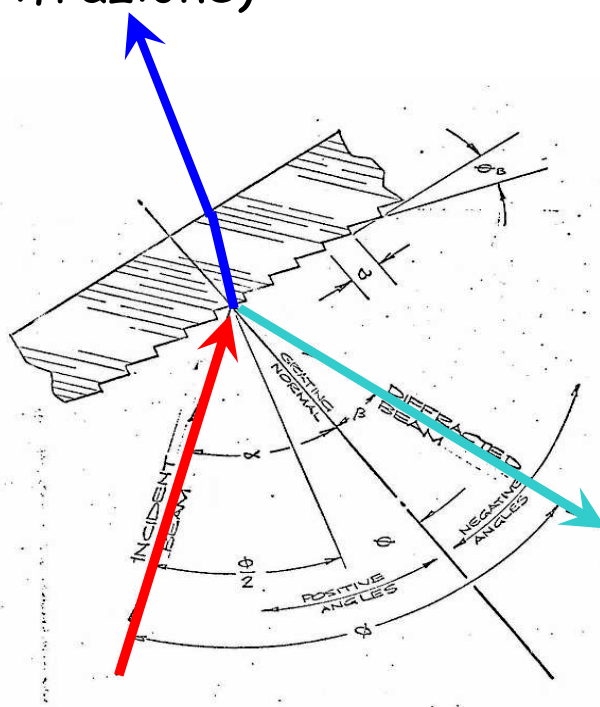
risoluzione

$$\alpha_{\min} \approx m \frac{\lambda}{W}$$

dispersione

$$\Delta\alpha_1 \approx \frac{1.5}{w} \Delta\lambda$$

"Grism"  
(per rifrazione)



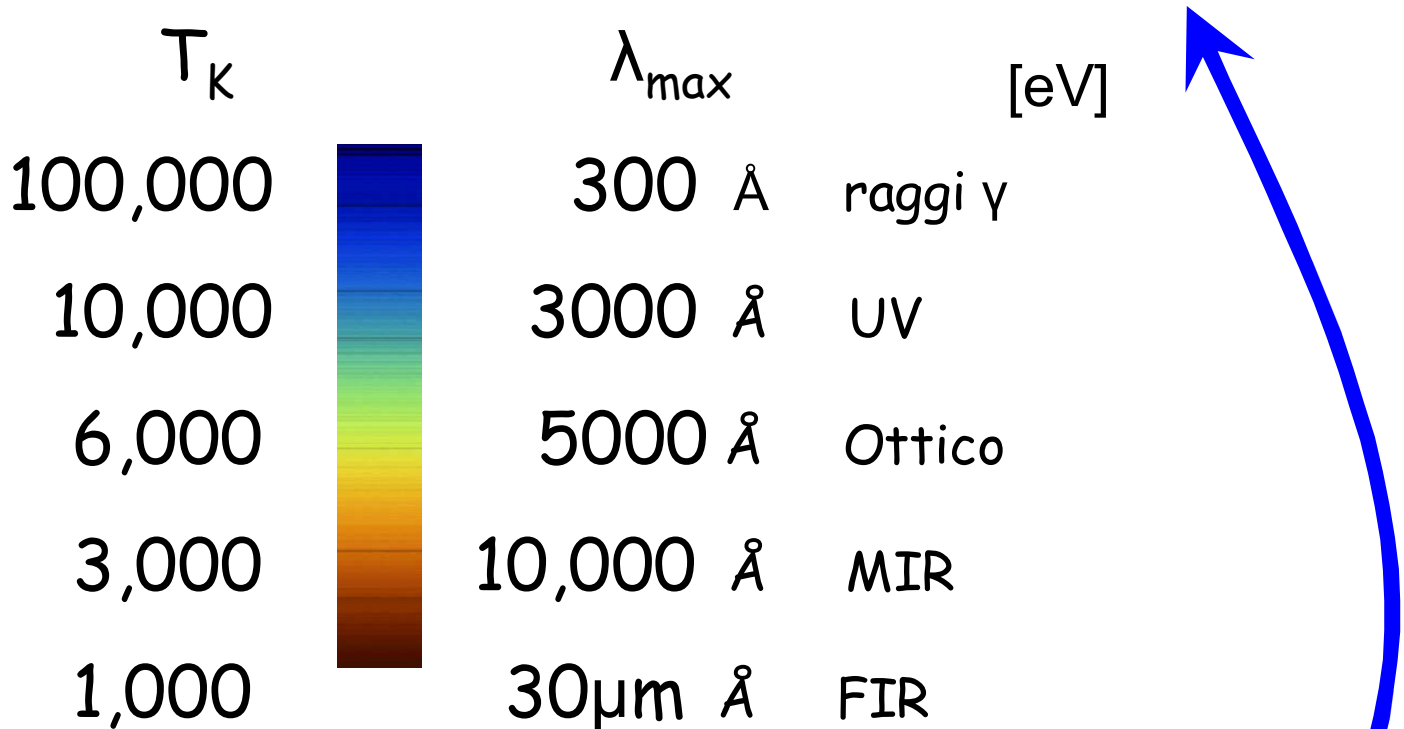
$$\frac{\Delta\alpha}{\alpha} \approx 1.5 \left( \frac{W}{w} \right) \frac{\Delta\lambda}{\lambda}$$

"Grid"  
(per riflessione)

**Legge di Wien :**

$$\lambda_{\max} T \propto \text{const}$$

$$\frac{\lambda_{\max}}{5500} = \frac{5780}{T_K} \quad \longrightarrow \quad \lambda_{\max} \approx \frac{310^7}{T_K} \text{ [\AA]}$$

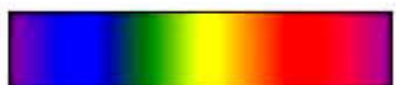


**Equipartizione dell'energia :**

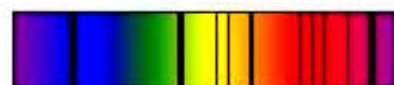
$$E \approx 3kT = 4.2 \cdot 10^{-16} T_K \approx h\nu = \frac{hc}{\lambda}$$

$$\langle \lambda \rangle \approx \frac{hc}{kT} = \frac{6.6 \cdot 10^{-27} \times 3 \cdot 10^{10}}{4.2 \cdot 10^{-16} T_K (10^{-8})} = \boxed{\frac{4.7 \cdot 10^7}{T_K}} \text{ [\AA]}$$

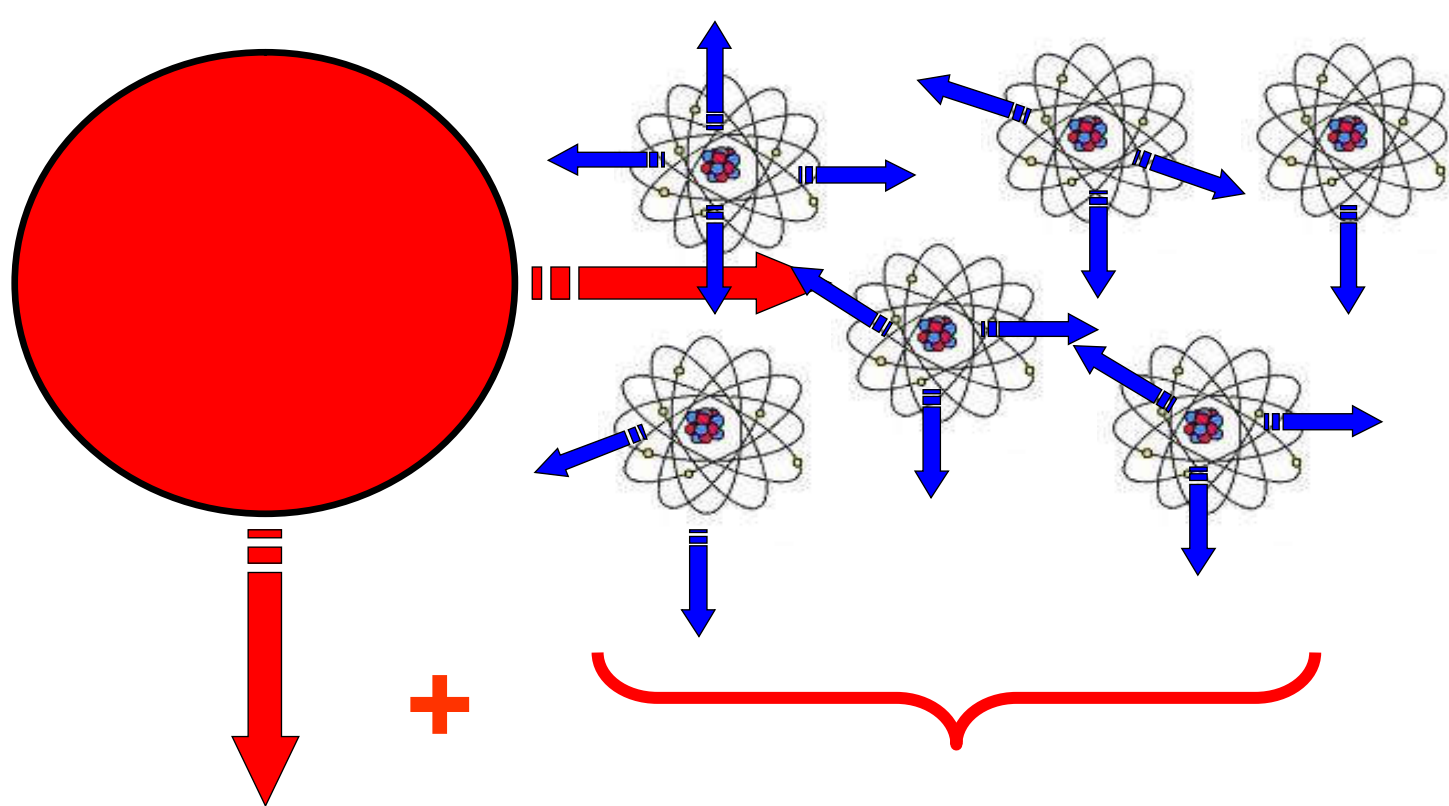
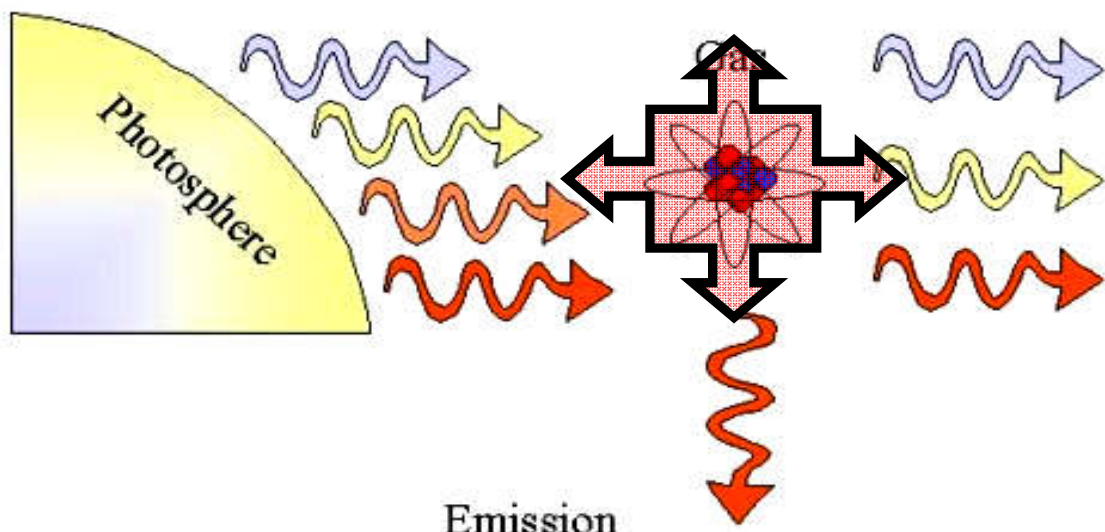
# Emissione & Assorbimento



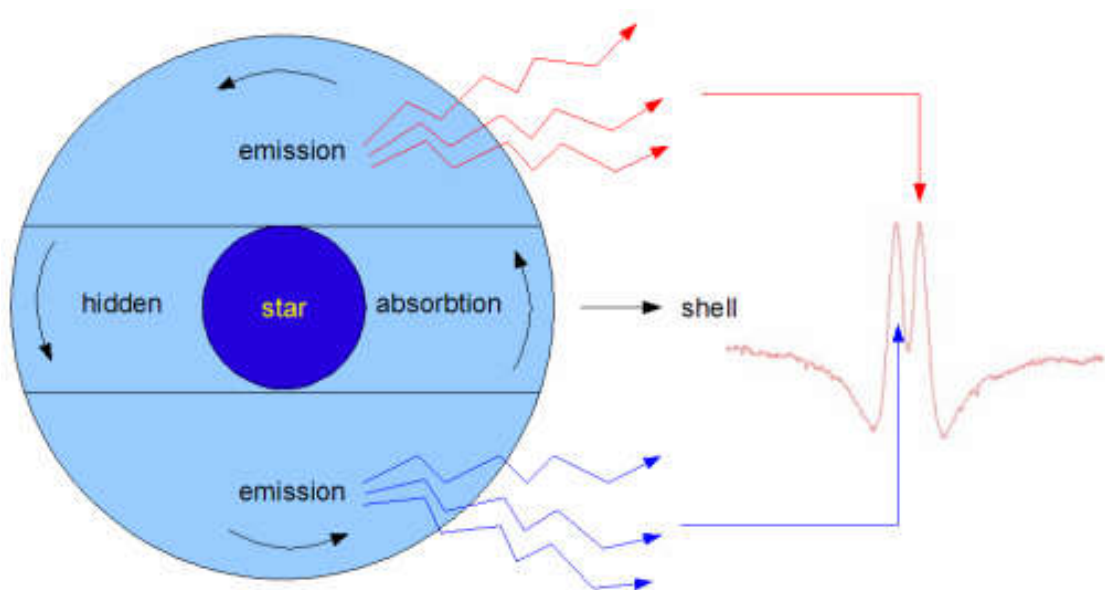
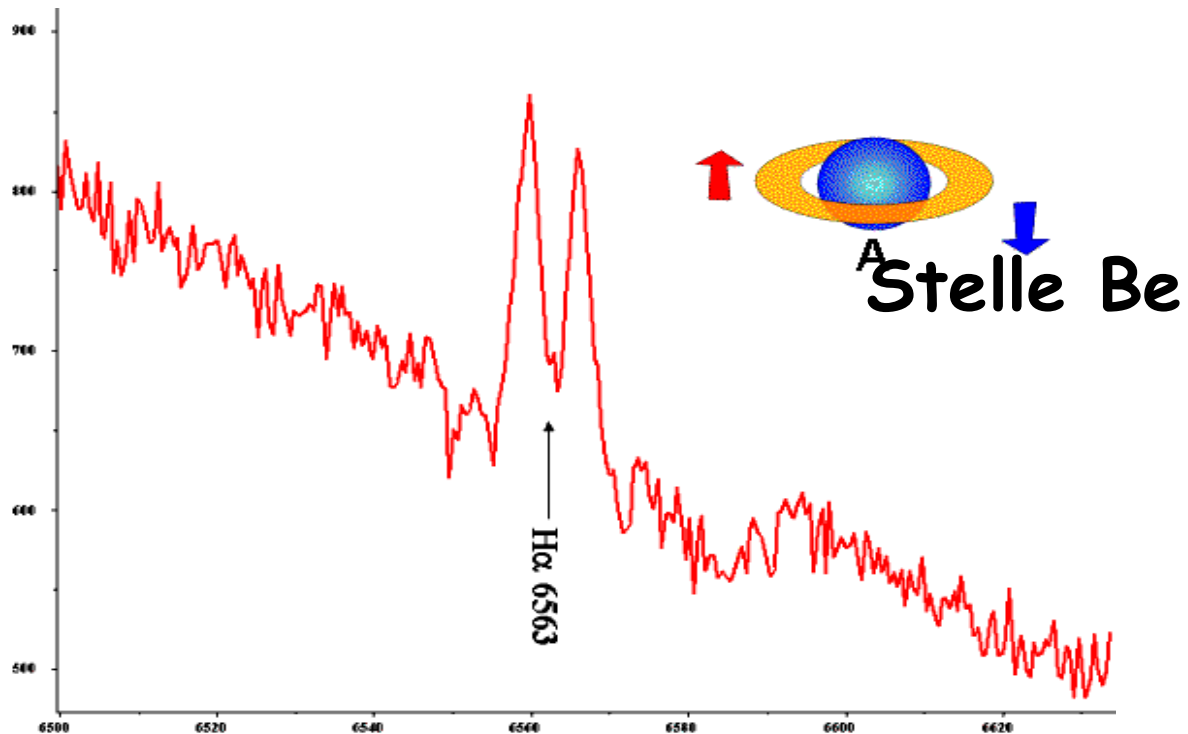
Black body spectrum  
(spettro di corpo nero)



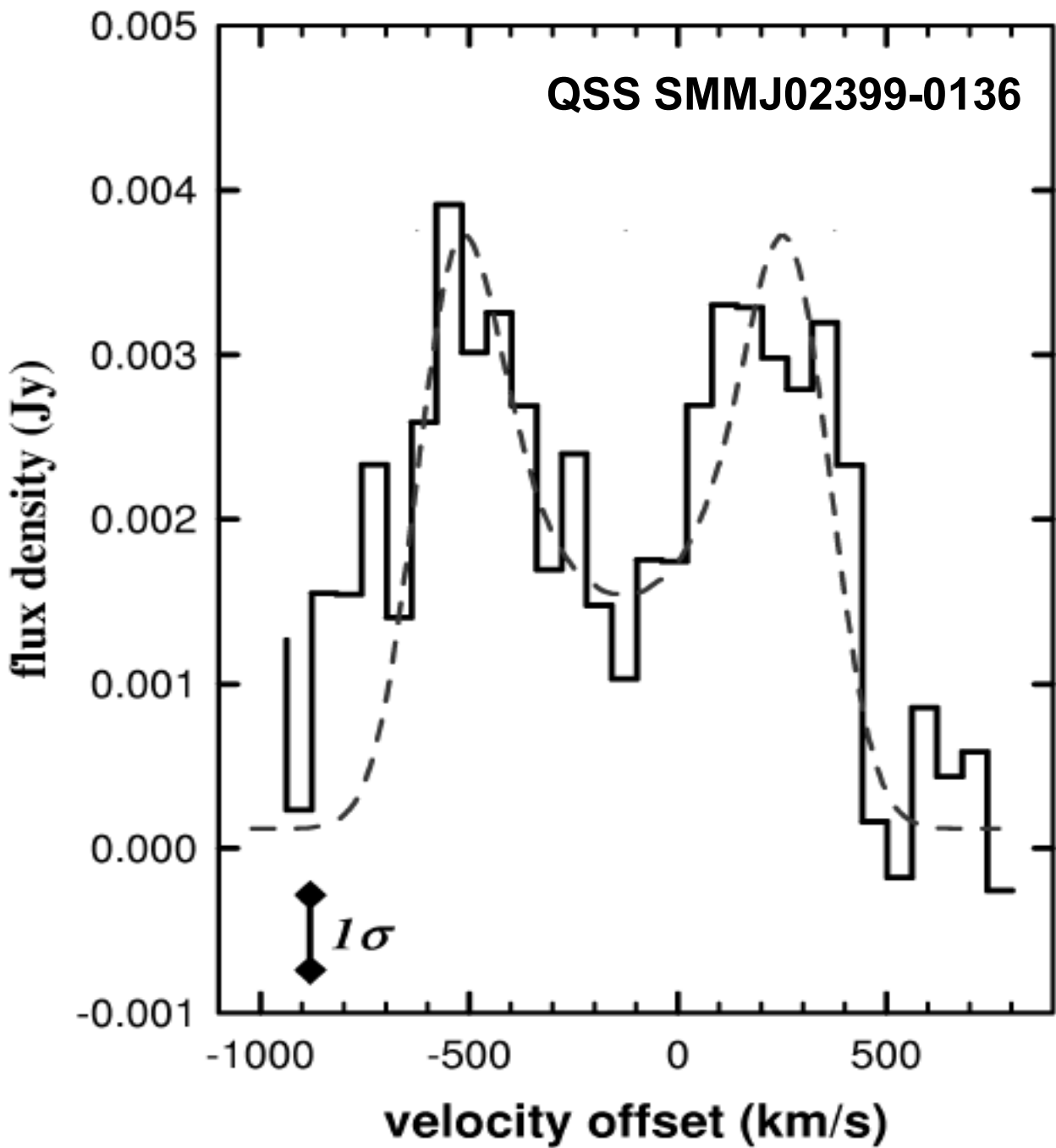
Atomic Absorption  
(Assorbimento atomico)



# Effetti della rotazione (emissione)



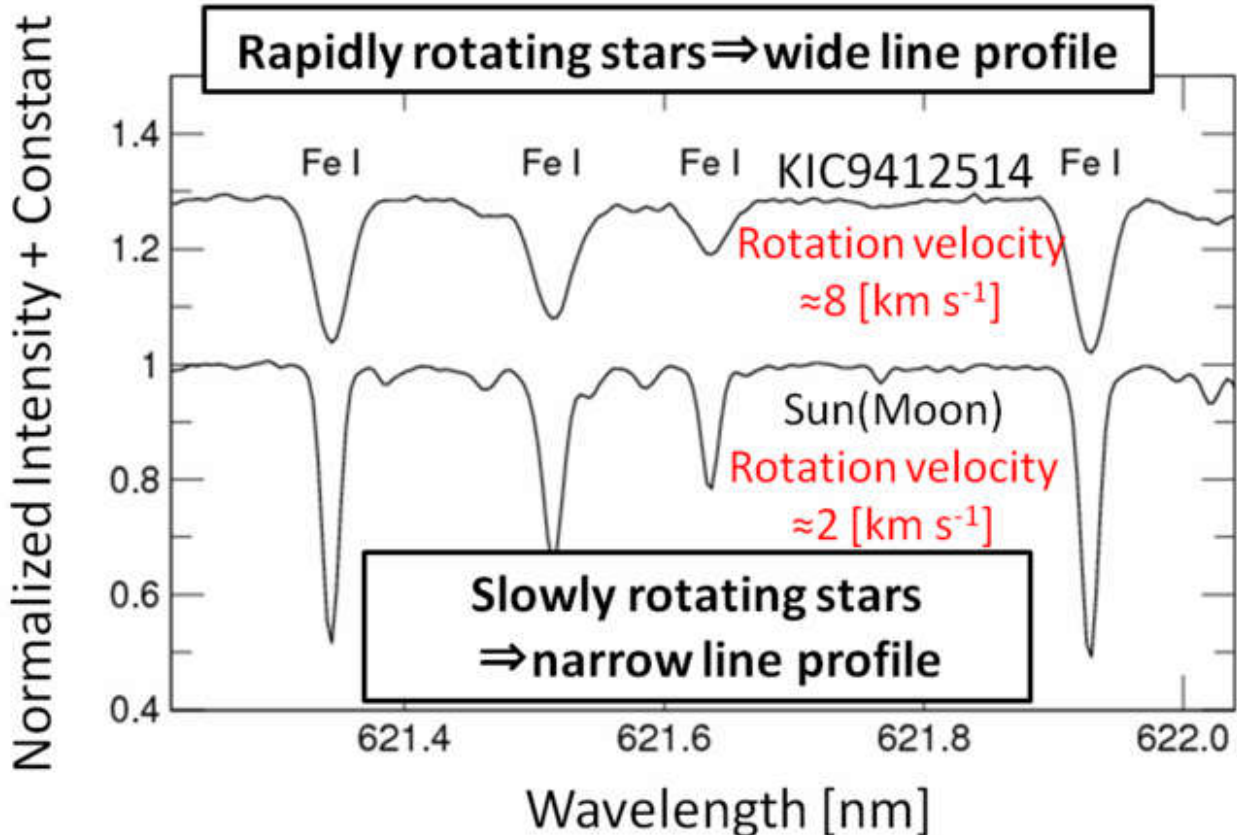
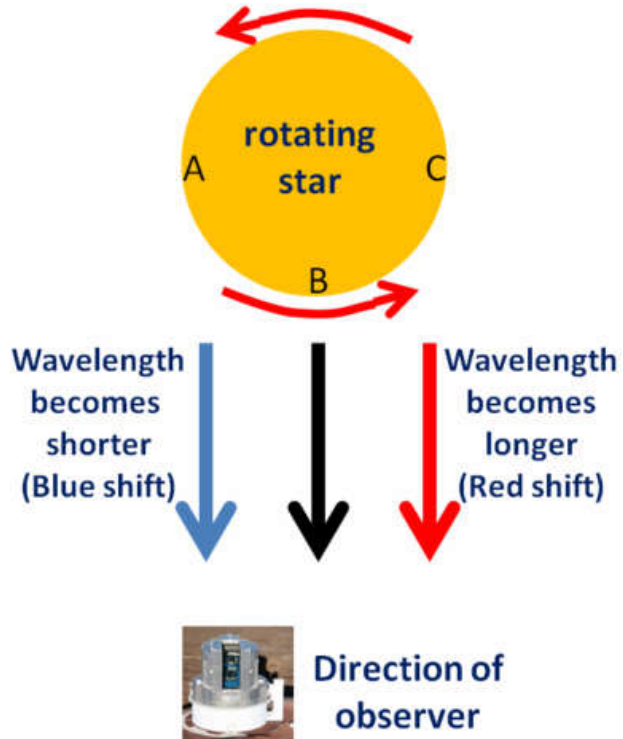
# Effetti della rotazione (emissione)



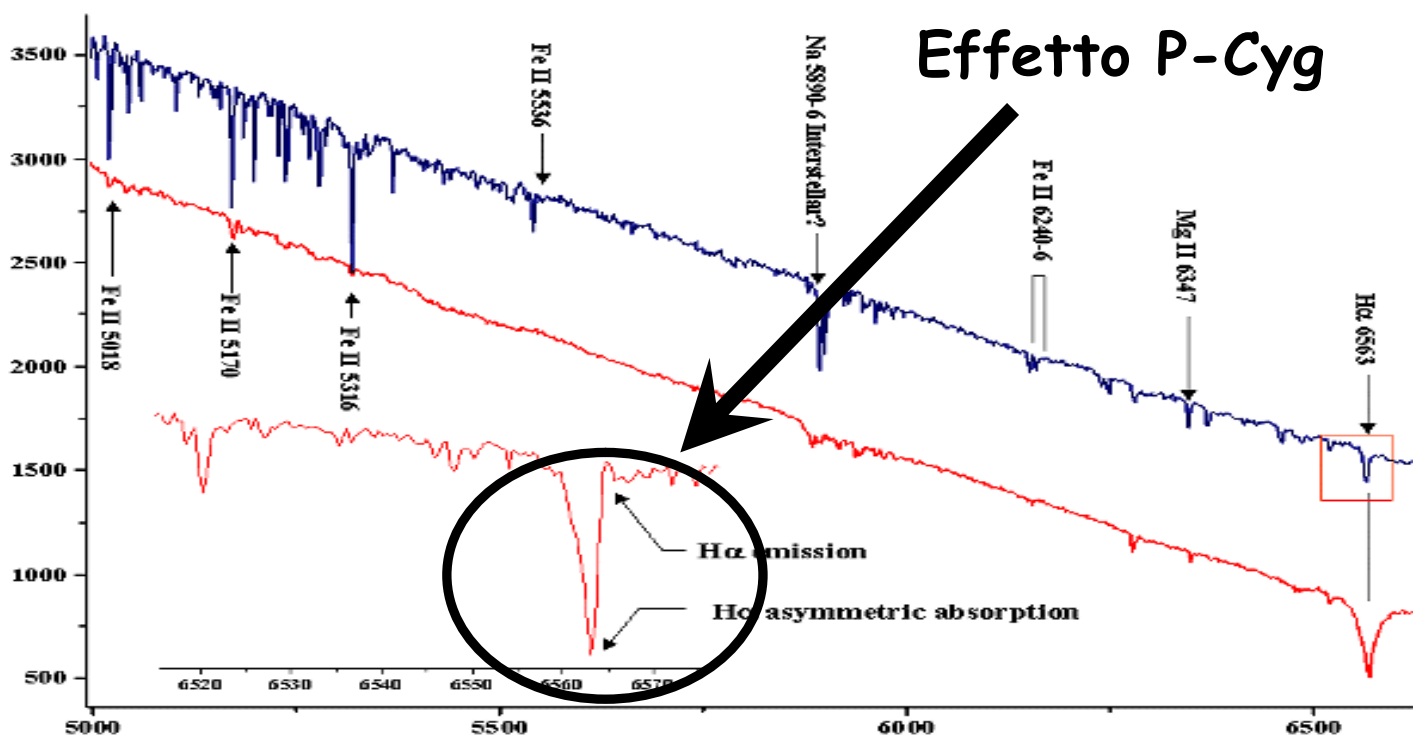
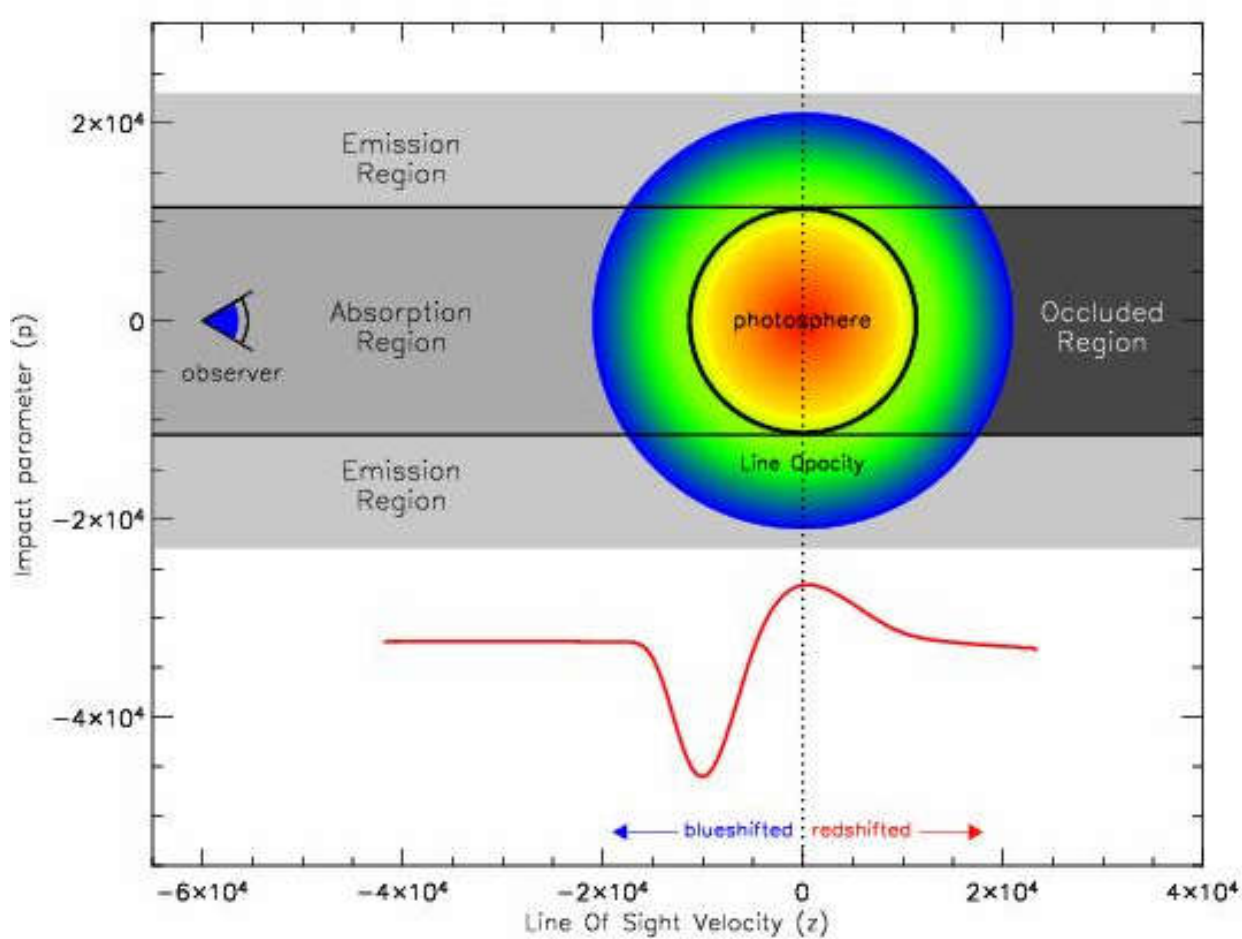
"SMMJ02399-0136 appears to contain a massive molecular ring/disk which rotates about a buried type 2 QSO. Its dynamical mass of  $>3.10^{11}$  Msun within a radius of 8 kpc"

A Very Massive Submillimeter Galaxy at  $z = 2.8$  (Genzel et al. 2003)

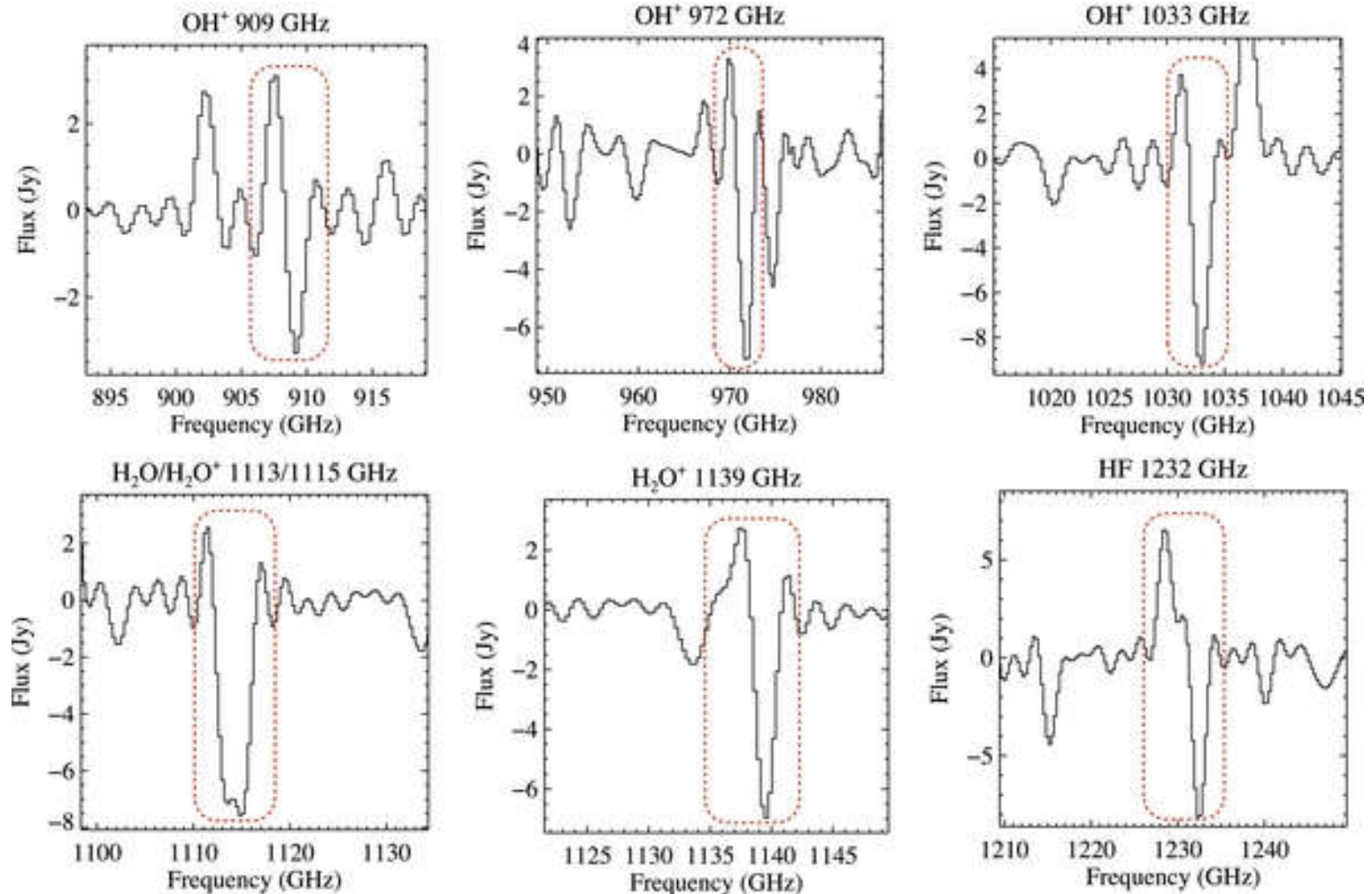
# Effetti della rotazione (assorbimento)



# L'effetto P Cygni

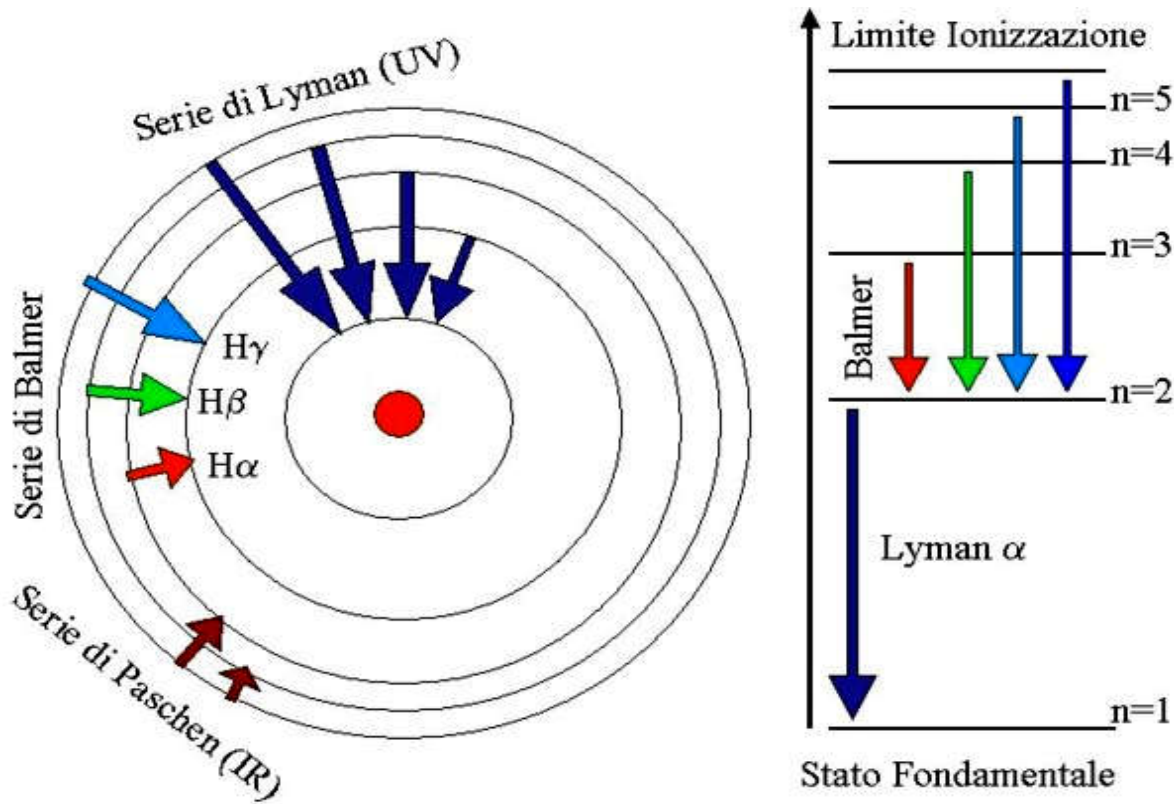


# L'effetto P Cygni (Arp 220)



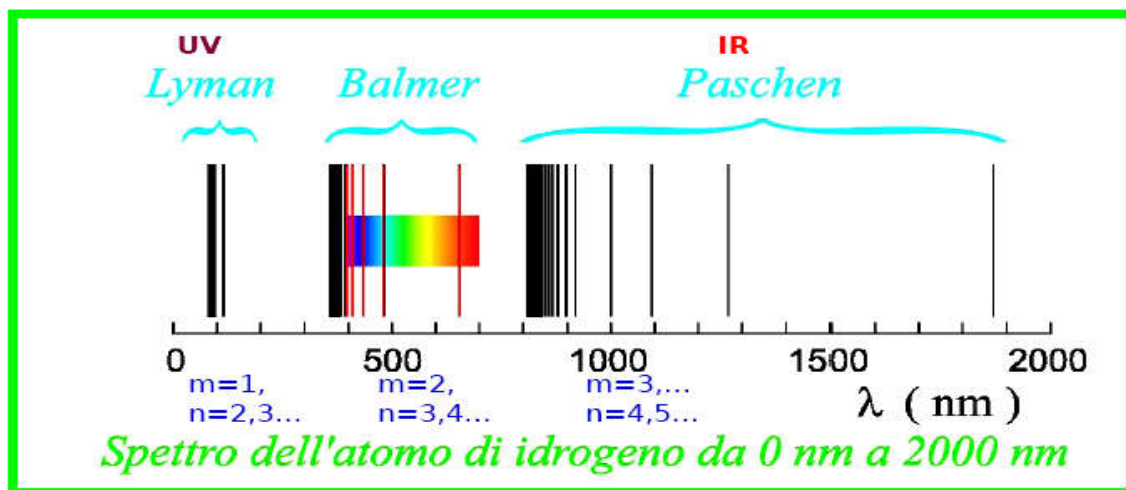
Arp 220 is the nearest Ultra Luminous Infrared galaxy (ULIRG) at a distance of about 77 Mpc and  $z \sim 0.0181$ . It has  $LFIR \sim 10^{12} L_{\odot}$ , and is one of the most popular templates for studies of high- $z$  dusty galaxies. (Rangwala et al., 2011)

# Le righe dell'Idrogeno



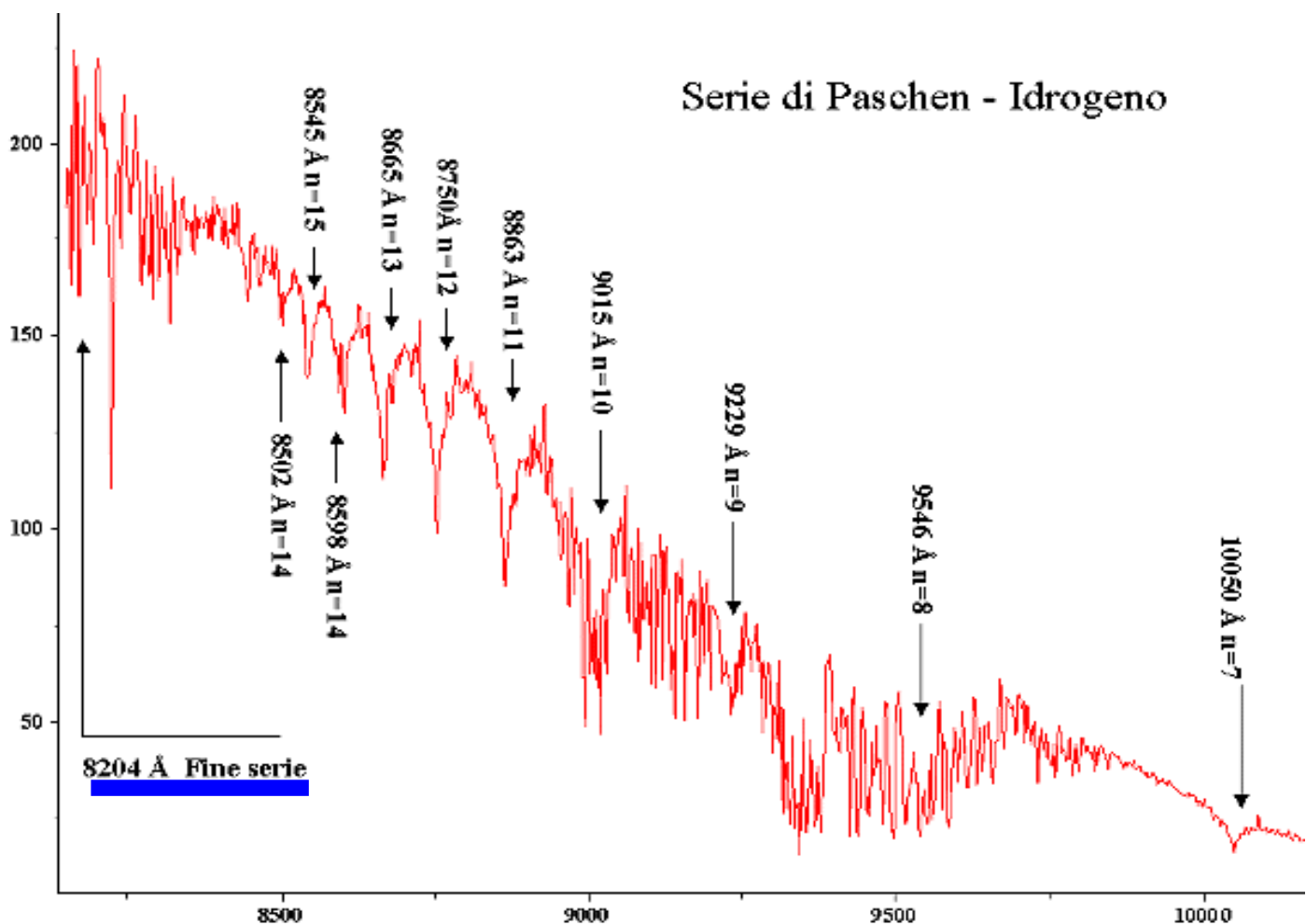
**Righe emesse non solo nel visibile**

$$\frac{1}{\lambda} = R \left( \frac{1}{m^2} - \frac{1}{n^2} \right) \quad m=1,2,3,\dots \quad n=m+1,\dots$$



# Le serie di righe

Nome della serie	Anno della scoperta	<i>m</i> nella formula di Rydberg	Limite della serie (nm)	$\lambda_{\max}$ ( $n=m+1$ ) (nm)	Regione spettrale
<b>Lyman</b>	1906-1914	1	<b>91.126</b>	<b>121.5</b>	UV lontano
<b>Balmer</b>	(1885)	2	<b>364.506</b>	<b>656.1</b>	Visibile-UV
<b>Paschen</b>	1908	3	<b>820.14</b>	<b>1874.6</b>	Infrarosso
<b>Brackett</b>	1922	4	<b>1458.03</b>	<b>4050.1</b>	Infrarosso
<b>Pfund</b>	1924	5	<b>2278.17</b>	<b>7455.8</b>	Infrarosso
<b>Humphreys</b>	1953	6	<b>3280.56</b>	<b>12365.1</b>	Infrarosso
<b>Hansen-Strong</b>	1973	7	<b>4465.21</b>	<b>19051.5</b>	Infrarosso

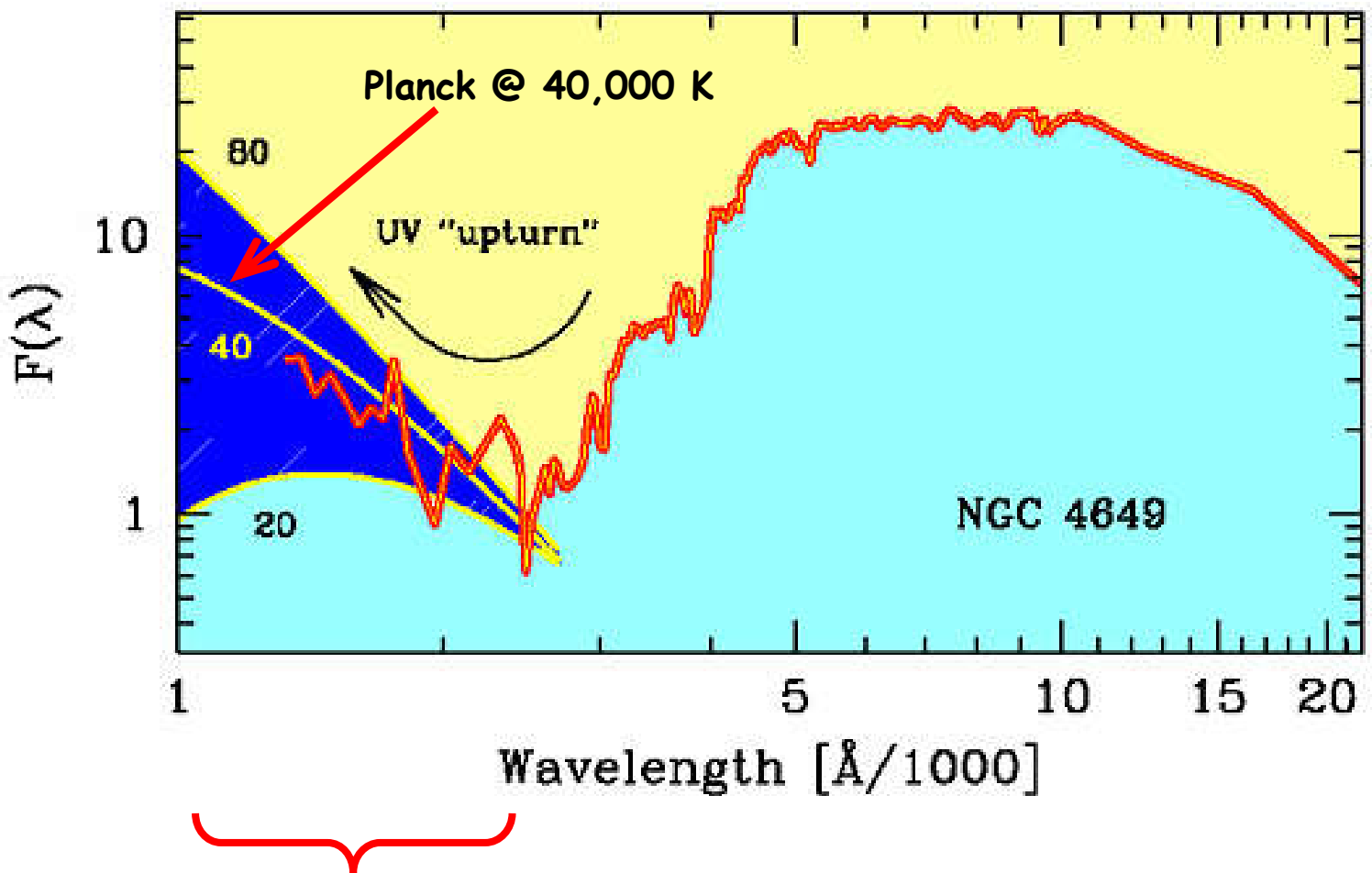


**Articoli consigliati (vedi Webpage):**

<http://www.bo.astro.it/~eps/lezioni/lezioni.html>

- **Galaxy Colors (Buzzoni 2005)**
- **Energetic & Chemical evolution of Spirals (Buzzoni 2011)**
- **Spectral Properties of Galaxies (Kennicutt 1992)**
- **Galaxy Spectral Atlas (Kennicutt 1992)**
- **SFR & Hubble Sequence (Kennicutt 1988)**
- **SFR in the MW (Kennicutt & Evans 2012)**
- **SFR (Schmidt 1959)**
- **Galaxy mass assembly (Pan 2015)**

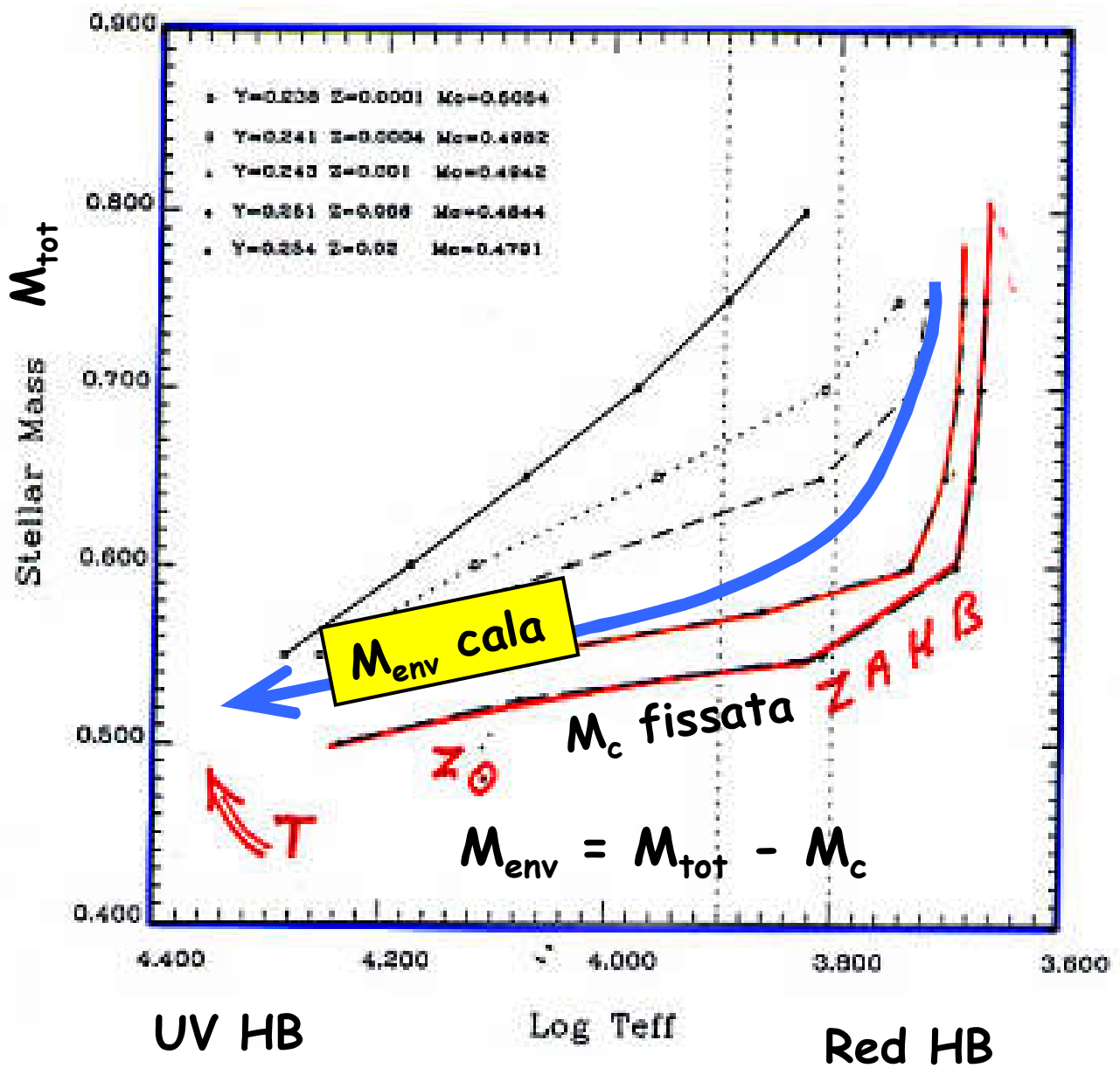
# L'emissione UV nelle SSPs: l'UV Upturn nelle galassie ellittiche



$$\left[ \frac{\text{Integrale Planck}}{\text{Bolometrico}} \right] = \begin{matrix} 20,000 & 40,000 & 80,000 \text{ K} \\ 1.4\% & 2.1\% & 6.0\% \end{matrix}$$

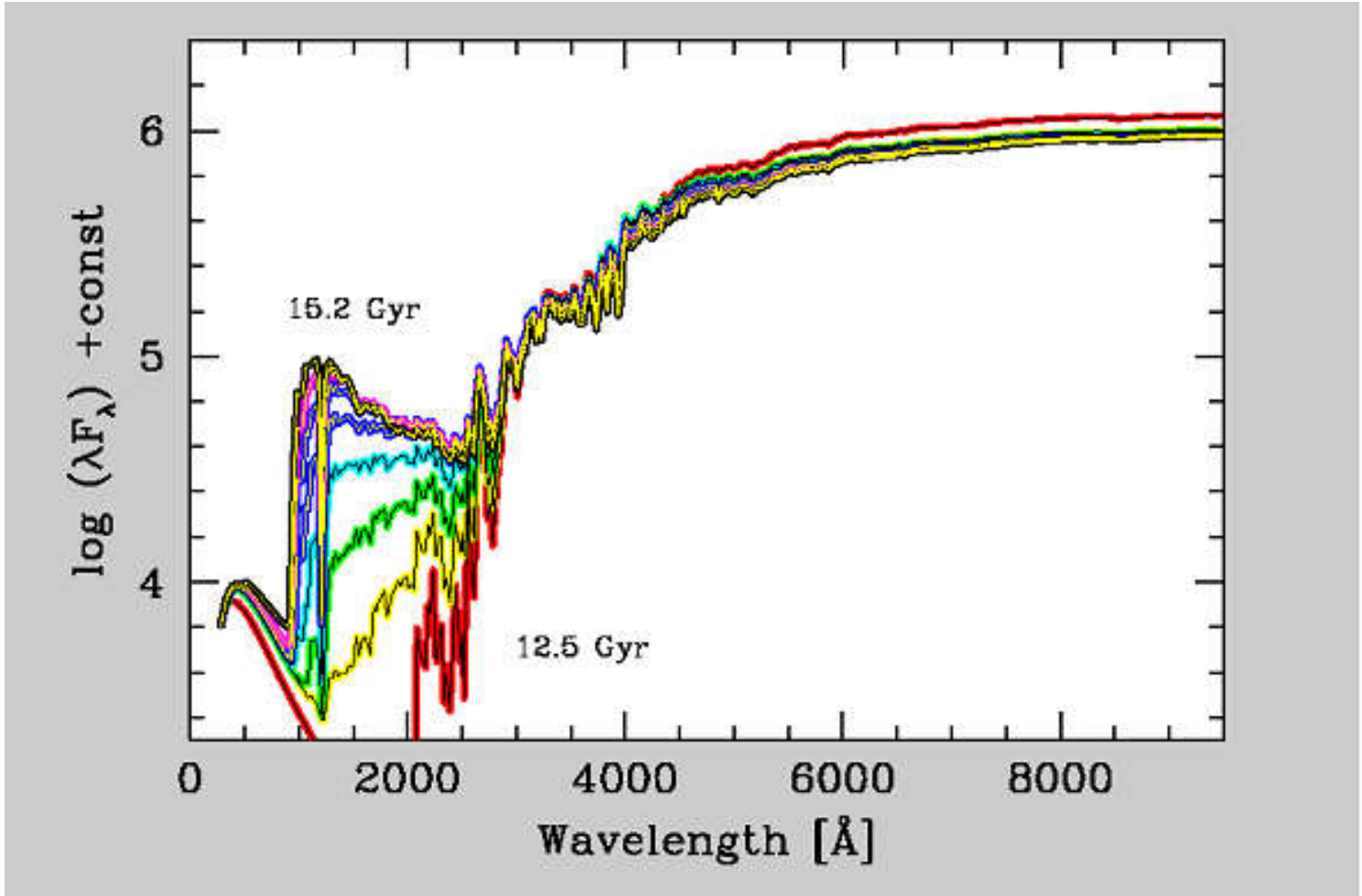
# Il meccanismo della Massa di core in HB

Castellani (1991)



- $M_{\text{env}} \text{ cala se}$  {
- 1) Aumenta  $M_c$  ( $= Y \uparrow$  perche'  $Z \uparrow$ )
  - 2) Aumenta la "mass loss" ( $= Z \uparrow ??$ )

# Evoluzione spettrale dell'UV upturn



A parità di efficienza del meccanismo che modula  $M_{env}$ , se aumenta  $M_{TO}$  possiamo aspettarci che aumenti anche  $M_{HB}$ . Siccome la  $T_{HB}$  è molto sensibile a  $M_{HB}$ , se  $t \uparrow$  allora  $M_{TO} \uparrow$  e  $M_{HB} \uparrow$ . Quindi  $M_{env} \uparrow$  e  $T \downarrow$ . Quindi il Braccio Orizzontale tende velocemente al rosso e l'UV upturn scompare:

$$\frac{dt}{t} \approx -2 \frac{dM_{TO}}{M_{TO}} \approx -2 \frac{dM_{HB}}{M_{HB}}. \text{ Se } \frac{dM_{HB}}{M_{HB}} \approx 0.1 \Rightarrow \frac{dt}{t} \approx 0.2$$

Quindi, andando indietro di circa 2-3 Glyr ( $z \sim 0.2-0.3$ ) l'effetto dovrebbe scomparire.

M. CASTELLANI et al. (1994)

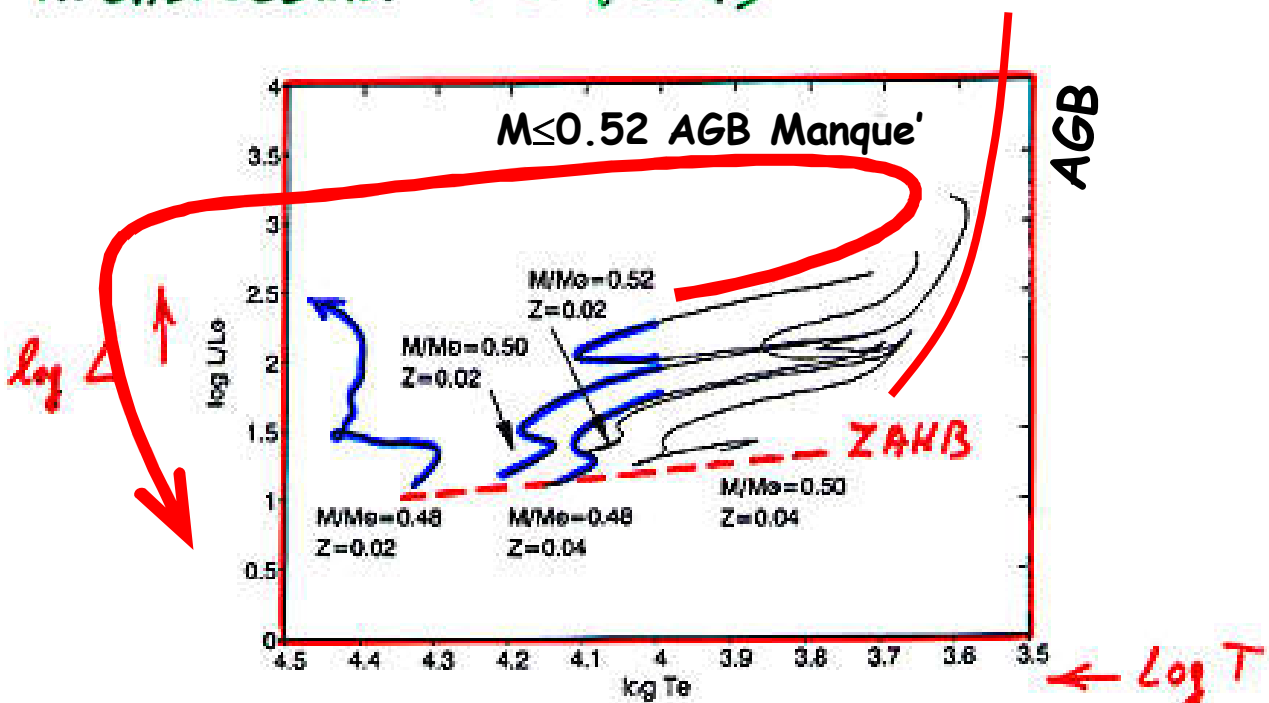


FIG. 1.—The H-R diagram of the models evolved at constant mass covering the central He-burning phase and (in some models) the initial He shell-burning phases.

V. CASTELLANI & TORNAMBÉ (1998)

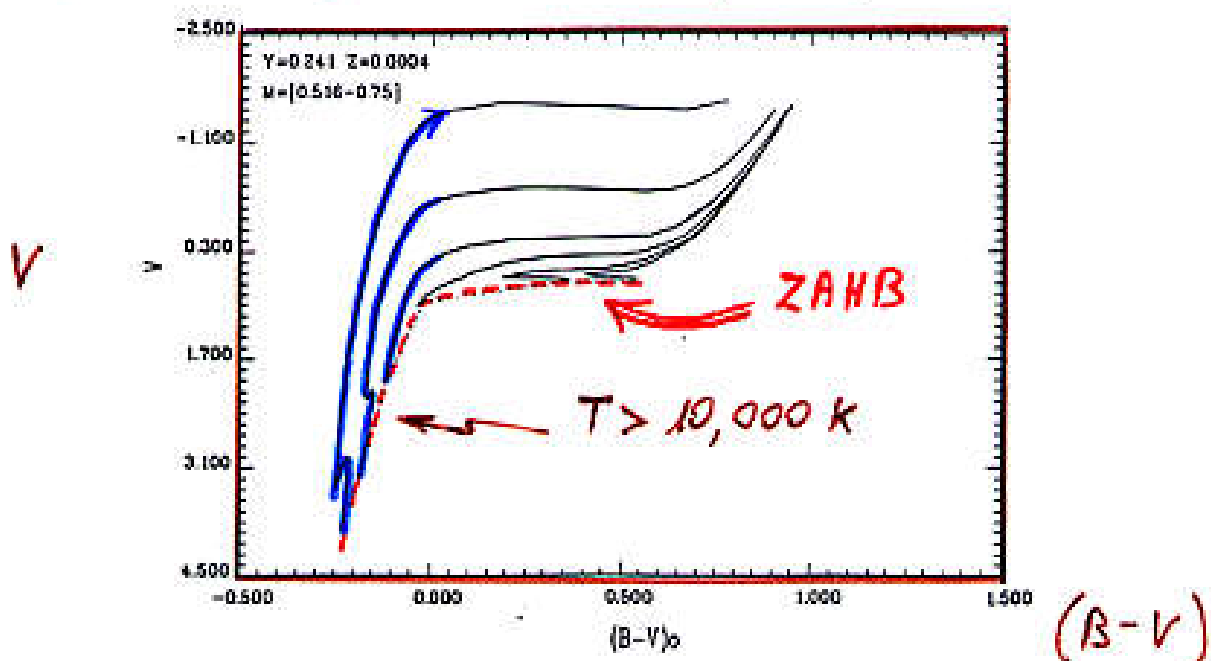


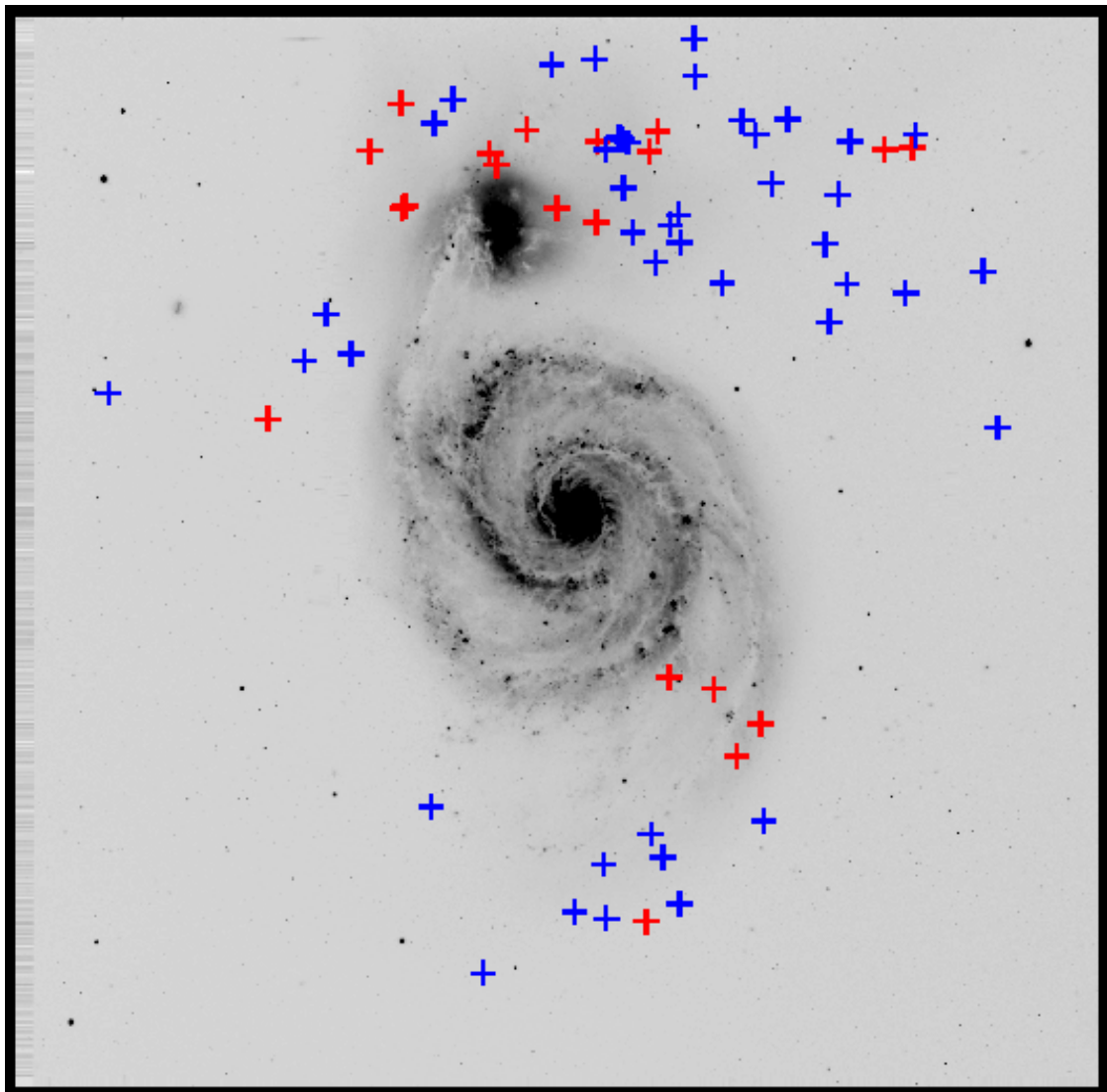
Fig. 5. The evolutionary paths in the  $V, B - V$  plane of HB models with  $Z = 0.0004$  and for selected values of the stellar mass in the labeled range of masses

**Articoli consigliati (vedi Webpage):**

<http://www.bo.astro.it/~eps/lezioni/lezioni.html>

- **SSP Theory (Renzini & Buzzoni 1986)**
- **Galaxy Colors (Buzzoni 2005)**
- **UV Upturn (O'Connell 1999)**
- **UV Upturn (Ali et al. 2018)**
- **Balmer break (Hamilton 1985)**
- **Lick indices (Worley et al. 1994)**

# Le Nebulose Planetarie



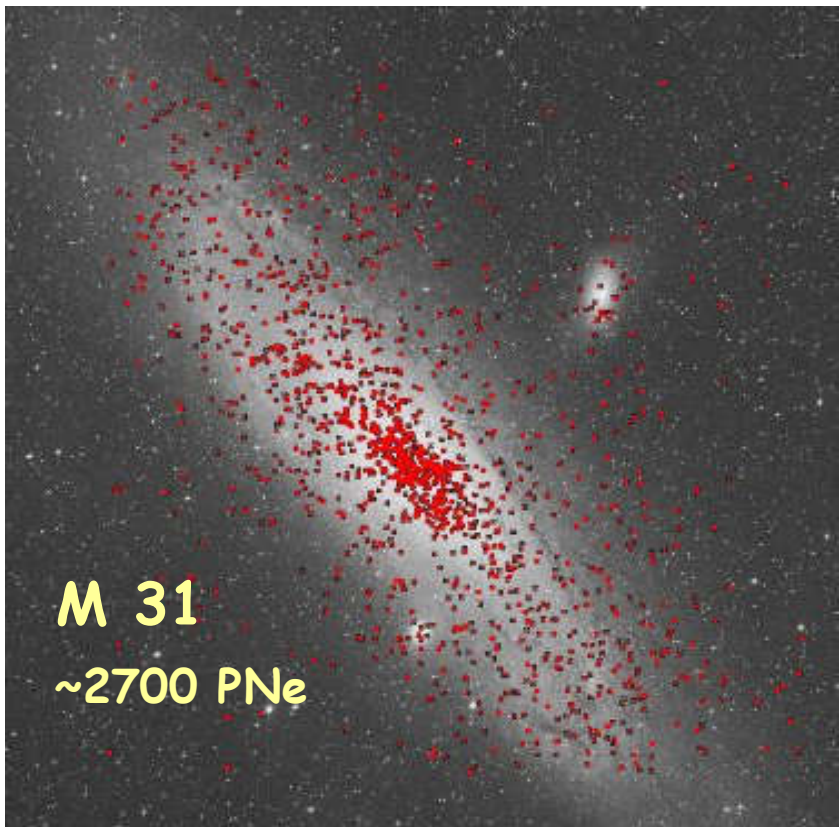
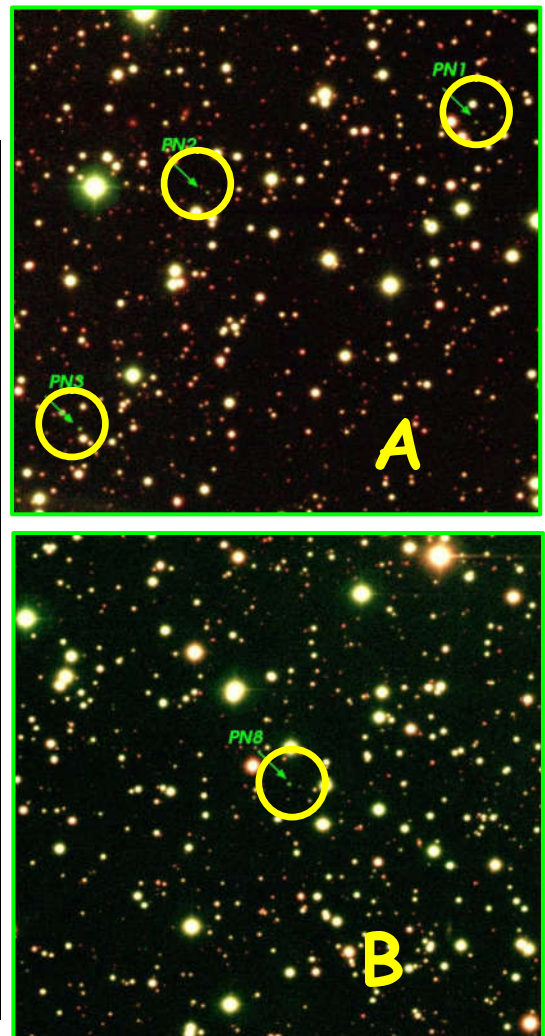
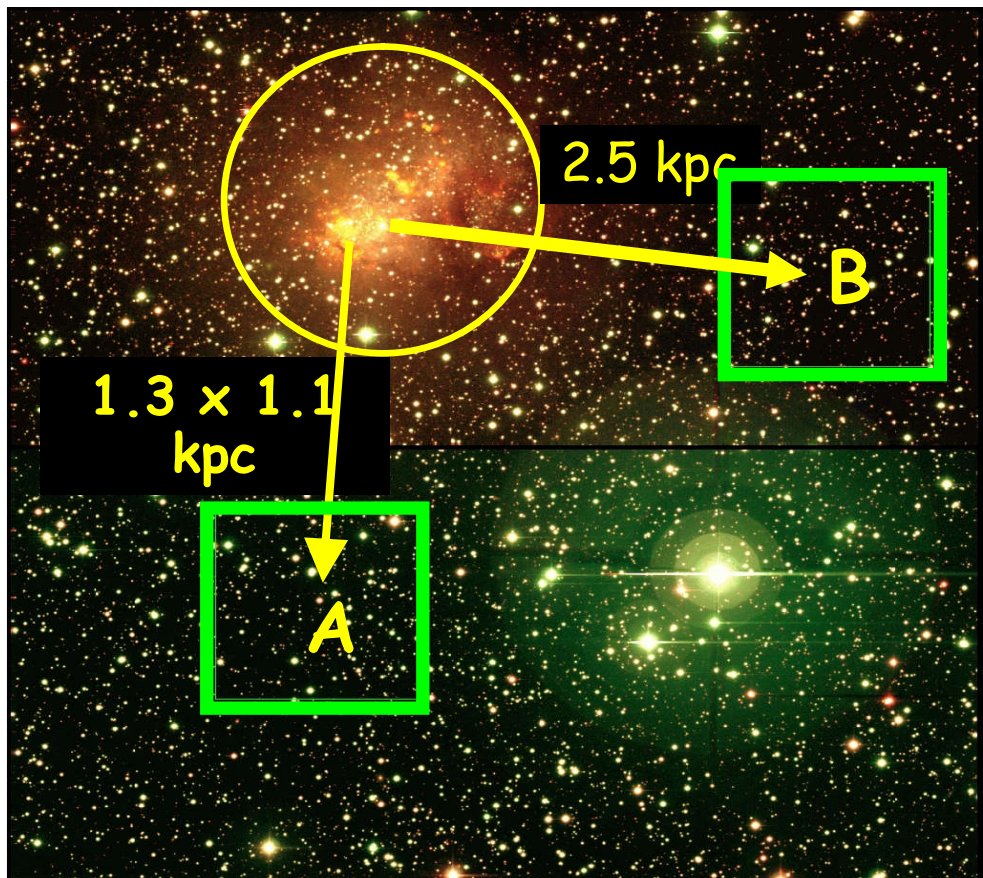
Feldmeier, Ciardullo & Jacoby (1997)

Planetary Nebulae follow **Luminosity** not surface brightness!

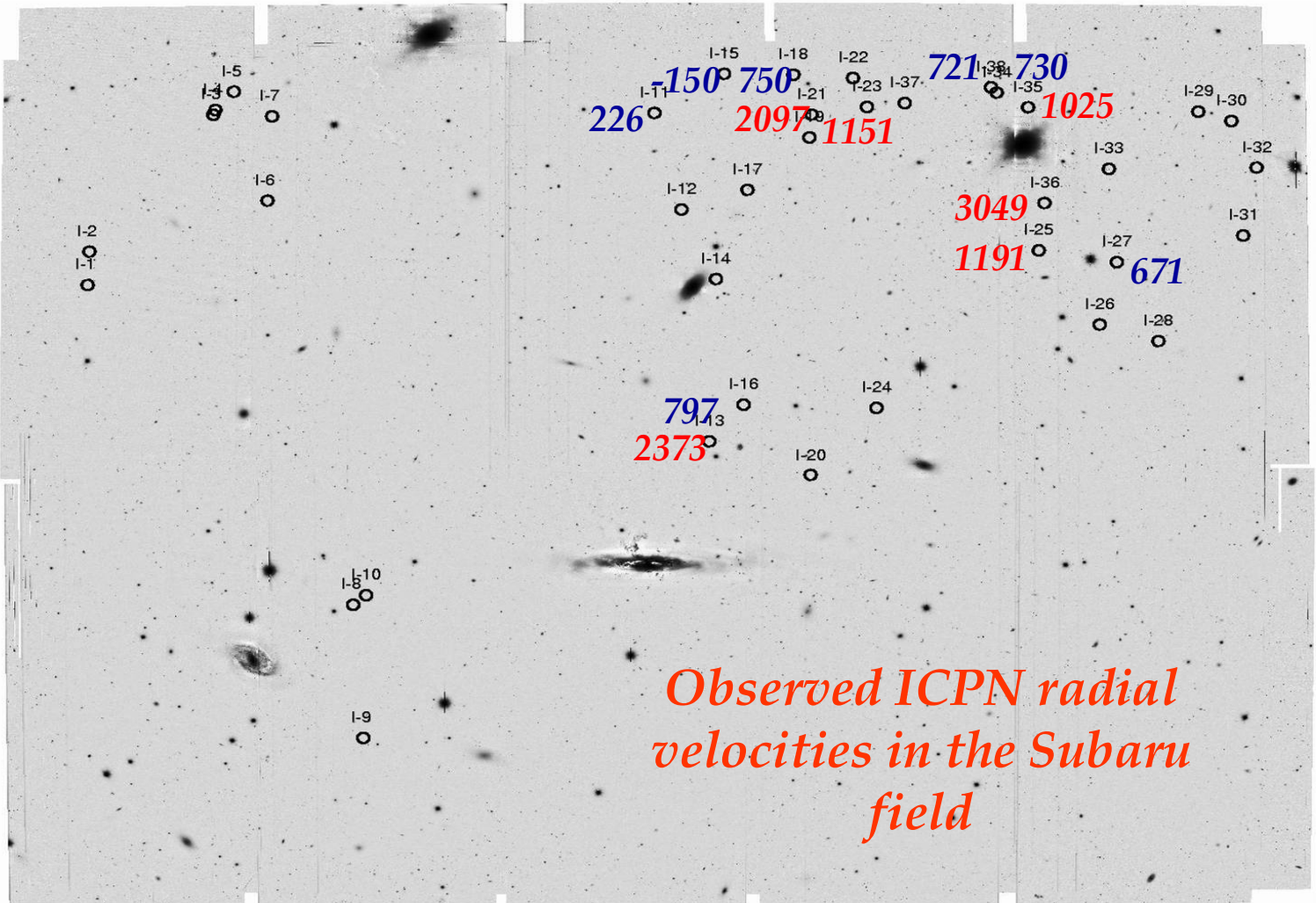
Stars can exist at great distances from luminous galaxies

# Il censimento delle PNe nelle galassie del Gruppo Locale

Magrini et al. 2003 A&A 407 51



# Planetarie intra-galattiche nell'Ammasso della Vergine



(Arnaboldi et al. 2002)

$$N_{PN} = BL_{tot}\tau_{PN} \longrightarrow \alpha = \frac{N_{PN}}{L_{tot}} = B\tau_{PN}$$

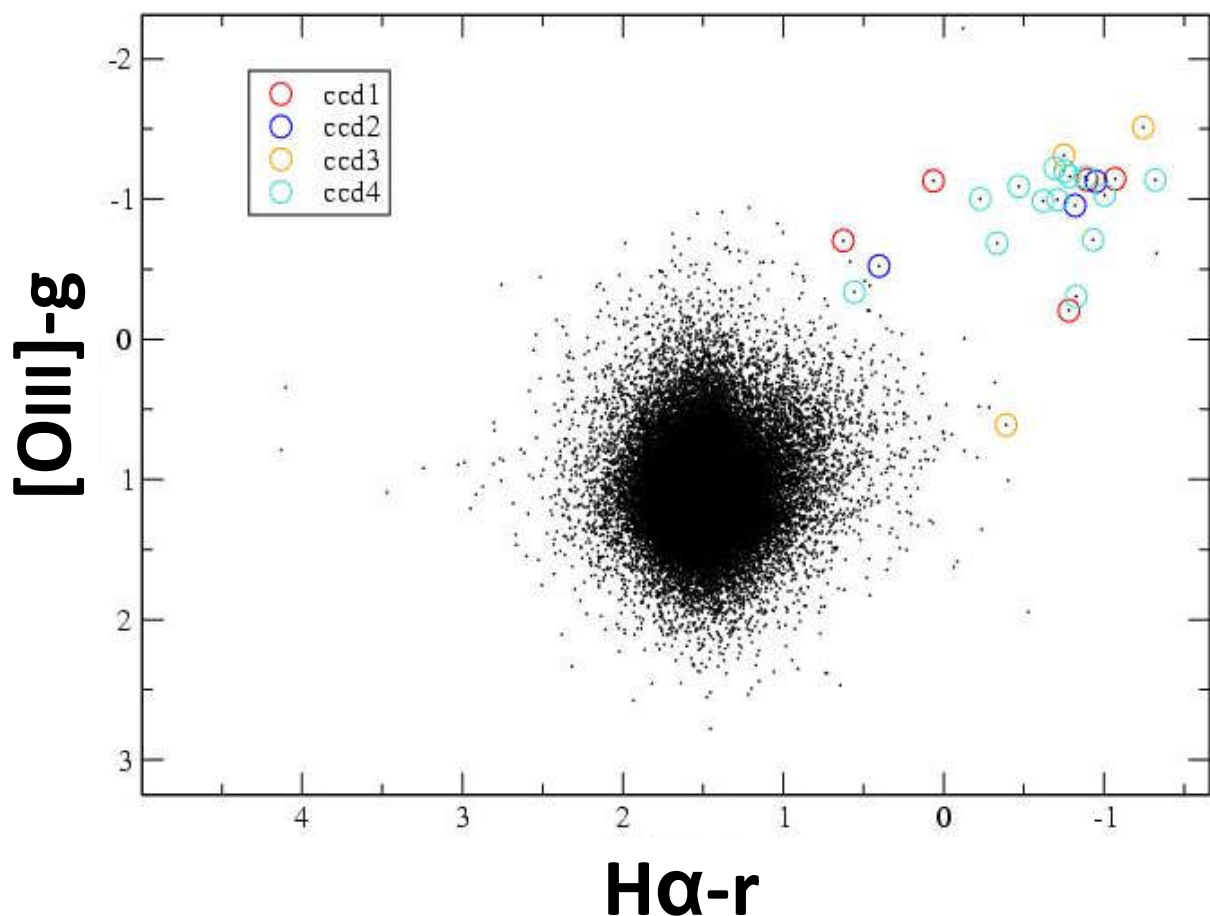
quindi  $\alpha = \frac{N_{PN}}{L_{tot}} \approx 2 \times 10^{-11} \times 3 \times 10^4 = 6 \times 10^{-7}$

Ovvero, 1 PN campiona:  $L_{tot} \approx \frac{1}{\alpha} \approx 1.7 \times 10^6 L_{sun}$

# [OIII]-g vs. H $\alpha$ -r color-color diagrams

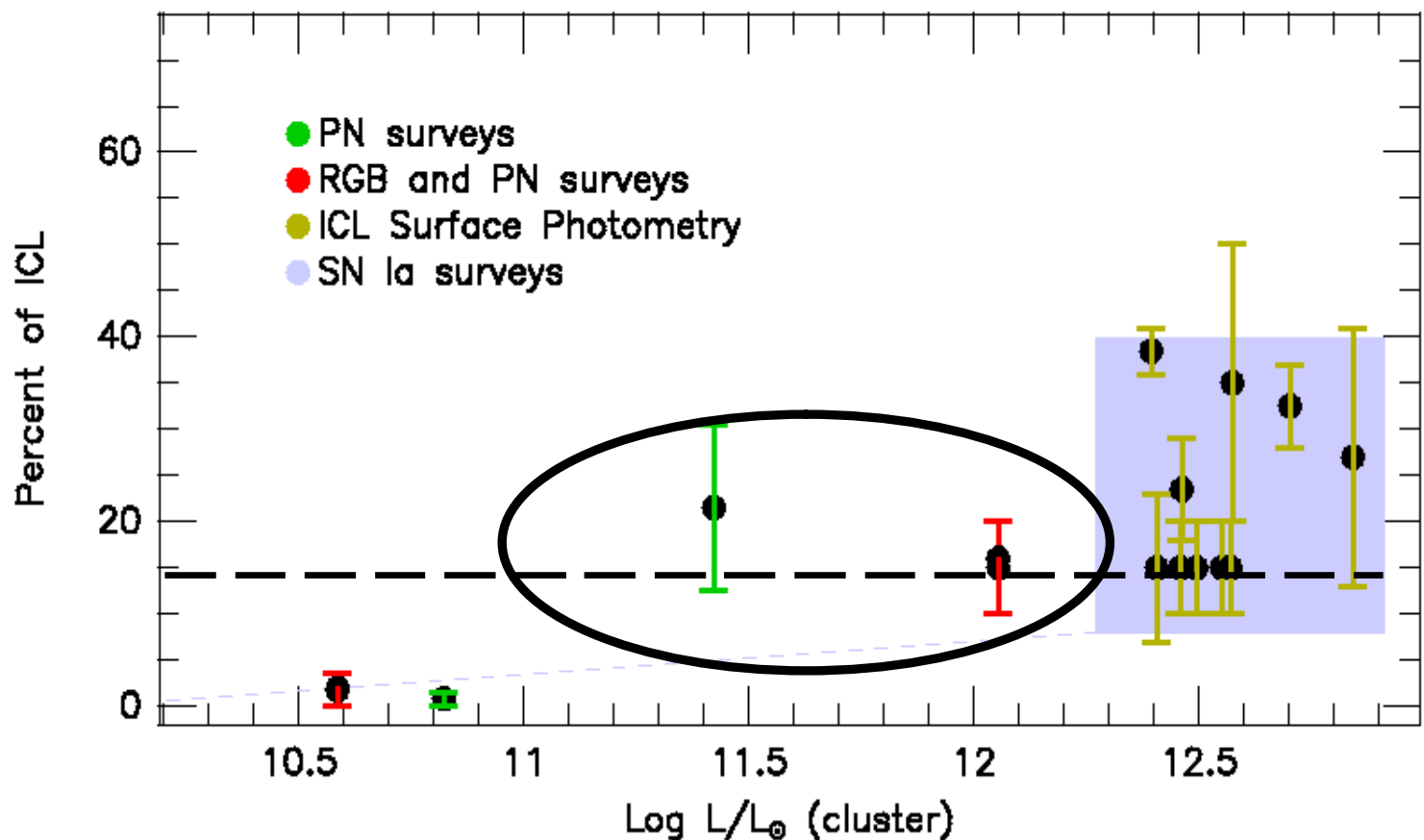
**NGC 205**

Planetary Nebulae in NGC205, field B



# PNe e Intra-Cluster Luminosity (ICL)

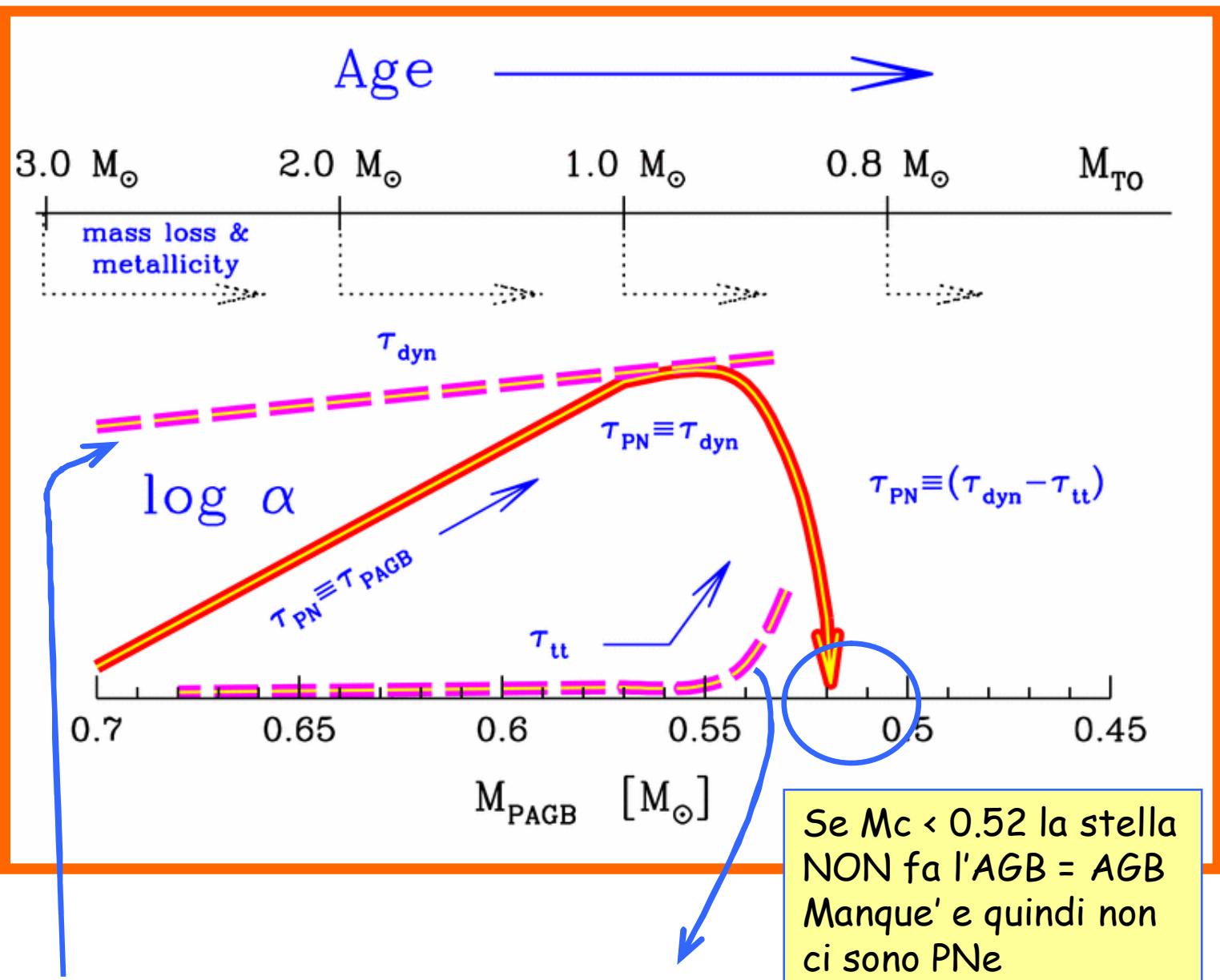
(Ciardullo et al. 2003)



Per l'Ammasso della Vergine, si valuta una ICL dell'ordine del 15% della L dell'intero ammasso.

# Tempi scala di visibilità delle PNe

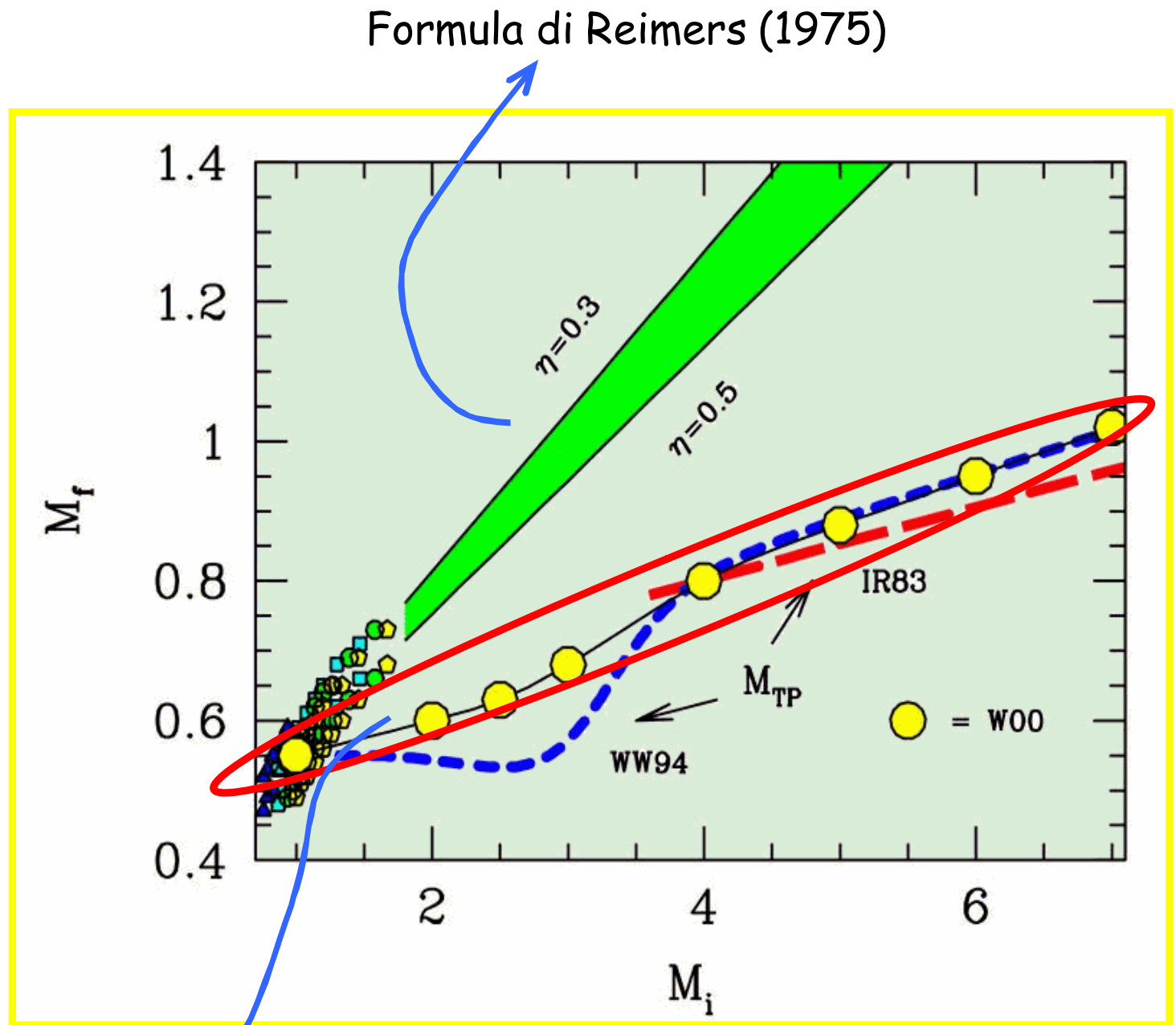
Buzzoni, Arnaboldi & Corradi (2006)



Tempo dinamico  
(evaporazione inviluppo)  
 $V \sim 10$  km/sec

Tempo di transizione  
da AGB freddo a  
 $T \sim 50,000$  K

# Massa iniziale e finale delle stelle

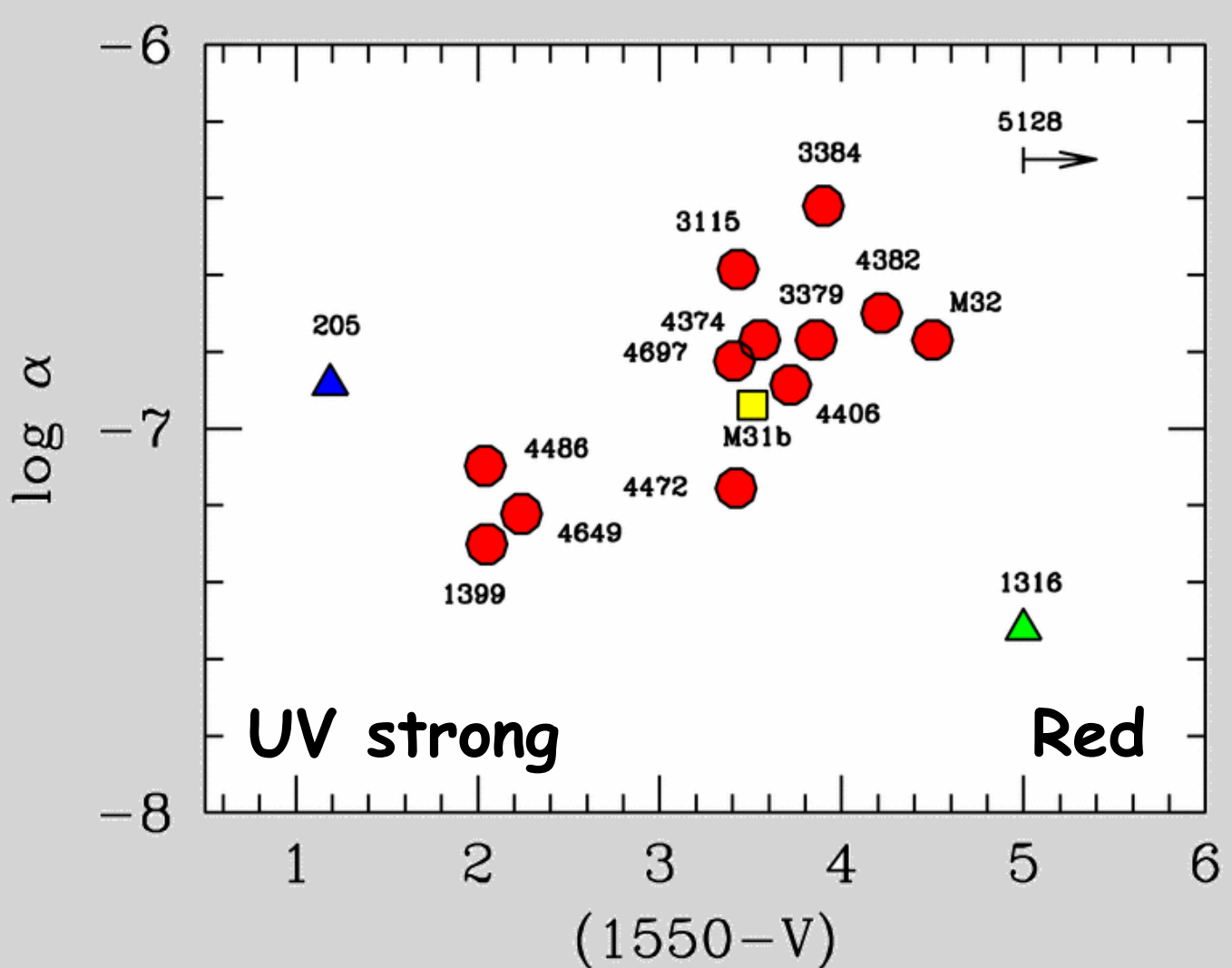


Buzzoni, Arnaboldi & Corradi (2006)

Osservazione empirica di Weidemann (2000) dagli ammassi aperti Galattici, dove  $M_i = M_{TO}$ , e  $M_f = M_{WD}$

Si vede che le PNe devono avere sempre una massa  $\ll 1M_{\text{sun}}$

# PNe e UV upturn nelle galassie ellittiche



Buzzoni, Arnaboldi & Corradi (2006)

Un forte UV da stelle HB implica molte stelle AGB  
manque' e quindi a↓

**Articoli consigliati (vedi Webpage):**

<http://www.bo.astro.it/~eps/lezioni/lezioni.html>

- **SSP Theory (Renzini & Buzzoni 1986)**
- **ICM & Planetary Nebulae (Arnaboldi 2003)**
- **Planetary Nebulae (Buzzoni et al. 2006)**

# Entropia Fotometrica

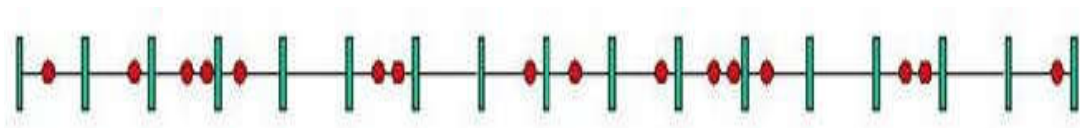
## What a Photometric Entropy theory is for?

Entropy is a measure of the intrinsic “variance” of a stellar aggregate along the different spectral range of observation.

- Surface-brightness Fluctuations
- Crowding
- Diagnostics from Narrow-band Spectroscopy

# Some Fundamentals

$$p(x) = \frac{e^{-\lambda} \lambda^x}{x!} \quad \text{for } \lambda > 0 \quad \text{and } x = 0, 1, 2, \dots$$



1, 2, 3, .......

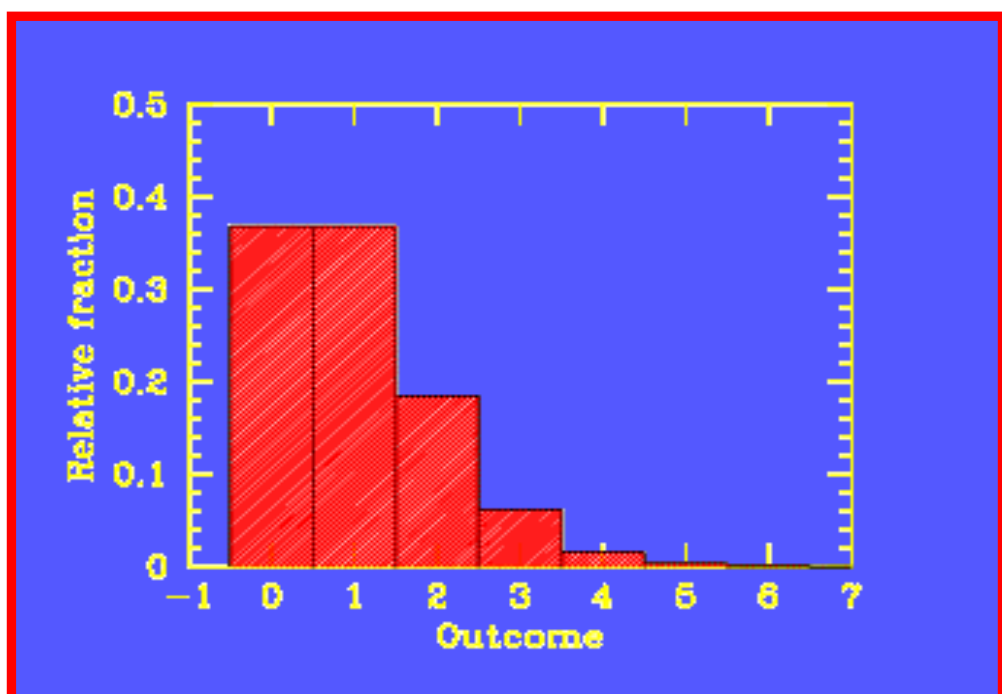
.....  $N_{tot}$

→  $N = 1 \pm 1$  for each cell  $L_{tot} = \sum \ell_* = N_{tot} \ell_*$

$$\sigma(N_{tot}) = \sqrt{\sum 1} = \sqrt{N_{tot}}$$

$$\sigma(L_{tot}) = \sqrt{\sum \ell_*^2} = \ell_* \sqrt{N_{tot}}$$

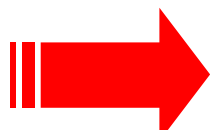
$$\sigma(L_{tot})/L_{tot} = 1/\sqrt{N_{tot}}$$



More generally, if  $\ell_*$  is NOT a constant, we can still define

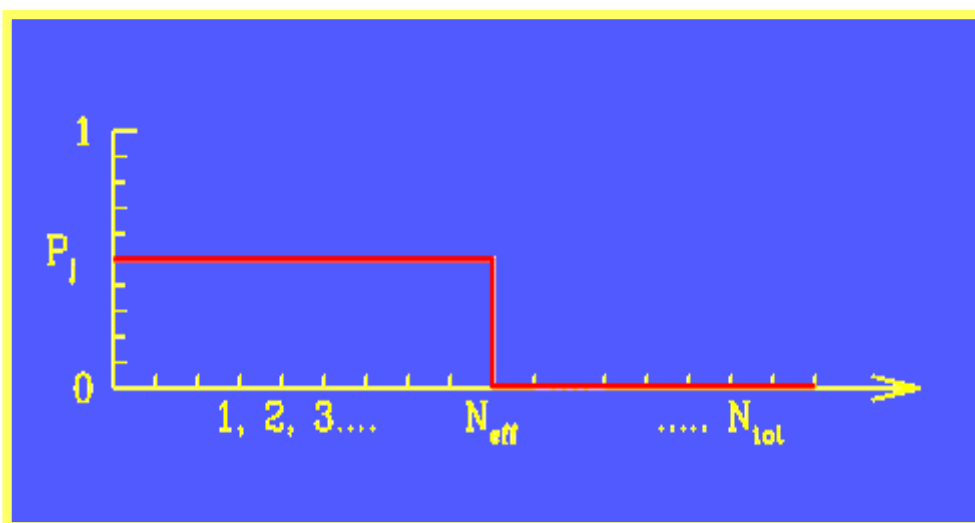
where, always,

$$N_{\text{eff}} \leq N_{\text{tot}}$$



$N_{\text{eff}}$  will depend on  $\lambda$  as  $\ell_*$  depends on  $\lambda$

$$S = \log(N_{\text{eff}}/N_{\text{tot}})$$

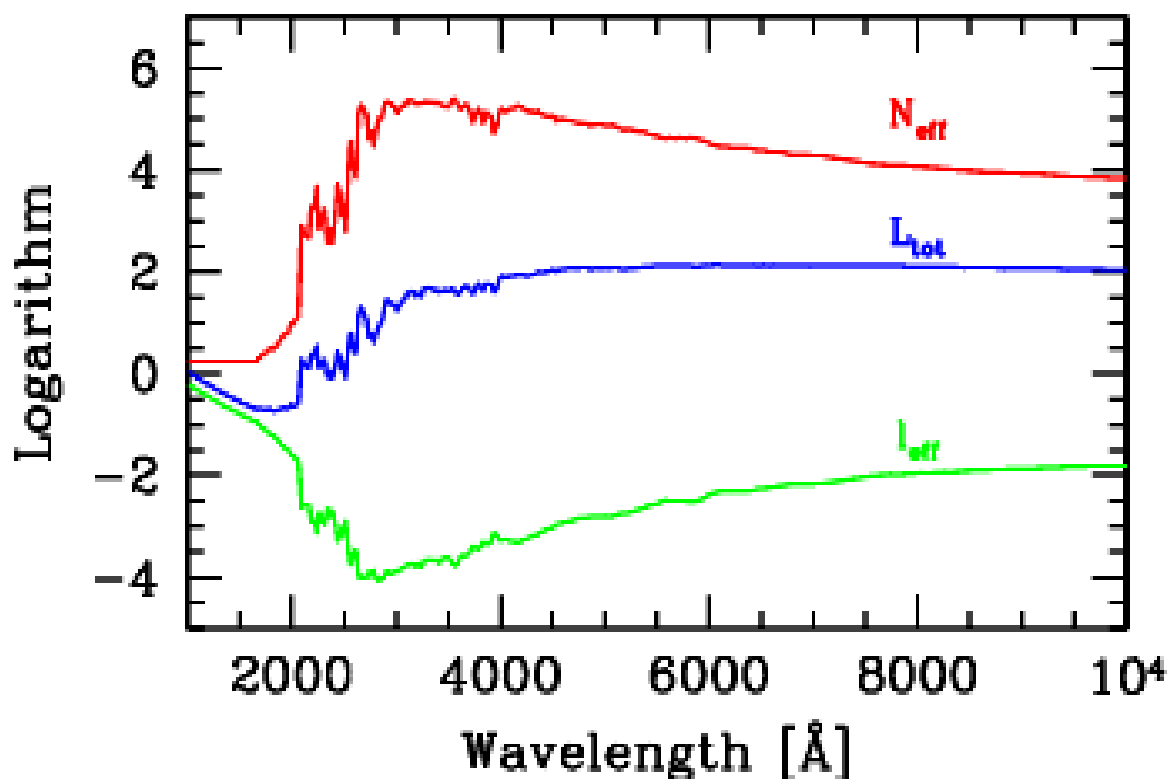


Quite importantly,  
 $S = S(\lambda)$

In order to fix  $N_{\text{eff}}$  (and Entropy) we need a photometric argument

$$\sigma^2(L_{\text{tot}}) / L_{\text{tot}} = \sum \ell_*^2 / \sum \ell_* = \ell_{\text{eff}}$$

At every  $\lambda$ , it must be:



Buzzoni (1993), A&Ap, 275, 433

Cerviño et al. (2002), A&Ap, 381, 51

# Teoria dettagliata

CASO A)  $N$  stelle di fissata luminosità  $\ell_*$

$$L_{\text{TOT}} = \sum^N \ell_* = N \ell_*$$

$$\sigma_{L_{\text{TOT}}} = \left( \sum \sigma_j^2 \right)^{\frac{1}{2}} \quad \forall * \quad m=1 \pm 1 \quad (\text{Poisson})$$

$$\left( \sum (l_* + 1)^2 \right)^{\frac{1}{2}} \rightarrow (N l_*^2)^{\frac{1}{2}} \rightarrow l_* \sqrt{N}$$

Quindi:

$$\frac{\sigma_L}{L_{\text{TOT}}} = \frac{l_* \sqrt{N}}{l_* N} = \frac{1}{\sqrt{N}}$$

CASO B)  $N$  stelle tutte diverse

$$L_{\text{TOT}} = \sum^N \ell_j = N \langle \ell \rangle \quad \text{dove } \langle \ell \rangle = \frac{\sum \ell_j}{N}$$

$$\sigma_{L_{\text{TOT}}} = \left( \sum \ell_j^2 \right)^{\frac{1}{2}} = \sqrt{N} \langle \ell^2 \rangle \quad \text{dove } \langle \ell^2 \rangle = \frac{\sum \ell_j^2}{N}$$

media quadratica

$$\text{dove } K = \left[ \frac{\langle \ell^2 \rangle}{\langle \ell \rangle^2} \right]^{\frac{1}{2}}$$

$K > 1$  perché  $\langle \ell \rangle^2 < \langle \ell^2 \rangle$

$$\frac{K}{\sqrt{N}} = \frac{1}{\sqrt{N_{\text{eff}}}} \Rightarrow \frac{N_{\text{eff}}}{N} = \frac{1}{K^2}$$

Quindi è sempre  $N_{\text{eff}} \leq N$

Definiamo ENTRPIA FOTOMETRICA:

$$S = -2 \log K = \log \frac{N_{\text{eff}}}{N}$$

## Analisi della varianza

$$\sigma_{L_{TOT}}^2 = \sum l_i^2$$

$$\frac{\sigma_L^2}{L_{TOT}} = \frac{N \langle l^2 \rangle}{N \langle l \rangle} \rightarrow \text{Questo rapporto ha le dimensioni di una luminosità}$$

quindi  $\ell_{app} = \frac{\langle l^2 \rangle}{\langle l \rangle} = \frac{\sum l^2}{\sum l}$

Che relazione c'è fra  $N_{app}$  e  $\ell_{app}$ ?

$$N_{app} \cdot \ell_{app} = \frac{N}{k^2} \frac{\langle l^2 \rangle}{\langle l \rangle} = \frac{N \cancel{\langle l^2 \rangle} \langle l \rangle^2}{\cancel{\langle l^2 \rangle} \cancel{\langle l \rangle^2}} = N \langle l \rangle^2$$

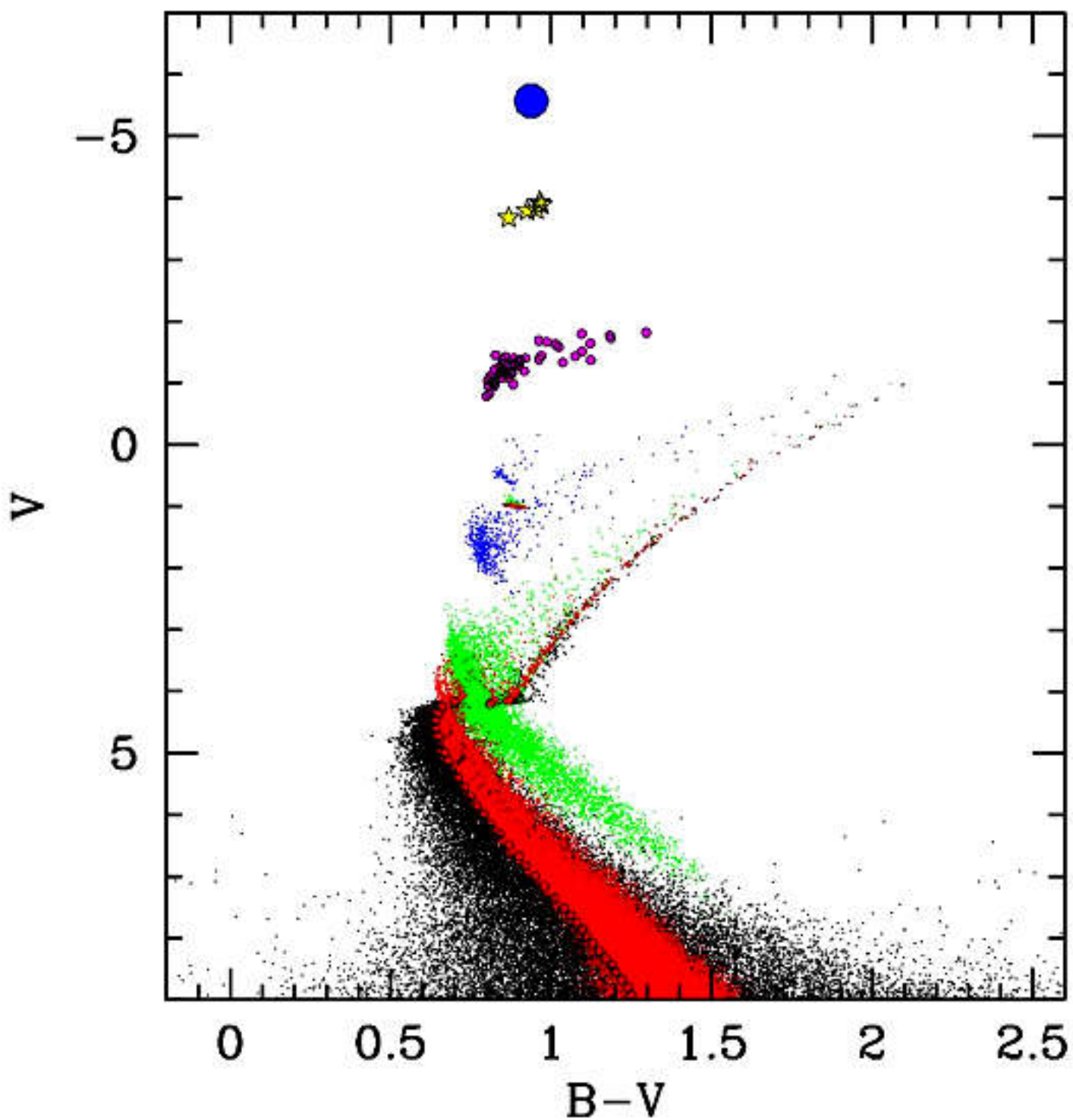
$\downarrow$   
 $N \frac{\sum l}{N}$

Quindi  $N_{app} \times \ell_{app} = L_{TOT}$

SSP

(Age, [Fe/H], IMF)

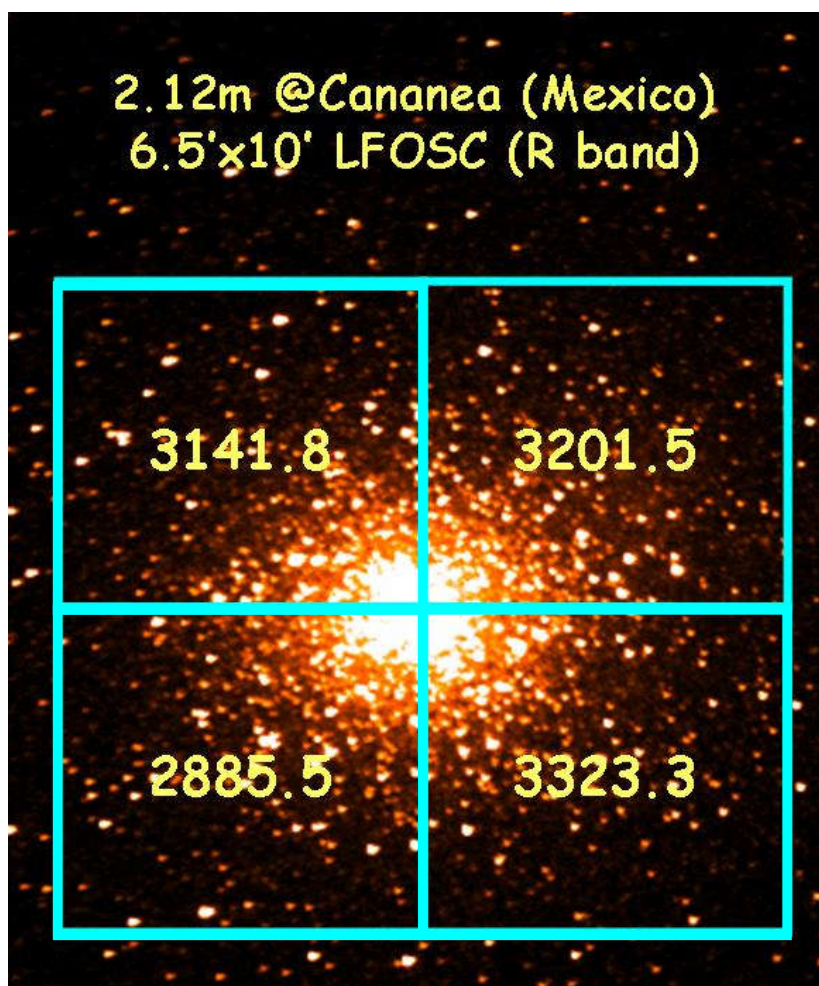
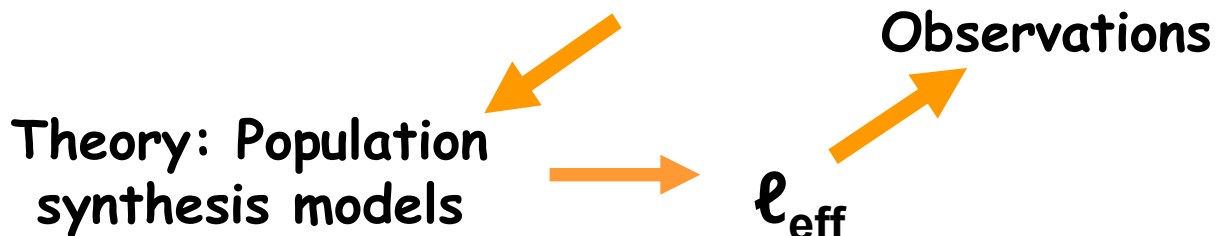
(15 Gyr, 0.0, Salpeter)



# Surface-Brightness Fluctuations: an alternative approach for the case of M53

First application of the theory to galx's: Tonry & Schneider (1988) and Tonry (1991)

$$\sigma^2(L_{\text{tot}}) / L_{\text{tot}} = \sum \ell_*^2 / \sum \ell_* = \ell_{\text{eff}}$$

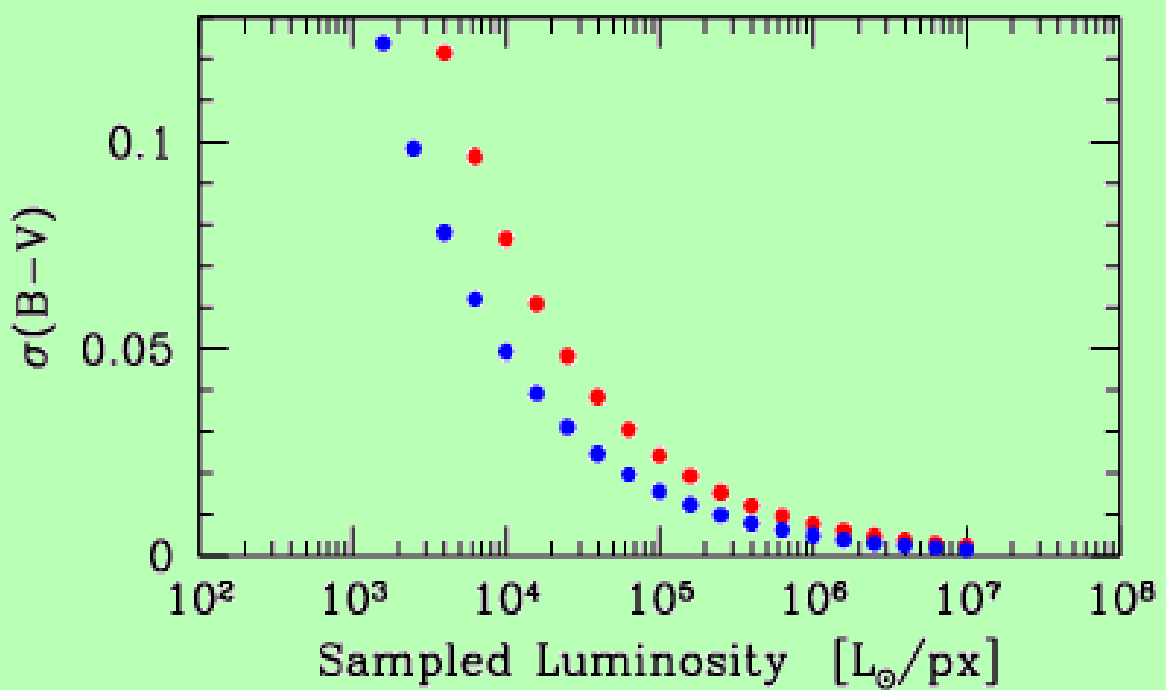


$$L_{(\text{quad})} = 3138 \pm 184$$

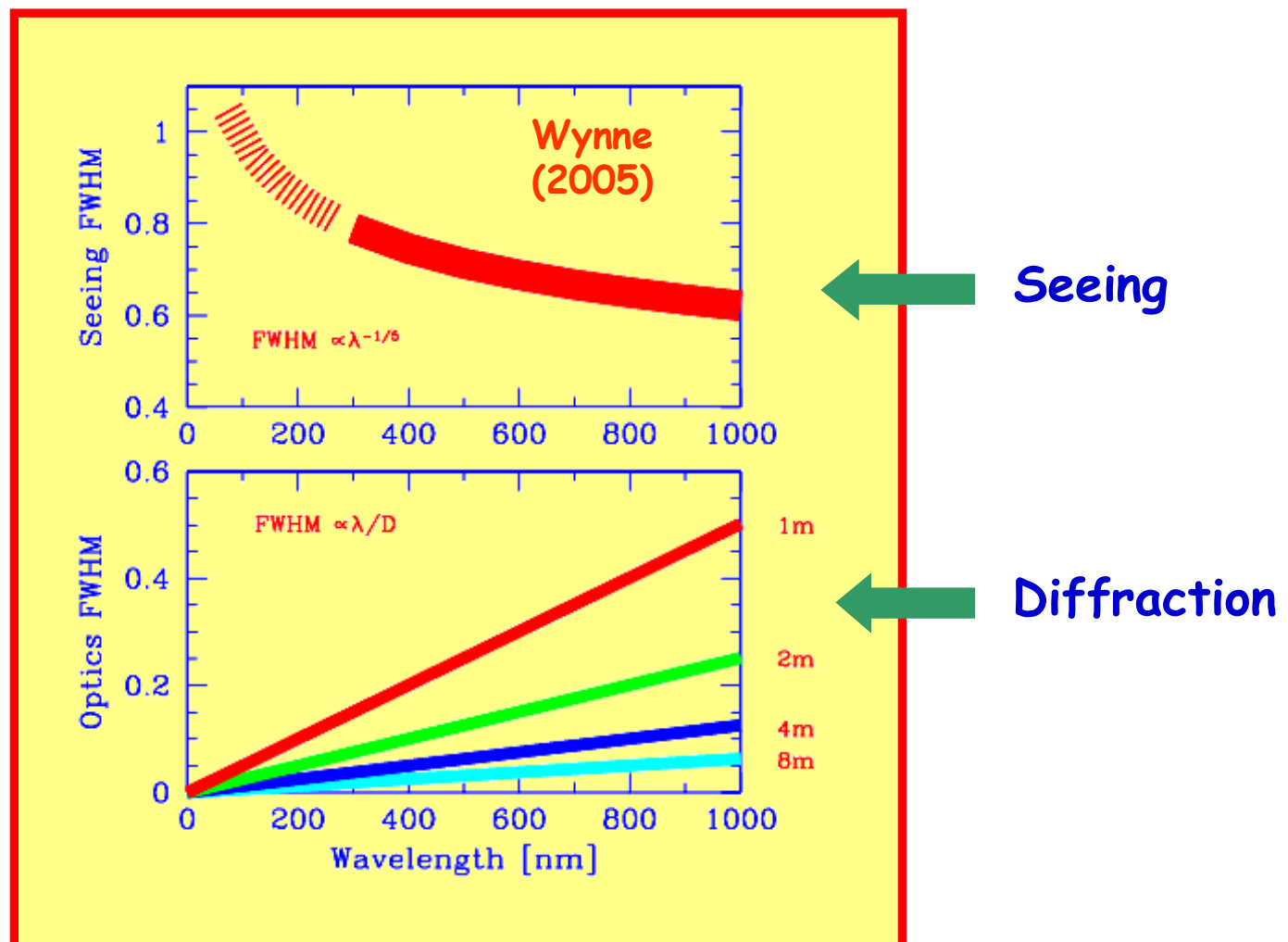
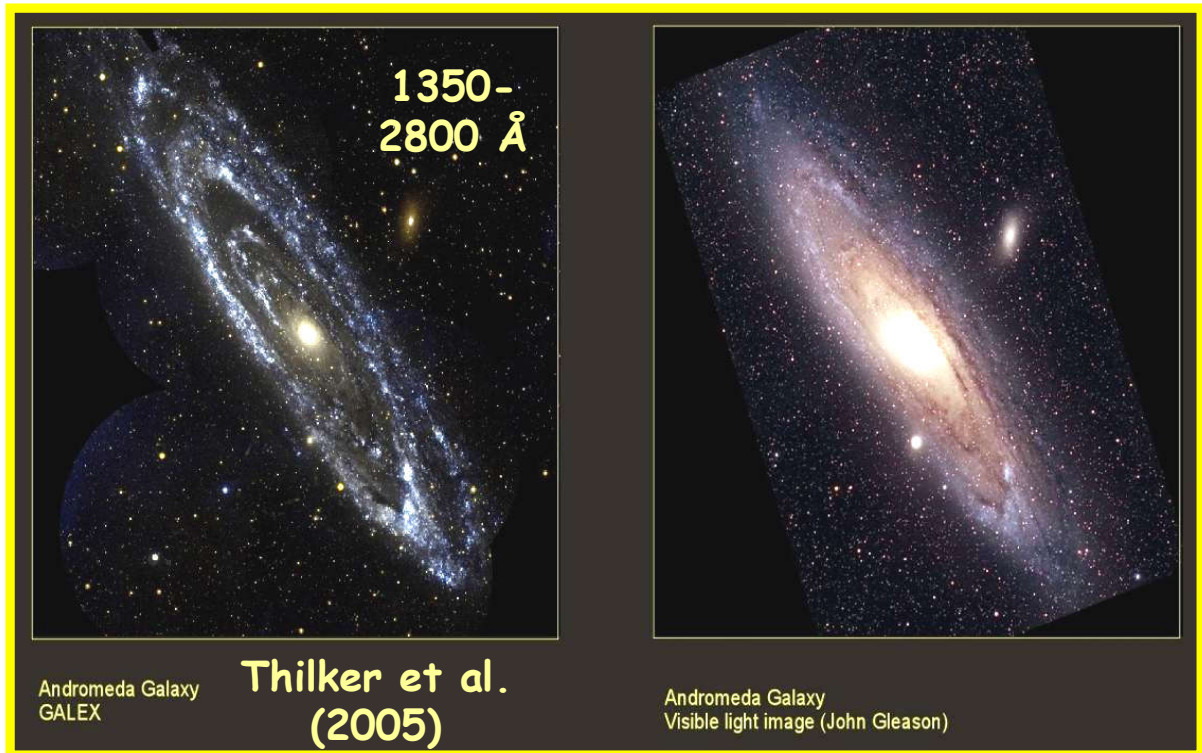
# Luminosity Sampling and Intrinsic Color Fluctuations

$$\Delta\text{mag} = \sigma(L_{\text{tot}})/L_{\text{tot}} = 1/\sqrt{N_{\text{eff}}}$$

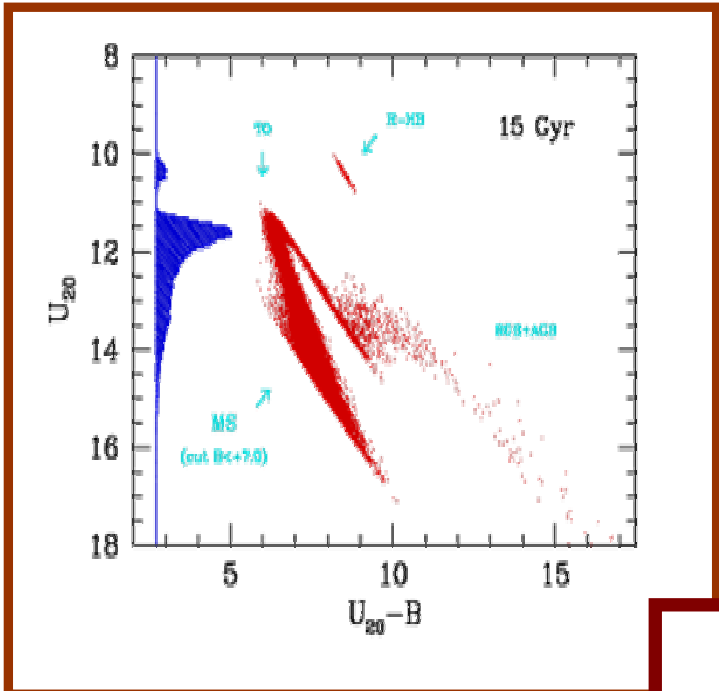
$$\sigma(B-V) = [\sigma(B)^2 + \sigma(V)^2]^{1/2} = (1/N_{\text{eff}}^B + 1/N_{\text{eff}}^V)$$



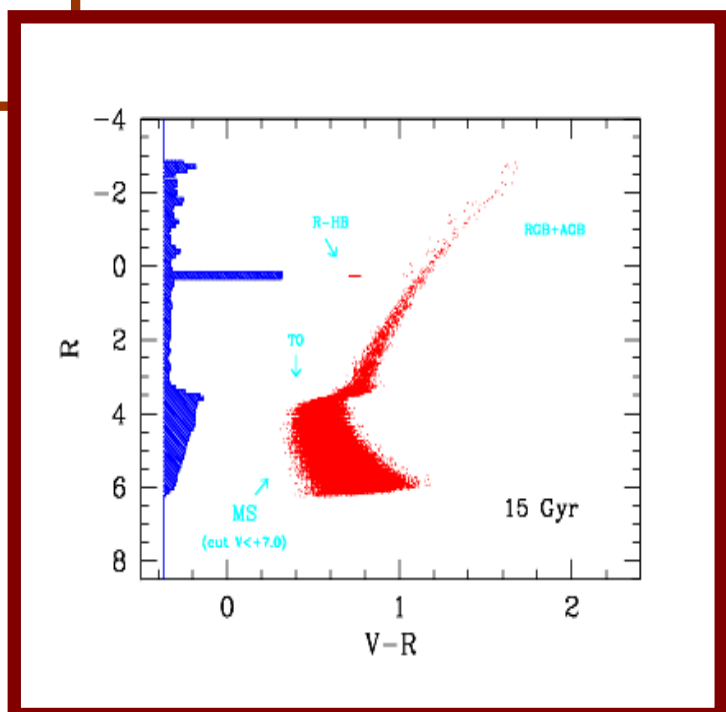
# Crowding & Optical opacity



# Oligarchy vs. Democracy

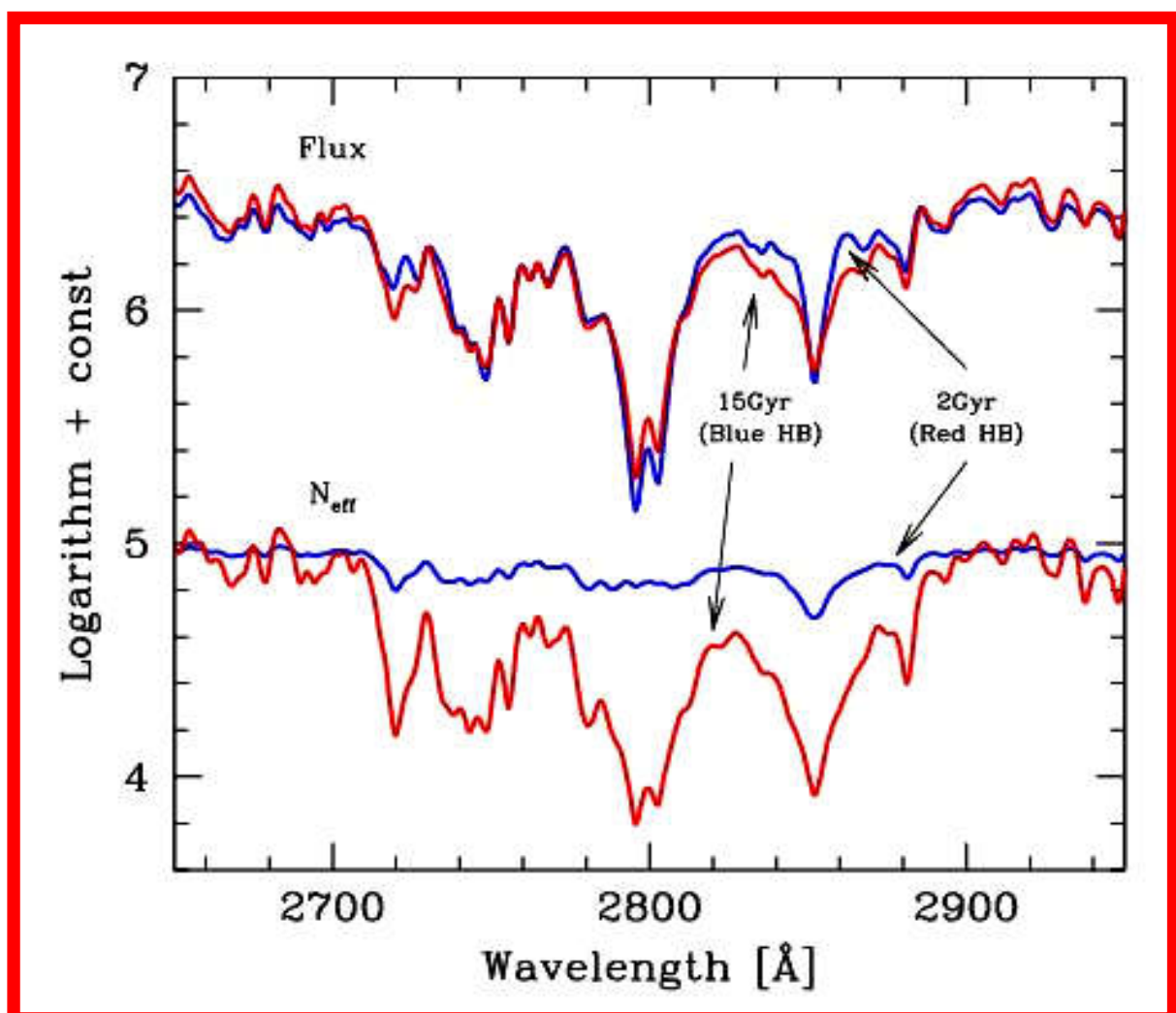
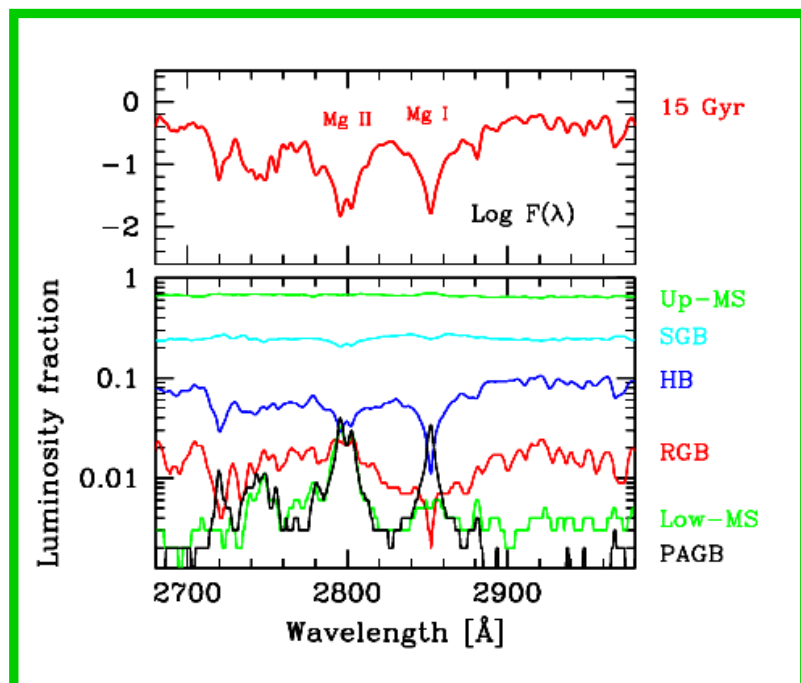


2000 Angstroms



7000 Angstroms

# Recovering the Age-Metallicity degeneracy



**Articoli consigliati (vedi Webpage):**

<http://www.bo.astro.it/~eps/lezioni/lezioni.html>

- **SBF (Buzzoni 1993)**
- **SBF (Tonry & Schneider 1988)**
- **SBF & Photometric Entropy (Buzzoni 2005)**
- **SBF & Photometric Entropy (Cerviño & Luridiana 2005)**

# Spettri & masse delle galassie

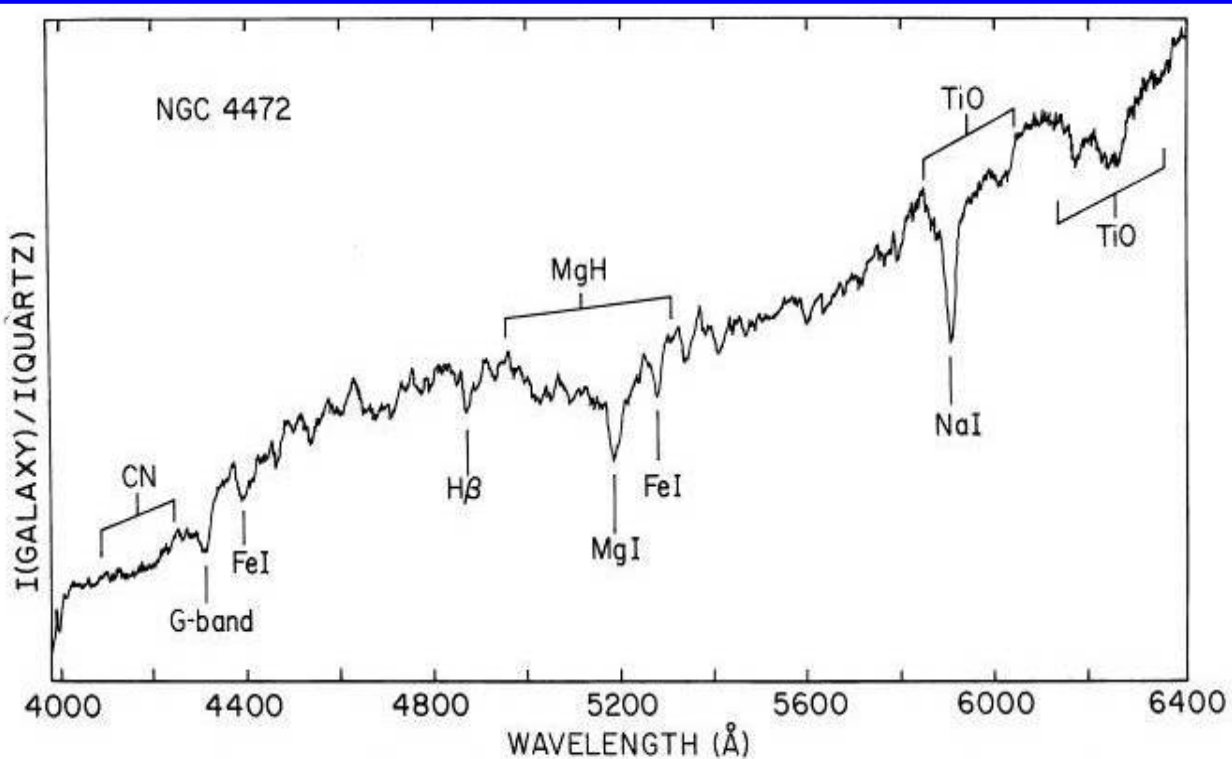


FIG. 1.—Typical scan of giant elliptical galaxy, divided by the tungsten lamp (denoted by “quartz”)

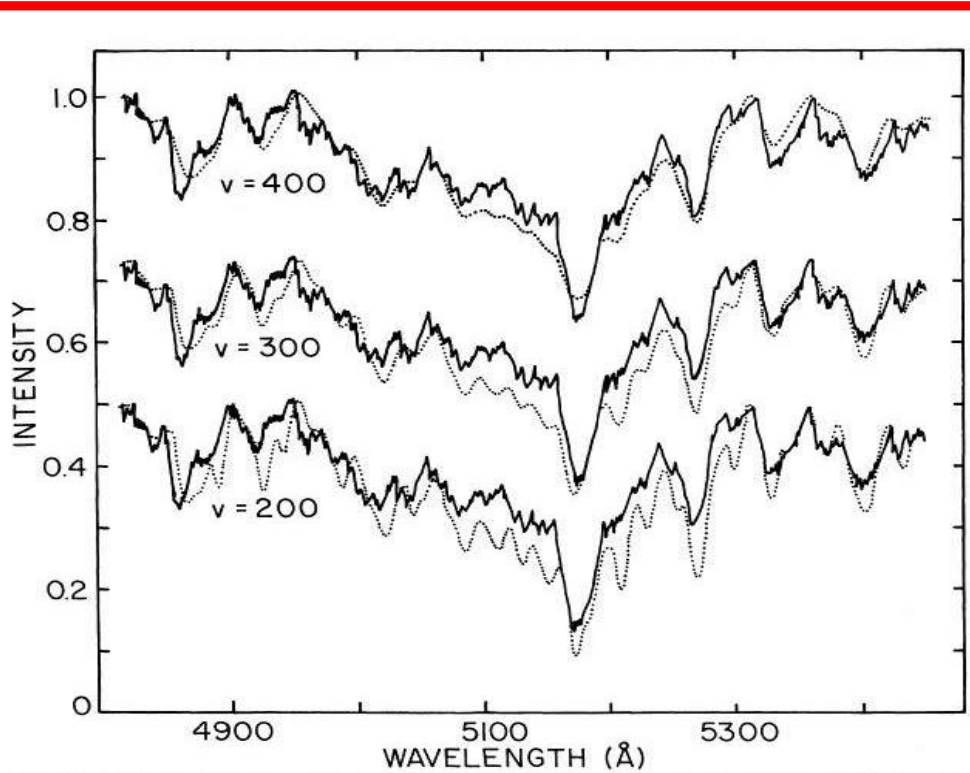


FIG. 3.—NGC 4472 compared with standard star HR 1805 (K3 III), broadened by various line-of-sight velocities (dotted line)

# La legge di Faber-Jackson (1976)

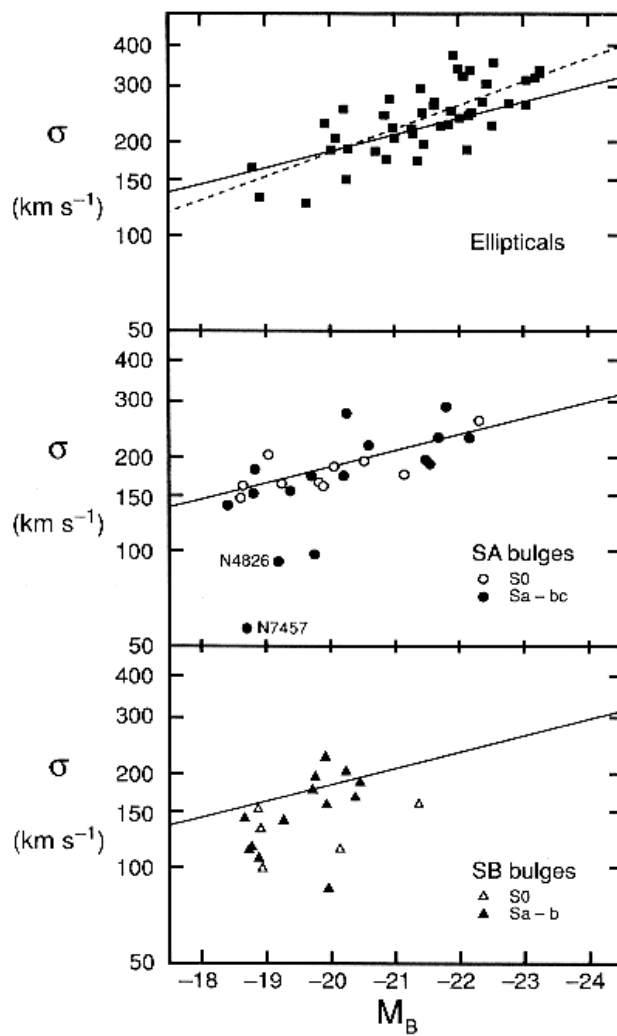


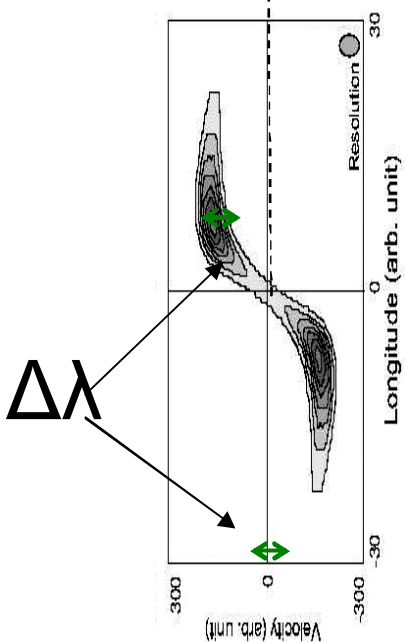
Fig. 6. Correlation between central velocity dispersion  $\sigma$  and absolute magnitude  $M_B$  for elliptical galaxies and for bulges of unbarred (SA) and barred (SB) disk galaxies. The solid line is a fit to the galaxies in the middle panel; the dashed line is a fit to the ellipticals. Except for the NGC 4826 point, this figure is from Kormendy and Illingworth (1983).

$$\left\{ \begin{array}{l} v^2 \approx \frac{GM}{R} \\ \mu = \frac{L}{\pi R^2} \approx \text{const} \\ \left( \frac{M}{L} \right) = \text{const} \end{array} \right. \quad \left. \begin{array}{l} \text{Se il moto e' caotico,} \\ \text{allora } v^2 \equiv \sigma^2 \end{array} \right\} \boxed{\sigma^4 \propto \mu L}$$

M82

# Spettri & Massa delle Spirali

@SUBARU  
(Japan)

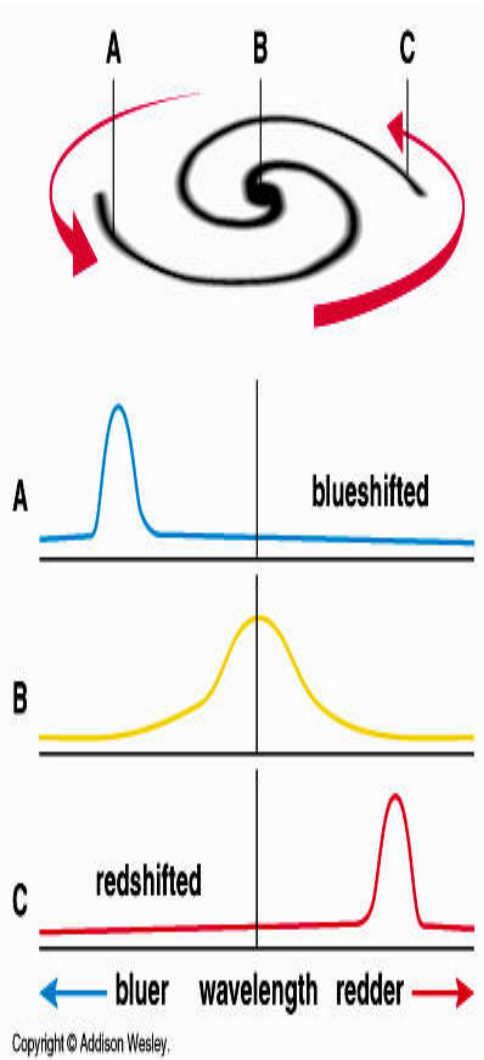


$$\frac{\Delta \lambda}{\lambda} = \frac{v}{c}$$

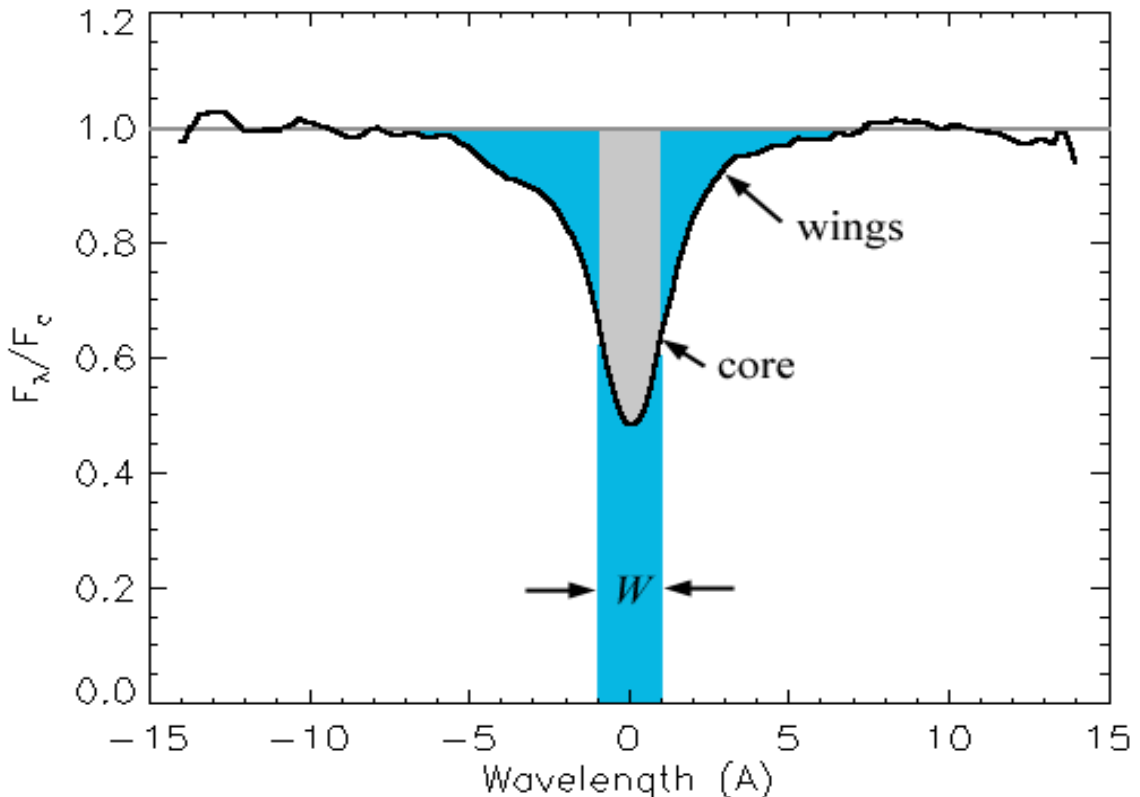
$$\frac{v^2}{R} = \frac{GM}{R^2}$$

Acc.  
centrifuga

Acc.  
gravitazionale

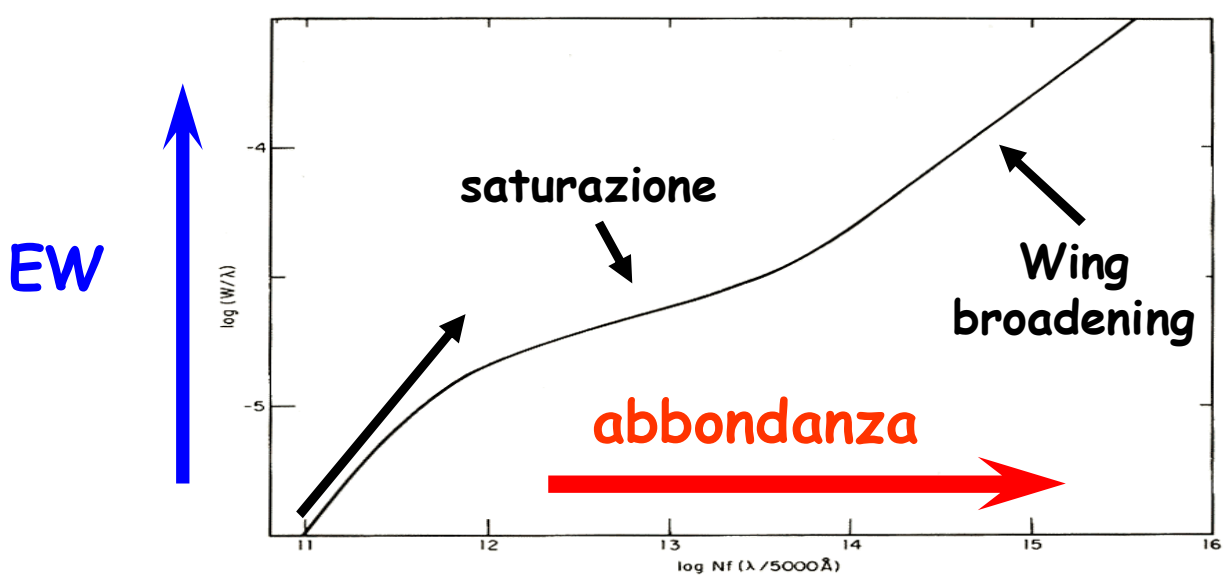


# Forza di indice e Ampiezza equivalente

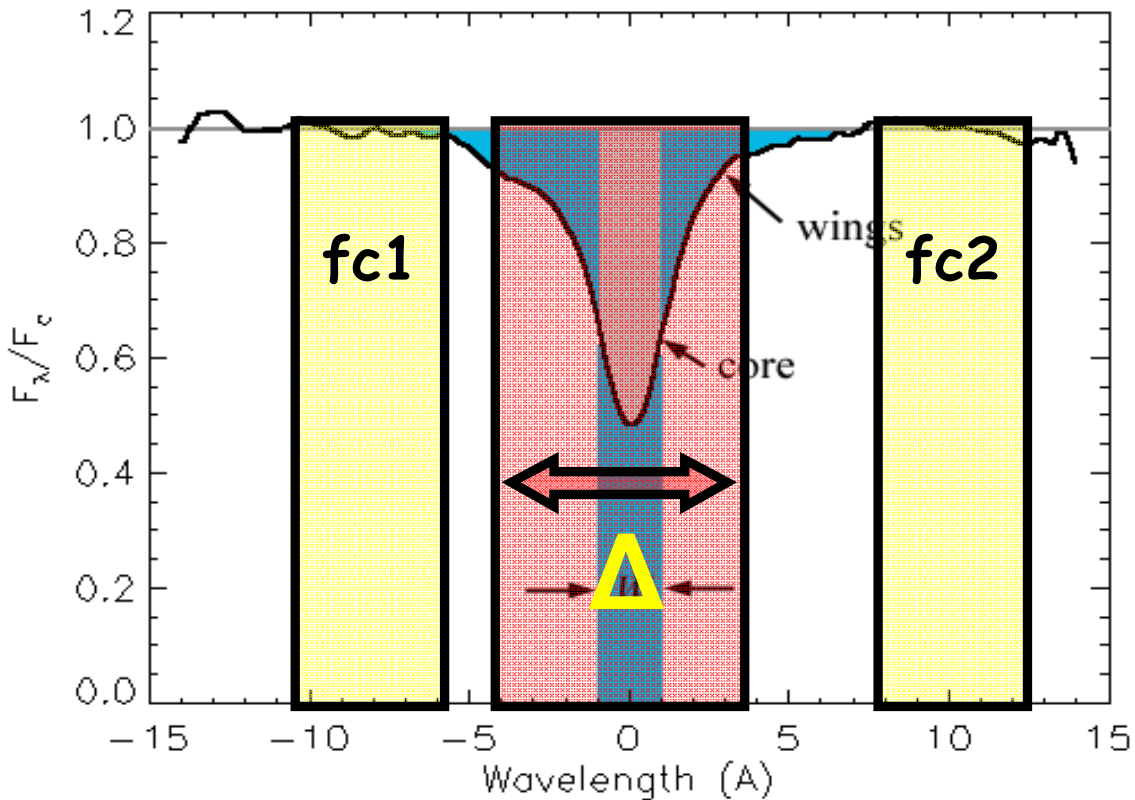


$$EW = \int \frac{f_c - f_f}{f_c} d\lambda$$

a  $T_{\text{eff}}$  fissato!!



# Indici in EW e in magnitudini



Tipicamente,

- se la riga è **atomica**, l'indice si misura in **EW**
- se la banda è **molecolare** si misura in **mag**

$$I_A = \Delta \frac{(f_c - f_f)}{f_c}$$

$$I_{\text{mag}} = -2.5 \log \left[ 1 - \left( \frac{I_A}{\Delta} \right) \right]$$

$$I_{\text{mag}} = -2.5 \log \left( \frac{f_f}{f_c} \right)$$

$$I_A = \Delta \left[ 1 - 10^{-0.4 I_{\text{mag}}} \right]$$

# Il sistema di Lick

TABLE I  
INDEX DEFINITIONS

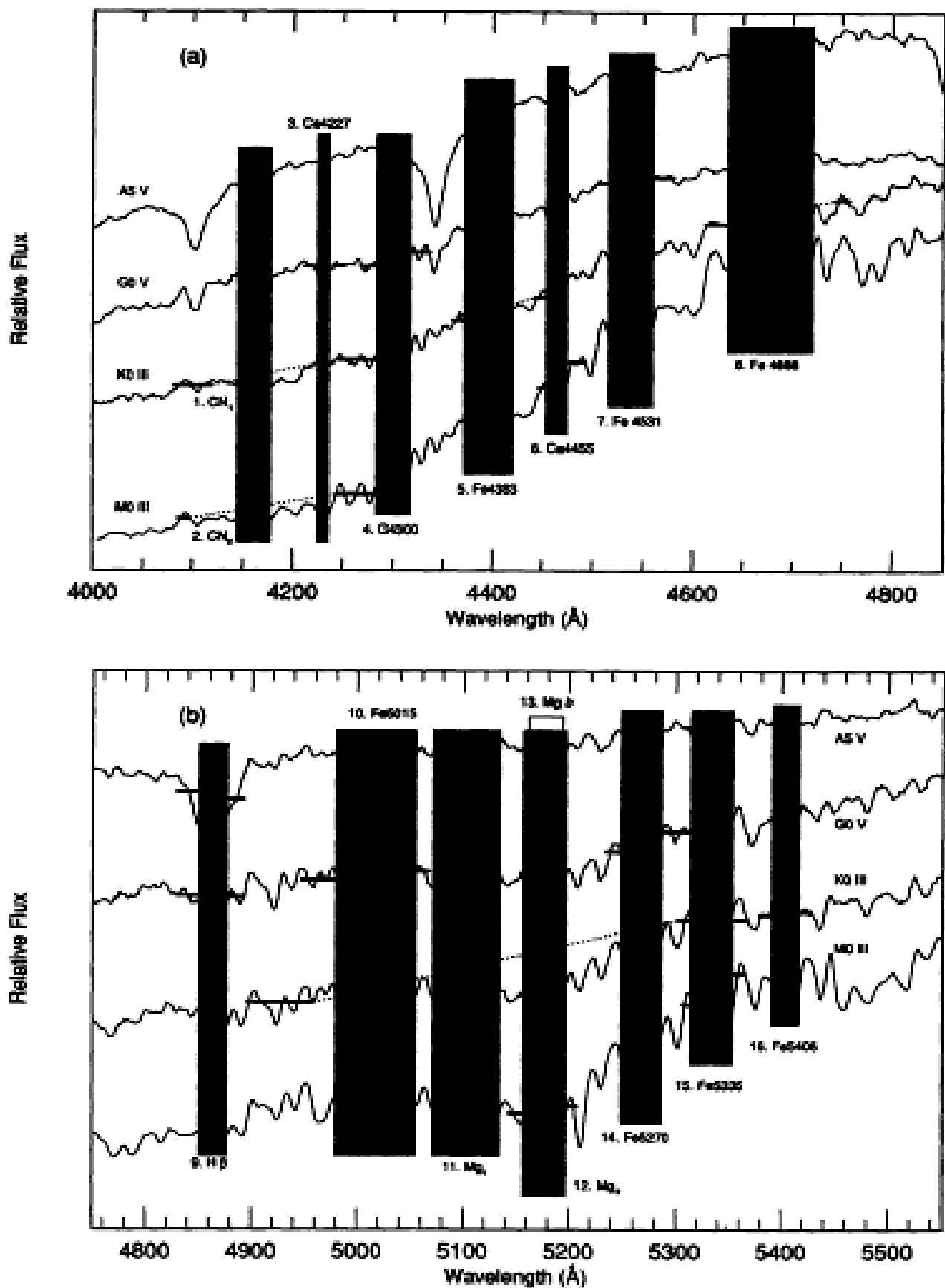
	Name	Index Bandpass	Pseudocontinua	Units	Measures	Error <sup>1</sup>	Notes
01	CN <sub>1</sub>	4143.375-4178.375	4081.375-4118.875 4245.375-4285.375	mag	CN, Fe I	0.021	
02	CN <sub>2</sub>	4143.375-4178.375	4085.125-4097.625 4245.375-4285.375	mag	CN, Fe I	0.023	2
03	Ca4227	4223.500-4236.000	4212.250-4221.000 4242.250-4252.250	Å	Ca I, Fe I, Fe II	0.27	2
04	G4300	4282.625-4317.625	4267.625-4283.875 4320.125-4336.375	Å	CH, Fe I	0.39	
05	Fe4383	4370.375-4421.625	4360.375-4371.625 4444.125-4456.625	Å	Fe I, Ti II	0.53	2
06	Ca4455	4453.375-4475.875	4447.125-4455.875 4478.375-4493.375	Å	Ca I, Fe I, Ni I, Ti II, Mn I, V I	0.25	2
07	Fe4531	4515.500-4560.500	4505.500-4515.500 4561.750-4580.500	Å	Fe I, Ti I, Fe II, Ti II	0.42	2
08	Fe4668	4635.250-4721.500	4612.750-4631.500 4744.000-4757.750	Å	Fe I, Ti I, Cr I, Mg I, Ni I, C <sub>2</sub>	0.64	2
09	H $\beta$	4847.875-4876.625	4827.875-4847.875 4876.625-4891.625	Å	H $\beta$ , Fe I	0.22	3
10	Fe5015	4977.750-5054.000	4946.500-4977.750 5054.000-5065.250	Å	Fe I, Ni I, Ti I	0.46	2,3
11	Mg <sub>1</sub>	5069.125-5134.125	4895.125-4957.625 5301.125-5366.125	mag	MgH, Fe I, Ni I	0.007	3
12	Mg <sub>2</sub>	5154.125-5196.625	4895.125-4957.625 5301.125-5366.125	mag	MgH, Mg b, Fe I	0.008	3
13	Mg b	5160.125-5192.625	5142.625-5161.375 5191.375-5206.375	Å	Mg b	0.23	3
14	Fe5270	5245.650-5285.650	5233.150-5248.150 5285.650-5318.150	Å	Fe I, Ca I	0.28	3
15	Fe5335	5312.125-5352.125	5304.625-5315.875 5353.375-5363.375	Å	Fe I	0.26	3
16	Fe5406	5387.500-5415.000	5376.250-5387.500 5415.000-5425.000	Å	Fe I, Cr I	0.20	2,3
17	Fe5709	5698.375-5722.125	5674.625-5698.375 5724.625-5738.375	Å	Fe I, Ni I, Mg I Cr I, V I	0.18	2
18	Fe5782	5778.375-5798.375	5767.125-5777.125 5799.625-5813.375	Å	Fe I, Cr I Cu I, Mg I	0.20	2
19	Na D	5878.625-5911.125	5862.375-5877.375 5923.875-5949.875	Å	Na I	0.24	
20	TiO <sub>1</sub>	5938.375-5995.875	5818.375-5850.875 6040.375-6105.375	mag	TiO	0.007	
21	TiO <sub>2</sub>	6191.375-6273.875	6068.375-6143.375 6374.375-6416.875	mag	TiO	0.006	

FWHM = 8.5 Å

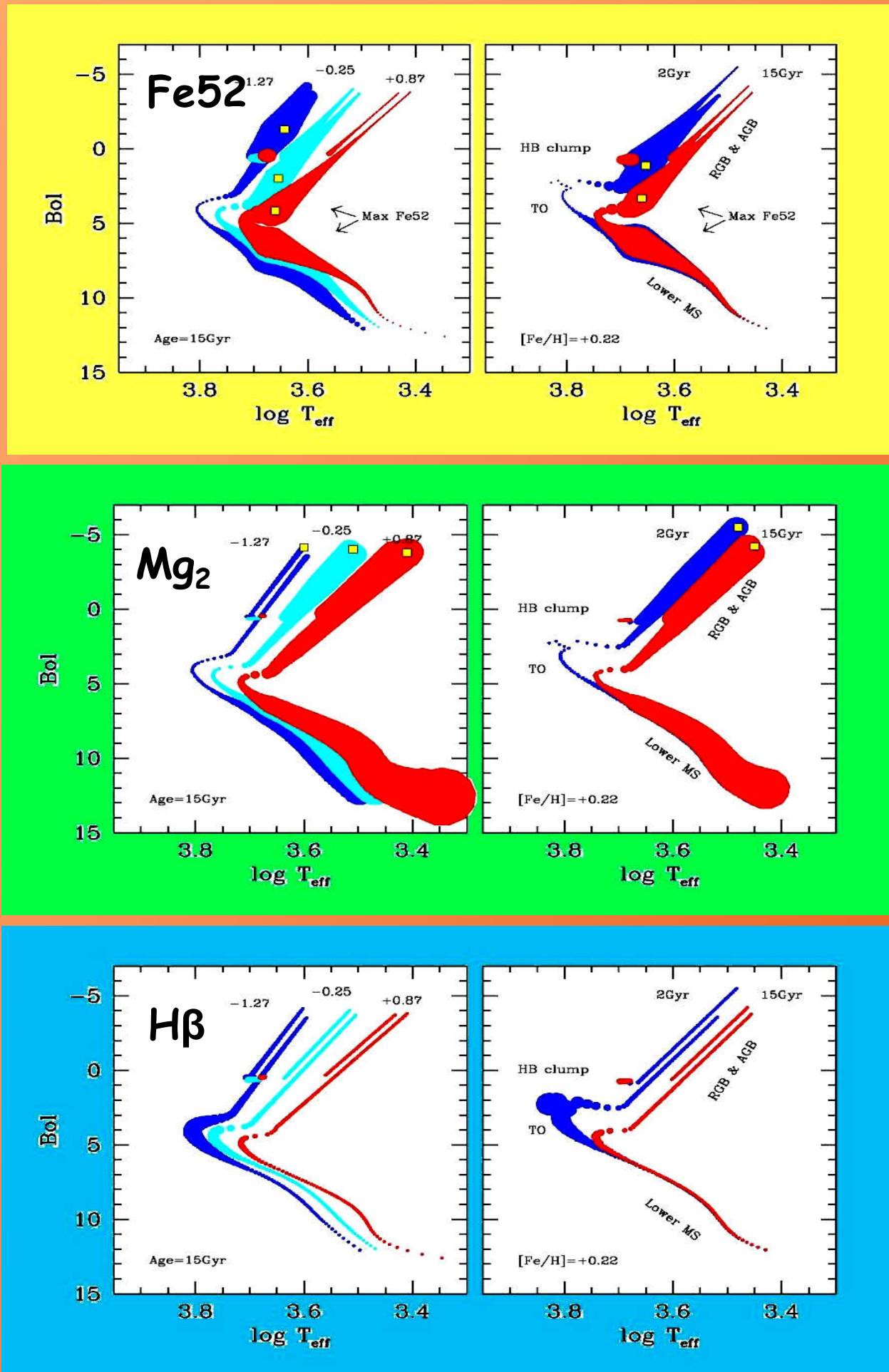
Worthey et al. (1994)

+ Trager et al. (1998)

# Indici Blu-Vis



# Narrow-band indices & SSP tomography

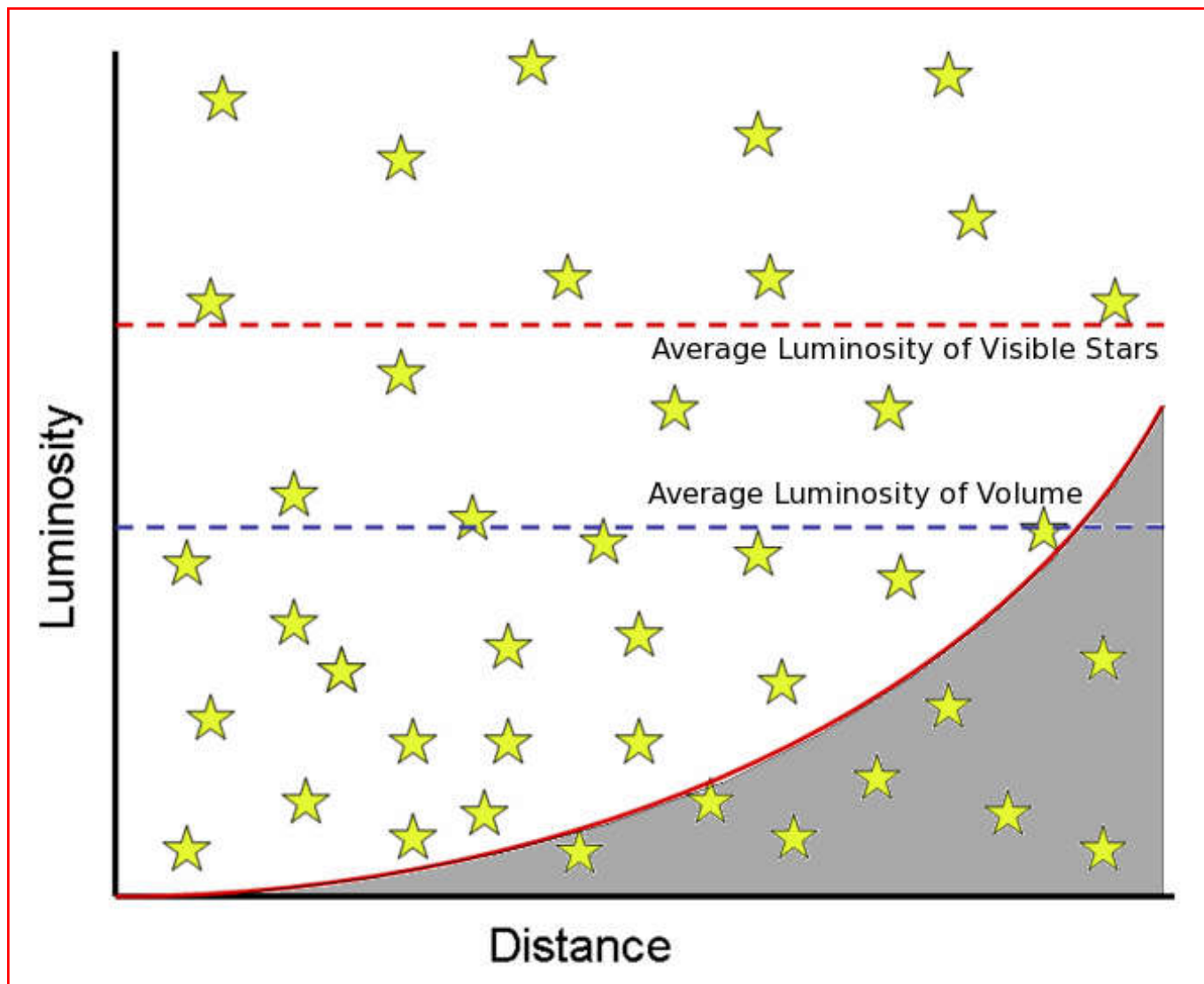


**Articoli consigliati (vedi Webpage):**

<http://www.bo.astro.it/~eps/lezioni/lezioni.html>

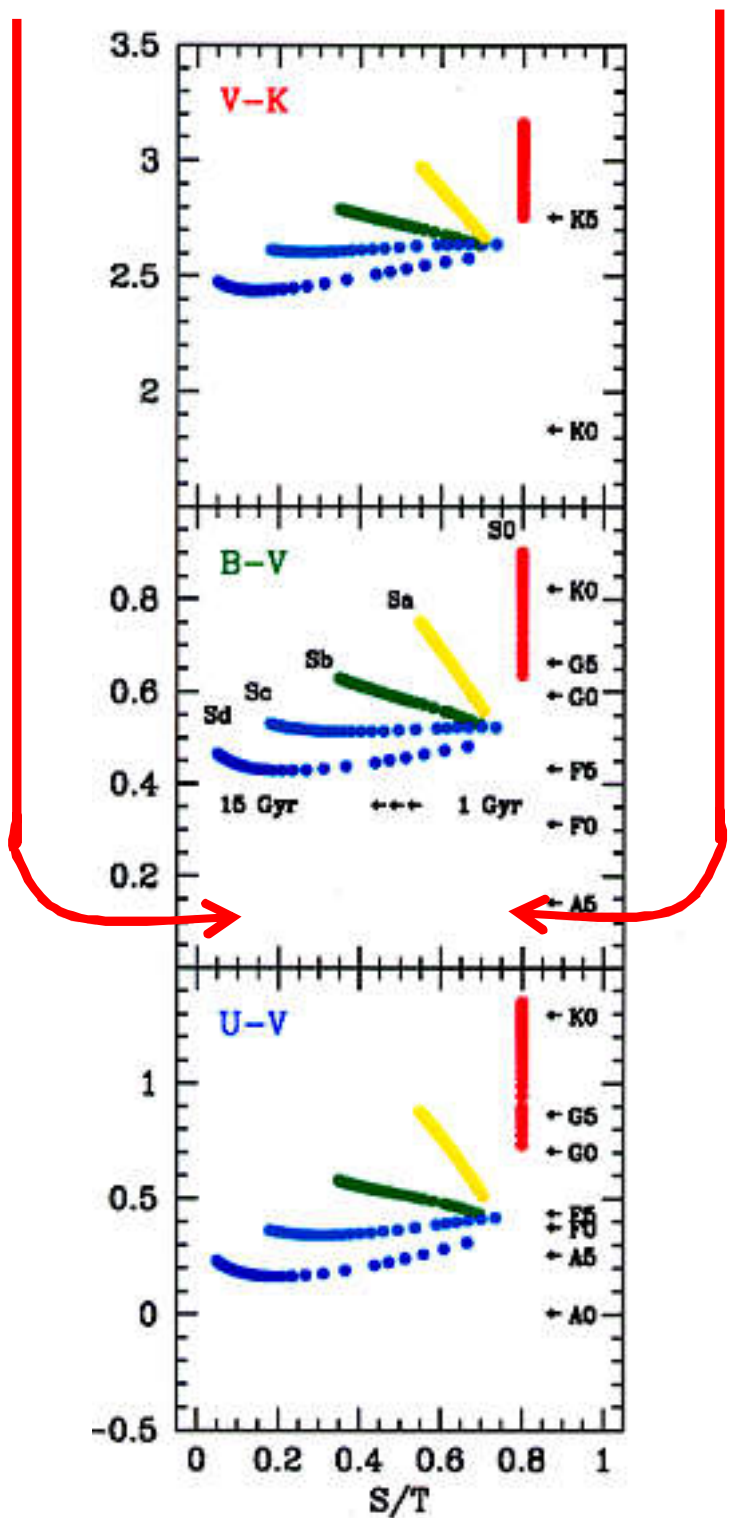
- **Spectral Properties of Galaxies (Kennicutt 1992)**
- **Galaxy Spectral Atlas (Kennicutt 1992)**
- **Faber & Jackson (1976)**
- **Balmer break (Hamilton 1985)**
- **Lick indices (Worley et al. 1994)**

# Il bias di Malmquist



# Bias morfológico & Bias fotométrico

Disk-dominated      Bulge-dominated

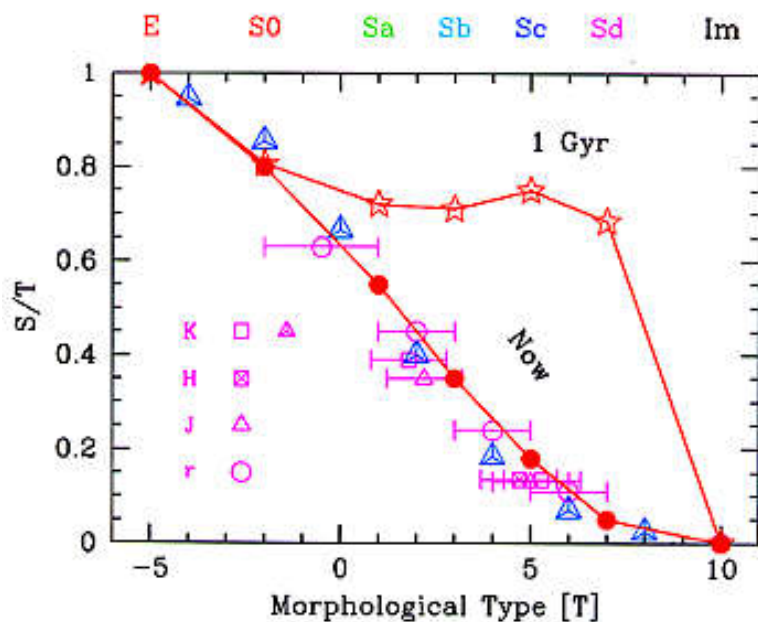
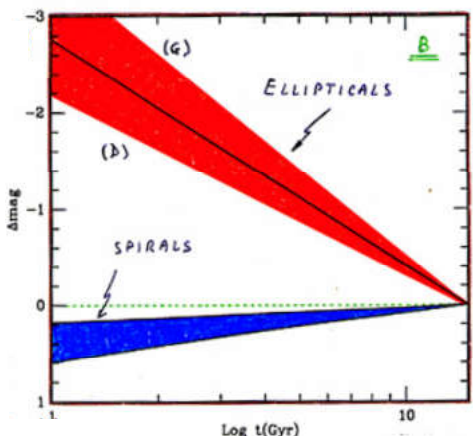


$L(\text{Spheroid})/L(\text{Tot})$

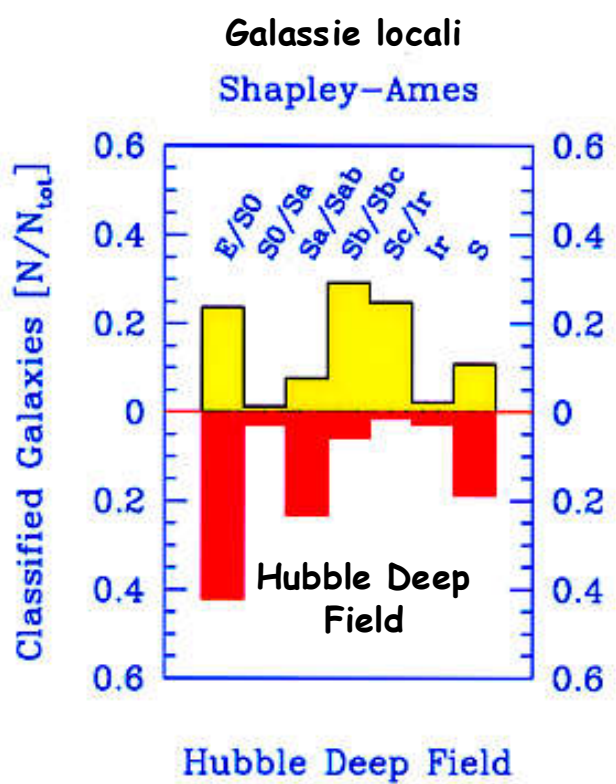
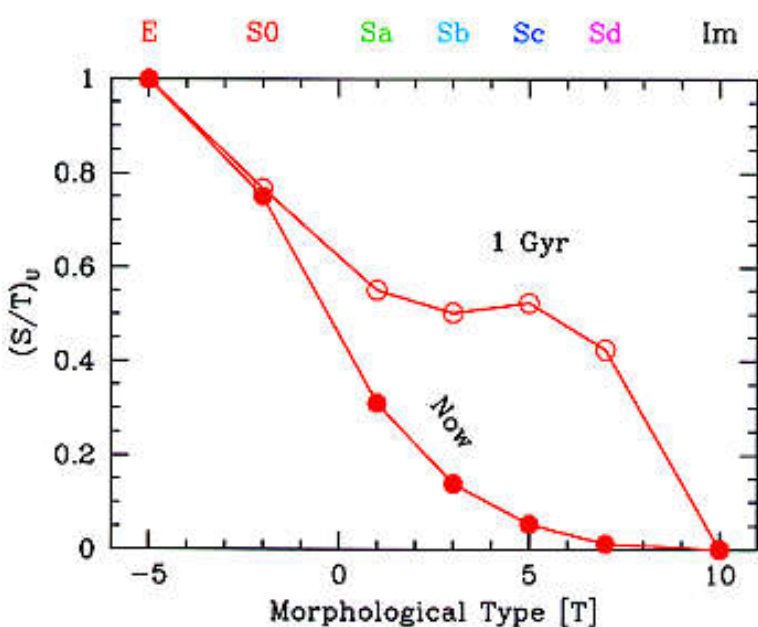
# Bias Morfologico

All'aumentare del redshift

- 1) Andiamo indietro nel tempo  
(bulge +luminoso e disco -luminoso)
- 2) La morfologia tende ad essere quella nell'Ultravioletto



Buzzoni (2005)



Van den Bergh et al. (1996)

# II Redshift

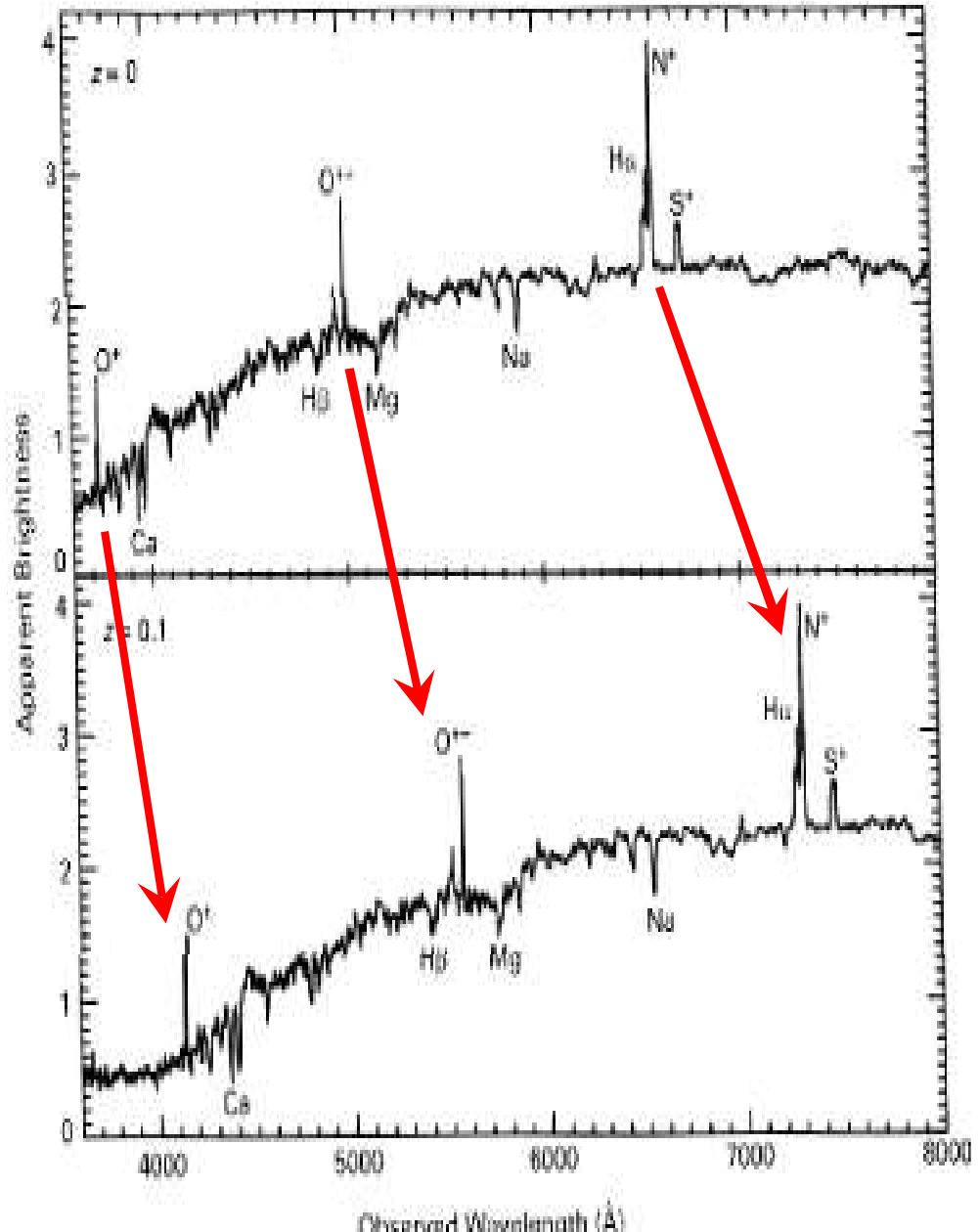


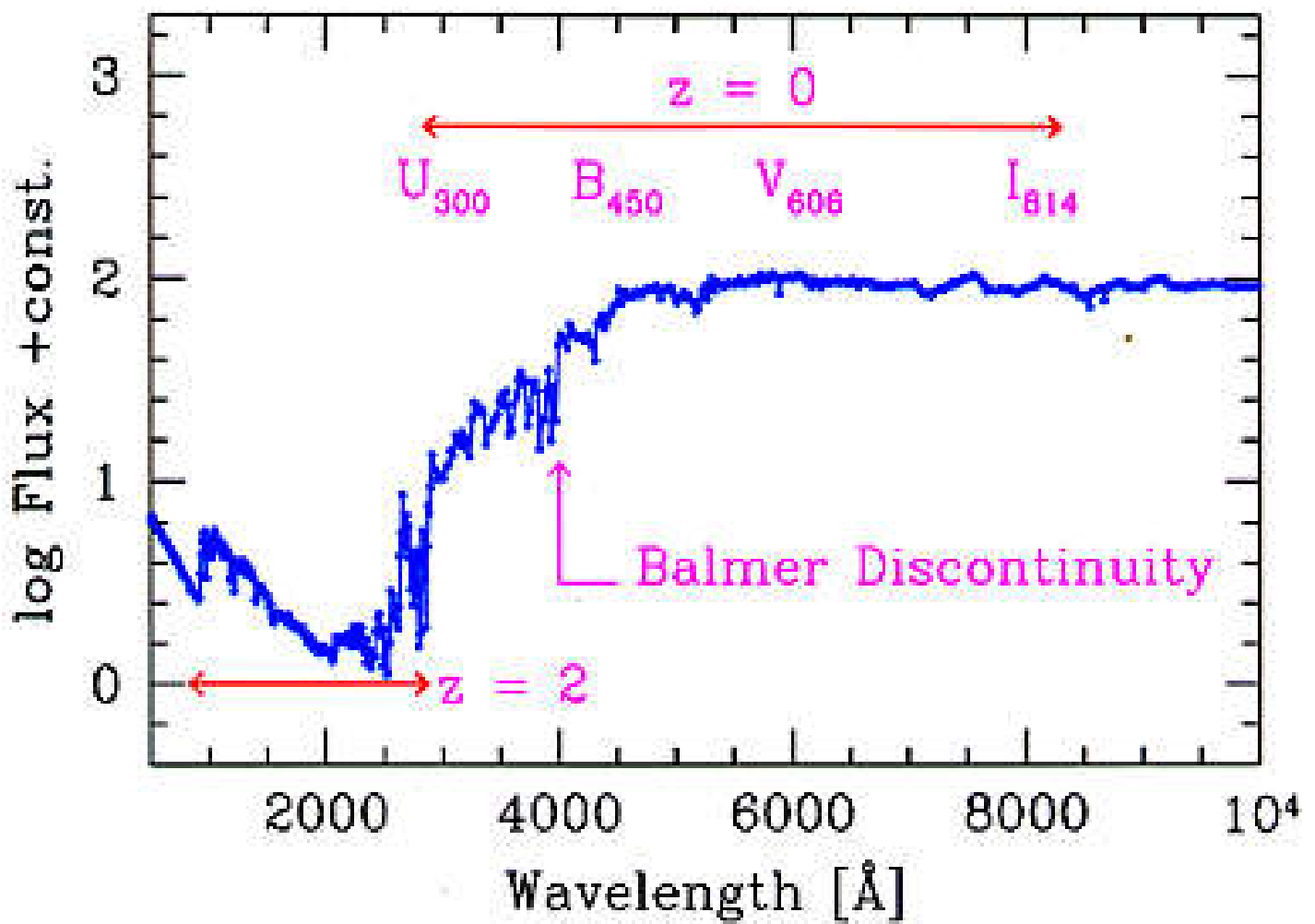
Figure 2.20 K. J. Webb

$$\frac{\lambda_{\text{oss}} - \lambda_{\text{lab}}}{\lambda_{\text{lab}}} = z$$

$$\frac{\Delta\lambda}{\lambda} = \frac{v}{c} = z$$

$$\frac{\lambda_{\text{oss}}}{\lambda_{\text{lab}}} = (1 + z)$$

# L'effetto di "stretching"



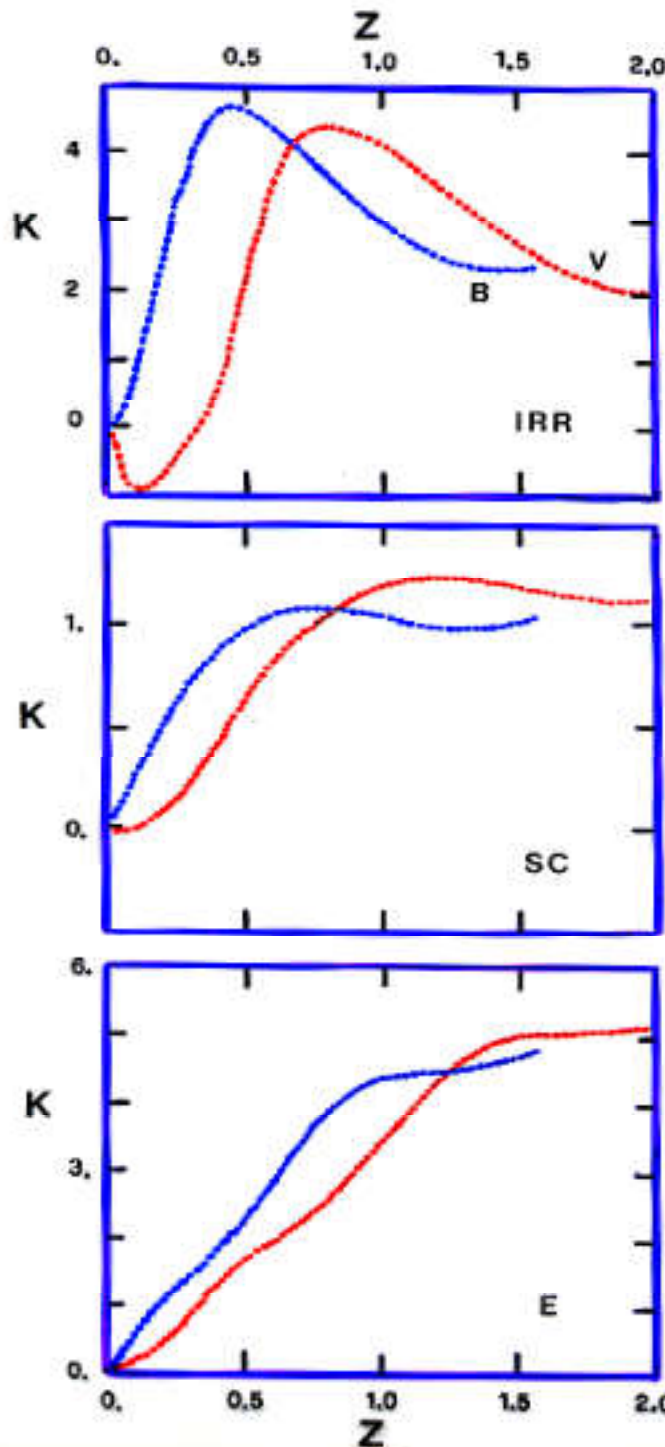
Massarotti et al. (2001)

# Correzione k

$$M - M_0 = 5 \log \frac{\ell}{\ell_0} + K(z) + \epsilon(z)$$

$$K(z) = 2.5 \log(1+z) - 2.5 \log \int F(\lambda/(1+z)) R_\lambda d\lambda / \int F_\lambda R_\lambda d\lambda$$

$$\epsilon(z) = -2.5 \log \int F(\lambda/(1+z); t_z) R_\lambda d\lambda / \int F(\lambda/(1+z); 0) R_\lambda d\lambda$$

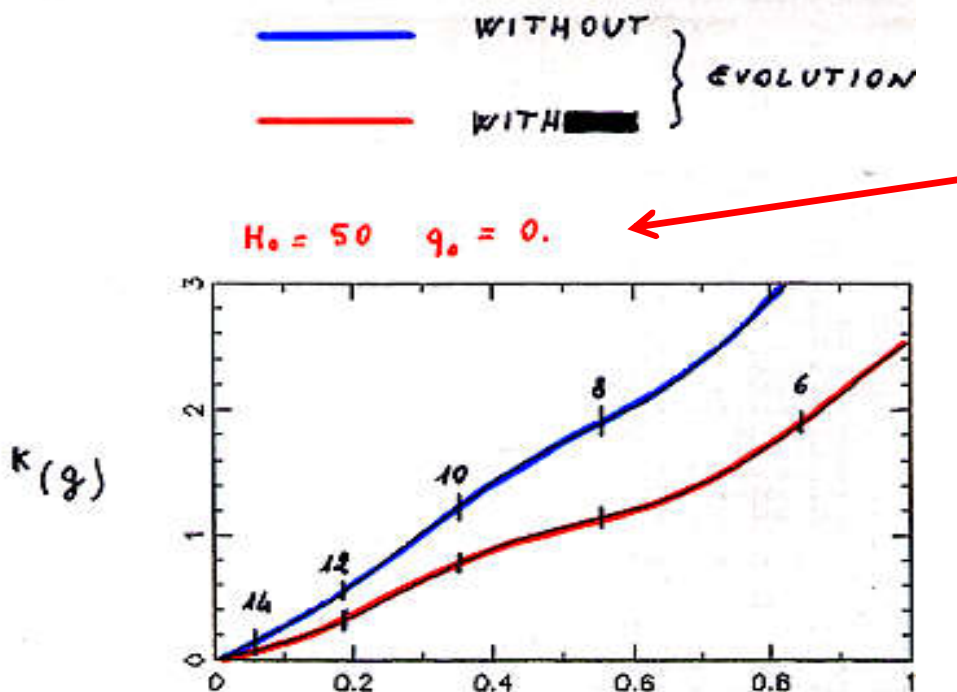


Notare che  $\forall$  morfologia

$$\lim_{z \rightarrow 0} k = +2.5 \log(1+z)$$

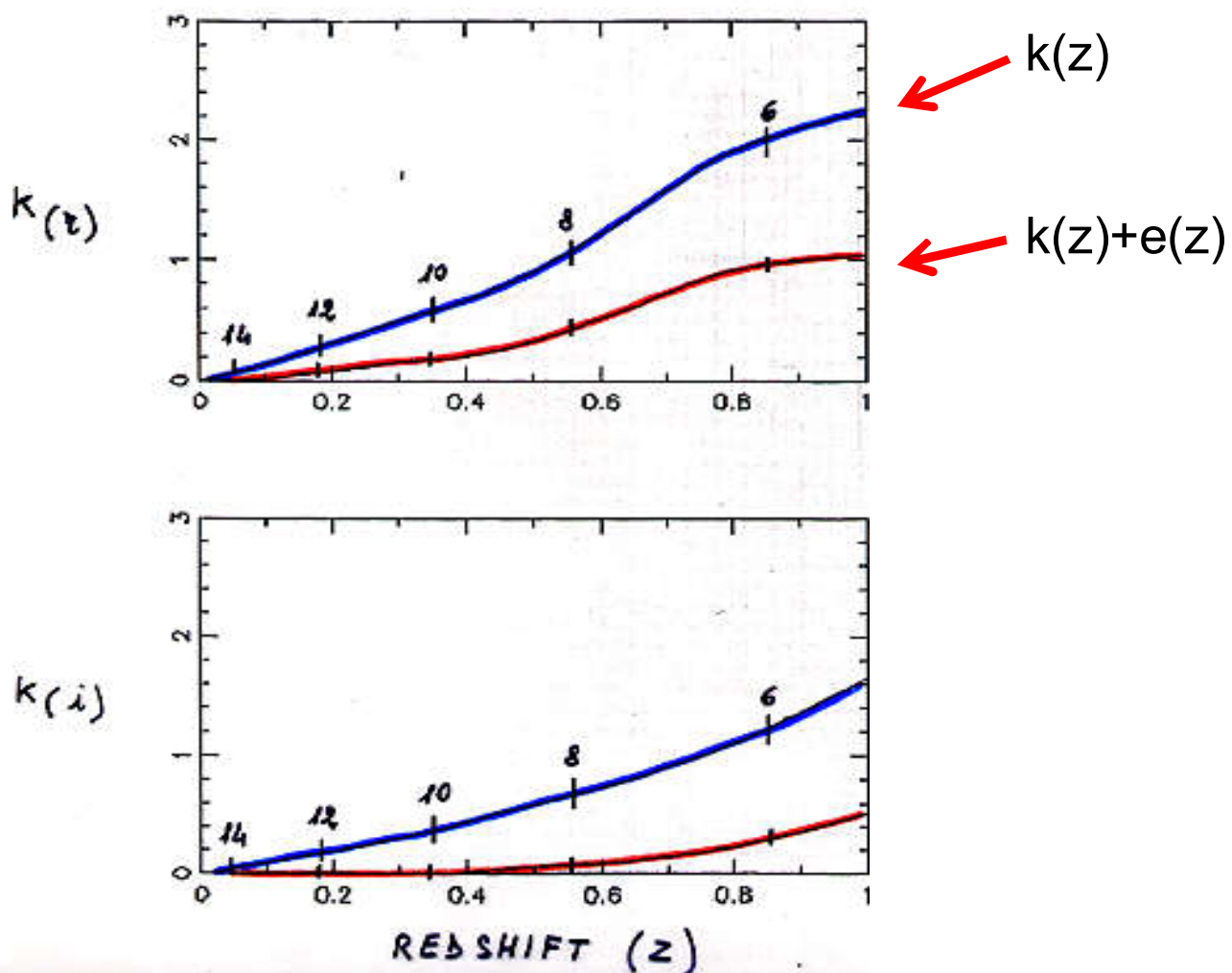
Dato che  $F(\lambda/(1+z)) \rightarrow F(\lambda)$

# Esempi di correzione $k$ passiva ( $k$ ) ed evolutiva ( $k+e$ )

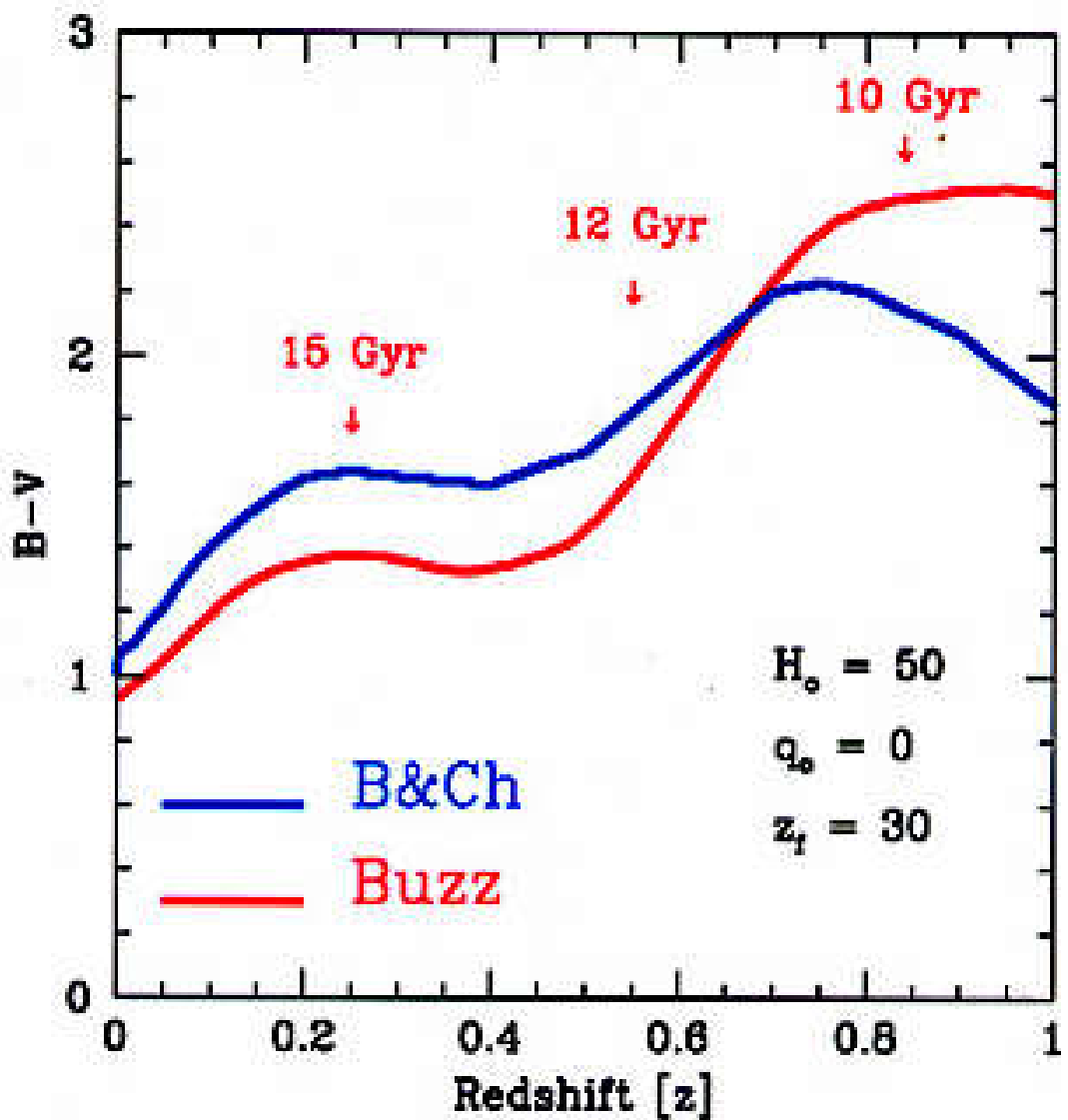


Importante!:

La correzione evolutiva  $e(z)$  dipende dal modello cosmologico assunto



# Apparent Color vs. Redshift

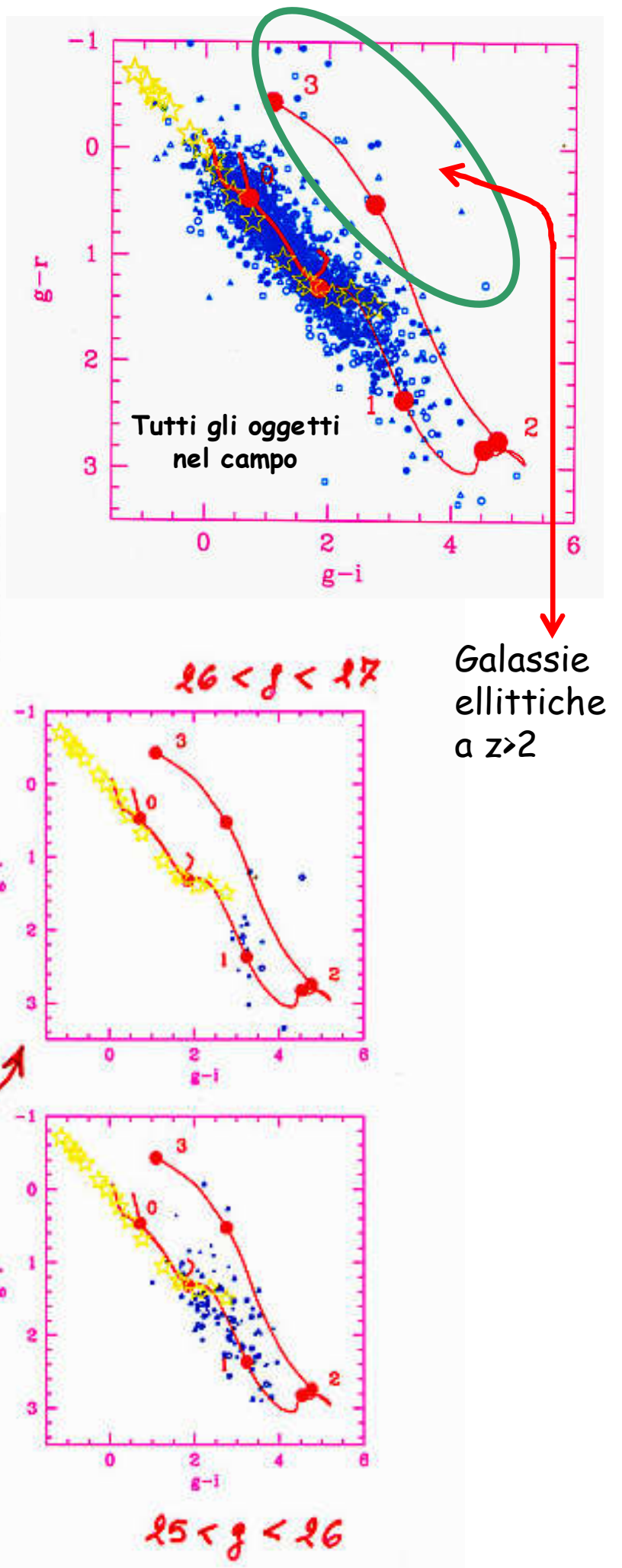


$$(B-V)_z = (B-V)_o + (k_B - k_V) + (e_B - e_V)$$

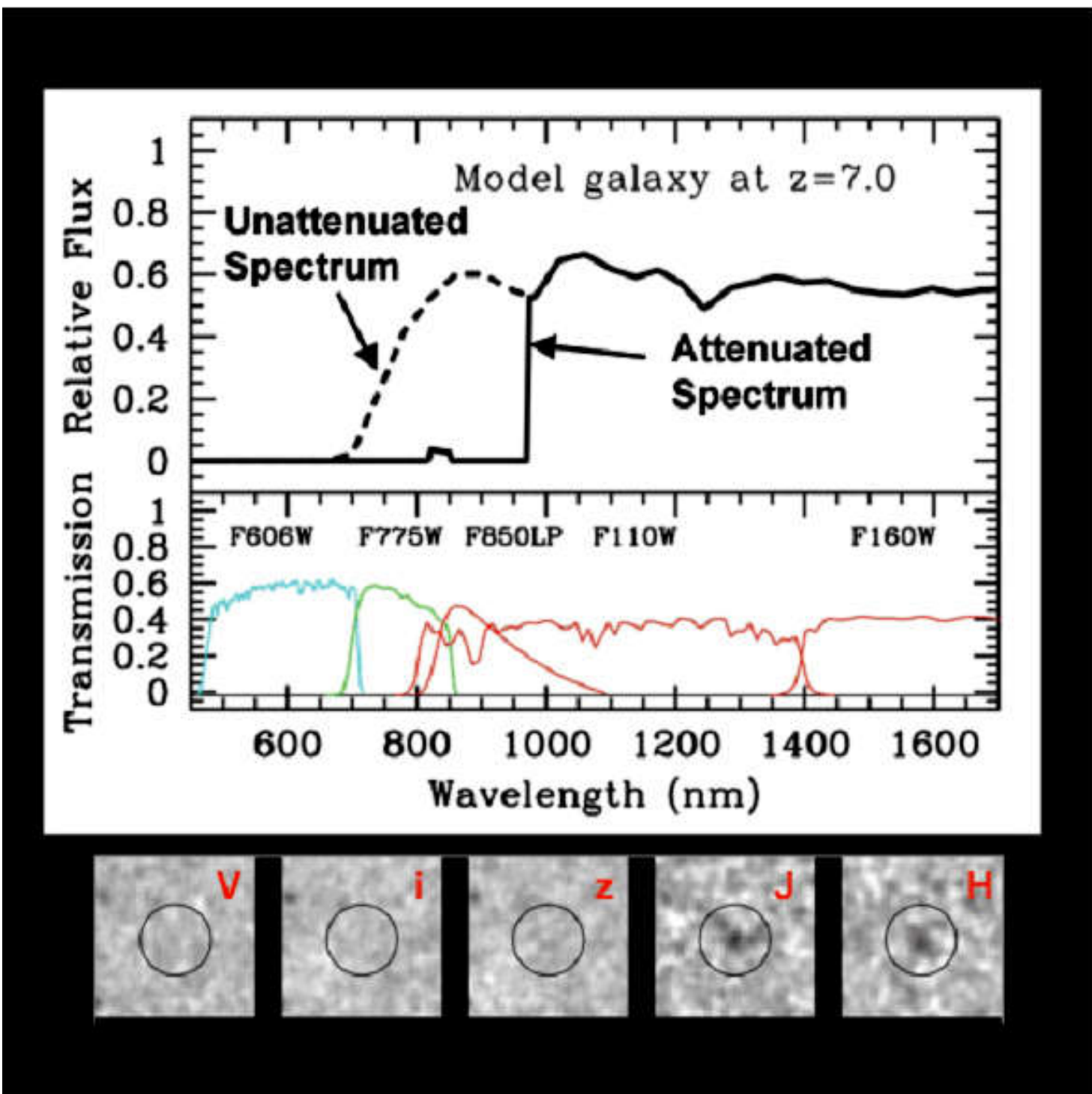
Colore  
apparente      Colore  
restframe

Opzionale, nel caso si voglia/possa  
tenere in conto della evoluzione  
con z

# Selezione fotometrica delle galassie ad alto redshift: un esempio



# Selezione fotometrica delle galassie ad alto redshift: "Dropout galaxies"



Steidel et al. (1996)

**Articoli consigliati (vedi Webpage):**

<http://www.bo.astro.it/~eps/lezioni/lezioni.html>

- **Galaxy Colors (Buzzoni 2005)**
- **Spectral Properties of Galaxies (Kennicutt 1992)**
- **Galaxy Spectral Atlas (Kennicutt 1992)**
- **Balmer break (Hamilton 1985)**
- **SFR & Hubble Sequence (Kennicutt 1988)**
- **Cosmic SFR (Madau & Dickinson (2014))**
- **Galaxy mass assembly (Pan 2015)**
- **k-correction (Hogg et al. 2002)**